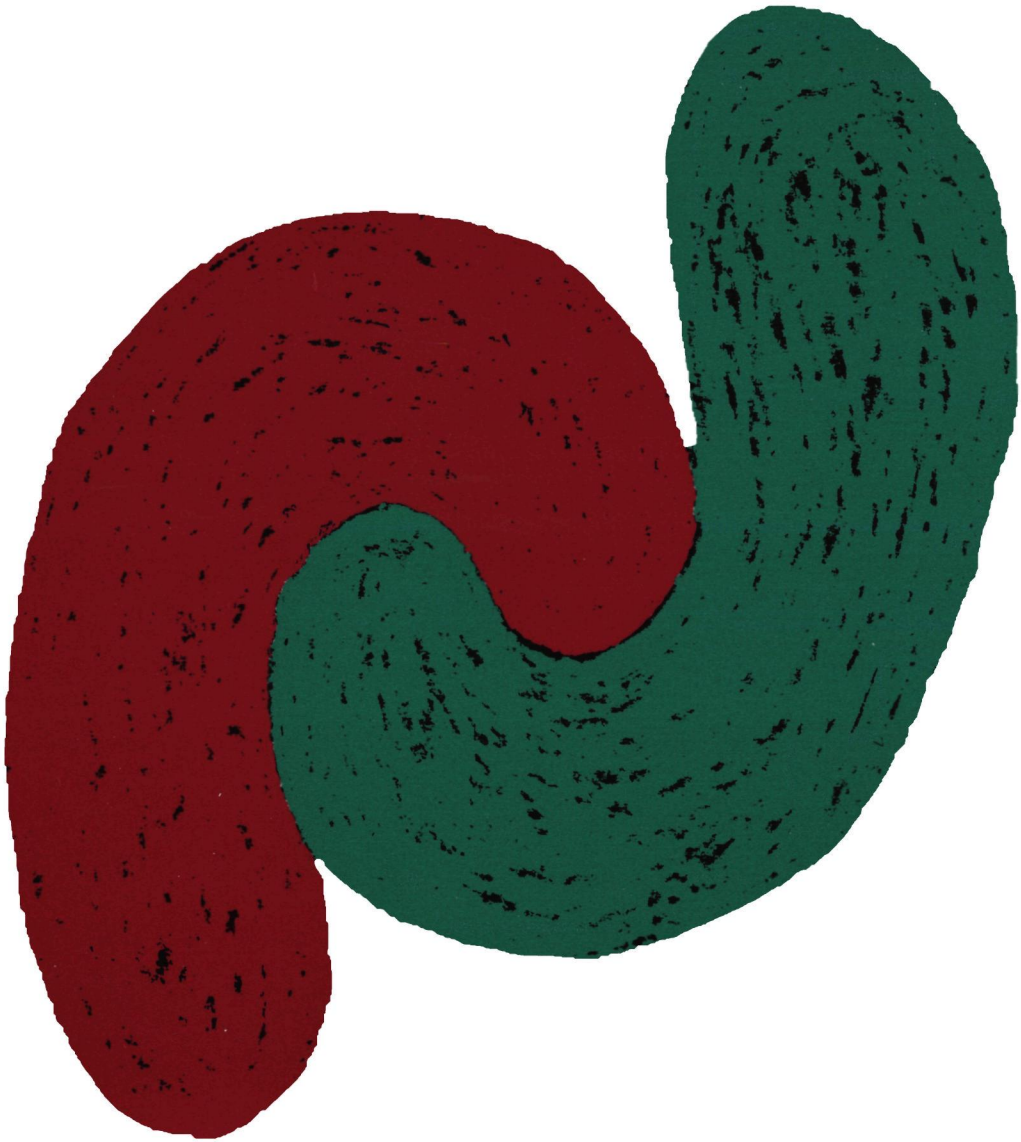

Synthesis, Binding Properties and Reactivity of Molecular Clips

EEN WETENSCHAPPELIJKE PROEVE OP HET GEBIED VAN DE NATUURWETENSCHAPPEN

PROEFSCHRIFT

TER VERKRIJGING VAN DE GRAAD VAN DOCTOR AAN DE KATHOLIEKE UNIVERSITEIT NIJMEGEN, VOLGENS BESLUIT VAN HET COLLEGE VAN DECANEN IN HET OPENBAAR TE VERDEDIGEN OP DONDERDAG 13 JUNI 1996 DES NAMIDDAGS OM 3.30 UUR PRECIES

DOOR

JOOST NICOLAAS HENDRIK REEK

GEBOREN OP 23 JUNI 1967 TE S'-HERTOGENBOSCH

Promotor:	**Prof. Dr. R. J. M. Nolte**	
Copromotor:	**Dr. A. E. Rowan**	
Manuscriptcommissie:	**Dr. R. P. Sijbesma**	**(T.U.E.)**
	Dr. H. K. A. C. Coolen	**(Solvay Duphar)**

Omslagontwerp: **M. F. Huls**

ISBN 90-9009555-1

Dankwoord

Na vier jaar promotieonderzoek krijg ik het gevoel iets van Einsteins relativiteitstheorie te begrijpen. Aan de ene kant vlogen deze vier jaar voorbij en aan de andere kant maakt het dat ik na deze periode ongeveer een derde van mijn leven op de universiteit rondloop. Kortom, tijd is relatief. De basis van deze relativiteit ligt bij het feit dat veel mensen er voor gezorgd hebben dat deze periode van mijn leven een hele aangename was. Deze mensen wil ik graag bedanken! Veel mensen zijn ook betrokken geweest bij de totstandkoming van dit proefschrift. Ook deze mensen wil ik graag bedanken.
Prof. Dr. Roeland Nolte wil ik bedanken voor zijn enthousiaste en stimulerende stijl van begeleiden en het vertrouwen, de mogelijkheden en de vrijheden die hij mij heeft gegeven. Met Dr. Alan Rowan heb ik prettig samengewerkt en ik ben hem zeer erkentelijk voor het kritisch doorlezen van het manuscript.
Ik wil alle studenten (Reek & Zonen B.V.) die een bijdrage hebben geleverd aan dit proefschrift bedanken voor de symbiotische manier van samenwerken, die mij in elk geval erg goed bevallen is. Alex, jij was degene die de minste begeleiding nodig had, maar ik ben er nog niet helemaal achter of dat door jouw persoonlijkheid of door jouw werktijden kwam. Hans, ik heb veel waardering voor het werk dat jij gedaan hebt, maar ik moet jou helaas toch, bij deze, iedere tweede donderdag van de maand "de nutsenman" maken. Alexander, nu werk je alleen in de zuurkast en het is nog steeds een rommeltje. Ik denk dat al die kolven met meuk, waar geen naam op stond, toch van jou afkomstig waren. Jeroen, het feit dat de rest van de groep ons altijd als twee broertjes zag, zegt mij genoeg. ls *hanse* | grep computer > handig scripts. Hans, hiermee geef ik aan dat de handige tips die met unix te maken hadden en jouw hulp bij het "ontplakbandiseren" van de plaatjes het leven een stuk aangenamer maakte. Timo, fruithapje??? Frank, je werkte niet voor mij, maar je wilde toch graag verbindingen voor mij maken. Helaas heb ik te weinig tijd gehad om daar nog iets moois mee te doen.
Collega's zijn erg belangrijk geweest omdat ze mede de sfeer bepalen en behulpzaam waren in het onderzoek en zo een wetenschappelijke bijdrage hebben geleverd. Appie, bij jou heb ik een echt "samen uit samen thuis" gevoel, omdat we alle stadia in de promotie tegelijk doorliepen. Hanny en Nico, mag ik jullie nog eens uit bed bellen op een zondag om 15.00 uur om een motor aan te duwen? Bertje, Gerben, Alan, Fokke, Hein, Patricia, Rudi, Stan, René, Gino, Hans, Hans, Alexander en Peter zijn alle collega's in en rond practicumzaal VII, die ik samen met de collega's van de derde en vierde verdieping graag voor vier mooie jaren wil bedanken. Hans Adams, jouw bijdrage aan de goede sfeer wil ik ook zeker even noemen.
Omdat mijn handen iets te groot zijn voor de handschoenen van de "glove box" van de CV apparatuur heb ik de handen van andere mensen tijdelijk moeten lenen. Annie, Bert en Stevie (ja, alles staat op flop onder de juiste naam) zijn mij te hulp geschoten om dit probleem op te lossen. Martin Feiters bedank ik voor de EPR metingen die hij heeft uitgevoerd, Huub Geurts voor de hulp bij de

elektronenmicroscopie en Nico voor het uitvoeren van de poederdiffractie-experimenten.
Helene Amatdjais, Peter van Galen, Pieter van der Meer, Wim van Luyn, Ad Swolfs en Chris Kroon gaven goede analytische en technische ondersteuning. Bij Sandra Tijdink kon ik altijd terecht voor administratieve en logistieke zaken. Ook de mensen die klaar stonden bij de NMR apparatuur, met name Jos Joordens, Gerda Nachtegaal en Paul Schlebos, ben ik zeer erkentelijk. De mensen van het CAOS-CAMM centrum en met name Hilbert Bruins Slot en Hens Borkent, wil ik bedanken voor de hulp bij het gebruik maken van de computer faciliteiten en Roel Fokkens voor de hoge resolutie massabepalingen die hij heeft gedaan.
Prof. P.T. Beurskens en zijn medewerkers van de afdeling Kristallografie en met name René de Gelder bedank ik voor het oplossen van de kristalstructuren. Dr. Peter Grootenhuis en Dr. V.J. van Geerestein van de CMC afdeling van Organon te Oss, hebben mij thuisgebracht in de wereld van de modelling. Met Bert Lutz en Prof. Dr. J.H. van der Maas heb ik een prettige samenwerking gehad op het gebied van de IR-metingen.
I want to thank Prof. M.J. Crossley for providing some porphyrin compounds, which were used for the synthesis of the nice porphyrin clips described in Chapter 7.
I appreciate the hospitality of Prof. Dr. J.-P. Sauvage during my stay in Strassbourg and I want to thank him for giving me the opportunity to visit his laboratory.
Ik wil graag twee mensen uit groep van Prof. de Schryver in Leuven, namelijk Steven en Frank, bedanken voor de metingen die daar zijn uitgevoerd. Steven, het spijt me dat ik door mijn enthousiasme jouw nachtrust heb verstoord.
Prof. Dr. P.W.N.M. van Leeuwen, Dr. P.C.J. Kamer en Dr. P. Wehman hebben geholpen bij de katalytische experimenten onder hoge druk, die in Amsterdam op een veilige manier zijn uitgevoerd.
Buiten de Chemie wil ik een aantal mensen noemen, die een indirecte maar toch een belangrijke rol gespeeld hebben. Ten eerste zijn dat mijn ouders, die mij de mogelijkheid gaven om te doen wat ik wilde doen en altijd achter mijn beslissingen stonden. Joep en Stephan bedank ik voor de begeleiding bij de "culturele" ontspanning. De mannen van het Heren 1 team van AquaNovio94 schepten iedere week weer de mogelijkheid tot afreageren tijdens het gezamenlijk opgevoerde "waterballet".
Mariëlle, jouw begrip en steun en überhaupt jouw aanwezigheid hebben ervoor gezorgd dat de spreekwoordelijke laatste loodjes uiteindelijk toch niet zo zwaar waren.

Contents

Chapter 1

General Introduction

1.1 INTRODUCTION

The design and construction of novel molecules which interact with other molecules via non-covalent interactions to form complexes is recognized as a new area in organic chemistry. It was opened in 1967, when Pedersen[1] discovered the ability of crown ether compounds to complex alkali and alkaline earth metal ions. Shortly thereafter Lehn[2] and Cram[3] developed more complicated receptors for alkali metal ions, which were termed cryptands and spherands. This new research area, currently referred to as "supramolecular chemistry", has grown rapidly and resulted in many new compounds and complexes 'glued' together by relatively weak interactions. These weak interactions are generally hydrophobic (solvophobic) interactions, hydrogen bonding, electrostatic and Van der Waals interactions, and π-π stacking interactions. The design of many of these compounds is often inspired by nature, where these weak interactions play an important role. Many process in biological systems are based on the association of molecules, forming complexes and larger aggregates, e.g. enzyme-substrate complexes[4] and DNA-protein complexes.[5] The major goals in supramolecular chemistry to date have been the syntheses of systems which model natural complexes, these being the development of enzyme mimics and the construction of large assemblies of molecules. In the former case substrate selectively, regio and stereo selectivity, and reaction enhancement are the prime enzyme properties which it is hoped supramolecular systems can mimic. The construction of large molecular assemblies is a more recent exciting development and is expected to generate new materials with novel properties.[6]

In our laboratory the design of receptor molecules for aromatic guests, based on the concave building block diphenylglycoluril (**1**) is under investigation. Functionalization of this building block with aromatic side-walls gives clip-shaped molecules (**2**) which are capable of binding dihydroxybenzenes by means of hydrogen bonding and π-π stacking interactions.[7] Using 2,7-dimethoxynaphthalene rings as side-

walls, a receptor molecule (**3**) was synthesized in which the clip-shaped cavity was induced by the binding of an electron poor aromatic guest, e.g. dinitrobenzene.[8] Functionalization of the side-walls with long 'tails' resulted in molecular assemblies with tunable thermotropic and lyotropic liquid-crystalline behaviour.[9]

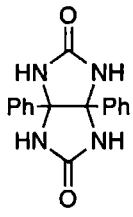

1

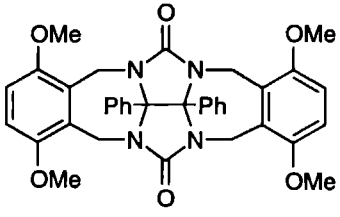

2

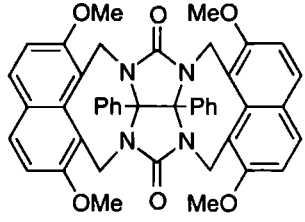

3

Clip molecule **2** has been functionalized with catalytic sites incorporated in the side-wall, in order to position a binding site nearby a catalytically active site (**4**).[10] These functionalized molecules were designed to be enzyme mimics, however, studies revealed that the binding site is no longer accessible to guest molecules when the clip was functionalized.

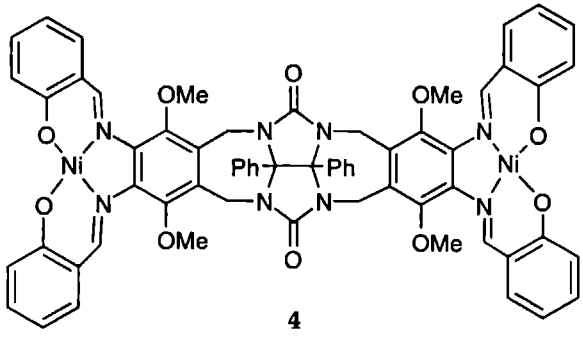

4

The work described in this thesis, involves the design and modification of molecular clips based on diphenylglycoluril, in order to combine the binding site with an active function. In Chapter 2, the syntheses of novel clip-shaped molecules having only one side-wall or different side-walls is described. This resulted in molecules which have only one catalytically active center incorporated in one side-wall nearby the cleft-shaped binding site. In Chapter 3 a detailed binding study of dihydroxybenzenes in clip-shaped molecules is presented. The thorough study of the binding properties of these molecules enabled the separate contributions of the interactions involved in the complex formation to be analyzed. The newly synthesized clip molecules were used to study the conformational and binding behaviour of clip molecules with naphthalene side-walls, which is presented in Chapter 4. These receptor molecules were found to be

able to complex Ag^+ by an induced fit mechanism. In the course of these investigations it was discovered that some clip molecules dimerize in solution and in the solid state. The origin of the dimerization process is discussed in Chapter 5, and it will be shown that a detailed understanding of this process can be useful in the construction of novel organic structures in the solid state. In Chapter 6 clip molecules with water soluble groups attached to the diphenylglycoluril framework, are presented. It appears that the dimerization of these clip molecules in aqueous solution is hydrophobically driven, resulting in the formation of large aggregates of well-defined shape and size, which are tunable by the addition of guest molecules. Clip-shaped molecules which are functionalized with porphyrin containing side-walls are discussed in Chapter 7. These functionalized receptors were designed in order to study the influence of an aromatic guest bound between a donor side-wall (Zn-porphyrin) and an acceptor side-wall (benzoquinone), on the electron transfer behaviour of the system. In the last chapter initial studies for the application of the functionalized clips as supramolecular catalysts will be presented and discussed.

1 2 LITERATURE SURVEY

The aim of this survey is to give an impression of the recent developments in certain specific areas of supramolecular chemistry rather than a detailed overview which covers all aspects of supramolecular chemistry This survey will be concerned mainly with the topics presented in this thesis, *i e* host-guest chemistry, supramolecular architectures, supramolecular photochemistry, and supramolecular catalysis

1.2.1 Host-guest chemistry[11]

Host-guest chemistry involves the binding of a substrate molecule (guest) in a receptor molecule (host) The process of molecular recognition between two species, is based on steric and interactional complementarity Several types of interactions can be involved in the latter A combination of more than one interaction will generally lead to more selective and stronger binding of the substrate in the receptor The first and simplest receptor synthesized was a crown ether, which was capable of binding ions using only ion-dipole interactions [1] Other receptor molecules which are able to complex ions are the slightly more complicated cryptands,[2] spherands,[3] and cyclophanes [12] The binding of non-charged guest molecules, however, necessitated the design of receptor molecules with binding abilities based on other non-covalent interactions Cyclodextrins[13] and some functionalized cyclophanes[14] (Figure 1) are able to bind aromatic guests in aqueous solution using predominantly hydrophobic interactions This hydrophobic effect enables very high binding constants to be achieved, e g as high as $10^5\ M^{-1}$ for guest molecules bound in a cyclodextrin dimer,[15] but with relatively low guest selectivity

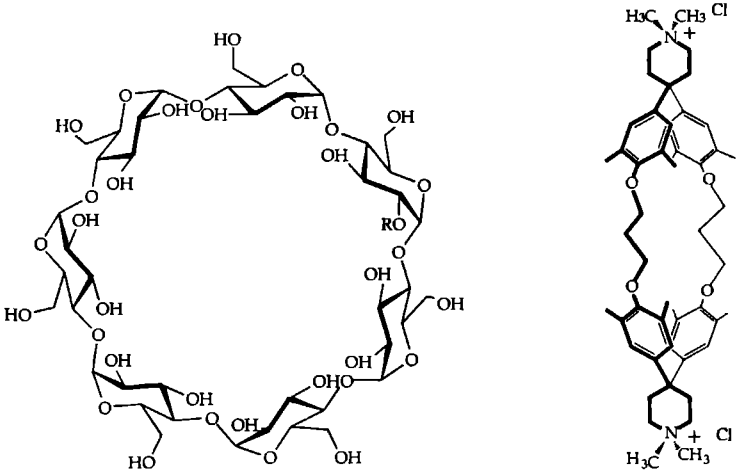

Figure 1 *The structure of a cyclodextrin (left) and a cyclophane receptor molecule (right)*

The strong binding of quaternary ammonium compounds in cyclophanes, which are constructed from benzene rings (Figure 1), indicate that cation-π interactions can also contribute significantly to binding.[16] This interaction has been reported for several other receptor systems[17] and it was proposed recently that this interaction is an attractive electrostatic interaction involving the cation and the quadropole moment of the aromatic ring.[18] It has been postulated[18] that these interactions also play an important role in the binding of cationic substrates in proteins, since the cation-π interaction can compete with the aqueous solvation of the cation.

It is considerably more difficult to obtain strong binding in organic solvents, since the hydrophobic effect is not present. Many examples have appeared in the literature where complex formation is based on hydrogen bonding.[19] Rebek *et al.*,[20] for example, have used Kemp's triacid to design receptor molecules, capable of binding amino acids, heterocyclic amines and diketopiperazines. In related work, it was shown that the binding of 9-ethyladenine to receptor molecules based on this triacid is enhanced when additional π-π interactions are involved.[21] A larger binding energy of approximately 0.4 kcal/mol per benzene ring was obtained upon increasing the stacking surfaces (see Figure 2).

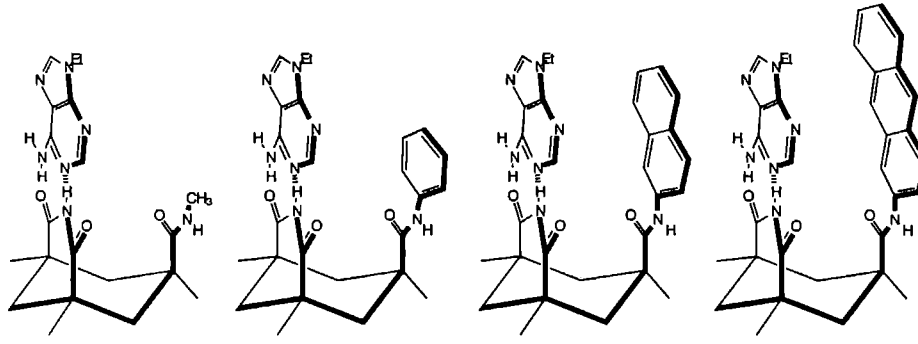

ΔG = -2.1 kcal ΔG = -2.5 kcal ΔG = -2.9 kcal ΔG = -3.4 kcal

Figure 2: *The binding of 9-ethyladenine is stepwise increased when the π-π stacking surface of the receptor is enlarged.*

Cleft-shaped and tweezer-like molecules are obtained when two aromatic surfaces are used to increase stacking interactions between host and guest. The cleft-shaped molecule synthesized by Harmata *et al.*[22] was found to form complexes with trinitrobenzene in the solid state (Figure 3a). The molecular tweezer of Zimmerman,[23] which was studied in detail, was capable of binding 2,4,5,7-tetranitrofluorenone in chloroform. Comparison of the binding properties of this tweezer with a similar receptor but with only one aromatic π-surface (Figure 3c), showed that the addition of a second π-stacking interaction enhanced the binding to a greater extent than would be

expected assuming a simple additivity effect. This large increase in binding energies was attributed to favourable entropy effects.

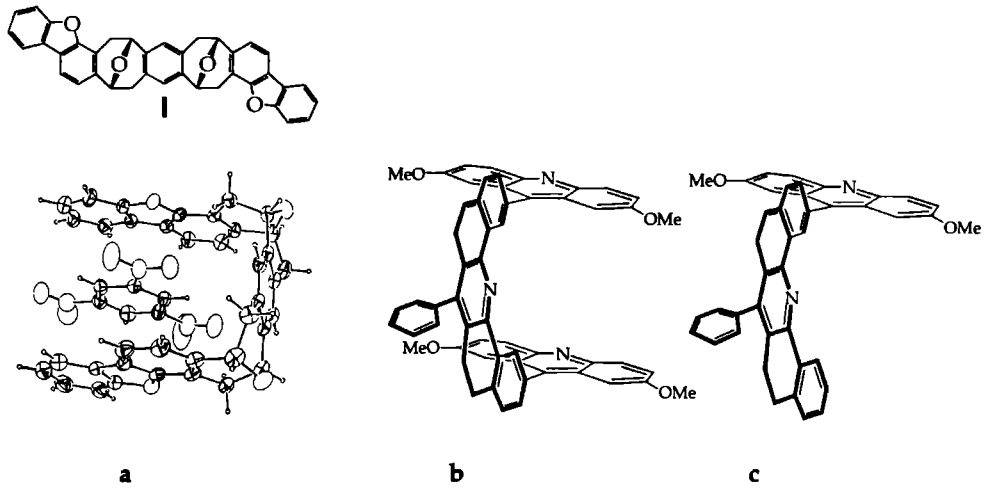

Figure 3: *The cleft shape receptor molecule of Harmata (a) and the molecular tweezers of Zimmerman (b and c).*

Whitlock *et al.*[24] have designed a series of receptors with concave binding sites which form complexes with nitrophenols in chloroform (Figure 4a). A study of the effect of size of the cavity on the supramolecular stability of the complex revealed that very high binding constants (K_a = 420,000 M^{-1} in $CDCl_3$) can be achieved, by the fine tuning of the cavity size.[25] This high binding capacity was attributed to a combination of a solvation effect (K_a = 26,000 M^{-1} in CD_2Cl_2) and the 'snugness' of fit. The latter effect being a result of maximized Van der Waals contacts. This 'snugness of fit' was also observed by Collet[26] and Cram,[27] who both synthesized a series of rigid cavity-containing compounds (Figure 4b). Collet *et al.*[26] connected two cyclotriveratrylenes to

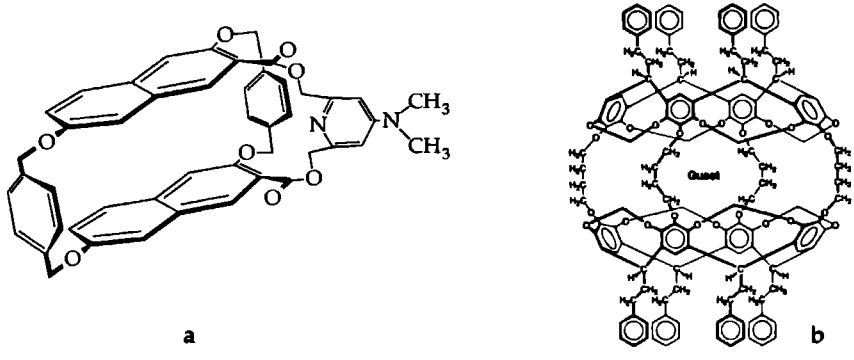

Figure 4: *The host molecule of Whitlock (a) and the carcerand of Cram (b).*

form a 'cryptophane', which was able to complex tetrahedral guest molecules, *i.e.* chloroform and tetramethylammonium ions. The 'carcerand' molecules of Cram have a very large cavity, which is able to stabilize photochemically unstable cyclobutadienes by supramolecular complexation.

1.2.2 Large supramolecular architectures[28]

In the above mentioned host-guest systems, it is clear that 1:1 complexes between a host and a guest are formed predominantly when the two components have both shape complementarity and directed attractive forces. Larger complexes can be formed, when molecules have several sites which can interact favourably with other molecules. The assembly of complementary building blocks can lead to organized systems with nanomeric dimensions. This process of self-assembly occurs frequently in nature and is used to form large functional macromolecular complexes such as DNA and DNA-protein complexes. A detailed knowledge of intermolecular forces is needed, in order to use this self-assembly principle to construct nano-structures with a certain function. In general most examples in the literature of such systems make use of hydrogen bonding interactions between the different building blocks.

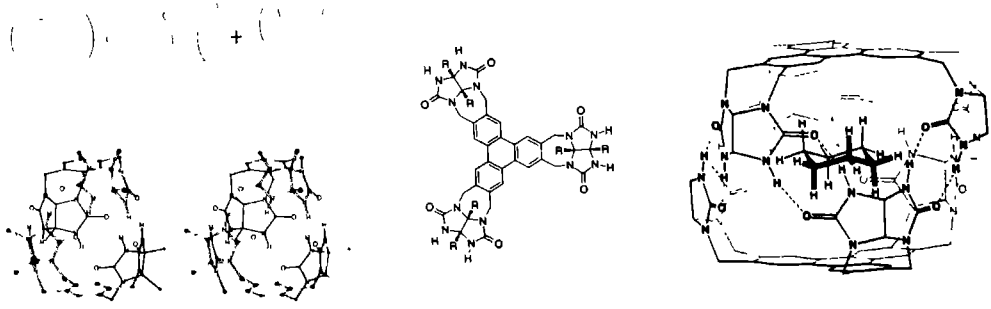

Figure 5: *Self-assembled host molecules which are able to bind guests.*

Rebek *et al.*[29] recently synthesized a receptor molecule based on diphenylglycoluril, which forms very strong tennis ball-shaped dimers. These 'tennis balls' consist of two concave units which assemble using hydrogen bonding. When the units of the dimer are enlarged it is possible to encapsulate benzene and cyclohexane guest molecules within the assembled host (Figure 5).[30] In the case of the dimer formed from monomeric building blocks consisting of three glycoluril units, the complex is formed via 12 hydrogen bonds.[31] The exchange between the free and the bound guest molecules appeared to be very slow (timescale of hours).

Whitesides et al.[32] have used melamine and cyanuric acid as complementary building blocks to construct "crinkled tapes" and so-called "Rosettes" and connected "Rosettes" (Figure 6). It was possible to construct larger assemblies, with a defined structure, by rational design. Menger *et al.*[33] have shown that very long and stable fibers, up to several centimeters in length, can be constructed using simple building blocks (Figure 7a). These fibers are thought to be built up from the self-assembly of many disk-shaped momers which are stacked on top of each other. Ghadiri *et al.*[34] have used cyclic peptides which stack via hydrogen bonding as building blocks, to form long nanotubes. These tubes which are hollow and have an internal diameter of 7-8 Å are almost micrometers in length, and are expected to have a variety of applications in the fields of chemistry, biochemistry and materials science.

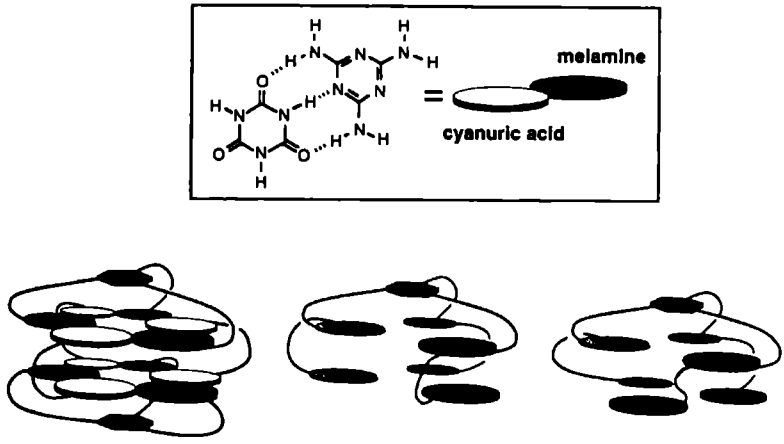

Figure 6: *Self-assembly based on complementary hydrogen bonding between melamine and cyanuric acid.*

The examples given so far are all based on self-assembly using hydrogen bonds. Stoddart *et al.* [35] have constructed numerous catenanes and rotaxanes with a high degree of control over the formed structures (Figure 8a), using π-π interactions. The formation of these assemblies is based on the favourable interaction between electro-deficient and electron-rich aromatic rings. These interactions have also been used by Otsuki *et al.*, to form pre-organized donor-acceptor units which crystallize into organic superstructures (Figure 8b).[36]

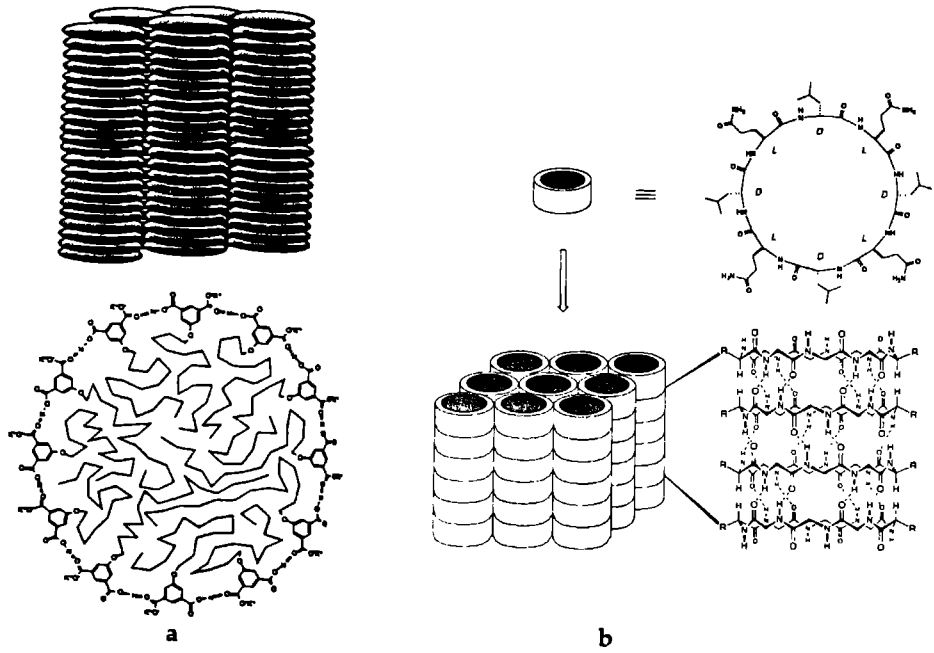

a b

Figure 7: *Long fibers formed by the monopotassium salt of 5-(hexadecyloxy)-isophthalic acid (a), and hollow tubular structures formed by cyclic peptides (b).*

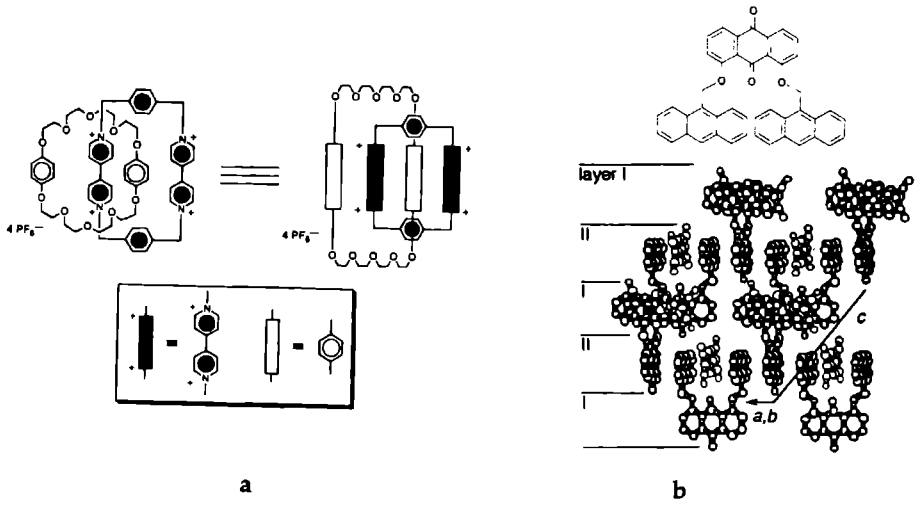

a b

Figure 8: *A typical catenane designed by Stoddart et al. (a), and a superstructure based on a pre-organized donor-acceptor unit (b).*

1.2.3 Supramolecular photochemistry[37,41]

Attempts to understand the mechanism of the highly complicated photosynthetic reaction centers has been a challenge for many years. A fast electron transfer over a long distance combined with a long lived charged separated state, are the key features

of the working mechanism of these reaction centers. The structure of the reaction centers of the purple photosynthetic bacteria *Rhodopseudomonas viridis*[38] and *Rhodobacter sphaeroides*.[39] have been elucidated and, in combination with spectroscopic[40] studies, has given a detailed insight into the mechanism of charge separation within these systems. The initial charge separation occurs at the so-called special pair, which consists of two covalently linked bacteriochlorophylls (see Figure

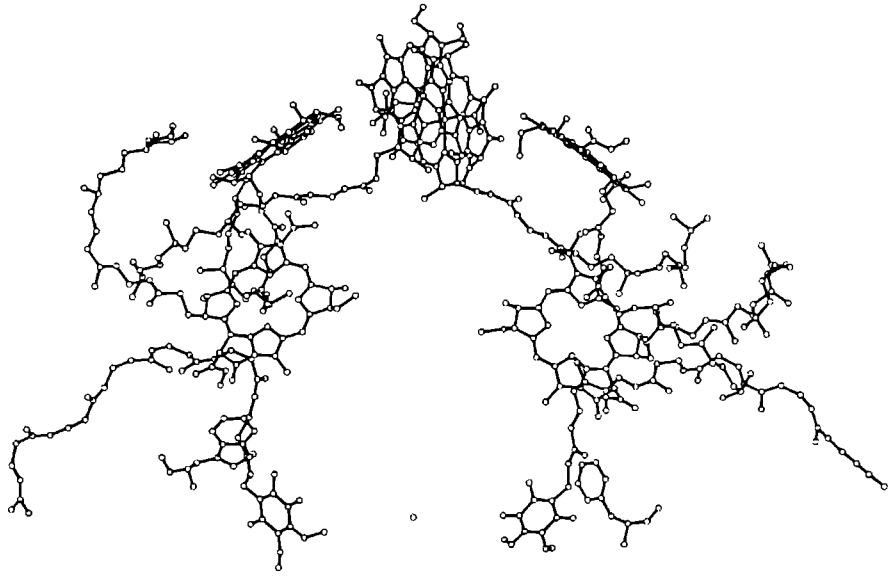

Figure 9: *The chromophores which are responsible for the electron transfer in the photosynthetic reaction center of Rhodopseudomonas viridis.*

9). An electron is then transferred very rapidly (± 3 ps) to the bacteriopheophytin and then to the quinone unit in approximately 200 ps. The charge recombination processes are relatively slow. A series of covalently linked porphyrin-quinone systems has been synthesized in order to mimic this electron transfer step from the bacteriopheophytin to the quinone.[41] Dervan *et al.* have performed a detailed study in order to get an insight into the variables influencing the electron transfer such as exothermicity and distance between the donor and the acceptor (Figure 10a).[42] Recently, some examples have been reported in which several covalently linked chromophores were studied in order to mimic multi-step electron transfer processes.[43] An example of a triad system synthesized by Wasielewski *et al.*,[43a] which displays a very fast photoinduced electron transfer, is shown in Figure 10b.

The supramolecular approach has been recognized recently as a very useful tool for the design of multichromophoric mimics. Examples using this approach are the

assembled bis(porphyrin)-stoppered rotaxane,[44] and the mixed porphyrin-ruthenium complexes[45] developed by Sauvage *et al.* (Figure 11). The former shows very fast photo-induced electron transfer between a zinc porphyrin and a gold porphyrin unit, due to mediation by the copper complex.

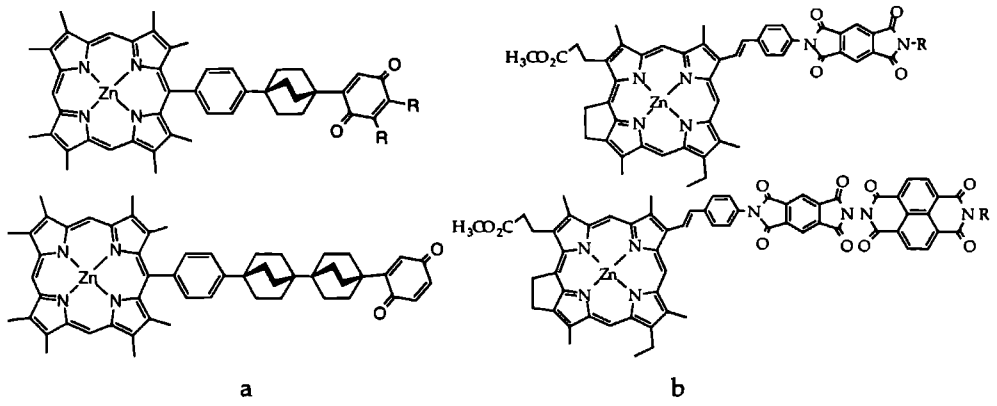

Figure 10: *The series of covalently linked porphyrin-quinone systems of Dervan et al. (a), and the coupled chromophores synthesized by Wasielewski et al. (b).*

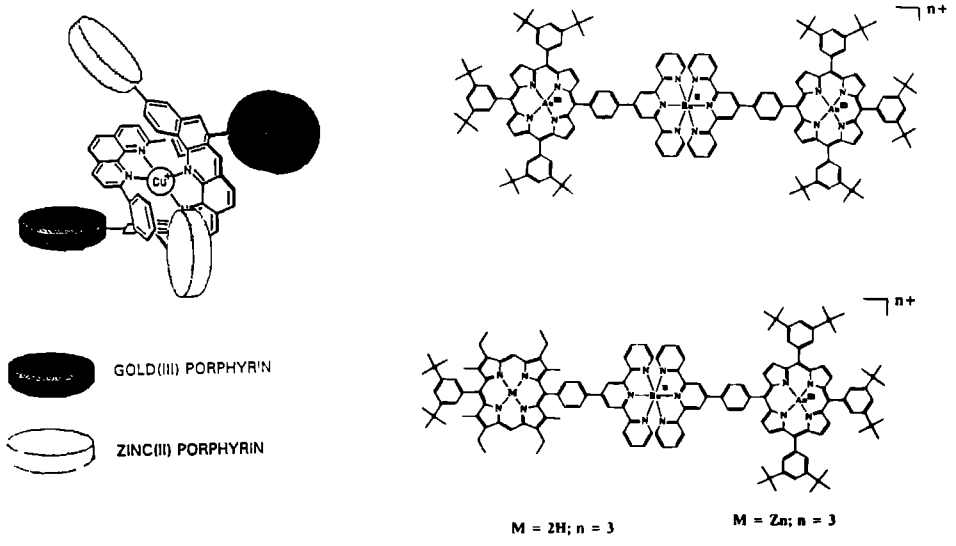

Figure 11: *Assembly of chromophores using ligand to metal interactions developed by Sauvage et al..*

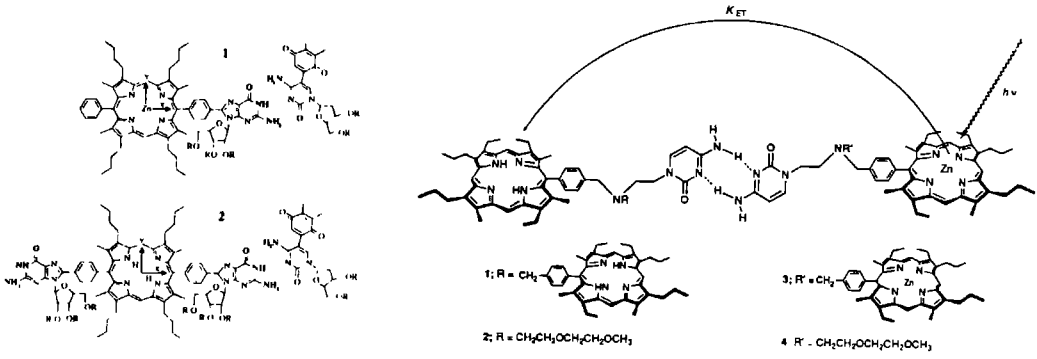

Figure 12. *Assemblies of chromophores based on hydrogen bonding showing photoinduced electron transfer and energy transfer behaviour.*

Sessler *et al.* have functionalized porphyrin molecules with nucleobases in order to assemble the chromophoric units by means of molecular recognition using hydrogen bonding.[46] These associated porphyrins showed an efficient photo-induced energy transfer over a center-to-center distance of 22.5 Å (Figure 12). Using the same type of approach it was shown that it is possible to achieve photo-induced electron transfer between an assembled complex of a zinc porphyrin donor and a quinone acceptor.[47]

The advantage of supramolecular chemistry in this field is that complex multi-chromophoric structures can be designed and constructed relatively easily. These systems are expected to aid in the understanding of multi-step electron transfer processes.

1.2.4 Supramolecular catalysis[48]

The combination of supramolecular chemistry and catalysis is a relatively new and exciting area. Addition of the aspect of molecular recognition to a synthetic catalyst is expected to lead to enhanced selectivity and increased efficiency. Such supramolecular systems are based upon the same principles as natural enzymes, these being the complexation of a substrate via non-covalent interactions in a binding pocket which is nearto an active site. Towards the goal of supramolecular catalysis several approaches have been used. Sanders *et al.*[49] have synthesized trimeric porphyrin host molecules, which are able to bind guests using ligand-to-metal interactions. These host molecules induce an exo-selectivity between the bound substrates in a Diels Alder reaction. For an acyl transfer reaction an efficient catalytic turnover without product inhibition was observed (Figure 13a).[50] The porphyrin units in this system are used to create a binding

site and are not used as catalytically active centers. The host system behaves as a frame upon which catalysis can occur.

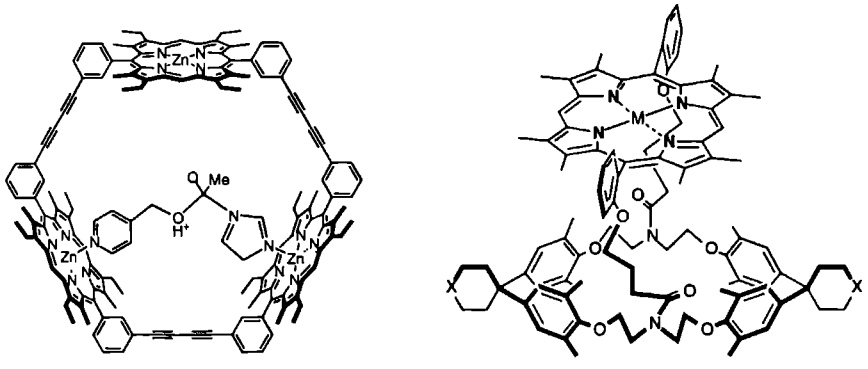

a b

Figure 13: *Reaction intermediate in an acyl transfer reaction catalysed by a trimeric porphyrin host (a), and a synthetic model of Cytochrome P-450 in which a porphyrin unit is connected to a cyclophane binding site (b).*

A different approach has been used by Diederich *et al.*,[51] who connected an iron porphyrin which is the catalytically active group to a cyclophane binding site. Small catalytic turn overs were found for the conversion of acenaphtene to acenaphtenone in the presence of an oxidant. A similar stragegy was used in systems in which a porphyrin molecule is connected to either one or two cyclodextrin units.[52] These supramolecular models are better catalysts for the epoxidation of alkenes which are bound in the hydrophobic cavity of the cyclodextrin, than a comparable catalyst without the cyclodextrin.

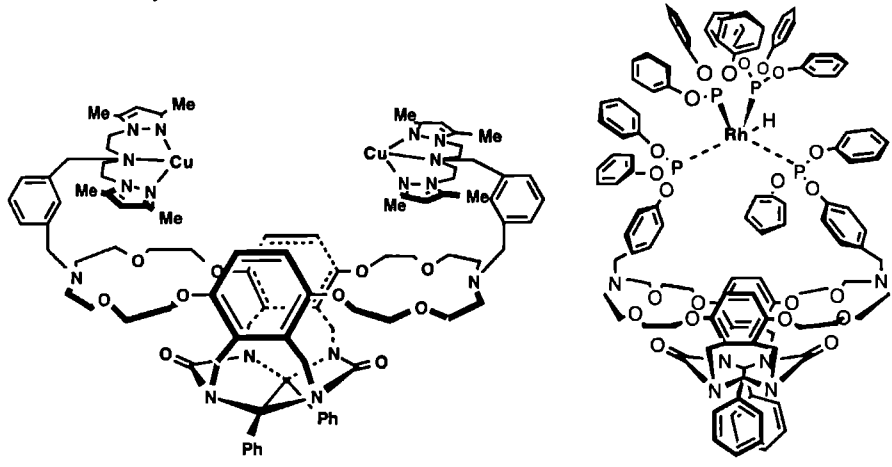

Figure 14: *Supramolecular catalysts with a binding site based on the diphenylglycoluril building block.*

Other examples of supramolecular catalyst based on active centers connected to a binding site have been developed by Nolte *et al.* (Figure 14). A basket-shaped receptor molecule was functionalized with a dicopper(II) pyrazole complex[53] and it was shown that this metallohost is able to oxidize benzylic alcohols in a stochiometric reaction. The substrate molecules which were complexed in the binding site reacted approximately $5*10^4$ times faster than those which were not bound. A similar system with a rhodium catalytic center connected to the same basket-shaped molecule was constructed.[54] This supramolecular catalyst, which is active in hydrogenation reactions, was shown to mimic properties of enzymes such as Michaelis Menten kinetics, substrate selectivity, reaction inhibition and rate enhancement by binding of cosubstrates or cofactors.

A final example of a supramolecular catalyst is that developed in the group of Corey.[55] An osmium catalyst for the enantioselective dihydroxylation of allylic alcohol substrates was designed. Although the term supramolecular catalyst was not mentioned, the approach used was to sandwich the substrate between the two aromatic surfaces of the ligand. Very high *ee* values were achieved using the catalyst. This example suggests that the conventional catalysts are now becoming similar to the supramolecular catalysts, since they are using the same principles as those of host-guest chemistry.

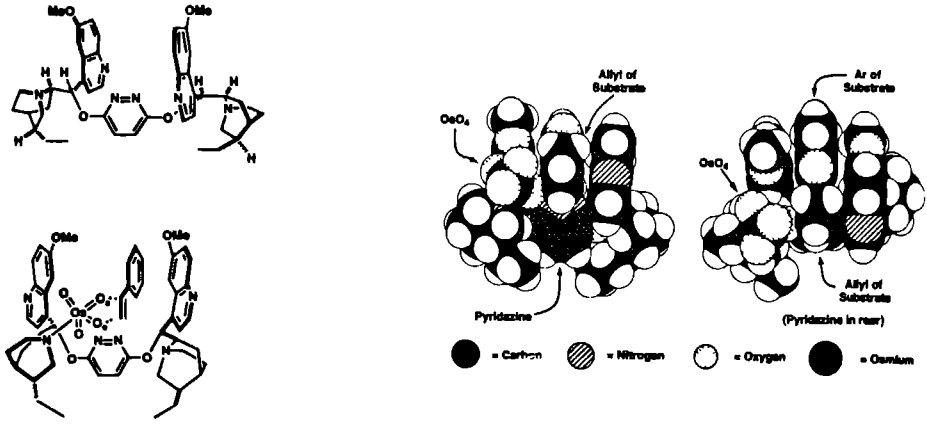

Figure 15: *A cleft shaped ligand with a catalytic site, and the calculated proposed complex.*

References

1 Pedersen, C. J. *J. Am. Chem. Soc.* **1967**, *89*, 2495 and 7017.

2 (a) Lehn, J.-M. *Angew. Chem.* **1988**, *100*, 91. (b) Dietrich, B.; Lehn, J.-M.; Sauvage, J.-P. *Tedrahedron Let.* **1969**, 2885 and 2889.

3 (a) Cram, D.J. *Angew. Chem.* **1988**, *100*, 1041. (b) Cram, D.J. *Science*, **1974**, *183*, 803, and references cited theirein.

4 Fresht, A. "*Enzyme structure and mechanism*", 2nd ed. **1985**, W. H. Freeman & Company, New York.

5 Stryer, L., "*Biochemistry*", 3rd. ed. **1988**, Freeman, New York.

6 (a) Service, R.F. *Science*, **1994**, *265*, 316. (b) Whitesides, G.M.; Mathias, J.P.; Seto, C.T. *Science*, **1991**, *254*, 1312. (c) Mann, S. *Nature* **1993**, *365*, 499.

7 Sijbesma, R. P.; Kentgens, A. P. M.; Lutz, E. T. G.; Van der Maas, J. H.; Nolte, R. J. M. *J. Am. Chem. Soc.* **1993**, *115*, 8999.

8 Sijbesma, R. P.; Wijmenga, S. S.; Nolte, R. J. M. *J. Am. Chem. Soc.* **1992**, *114*, 9807-9813.

9 van Nunen, J. L. M.; Stevens, R. S. A.; Picken, S. J.; Nolte, R. J. M. *J. Am. Chem. Soc.* **1994**, *116*, 8825.

10 Gosling, P. A.; Sijbesma, R. P.; Spek, A. L.; Nolte, R. J. M. *Recl. Trav. Chim. Pays-Bas* **1993**, *112*, 404.

11 Recent reviews: (a) Cram, D. J. *Top. Curr. Chem.* **1981**, *98*, 43. (b) Schneider, H-J.; *Angew. Chem.* **1991**, *103*, 1419. (c) Diederich, F. *Angew. Chem.* **1988**, *100*, 372. (d) Seel, C.; Vögtle, F. *Angew. Chem.* **1992**, *104*, 542. (d) Izatt, *Chem. Rev.* **1995**, *95*, and references cited therein (e) Izatt, R. M.; Bradshaw, J. S.; Pawlak, K.; Bruening, R. L.; Tarbet, B. *J. Chem. Rev.* **1992**, *92*, 1261, and references cited therein (f) Various authors in *Tetrahedron*, **1995**, *51*, vol. 2, topic molecular recognition. (g) Cram, D. J. *Nature* **1992**, *356*, 29. (h) Zimmerman, S. C. "*Bioorganic Chemistry Frontiers 2*", **1991**, Springer-Verlag Berlin heidelberg, 33. (i) Hamilton, A. D. "*Bioorganic Chemistry Frontiers 2*", **1991**, Springer-Verlag Berlin heidelberg, 115.

12 Diederich, F. "*Cyclophanes;*" Royal Society of Chemistry; Cambridge, **1991**.

13 (a) Bender, M.L.; Komiyama, M. "*Cyclodextrin Chemistry;*" Springer; Berlin, **1978**. (b) Cramer, F. "*Einschlußverbindungen,*" Springer, Berlin, **1954**.

14 (a) Benson, D. R., Valentekovich, R.; Diederich, F. *Angew. Chem.* **1990**, *102*, 213.; (b) Benson, D. R., Valentekovich, R.; Knobler, C.B.; Diederich, F. *Tetrahedron* **1991**, *47*, 2401. (c) Ferguson, S. B.; Diederich, F. *Angew. Chem.* **1986**, *98*, 1127.

15 Venema, F. Thesis, **1996**, Nijmegen.

16 Shepodd, T. J.; Petti, M. A.; Dougherty, D. A. *J. Am. Chem. Soc.* **1986**,*108*, 6085.

17 (a) Kearney, P. C. *et al., J. Am. Chem. Soc.* **1993**, *115*, 9907. and references therein (b) Dougherty, D. A. "*Comprehensive Supramolecular Chemistry*", **1995**, Vol 10,

Lehn, J. M. ed. (c) Garel, L.; Lozach, B.; Dutasta, J.-P.; Collet, A. *J. Am. Chem. Soc.* **1993**, *115*, 11652.

18 Dougherty, D. A. *Science*, **1996**, *271*, 163.

19 a) Conn, M. M.; Deslongchamps, G.; de Mendoza, J.; Rebek, Jr., J. *J. Am. Chem. Soc.* **1993**, *115*, 3548. (b) Blake, J. F.; Jorgensen, W. L. *J. Am. Chem. Soc.* **1990**, *112*, 7269. (c) Hamilton, A. D.; Little, D. *J. Chem. Soc., Chem. Commun.* **1990**, 297. (d) Goswami, S.; Hamilton, A. D. *J. Am. Chem. Soc.* **1989**, *111*, 3425. (e) Chang, S.-K.; Van Engen, D.; Fan, E.; Hamilton, A. D. *J. Am. Chem. Soc.* **1991**, *113*, 7640. (f) Fan, E.; Van Arman, S. A.; Kincaid, S.; Hamilton, A. D. *J. Am. Chem. Soc.* **1993**, *115*, 369. (g) Hayashi, T.; Miyahara, T.; Hashizume, N.; Ogoshi, H. *J. Am. Chem. Soc.* **1993**, *115*, 2049. (h) Murray, T. J.; Zimmerman, S. C. *J. Am. Chem. Soc.* **1992**, *114*, 4010. (i) Bell, T. W.; Liu, J. *J. Am. Chem. Soc.* **1988**, *110*, 3673. (j) Adrian, Jr., J. C.; Wilcox, C. S. *J. Am. Chem. Soc.* **1991**, *113*, 678. (k) Kelly-Rowley, A. M.; Cabell, L. A.; Anslyn, E. V. *J. Am. Chem. Soc.* **1991**, *113*, 9687.

20 (a) Rebek, J., Jr.; Nemeth, D. *J. Am. Chem. Soc.* **1985**, *107*, 6738. (b) Rebek, J., Jr.; Askew, B.; Nemeth, D.; Parris, K. *J. Am. Chem. Soc.* **1987**, *109*, 2432. (c) Rebek, J., Jr.; Askew, B.; Killoran, M.; Nemeth, D.; Lin, F.-T. *J. Am. Chem. Soc.* **1987**, *109*, 2426. (d) Jeong, K.-S.; Muehldoef, A. V.; Rebek, J., Jr. *J. Am. Chem. Soc.* **1990**, *112*, 6144.

21 (a) Askew, B.; Ballester, P.; Buhr, C.; Jeong, K.-S.; Jones, S.; Parris, K.; Williams, K.; Rebek, J., Jr.*J. Am. Chem. Soc.* **1989**, *111*. 1082. (b) Williams, K.; Askew, B.; Ballester, P.; Buhr, C.; Jeong, K.-S.; Jones, S.; Rebek, J., Jr.*J. Am. Chem. Soc.* **1989**, *111*, 1090.

22 (a) Haramata, M.; Barnes, C. L. *J. Am. Chem. Soc.* **1990**, *112*, 5655. (b) Haramata, M.; Barnes, C. L.; Rao Karra, S.; Elahmad, S. *J. Am. Chem. Soc.* **1994**, *116*, 8392.

23 (a) Zimmerman, S.C. Bioorganic Chemistry Fontriers 2, **1991**, Springer-Verlag, Berlin. 33-74 and references cited therein (b) Zimmerman, S. C.; Vanzyl, C. M. *J. Am. Chem. Soc.* **1987**, *109*, 7894. (c) Zimmerman, S. C.; Vanzyl, C. M.; Hamilton, G. S.*J. Am. Chem. Soc.* **1989**, *111*, 1373.

24 Whitlock B. J.; Whitlock, H. W. *J. Am. Chem. Soc.* **1990**, *112*, 3910-3915.

25 Whitlock B. J.; Whitlock, H. W. *J. Am. Chem. Soc.* **1994**, *116*, 2301-2311.

26 (a) Canceill, J.; Lacombe, L.; Collet, A. *J. Am. Chem. Soc.* **1986**, *108*, 4230. (b) Canceill, J.; Cesario, M.; Collet, A.; Guilhem, J.; Lacombe, L.; Lozach, B.; Pascard, C. *Angew. Chem.* **1989**, *101*, 1249.

27 Cram, D. J. *Angew. Chem., Int. Ed. Engl.* **1986**, *25*, 1039.

28 For recent reviews see: (a) Lawrence, D. S.; Jiang, T.; Levette, M. *Chem. Rev.* **1995**, *95*, 2229-2260. (b) Bernstein, J.; Davis, R. E.; Shimoni, L.; Chang, N.-L. *Angew. Chem.* **1995**, *107*, 1689. (c) Percec, V.; Heck, J.; Johansson, G.; Tomazos, D.;

Kawasumi, M.; Chu, P.; Ungar, G. *Pure Appl. Chem.* **1994**, 1719. (d) Lehn, J.-M. "*Supramolecular Chemisry*" **1995**, VCH, New York. see also ref 6.

29 (a) Wyler, R.; de Mendoza, J.; Rebek, Jr., J. *Angew. Chem. Int. Ed. Engl.* **1993**, *32*, 1699. (b) Branda, N.; Wyler, R.; Rebek, Jr., J. *Science* **1994**, *263*, 1267.

30 Meissner, R. S.; Rebek, Jr., J.; de Mendoza, J. *Science* **1995**, *270*, 1485.

31 Grotzfeld, R. M.; Branda, N.; Rebek, Jr., J. *Science* **1996**, *271*, 487.

32 (a) Zerkowski, J. A.; MacDonald, J. C.; Seto, C. T.; Wierda, D. A.; Whitesides, G. M. *J. Am. Chem. Soc.* **1994**, *116*, 2382-2391. (b) Zerkowski, J. A.; Whitesides, G. M. *J. Am. Chem. Soc.* **1994**, *116*, 4298-4304. (c) Mathias, J. P.; Seto, C. T.; Simanek, E. E.; Whitesides, G. M. *J. Am. Chem. Soc.* **1994**, *116*, 1725-1736. (d) Mathias, J. P.; Simanek, E. E.; Zerkowski, J. A.; Seto, C. T.; Whitesides, G. M. *J. Am. Chem. Soc.* **1994**, *116*, 4316-4325. (e) Mathias, J. P.; Simanek, E. E.; Whitesides, G. M. *J. Am. Chem. Soc.* **1994**, *116*, 4326-4320.

33 Menger, F.M.; Lee, S.E. *J. Am. Chem. Soc.* **1994**, *116*, 5987.

34 (a) Hartgerink, J. D.; Granja, J.R.; Milligan, R.A.; Ghadiri, M.R. *J. Am. Chem. Soc.* **1996**, *118*, 43. (b) Ghadiri, M.R.; Granja, J.R.; Milligan, R.A.; McRee, D.E.; Khazanovich, N. *Nature*, **1993**, *366*, 324.

35 (a) Ashton, P. R.; Ballardini, R.; Balzani, V.; Credi, A.; Gandolfi, M. T.; Menzer, S.; Pérez-García, L.; Prodi, L.; Stoddart, J. F.; Venturi, M.; White, A. J. P.; Williams, D. J. *J. Am. Chem. Soc.*, **1995**, *117*, 11171. (b) Amabilino, D. B.; Anelli, P. R.; Ashton, P. R; Brown, G. R.; Córdova, E.; Godínez, L. A.; Hanes, W.; Kaifer, A. E.; Philp, D.; Slawin, A. M. Z.; Spencer, N.; Stoddart, J. F.; Tolley, M. S.; Williams, D. J. *J. Am. Chem. Soc.*, **1995**, *117*, 11142. (c) P. R.; Ashton, P. R; Cleassens, C. G.; Hanes, W.; Menzer, S.; Stoddart, J. F.; White, A. J. P; Williams, D. J. *Angew. Chem.* **1995**, *107*, 1994. (d) Amabilino, D. B.; Stoddart, J. F.; Williams, D. J. *Chem. Mater.* **1994**, *6*, 1159.

36 Otsuki, J.; Oya, T.; Lee, S.-H.; Araki, K. *J. Chem. Soc. Chem. Commun.* **1995**, 2193.

37 For a general review: Balzani, V. *Tetrahedron*, **1992**, *48*, 10443.

38 (a) Deisenhofer, J.; Epp, O.; Mike, K.; Huber, R.; Michel, H. *J. Mol. Biol.* **1984**, *180*, 385. (b) Deisenhofer, J.; Epp, O.; Mike, K.; Huber, R.; Michel, H. *Nature* **1985**, *318*, 618. (c) Michel, H.; Epp, O.; Deisenhofer, J. *EMBO J.* **1986**, *5*, 2445.

39 Allen, J. P.; Feher, G.; Yeates, T. O.; Komiya, H.; Rees, D. C. *Proc. natn. Acad. Sci. U.S.A.* **1987**, *84*, 5730.

40 (a) For a review see: Fox, M. A. "*Photoinduced electron transfer*" **1988**, Chanon, M.A. ed. Elsevier, New York. (b) Barber, J. *Nature* **1988**, *333*, 114. (c) Feher, G.; Allen, J. P.; Okamura, M. Y.; Rees, D. C. *Nature* **1989**, *339*, 111. (d) Fleming, G. R.; Martin, J. L.; Breton, J. *Nature* **1988**, *333*, 190. (e) Barber, J.; Andersson, B. *Nature* **1994**, *370*, 31.

41 For a reviews see: (a) Wasielewski, M. R. *Chem. Rev.* **1992**, *92*, 435. (b) Kurreck, H. Huber, M *Angew. Chem.* **1995**, *107*, 929.

42 (a) Leland, B. A.; Felker, P. M.; Hopfield, J. J.; Zewail, A. H.; Dervan, P. B. *J. Phys. Chem.* **1985**, *89*, 5571. (b) Joran, A. D.; Leland, B. A.; Geller, G. G.; Hopfield, J. J.; Dervan, P. B. *J. Am. Chem. Soc.* **1984**, *106*, 6090. (c) Joran, A. D.; Leland, B. A.; Felker, P. M.; Zewail, A. H.; Hopfield, J. J.; Dervan, P. B. *Nature* **1987**, *327*, 508. (d) Kundkar, L. R.; Perry, J. W.; Hanson, J. E.; Dervan, P. B. *J. Am. Chem. Soc.* **1994**, *116*, 9700.

43 (a) Wiederrecht, G. P.; Niemczyk, M. P.; Svec, W.A.; Wasielewski, M. R.; *J. Am. Chem. Soc.* **1996**, *118*, 81. (b) Osuka, A.; Marumo, S.; Mataga, N.; Taniguchi, S.; Okada, T.; Yamazaki, I.; Nishimura, Y.; Ohno, T.; Nozaki, K. *J. Am. Chem. Soc.* **1996**, *118*, 155. (c) Osuka, A.; Okada, T.; Taniguchi, S.; Nozaki, K.; Ohno, T.; Mataga, N. *Tetrahedron. Lett.* **1995**, *36*, 5781.

44 (a) Chambron, J.-C.; Harriman, A.; Heitz, V.; Sauvage, J. -P. *J. Am. Chem. Soc.* **1993**, *115*, 6109. (b) Brun, A. M.; Atherton, S. J.; Harriman, A.; Heitz, V.; Sauvage, J. -P. *J. Am. Chem. Soc.* **1992**, *114*, 4632. (c) Collin, J. -P.; Harriman, A.; Heitz, V.; Odobel, F.; Sauvage, J. -P. *J. Am. Chem. Soc.* **1994**, *116*, 5679.

45 Harriman, A.; Odobel, F.; Sauvage, J.-P. *.J Am. Chem. Soc.* **1995**, *117*, 9461.

46 (a) Sessler, J. L.; Wang, B.; Harriman, A. *J. Am. Chem. Soc.* **1995**, *117*, 704. (b) Harriman, A.; Magda, D. J.; Sessler, J. L. *J. Phys. Chem.* **1991**, *95*, 1530.

47 Berman, A.; Izraeli, E. S.; Levanon, H.; Wang, B.; Sessler, J. L. *J. Am. Chem. Soc.* **1995**, *117*, 8252.

48 For a recent review: Feiters, M. C. "*Supramolecular Catalysis*" in "*Comprehensive Supramolecular Chemistry*", **1995**, Vol 10, Lehn, J. M. ed.

49 (a) Anderson, H. L.; Bashall, A.; Henrick, K.; McPartlin, M.; Sanders, J. K. M., *Angew. Chem.* **1994**, *106*, 445; (b) Walter, C. J.; Anderson, H. L.; Sanders, J. K. M., *J. Chem. Soc. Chem. Commun.* **1993**, 458.

50 Mackay, L. G.; Wylie, R. S.; Sanders, J. K. M., *J. Am. Chem. Soc.* **1994**, *116*, 3141.

51 (a) Benson, D. R.; Valentekovich, R.; Diederich, F. *Angew. Chem.* **1990**, *102*, 213. (b) Benson, D. R., Valentekovich, R.; Tam, S.-W; Diederich, F. *Helv. Chim. Acta*, **1993**, *76*, 2034.

52 Kuroda, Y.; Hiroshhige, T.; Sera, T.; Shiroiwa, Y.; Tanaka, H.; Ogoshi, H. *J. Am. Chem. Soc.* **1989**, *111*, 1912.

53 Martens, C. F.; Klein Gebbink, R. J. M.; Feiters, M. C.; Nolte, R. J. M. *J. Am. Chem. Soc.* **1994**, *116*, 5667.

54 (a) Coolen, H. K. A. C.; van Leeuwen, P. W. N. M.; Nolte R. J. M. *Angew. Chem.* **1992**, *31*, 905. (b) Coolen, H. K. A. C.; Meeuwis, J. A. M.; van Leeuwen, P. W. N. M.; Nolte R. J. M *J. Am. Chem. Soc.* **1995**, *117*, 11906.

55 Corey, E. J.; Guzman-Perez, A.; Noe, M. C. *J. Am. Chem. Soc.* **1994**, *116*, 12109.

Chapter 2

Synthesis, Conformational Analysis and Binding Properties of Molecular Clips with Two Different Side-walls

2.1 INTRODUCTION

There is currently great interest in the field of host-guest chemistry and in catalysis of reactions using simple enzyme mimics.[1] The focus of this interest has been primarily on the design and construction of molecules possessing a binding site for a substrate, which is positioned nearby a catalytically active center. In the case of enzymes the enzyme-substrate complex formation is generally dominated by hydrophobic effects with additional, relatively weak interactions such as hydrogen bonding, π-π stacking and dipolar interactions used to control substrate selectivity and orientation. The shape-complementary of the receptor site and the aforementioned weak interactions are of fundamental importance for achieving substrate, regio and enantioselectivity in the reaction. Early research into this area has revealed that cyclodextrins are ideal building blocks for the construction of simple enzyme-like catalysts.[2] As in natural enzymes, substrate binding in these mimics is dominated by hydrophobic interactions.[3] Simple modifications of the cyclodextrin molecules with basic functionalities has provided catalysts that are active towards ester hydrolysis and trans-esterification reactions.[4] A more recent example of a water soluble molecule with a binding site is that of Diedrich's cyclophane,[5] which when functionalized with a thiazolium[6] or a porphyrin group[7] proved to be a good enzyme mimic. Organic chemists are not, like nature, confined to the use of water as a solvent and consequently the enzyme approach can also be applied to molecular systems which are soluble in organic solvents. In these cases the main forces contributing to the complex stability are hydrogen bonding, electrostatic interactions, π-π stacking interactions and metal-to-ligand bonding. One of the more promising types of receptor molecules capable of binding guests in organic solvents are the tweezer-like or clip-shaped receptors. Zimmerman[8] and Whitlock[9] have constructed excellent examples of this type of molecules, showing high substrate binding and selectivity. The next step, however, to combine these types of receptors with a catalytically active site has

received considerably less attention. The most commonly used catalysts described in the literature are porphyrins and salophenes, the former species often being found in natural enzymes. Several examples of bridged, capped and fenced porphyrins as catalysts giving remarkable selectivities, have been reported.[10] Only in a limited number of systems, is the porphyrin located nearby a substrate binding site.[11] A good example of a supramolecular catalytic system, is the porphyrin trimer synthesized by Sanders.[12] In this relatively simple supramolecular system the porphyrin units are part of the binding site. Remarkable enhancements in selectivity for Diels Alder reactions were obtained on using simple metal-to-ligand bonding. In general, however, non-porphyrin supramolecular catalysts are very poorly described in the literature.[1,13]

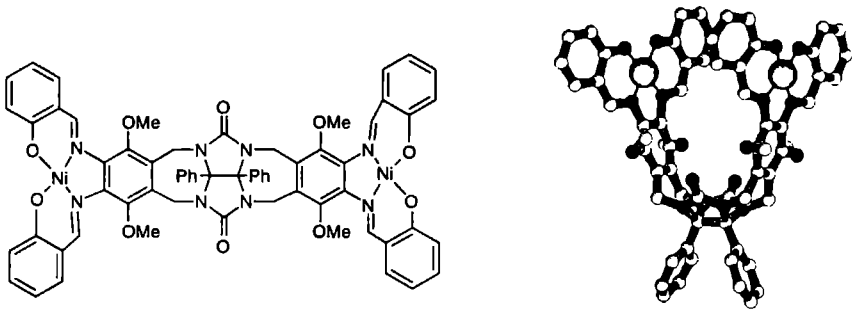

Figure 1. *X-ray structure of the double nickel(II) salophene functionalized molecular clip (see ref 18).*

One of the major goals of research in our group has been the design and synthesis of new types of cleft-shaped host molecules that can be functionalized with catalytically active components and used consequently as enzyme mimics. Previous work towards this goal has led to the development of clip[14] and basket-shaped[15] molecules which were found to be ideal hosts for hydroxybenzene substrates. Subsequent functionalization of these baskets with metal centers positioned above the cavity via flexible spacers, gave host molecules which were still able to bind dihydroxybenzenes, but in addition behaved as catalysts giving substrate selectivity,[16] and enhancement of reaction rates.[17] Another approach used to construct biomimetic catalyst was to functionalize the side-walls of a molecular clip with two metal salophene groups (Figure 1).[18] The obtained clip was unable, unfortunately, to bind guest molecules due to the steric hindrance of the methoxy groups blocking the cavity and the close

proximity of the two metal salophene units. In order to overcome this unfavourable interaction between the host and the guest it was necessary to design clip molecules with two different (aromatic) side-walls which would facilitate the mono-functionalization with a metal center. In this chapter the synthesis, characterization and preliminary binding studies of these new clip molecules are described.

2.2 RESULTS AND DISCUSSION

2.2.1 Synthesis

Previously developed starting compounds derived from diphenylglycoluril (DPG) which have been used in the synthesis of other molecular receptors are cyclic ether **1**,[14b] and the tetraacetoxy and the tetrachloro derivatives **2a** and **2b** (Chart I).[14a] Clip **3a** can be synthesized from **1** by means of an acid catalyzed amido alkylation reaction, and clips **3b**, **4** and **5a** are accessible from the more reactive compound **2b**. The first step in

Chart I

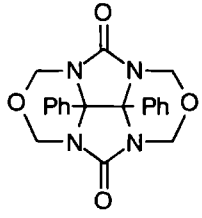

1

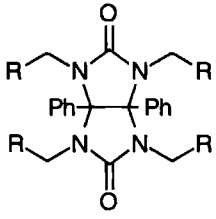

2a R= OAc
2b R= Cl

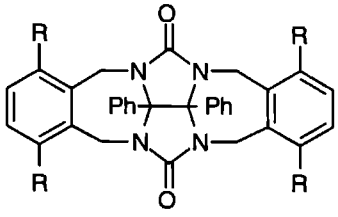

3a R=OMe
3b R=H

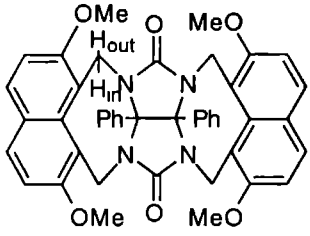

4

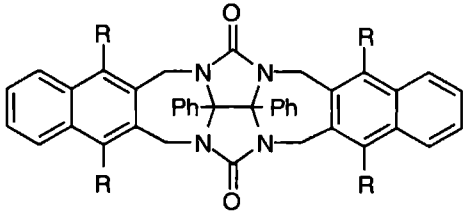

5a R=OMe
5b R=H

the synthesis of asymmetrically substituted clip molecules is the preparation of a mono-walled intermediate. Subsequent reaction of this species with a second side-wall will result in the desired compounds. In order to synthesize clip molecules functionalized with one ligand system, the mono-walled species have to be nitrated before the second wall is attached (*vide infra*). These steps will be described later.

Mono-walled molecules based on DPG

To obtain mono-walled host **7**, cyclic ether **1** was reacted with one equivalent of 1,4-dimethoxybenzene (1,4-DMB) in a mixture of acetic anhydride and TFA under a variety of different reaction conditions. In all cases the reaction product was an 1:1 mixture of **1** and **3a**, probably because the acetate functions in the intermediate **8** are activated by the attached aromatic wall towards a further amido alkylation reaction compared to the tetraacetate intermediate **2a**. Another possibility is that the first attached wall has a favourable pre-organization effect on the second 1,4-DMB molecule.

Chart I continued

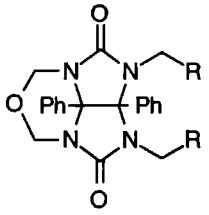

6a R=OAc
6b R=Cl

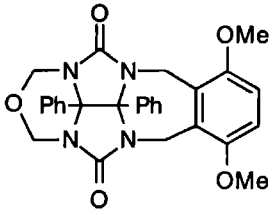

7

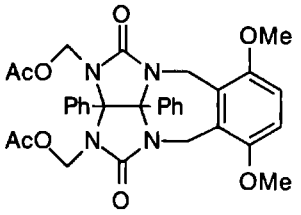

8

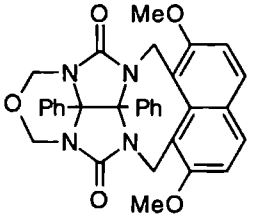

9

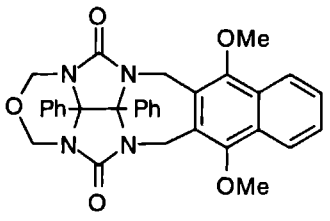

10

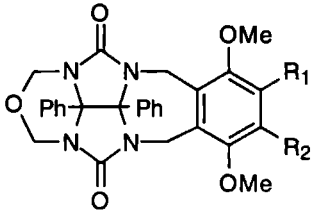

11a: R1 = NO_2 R2 = H
11b: R1 = NO_2 R2 = NO_2
11c: R1 = NH_2 R2 = NH_2

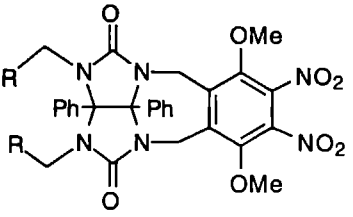

12a R = OAc
12b R = Cl

In order to overcome this problem a new starting compound **6b**, which has two sites of differing reactivity toward Friedel Crafts alkylation was synthesized. Compound **6b** was obtained from **1** in two steps: (i) a partial reaction of **1** with acetic anhydride using p-toluenesulfonic acid as a catalyst and subsequent separation of **6a** from **1** by column chromatography, yielding **6a** in 65%; (ii) substitution of the acetyl groups with chloride groups by stirring **6a** overnight in an 1:1 mixture of CH_2Cl_2 and thionyl chloride. This gave crystalline **6b** (92% yield) which was moisture sensitive.

Chart I continued

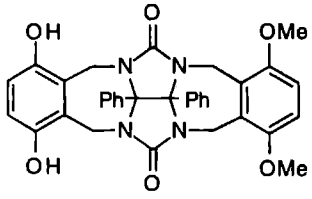

13

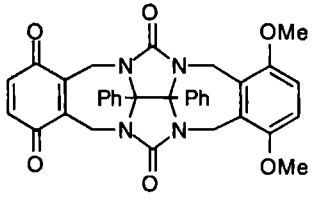

14

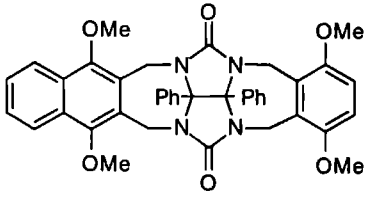

15

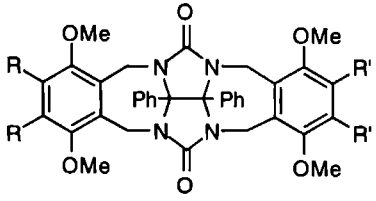

16a R=H, R'=NO_2
16b R=H, R'=NH_2
16c R,R'=NO_2
16d R,R'=NH_2

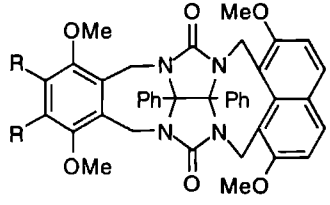

17a R=H
17b R=NO_2
17c R=NH_2

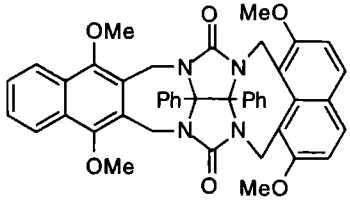

18

Reaction of **6b** with 1,4-DMB in 1,2-dichloroethane with $SnCl_4$ as a catalyst at both room temperature and at 0 °C again resulted in mixtures of **1** and **3a** as products. The reaction was performed at lower temperature, in order to better differentiate the reactivity of the sites of **6b**. To an 1:1 mixture of **6b** and 1,4-DMB in 1,2-dichloroethane

at -35°C, $SnCl_4$ was added slowly and the mixture was allowed to warm slowly to 0 °C overnight. The precipitate obtained was shown to be **7** (88% yield). A similar reaction of the tetrachloro derivative **2b** yielded a mixture of **1**, **7**, and **3a** (molar ratio 1:4:1), which could be separated by column chromatography to give **7** (58%). An alternative approach to obtain **7** was by performing the reaction at room temperature but in high dilution. Slow addition of a solution of 1,4-DMB to an 1,2-dichloroethane solution of **2b** and $SnCl_4$ again yielded a mixture of **1**, **7**, and **3a** (1:4:1), which yielded **7** (52% after column chromatography).

2,7-Dimethoxynaphthalene (2,7-DMN) and 1,4-dimethoxynaphthalene (1,4-DMN) are less reactive towards attack by **2b** than 1,4-DMB. An equimolar mixture of **2b** and 2,7-DMN in 1,2-dichloroethane containing 4 equivalents of $SnCl_4$ was heated under reflux to yield **9** in 71% after column chromatography. A similar reaction of **2b** with 1,4-DMN yielded **10** in 42%.

Molecular clips with two different side-walls

The mono-walled molecules **7**, **9**, and **10** could now be used as starting materials for the preparation of several new clips containing two different aromatic side-walls. Heating a mixture of **7** with hydroquinone in 1,2-dichloroethane with p-toluenesulfonic acid as a catalyst yielded **13** in 73%. This compound, which is insoluble in most organic solvents, was converted into a bright red compound **14** by aerial oxidation in DMSO using Cu_2Cl_2 as a catalyst (yield 77%).

Reactions of **7** and **9** with 1,4-DMN in mixtures of acetic anhydride and TFA yielded **15** and **18** in 70 and 65%, respectively. Analogous reactions of **9** and **10** with 1,4-DMB yielded **17a** and **15** in 94 and 97%, respectively.

Nitration reactions were carried out, in order to obtain clip molecules functionalized with a catalytic side-wall. Stirring compound **7** in acetic anhydride with two equivalents of nitric acid for 16h gave the mono-nitro compound **11a** as a crystalline precipitate in 80% yield. The analogous reaction with a mixture of **1**, **7**, and **3a** (molar ratio 1:4:1), gave a precipitate which was proved to be pure **11a** (yield: 80% based on **7**). Subsequent reaction of **11a** in acetic anhydride with 4 equivalents of nitric acid yielded the dinitro compound **11b** in 96%, after purification by column chromatography. Dinitro-clip **16a** was prepared in 96% yield by amido alkylation of **11b** with 1,4-DMB in acetic anhydride/TFA. Several nitration reactions with **17a** were carried out in order to obtain dinitro-clip **17b**. The clip molecule decomposed under the conditions necessary to nitrate the 1,4-DMB wall to give 2,7-dimethoxy-1,8-dinitronaphthalene as a side product. Compound **11b** was reacted, therefore, with acetic acid and *p*-toluenesulfonic

acid to give compound **12a**, which was treated subsequently with thionyl chloride in CH_2Cl_2 to give **12b**. This compound was now sufficiently reactive to undergo a Friedel Crafts reaction with 2,7-DMN to yield **17b** in 60% yield.

Chart I continued

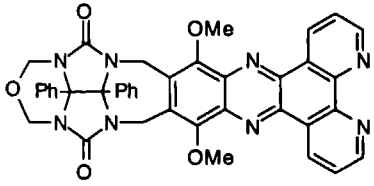

19

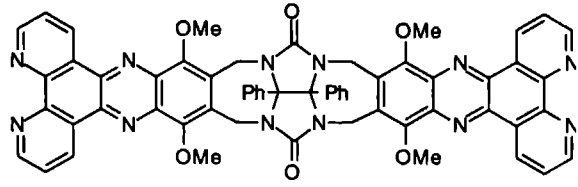

20

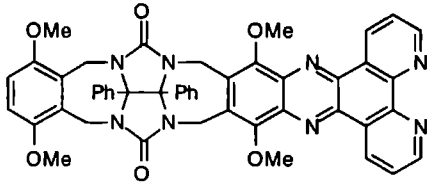

21

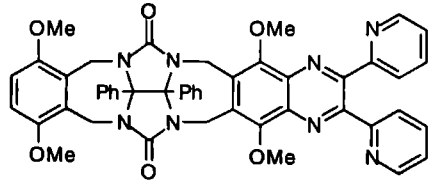

22

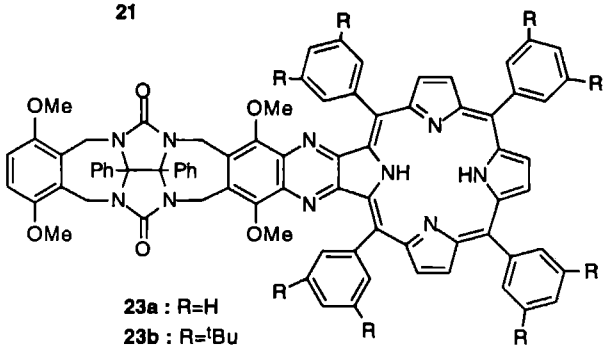

23a : R=H
23b : R=^{t}Bu

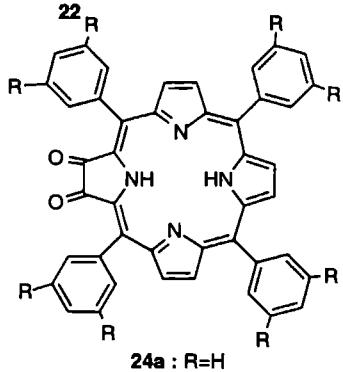

24a : R=H
24b : R=^{t}Bu

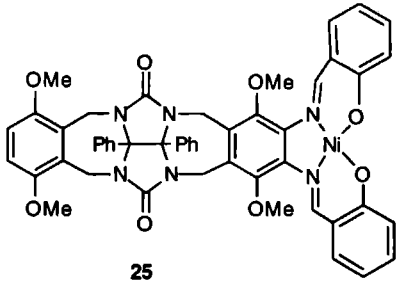

25

Chart I continued

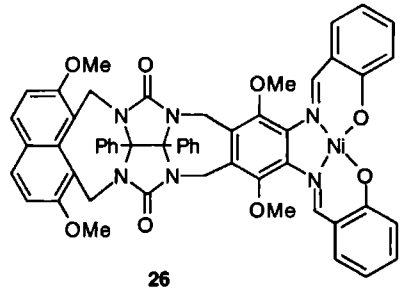

26

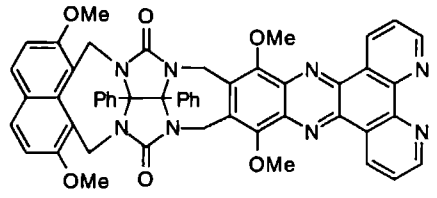

27

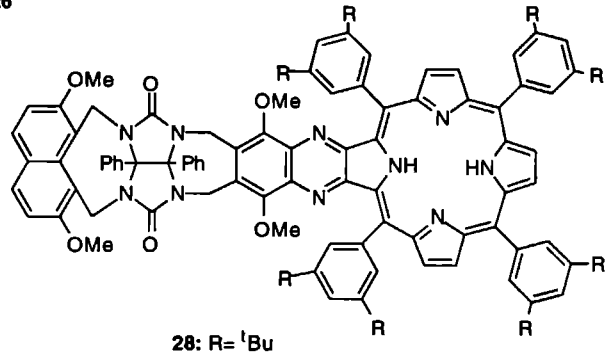

28: R= ^{t}Bu

Dinitro-compounds **11b**, **16a** and **17b** were reduced to the corresponding diamines, **11c**, **16b**, and **17c** using triethylammonium formate[19] as a hydrogen donor with Pd on carbon as a catalyst in a mixture of THF and methanol. These compounds were found to be very sensitive to oxidation and were used, therefore, without further purification for subsequent synthesis.

Clip molecules functionalized with catalytic side-walls

All clips containing one or two walls functionalized with a ligand were obtained by a condensation reaction of **11c**, **16b**, **16d**, or **17c** with a diketone precursor, or with salicylaldehyde. Heating **11c** with 1,10-phenanthroline-5,6-quinone[20] in a (1:1:1 (v/v)) mixture of MeOH/THF/CH_2Cl_2 over Mol. Sieves (3Å) yielded **19** in 79% after purification by column chromatography. Similar reactions of **16b** with 1,10-phenanthroline-5,6-quinone, 2,2'-pyridil and porphyrin diketone **24a**[21] gave compounds **21**, **22** and **23a** in 31, 71 and 28% yields, respectively. The condensation reaction of **16b** and 2,2'-pyridil or porphyrin-diketone **24** in pure dichloromethane resulted in significantly higher yields (52 and 92%, respectively). A clip molecule functionalized at one side with a salophene unit was obtained after a template condensation reaction of **16b** with salicylaldehyde and $Ni(OAc)_2$ yielding **25** in 90% yield. Mono-functionalized clip molecules having an opposing 2,7-DMN side-wall

were obtained by similar condensation reactions using **17c** as the diamine precursor, resulting in clip molecules **26-28** (yields 80%, 72% and 63%, respectively).

2.2.2 NMR Conformational analysis

It has been shown previously[14a] by our group that a naphthalene moiety which is connected to the DPG framework at the 1 and 8 positions can adopt two orientations: (a) upwards with respect to the phenyl ring on the convex side of the DPG unit (*anti*)

Table I. *Assignment of ^1H NMR signals to the conformers of* **9**, **17a**, *and* **18**[a]

Proton signal	**9**		**17a**		**18**	
	anti	*syn*	*anti*	*syn*	*anti*	*syn*
NCH_2O	5.37	5.66				
out[b]	(11.0)	(11.0)				
NCH_2O	4.29	4.44				
in[b]	(11.0)	(11.0)				
NCH_2Ph			5.39	5.68		
out[b]			(15.8)	(15.8)		
NCH_2Ph			3.85	3.74		
in[b]			(15.8)	(15.8)		
NCH_2Napht (2,7)	5.98	6.20	5.98	6.12	5.97	6.15
out[b]	(16.3)	(16.5)	(16.4)	(16.4)	(16.4)	(14.8)
NCH_2Napht (2,7)	4.19	5.11	4.10	4.95	4.09	4.96
in[b]	(16.3)	(16.5)	(16.4)	(16.4)	d	(14.8)
NCH_2Napht (1,4)					5.63	5.82
out[b]					(16.0)	(15.9)
NCH_2Napht (1,4)					3.84	3.93
in[b]					(16.0)	(15.9)
OCH_3	4.11	3.97	4.07	3.95	4.02	4.25
			3.75	3.93	3.90	3.96
Ph H-2,6[c]	d	6.42(*s*)	d	6.46(*s*)	d	6.50(*s*)
Ph H-3,5[c]	d	6.13(*s*)	d	6.13(*s*)	d	6.16(*s*)
Ph H-4[c]	d	6.25(*s*)	d	6.26(*s*)	d	6.28(*s*)
Ph H-2,3[e]			6.12	6.85		
Napht H-3 (2,7)	7.19	6.90	7.14	6.88	7.11	6.88
	(9.0)	(9.0)	(9.1)	(9.1)	(8.9)	(8.9)
Napht H-4 (2,7)	7.74	7.30	7.62	7.26	7.57	7.26
	(9.0)	(9.0)	(9.1)	(9.1)	(8.9)	(8.9)
Napht H-5,8 (1,4)					7.95	8.11
Napht H-6,7 (1,4)					7.41	7.51

[a]Shifts are in ppm; *J*-couplings (Hz) in parentheses; the designations (*s*) and (*a*) are used for the phenyl rings *syn* and *anti* with respect to the side-walls. [b]The designations *in* and *out* are used as indicated in Chart I. [c]Protons of the glycoluril framework. [d]No assignment could be made. [e]Protons of the 1,4-dimethoxybenzene side-wall.

and (b) downwards (*syn*) with respect to this ring. Compound **4** exists in three conformations in solution, which interconvert slowly on the NMR time scale, *syn-syn* (7.7%), *syn-anti* (89.6%) and *anti-anti*(2.7%).

Table II. *Assignment of ^1H NMR signals to the conformers of 26, 27 and 28*[a]

Proton signal	26		27		28	
	anti	*syn*	*anti*	*syn*	*anti*	*syn*
NC*H*$_2$Ph	5.50	5.65	5.89	6.08	5.85	6.13
out[b]	(15.9)	(15.8)	(16.4)	(15.9)	(15)	(15)
NC*H*$_2$Ph	3.88	3.86	3.96	4.01	3.82	3.95
in[b]	(15.9)	(15.8)	(16.4)	(15.9)	(15)	(15)
NC*H*$_2$Napht (2,7)	5.98	6.15	6.04	6.17	5.58	4.80
out[b]	(15.9)	(14.7)	(16.4)	(14.9)	(15)	(15)
NC*H*$_2$Napht (2,7)	4.09	4.98	4.12	4.98	3.96	2.70
in[b]	(15.9)	(14.7)	(16.4)	(14.9)	(15)	(15)
OCH$_3$	4.03	3.97	4.34	4.72	3.96	3.91
	3.52	3.81	4.05	3.99	3.55	3.85
Ph H-2,6[c]	7.36-	6.49	7.32-	6.54	7-7.3	6.75(*s*)
	6.95	(*s*)	6.98			7.23(*a*)
Ph H-3,5[c]	7.36-	6.19	7.32-	6.25	7-7.3	6.15(*s*)
	6.95	(*s*)	6.98			6.85(*a*)
Ph H-4[c]	6.60	6.29	7.32-	6.30	7-7.3	6.60(*s*)
		(*s*)	6.98	(7.3)		7,10(*a*)
Napht H-3 (2,7)	7.17	6.89	7.02	6.90	6.8-	6.8-
	(9.0)	(9.0)	(8.8)	(9.0)	7.3	7.3
Napht H-4 (2,7)	7.59	7.28	7.47	7.28	6.8-	6.8-
	(9.0)	(9.0)	(8.8)	(9.0)	7.3	7.3
Ar*H*	7.36-	7.36-				
	6.95	6.95				
ArNC*H*Ar	9.04	9.26				
Phenan*H*			9.50	9.67		
			9.22	9.29		
			7.72	7.84		
Porphyrin β*H*					8.94	8.94
					8.67	8.67
Porphyrin β*H*					(5)	(5)
					8.77	8.77
Porphyrin pyr *H*					-2.68	-2.68
Porphyrin Ar*H*					7.5-8.3	7.5-8.3
Porphyrin ArCC*H*					1.5-1.7	1.5-1.7

[a]Shifts are in ppm; *J*-couplings (Hz) in parentheses; the designations (*s*) and (*a*) are used for the phenyl rings *syn* and *anti* with respect to the side-walls. [b]The designations *in* and *out* are used as indicated in Chart I. [c]Protons of the glycoluril framework.

Compounds **9**, **17a**, and **18** which have one naphthalene wall connected at the 1 and 8 positions, were expected to exist in solution in only two conformations, *viz. syn* and

anti. The 400 MHz ^{1}H NMR spectra of these compounds in $CDCl_3$ at 298 K confirmed this. Nearly all signals of the respective conformers could be assigned with the help of COSY spectra (see Table I). The procedure that was followed for this assignment was similar to that described previously for **4**.[14a] The shielding effects of aromatic rings can be estimated with the help of the Johnson and Bovey[22] tables. It can be shown that the signals of the protons of the phenyl groups of the diphenylglycoluril framework on the *syn* side of one conformer are shifted upfield relative to the proton signals on the *anti* side. This method enables full assignment of the AX quartets of the NCH_2 protons and the signals of the wall protons for each of the conformers. The relative abundance of the different conformers of **9**, **17a**, and **18**, were determined by integration of these signals: 23% of the molecules of **9** were in the *syn* conformation and 77% in the *anti* conformation in $CDCl_3$ at 298 K. With **17a**, these values were 85 and 15%, and in the case of **18** 76 and 24%, respectively. This result is in agreement with the previously proposed idea that clip molecules with naphthalene walls connected at the 1,8-positions preferentially adopt a conformation in which the walls are optimally exposed to solvent molecules.[14a] For compound **4** this is achieved with the *syn-anti* conformation, for compound **9** with the *anti* conformation, and for compounds **17a** and **18** with the *syn* conformation. More details concerning these conformations will be presented in Chapter 4.

In addition to these model compounds, the conformational behaviour of the mono-functionalized clip molecules **26-28** was also studied by ^{1}H NMR (see Table 2). These molecules are important with respect to the overall goal of developing biomimetic catalytic systems. They were found to exist in two conformers with the *syn* conformers dominating: 68% for **26**, 68% for **27** and 55% for **28**.

2.2.3 Binding properties.

It is known from our earlier studies that the molecular clip **3a** is a good receptor for the complexation of dihydroxybenzenes, whereas **5a** is unable to bind such guests.[14d] This lack of binding of guest molecules was ascribed initially to the methoxy groups on the walls of **5a** which point inside the cavity and block the carbonyl functions from forming hydrogen bonds. Further studies indicate that, in addition to this steric effect, there is an unfavourable *i.e.* repulsive π-π interaction between the aromatic guest and the naphthalene side-walls which also results in a decrease in binding (*vide infra*).

Complexation studies with the guest olivetol (1,3-dihydroxy-5-pentylbenzene) were performed in order to obtain further insight into the influence of two different aromatic walls in the clip molecule, upon host-guest binding. The association constants (K_a's) and complex induced shift (CIS) values for a series of related clip

molecules were determined by ^1H NMR titrations as described previously.[14d] The trends in binding affinity of olivetol to selected clips are shown in Table III. It can be seen that a large drop in K_a is observed upon going from host molecules **3a** to **15** to **5a**. This highlights the fact that an 1,4-DMN wall (which can be considered as a functionalized 1,4-DMB wall) is unfavourable for guest binding compared with an 1,4-DMB wall. By comparing the association constant between olivetol and clip **3a** with that of clip **15** it can be seen that the presence of one 1,4-DMN side-wall in a clip considerably reduces the binding strength (25x), but does not totally block the cleft for binding. The binding of olivetol to cyclic ether **1** (K_a = 25 M^{-1}) increases when an 1,4-DMB wall is attached to this molecule (**7**, K_a = 40 M^{-1}), but decreases when this wall is an 1,4-DMN aromatic surface (**10**, K_a < 1 M^{-1}).

Table III. *Association constants and complex induced shift values of complexes between olivetol and different clips.*[a]

Clip	Ka /M^{-1}	CIS / ppm[b]
3a	1500	-0.51
15	55	-0.43
5a	<1	-
1	25	-
7	40	-0.34
10	<1	-
17a	1060[c]	-
18	90[c]	-
19	<1	-
20	<1	-
21	210	-0.36
22	125	-0.31
23a	30	-0.34
5b	60[d]	-
3b	175[d,e]	-
25	920	-0.44
26	1200	-0.40[f]

[a]The errors in the association constants are 10-30%. [b]CIS values of the *p*-dimethoxybenzene side-walls. [c]Value taken from Chapter 4. [d]Association constant of the complex with resorcinol. [e]Value taken from Chapter 3. [f]CIS values of the imine protons.

Clip molecules **17a** and **18** are able to bind an olivetol guest by an induced fit mechanism. The 2,7-DMN wall flips upon complexation of the guest molecule as depicted in Figure 2. The association constants for clips **17a** and **18** were determined by following the ratio of conformers as a function of the guest concentration.[14a] These experiments also revealed that the 1,4-DMN wall is very unfavourable for binding. A drop in association constant from K_a = 1060 M^{-1} (**17a**) to 90 M^{-1} (**18**) was observed

when the 1,4-DMB wall in the clip molecule was replaced by an 1,4-DMN wall (Table III). Since the change to an 1,4-DMN wall had such a great influence upon the host-guest binding it was decided to perform binding studies with **5b**, a molecule with naphthalene walls but without methoxy groups. In this case resorcinol was chosen as the guest molecule, in order that a comparison with previous studies could be made.[14d] Clip molecule **5b** was able to bind resorcinol (K_a = 70 M^{-1}), but with a significantly lower binding constant than was found for the clip with two benzene walls **3b** (K_a = 175 M^{-1}). When the methoxy groups of clip molecule **5a** are removed, the cleft is no longer blocked, however, the binding is still relatively weak (compared with that of **3b**) because of unfavourable π-π stacking interactions. These unfavourable π-π interactions are caused by a repulsive electrostatic interaction according to calculations using the Hunter and Sanders model[23] (see also Chapter 3). The formation of the hydrogen bonds between host and guest forces the guest into a geometry in which the π-π interaction with the aromatic side-walls is very unfavourable.

Comparison of the CIS value of clip **15** (-0.43 ppm) with that of **3a** (-0.51 ppm), indicates that in both complexes the guest molecule is positioned in a similar orientation. Calculations were carried out with a computer program based on the Johnson and Bovey tables of ring current shifts,[22] which showed that the guest is less deeply bound in the cavity of clip **15** than in the cavity of clip **3a**.[14d] This might be important when a guest molecule has to be bound nearby a catalytically active site, e.g. a metal center bound to ligands **19-23**.

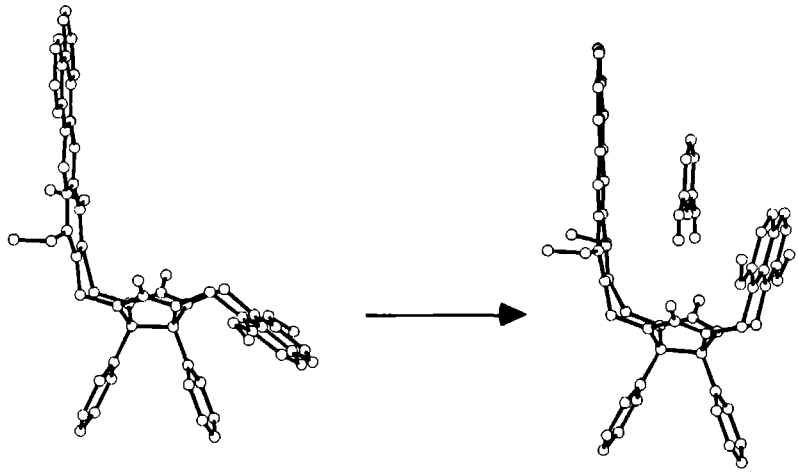

Figure 2. *Binding of a resorcinol guest molecule by an 'induced fit' mechanism in a clip containing an 1,8-connected naphthalene side-wall.*

The binding properties of the ligand functionalized molecular clips **19-26** are important with respect to the aims outlined in the Introduction. The mono-phenanthroline clip **21** is capable of binding olivetol (K_a = 210 M^{-1}), whereas the di-phenanthroline clip **20**, is not a good host (K_a < 1 M^{-1}). This is in line with the binding results obtained with clip molecules **3a**, **5a** and **15** (*vide supra*), and is due to the repulsive nature of the two large electronegative side-walls of **20**, and the steric effects of the methoxy groups which partly block the carbonyl groups. Porphyrin clip **23a** and dipyridine clip **22** are also capable of binding olivetol in their clefts (K_a = 30 and 125 M^{-1} respectively). The observed binding constants are lower the binding constant of mono phenanthroline clip **21** due to steric effects. In clip **22** the pyridyl groups are positioned orthogonally to the wall of the cleft, leading to steric congestion when the guest is bound. Porphyrin clip **23a** contains phenyl groups attached to the porphyrin ring which are pointing slightly into the cleft, as is evident from the X-ray structure of this molecule (see Chapter 7). These phenyl groups cause steric repulsion, resulting in a lower association constant. Mono-walled clip molecule **19** is not able to bind olivetol, which is in line with the binding properties of **10**. The CIS values of the complexes between the clips **21**, **22** and **23** and olivetol, again suggest that the guest is binding with approximately the same geometry but less deeply than in clip **3a**.[14d]

It is clear from the binding studies with compounds **15** and **18** that 2,7-DMN side-walls gives rise to slightly higher binding constants than 1,4-DMB side-walls. This is also the case for the clips containing a catalytically active nickel salophene side-wall. Compound **25** binds olivetol with an association constant of K_a = 920 M^{-1} which is slightly lower than the K_a = 1200 M^{-1} measured for **26**. These binding constants are, however, both higher than those observed for the 1,4-DMN containing clips **15** and **18**. This is probably an effect of the lower electron density of the nickel salophene functionalized side-wall, which reduces the electrostatic repulsion between this side-wall and the aromatic ring of the bound guest molecule.

Further detailed binding studies with the new clip molecules as well as catalytic studies are reported in Chapters 3, 4 and 8.

2.3 CONCLUSIONS

A new general synthetic route to molecular clips with two different side-walls starting from the new precursor **6b** and the known compound **2b** is described. A variety of clips which are shown to be able to bind dihydroxy-substituted aromatic guests in chloroform by means of hydrogen bonding and π-π-interactions have been synthesized via this route. Some clips have been functionalized on one side-wall with metal binding ligand systems, *viz.* phenanthroline, pyridine, Ni-salophen and

porphyrin for future applications in synzymatic catalysis. This resulted in clips possessing a catalytic group or a ligand system incorporated in the side-wall, which are still capable of binding dihydroxybenzenes. These molecules can be seen as simple enzyme mimics since they possess a ligand system that can be turned easily into a catalytic center rigidly attached to a binding site.

2.4 EXPERIMENTAL SECTION

2.4.1 General

Thionyl chloride and triethylammonium formate were distilled prior to use. THF and diethyl ether were distilled under nitrogen from sodium benzophenone ketyl. Dichloromethane and chloroform were distilled from $CaCl_2$. 1,2-Dichloroethane and methanol were distilled from CaH_2. All other solvents and chemicals were commercial materials and used as received. Merck Silica Gel (60H) was used for column chromatography and Merck Silica Gel F_{254} plates for thin layer chromatography. IR spectra were recorded on a Perkin Elmer FTIR 1720-Xspectrometer. ^1H NMR spectra were recorded on Bruker WH-90, Bruker AC-100, Bruker WM-200, and Bruker AM-400 instruments. Chemical shifts (∂) are reported in ppm downfield from internal $(CH_3)_4Si$ Abbreviations used are s = singlet, d = doublet, m = multiplet, br = broad. FAB-MS spectra were recorded on a VG 7070E instrument, the matrix used was *m*-nitrobenzylalcohol. Elemental analyses were determined with a Carlo Erba Ea 1108 instrument.

2.4.2 Compounds

The syntheses and properties of compounds **1**, **2a**, **2b**, **3a**, **3b**, **4**, **5a**[14] and of **16c** and **16d**[18] have been described elsewhere. 1,10-Phenanthroline-5,6-quinone was synthesized from 1,10-phenanthroline monohydrate according to literature procedures.[20] 17,18-Dioxoporphyrins **24a** and **24b** were kindly provided by Prof. M. J. Crossley.[21]

1,4-Dimethoxynaphthalene. A mixture of 5.0 g (31 mmol) of 1,4-dihydroxynaphthalene, 17.5 g (0.312 mol) of powdered KOH and 11 mL (66 mmol) of dimethylsulfate in 100 mL of DMSO was stirred for 1 h. The mixture was then poured into 500 mL of water and the product was extracted with 200 mL of CH_2Cl_2. The organic layer was washed with aqueous 1N HCl, aqueous 1N NaOH (2x) and water and dried over $MgSO_4$. After evaporation of the solvent in vacuo and purification of the residue by column chromatography (CH_2Cl_2/MeOH 199:1, v/v), 5.4 g (92%) of 1,4-dimethoxynaphtalene was obtained as a white solid: mp 140°C.

6,8,15,16b,16c,17-Hexahydro-16b,16c-diphenyl-7H,16H-6a,7a,15a,16a-tetraazanaphto[5,6] azuleno[2,1,8-ij]naphto[f]azulene-7,16-dione (5b). To a suspension of 900 mg (16 mmol)

of KOH in 2 mL of DMSO was added 300 mg (1.0 mmol) of diphenylglycoluril and 650 mg (2.7 mmol) of α,α'-dibromo-2,3-dimethylnaphthalene. The mixture was stirred for 16 hrs and then poured into 20 mL of water. The compound was extracted with 20 mL of CH_2Cl_2, the organic layer was washed with aqueous 1N NaOH, water, and dried over $MgSO_4$. After evaporation of the solvent the compound was purified by column chromatography (eluent CH_2Cl_2) and recrystallization from $CHCl_3$ yielding 184 mg white powder (31%). Mp > 310°C; ^{1}H NMR ($CDCl_3$) δ 7.70 (s, 4H, Naphth*H*), 7.70-7.60 and 7.45-7.30 (2m, 8H, Naphth*H*), 7.18 (s, 10H, ArH), 5.01 and 4.27 (2d, 8H, NCHHAr, *J* = 16 Hz); FAB-MS *m/z* 599 $(M+H)^+$. Anal. Calcd. for $C_{40}H_{30}N_4O_2 \cdot (CHCl_3)$: C, 68.58; H, 4.35; N, 7.80. Found: C, 67.96; H, 4.66; N, 7.29.

Acetic acid 3-acetoxymethyltetrahydro-1,4-dioxo-2a,7b-diphenyl-6-oxa-2,3,4a,7a-tetraazacyclopenta[cd]inden-2-ylmethyl ester (6a). A suspension of 3.18 g (8.40 mmol) of **1** and 80 mg (0.42 mmol) of p-toluenesulfonic acid monohydrate in 15 mL of acetic anhydride was heated to reflux. After the mixture became clear, it was instantly cooled in an ice-bath. Diethyl ether (15 mL) was added and the resulting precipitate was filtered off, washed with diethyl ether and dried under vacuum. After column chromatography (CH_2Cl_2/MeOH, 99:1 v/v), 2.62 g (65%) of **6a** was obtained as a white solid: Mp 228°C; IR (KBr) 1756, 1737 (C=O), 1237 (COC); ^{1}H NMR ($CDCl_3$) δ 7.20-6.95 (m, 10H, ArH), 5.65 and 4.47 (2d, 4H, NC*H*$_2$OAc, *J* = 11.4 Hz), 5.62 and 5.33 (2d, 4H, NC*H*$_2$O, *J* = 11.1 Hz), 2.07 (s, 6H, $COCH_3$); FAB-MS *m/z* 481 $(M+H)^+$. Anal. Calcd. for $C_{24}H_{24}N_4O_7$: C, 60.00; H, 5.03; N, 11.66. Found: C, 60.12; H, 4.99; N, 11.55.

2,3-Bis-chloromethyldihydro-2a,7b-diphenyl-6-oxa-2,3,4,7a-tetraazacyclopenta-[cd]indene-1,4-dione (6b). Compound **6a** (1.11 g, 2.31 mmol) was stirred under nitrogen for 16 hrs in a mixture of 2 mL of CH_2Cl_2 and 3 mL (41 mmol) of $SOCl_2$. After addition of 5 mL of diethyl ether the precipitate was filtered off, washed with diethyl ether and dried under vacuum. Yield: 0.92 g (92%) of **6b** as a white hygroscopic solid: ^{1}H NMR ($CDCl_3$) δ 7.28-6.92 (m, 10H, ArH), 5.40 and 5.33 (2d, 4H, NC*H*$_2$Cl, *J* = 11.0 Hz), 5.65 and 4.47 (2d, 4H, NC*H*$_2$O, *J* = 11.1 Hz); FAB-MS *m/z* 397 $(M-Cl)^+$. Due to the instability of the compound no satisfactory elemental analysis could be obtained.

Mono-walled compound 7. Method A: A stirred suspension of 0.95 g (2.2 mmol) of **6a** and 0.30 g (2.2 mmol) of 1,4-dimethoxybenzene in 100 mL of 1,2-dichloroethane was cooled under nitrogen to -35°C in an acetone/CO_2-bath. $SnCl_4$ (1 mL, 8 mmol) was added and the mixture was allowed to warm slowly to 0°C. A precipitate was formed, which was filtered at 0°C, washed with diethyl ether and redissolved in 100 mL of dichloromethane. The organic layer was washed with aqueous 1N HCl and water, dried ($MgSO_4$) and concentrated *in vacuo*. Yield: 0.96 g (88%) of **7** as a white solid.

Method B: A stirred suspension of 1.07 g (2.2 mmol) of **2b** and 0.30 g (2.2 mmol) of 1,4-dimethoxybenzene in 100 mL of 1,2-dichloroethane was cooled under nitrogen to -35°C in an acetone/CO_2-bath. $SnCl_4$ (1 mL, 8 mmol) was added. The mixture was allowed to warm slowly to 0°C and 10 mL of aqueous 6N HCl was added. After stirring for 15 min, the organic layer was washed with water and concentrated *in vacuo*. A mixture of **1**, **7** and **3a** was obtained (molar ratio 1:4:1) which could be separated by column chromatography ($CHCl_3$/MeOH, 197:3, v/v) to yield 0.63 g (58%) of **7**.
Method C: To a stirred solution of 1.0 g (2.0 mmol) of **2b** and 1 mL (8 mmol) of $SnCl_4$ in 200 mL of degassed 1,2-dichloroethane (2 mL/min) a solution of 0.28 g (2.0 mmol) of 1,4-dimethoxybenzene in 100 mL of 1,2-dichloroethane was added slowly. After the addition of 10 mL of 6N aqueous HCl the mixture was stirred for another 15 min. The organic layer was washed with water and concentrated *in vacuo*. A mixture of **1**, **7**, and **3a** was obtained (molar ratio 1:4:1) which could be separated by column chromatography as described under method B. Yield: 0.52 g (51%) of **7**: Mp 381°C (dec); ^{1}H NMR ($CDCl_3$) δ 7.30-7.00 (m, 10H, ArH), 6.83 (s, 2H, ArH), 5.65 and 3.80 (2d, 4H, NCH_2Ar, J = 15.8 Hz), 5.50 and 4.40 (2d, 4H, NCH_2O, J = 11.0 Hz), 3.87 (s, 6H, OCH_3); FAB-MS *m/z* 499 $(M+H)^+$. Anal. Calcd for $C_{28}H_{26}N_4O_5$: C, 67.46; H, 5.26; N, 11.24. Found: C, 67.63; H, 5.15; N, 11.18.

Mono-walled compound 9. A mixture of 2.0 g (4.1 mmol) of **2b**, 1.0 g (5.3 mmol) of 2,7-dimethoxynaphthalene and 1.5 mL (12 mmol) of $SnCl_4$ was refluxed under nitrogen for 50 min in 100 mL of degassed 1,2-dichloroethane. After this period, 10 mL of aqueous 6N HCl was added and the mixture was refluxed for an additional 15 min. After cooling, CH_2Cl_2 (50 mL) was added and the organic layer was washed with aqueous 1N HCl, aqueous 1N NaOH (2x) and water, and concentrated *in vacuo*. Column chromatography (CH_2Cl_2/MeOH, 99:1 v/v) gave 1.6 g (71%) of **9** as a white solid: Mp 315°C (dec); ^{1}H NMR ($CDCl_3$) see Table I; FAB-MS *m/z* 549 $(M+H)^+$. Anal. Calcd. for $C_{32}H_{28}N_4O_5$: C, 70.06; H, 5.14; N, 10.21. Found: C, 70.20; H, 5.22; N, 9.99.

Mono-walled compound 10. A mixture of 2.4 g (4.9 mmol) of **2b**, 1.1 g (5.9 mmol) of 1,4-dimethoxynaphthalene and 1.5 mL (12 mmol) of $SnCl_4$ was refluxed under nitrogen for 5 min in 100 mL of degassed 1,2-dichloroethane. After this period 10 mL of aqueous 6N HCl was added and the mixture was refluxed for an additional 15 min. After cooling, CH_2Cl_2 (50 mL) was added and the organic layer was washed with aqueous 1N HCl, aqueous 1N NaOH (2x) and water, and concentrated *in vacuo*. Column chromatography ($CHCl_3$/EtOAc, 95:5 v/v) gave 1.1 g (42%) of **10** as a white solid: Mp 377°C (dec); ^{1}H NMR ($CDCl_3$) δ 8.10 (m, 2H, Napht H-5,8), 7.53 (m, 2H, Napht H-6,7), 7.27-7.00 (m, 10H, ArH), 5.81 and 4.03 (2d, 4H, NCH_2Ar, J = 15.9 Hz), 5.52 and

4.43 (2d, 4H, NCH_2O, J = 11.0 Hz), 4.20 (s, 6H, OCH_3); FAB-MS m/z 549 $(M+H)^+$. Anal. Calcd. for $C_{32}H_{28}N_4O_5$: C, 70.06; H, 5.14; N, 10.21. Found: C, 70.08; H, 5.18; N, 10.15.

Mononitro compound 11a. To an ice-cooled suspension of **7** (0.49 g, 0.99 mmol) in 2 mL of acetic anhydride was *carefully* and *slowly* added 0.5 mL of aqueous 53% HNO_3. The resulting solution was allowed to warm to room temperature and stirred for 16 hrs. A crystalline precipitate was filtered off and washed with acetic acid and cold ethanol. Yield: 0.43 g (80%) of **11a** as a pale yellow solid: Mp 303°C (dec); ^1H NMR ($CDCl_3$) d 7.39 (s, 1H, ArH), 7.22-7.03 (m, 10H, ArH), 5.69, 5.65, 3.95 and 3.84 (4d, 4H, NCH_2Ar, J = 15.8 Hz), 5.51 and 4.43 (br d, 4H, NCH_2O, J = 11.0 Hz), 4.10 and 3.96 (2s, 6H, OCH_3); FAB-MS m/z 544 $(M+H)^+$. Anal. Calcd. for $C_{28}H_{25}N_5O_7$: C, 61.87; H, 4.64; N, 12.88. Found: C, 62.03; H, 4.67; 12.69.

Dinitro compound 11b. To an ice-cooled suspension of **11a** (0.35 g, 0.65 mmol) in 2 mL of acetic anhydride was *carefully* and *slowly* added 1 mL of aqueous 53% HNO_3. The resulting solution was allowed to warm to room temperature. The mixture was stirred for 16 hrs and then poured into 100 mL of water. The product was extracted with 50 mL of CH_2Cl_2. The organic layer was washed twice with aqueous 1N NaOH and with water, and concentrated in vacuo. After purification by column chromatography (CH_2Cl_2/EtOH, 99:1 v/v), 0.35 g (94%) of **11b** was obtained as a pale yellow solid. A sample was recrystallized from acetic acid: Mp 376°C (dec); ^1H NMR ($CDCl_3$) δ 7.30-7.00 (m, 10H, ArH), 5.57 and 3.98 (2d, 4H, NCH_2Ar, J = 15.8 Hz), 5.52 and 4.46 (2d, 4H, NCH_2O, J = 11.0 Hz), 4.19 (6H, OCH_3); FAB-MS m/z 589 $(M+H)^+$. Anal. Calcd. for $C_{28}H_{24}N_6O_9 \cdot (CH_3COOH)$: C, 55.54; H, 4.35; N, 12.96. Found: C, 55.68; H, 4.12; N, 13.05.

Diamino compound 11c. Compound **11b** (0.10 g, 0.17 mmol) was suspended in a degassed mixture of 5 mL of methanol and 5 mL of THF. Palladium on carbon (25 mg) and 0.5 mL (3.4 mmol) of triethylammonium formate were added. The mixture was stirred under nitrogen for 16 hrs and filtered under nitrogen and the residue was washed with CH_2Cl_2 (5 mL). The resulting solution of **11c** was used without purification for further synthesis. An aliquot of the solution was evaporated to dryness for analysis: ^1H NMR ($CDCl_3$) δ 7.25-7.04 (m, 10H, ArH), 5.43 and 3.91 (2d, 4H, NCH_2Ar, J = 15.8 Hz), 5.53 and 4.45 (2d, 4H, NCH_2O, J = 11.1 Hz), 3.92 (s, 6H, OCH_3); the signals of the amino groups were too broad to be detected. FAB-MS m/z 529 $(M+H)^+$. Due to the instability of the compound no satisfactory elemental analysis could be obtained.

Mono-walled compound 12a. A mixture of 0.43 g (0.73 mmol) of **11a**, 50 mg (0.26 mmol) of p-toluenesulfonic acid monohydrate and 2 mL of acetic anhydride was stirred at 110°C for 3 hrs. After cooling, 8 mL of methanol was added and the mixture

was poured in 100 mL of aqueous 2N NaOH. The product was extracted with 2x 50 mL of CH_2Cl_2. The combined organic layers were washed with water, dried ($MgSO_4$) and evaporated to dryness. Yield 0.48 g (95%) of **12a** as a pale yellow solid. A sample was recrystallized from acetic acid: Mp 98-102°C; ^{1}H NMR ($CDCl_3$) δ 7.34-6.82 (m, 10H, ArH), 5.63 and 5.28 (2d, 4H, NC*H*$_2$OAc, *J* = 11.5 Hz), 5.62 and 3.92 (2d, 4H, NC*H*$_2$Ar, *J* = 16.4 Hz), 4.17 (s, 6H, OCH_3), 2.02 (s, 6H, $COCH_3$); FAB-MS *m/z* 631 $(M\text{-}OAc)^+$, 713 $(M+Na)^+$. Anal. Calcd. for $C_{32}H_{30}N_6O_{12}\cdot 0.5(CH_3COOH)$: C, 55.00; H, 4.48; N, 11.66. Found: C, 54.88; H, 4.63; N, 11.63.

Mono-walled compound 12b. Compound **12a** (0.48 g, 0.73 mmol) was stirred under nitrogen for 16 hrs in a mixture of 2 mL of CH_2Cl_2 and 4 mL of $SOCl_2$. The solvent was removed *in vacuo* to yield 0.45 g (100%) of **12b** as a pale yellow hygroscopic solid: ^{1}H NMR ($CDCl_3$) δ 7.37-6.83 (m, 10H, ArH), 5.59 and 3.91 (2d, 4H, NC*H*$_2$Ar, *J* = 16.0 Hz), 5.41 and 5.25 (2d, 4H, NC*H*$_2$Cl, *J* = 11.5 Hz), 4.17 (s, 6H, OCH_3); FAB-MS *m/z* 573 $(M\text{-}2Cl+H)^+$. Due to the instability of the compound no satisfactory elemental analysis could be obtained.

5,7,12,13b,13c,14-Hexahydro-1,4-dihydroxy-8,11-dimethoxy-13b,13c-diphenyl-6*H*,13*H*-5a,6a,12a,13a-tetraazabenz[5,6]azuleno[2,1,8-*ija*]benz[f]azulene-6,13-dione (13). A suspension of 0.77 g (1.5 mmol) of **7** and 0.61 g (3.2 mmol) of p-toluenesulfonic acid monohydrate in 10 mL of degassed 1,2-dichloroethane was refluxed under nitrogen for 10 min over Mol Sieves 4 Å. To the resulting clear solution 0.34 g (3.1 mmol) of hydroquinone was added and the mixture was refluxed over Mol Sieves for an additional 1 hr. After cooling, 5 mL of methanol was added and the precipitate was collected by filtration and washed with methanol. After recrystallization from DMSO, 0.67 g (73%) of **13** was obtained as a white solid: Mp 325°C (dec); ^{1}H NMR (DMSO-d_6) δ 8.76 (s, 2H, OH), 7.28-6.90 (m, 10H, ArH), 6.77 and 6.44 (2s, 4H, ArH), 5.37, 5.26, 3.63 and 3.50 (4d, 8H, NC*H*$_2$Ar, *J* = 15.8 Hz), 3.69 (s, 6H, OCH_3); FAB-MS *m/z* 591 $(M+H)^+$. Anal. Calcd. for $C_{34}H_{28}N_4O_6$: C, 69.14; H, 5.12; N, 9.49. Found: C, 69.24; H, 5.19; N, 9.31.

Clip molecule 14. Compound **13** (0.13 g, 0.22 mmol) was dissolved in 5 mL of DMSO. Cu_2Cl_2 (50 mg) and 0.5 mL of pyridine were added and air was bubbled through the mixture for 2 hrs. The resulting red suspension was poured into 50 mL of aqueous 1N HCl and the product was extracted with 50 mL of $CHCl_3$. The organic layer was washed with aqueous 1N HCl, 5% aqueous NH_3 (2x) and with water (2x), and concentrated *in vacuo*. After purification by column chromatography (CH_2Cl_2/MeOH, 98:2 v/v), 0.10 g (77%) of **14** was obtained as a red solid: Mp 312°C (dec); IR 1734, 1714 (C=O), 1655 (C=C); ^{1}H NMR ($CDCl_3$) δ 7.35-6.85 (m, 10H, ArH), 6.72 and 6.65 (2s, 4H, ArH and CH), 5.64, 5.50, 3.77 and 3.67 (4d, 8H, NC*H*$_2$Ar, *J* = 15.8 Hz), 3.80 (s, 6H, OCH_3); FAB-MS *m/z* 591

$(M+4H)^+$. Anal. Calcd. for $C_{34}H_{28}N_4O_6 \cdot (CH_2Cl_2)$: C, 62.41; H, 4.49; N, 8.32. Found: C, 62.29; H, 4.55; N, 8.38.

Clip molecule 15. Method A: A solution of 0.27 g (0.49 mmol) of **10** and 75 mg (0.54 mmol) of 1,4-dimethoxybenzene in 1 mL of acetic anhydride and 1 mL of trifluoroacetic acid was heated for 1 hr at 95°C. After cooling, 4 mL of methanol was slowly added and the resulting precipitate was filtered off, washed with diethyl ether and dried under vacuum. Yield: 106 mg (97%) of **15** as a white solid.
Method B: A solution of 0.32 g (0.64 mmol) of **7** and 0.24 g (1.29 mmol) of 1,4-dimethoxynaphthalene in 2 mL of acetic anhydride and 2 mL of trifluoroacetic acid was heated for 3 hrs at 95°C. After cooling, 8 mL of methanol was slowly added and the resulting precipitate was filtered off, washed with diethyl ether and dried under vacuum. Yield: 0.30 g (70%) of **15**: Mp 263°C (dec); ^{1}H NMR ($CDCl_3$) δ 8.05 (m, 2H, Napht H-5,8), 7.48 (m, 2H, Napht H-6,7), 7.35-6.95 (m, 10H, ArH), 6.67 (s, 2H, ArH), 5.73, 5.59, 3.94 and 3.79 (4d, 8H, NCH_2Ar, J = 16.0 Hz), 4.08 and 3.76 (2s, 12H, OCH_3); FAB-MS *m/z* 669 $(M+H)^+$. Anal. Calcd. for $C_{40}H_{36}N_4O_6$: C, 71.84; H, 5.43; N, 8.38. Found: C, 72.07; H, 5.36; N, 8.21.

5,7,12,13b,13c,14-Hexahydro-1,4,8,11-tetramethoxy-2,3-dinitro-13b,13c-diphenyl-6*H*,13*H*-5a,6a,12a,13a-tetraazabenz[5,6]azuleno[2,1,8-*ija*]benz[f]azulene-6,13-dione (16a). Starting from **11b** (0.35 g, 0.60 mmol) and 1,4-dimethoxybenzene (90 mg, 0.65 mmol) this compound was synthesized as described for **15** (method A). Yield: 0.40 g (96%) of **16a** as a pale yellow solid. A sample was recrystallized from acetic acid for analysis: IR 1708 (C=O), 1546, 1358 (N-O); ^{1}H NMR ($CDCl_3$) δ 7.30-6.95 (m, 10H, ArH), 6.85 (s, 2H, ArH), 5.61 and 3.80 (2d, 4H, NCH_2Ar, J = 15.9 Hz), 5.52 and 3.88 (2d, 4H, NCH_2Ar, J = 16.4 Hz), 4.07 and 3.82 (2s, 12H, OCH_3); FAB-MS *m/z* 709 $(M+H)^+$. Anal. Calcd. for $C_{36}H_{32}N_6O_{10} \cdot (CH_3COOH)$: C, 59.36; H, 4.72; N, 10.94. Found: C, 59.61; H, 4.59; N, 10.82.

5,7,12,13b,13c,14-Hexahydro-1,4,8,11-tetramethoxy-2,3-diamino-13b,13c-diphenyl-6*H*,13*H*-5a,6a,12a,13a-tetraazabenz[5,6]azuleno[2,1,8-*ija*]benz[f]azulene-6,13-dione (16b). Compound **16a** (0.21 g, 0.30 mmol) was suspended in a degassed mixture of 10 mL of methanol and 10 mL of THF. Palladium on carbon (50 mg) and 1 mL (7 mmol) of triethylammonium formate were added. The mixture was stirred under nitrogen for 16 hrs, filtered under nitrogen, and the residue was washed with CH_2Cl_2 (10 mL). The resulting solution of **16b** was used without purification for further synthesis. An aliquot of the solution was evaporated to dryness for analysis: Mp 311°C (dec); ^{1}H NMR ($CDCl_3$) δ 7.18-6.92 (m, 10H, ArH), 6.71 (s, 2H, ArH), 5.60, 5.36, 3.83 and 3.78 (4d, 8H, NCH_2Ar, J = 15.8 Hz), 5.0-4.0 (br s, 4H, NH_2), 3.82 and 3.77 (2s, 12H, OCH_3); FAB-MS *m/z* 649 $(M+H)^+$. Due to the instability of the compound no satisfactory elemental analysis could be obtained.

Clip molecule 17a. Starting from **9** (0.38 g, 0.69 mmol) and 1,4-dimethoxybenzene (0.11 g, 0.80 mmol) this compound was synthesized as described for **15** (method A). Yield: 0.43 g (93%) of **17a** as a white solid: Mp 317°C (dec); IR 1727, 1712 (C=O); ^{1}H NMR ($CDCl_3$) see Table I; FAB-MS *m/z* 669 $(M+H)^+$.Anal. Calcd. for $C_{40}H_{36}N_4O_6$: C, 71.84; H, 5.43; N, 8.38. Found: C, 71.85; H, 5.43; N, 8.37.

Dinitro compound 17b. To a solution of 0.45 g (0.70 mmol) of **12b** and 0.26 g (1.4 mmol) of 2,7-dimethoxynaphthalene in 40 mL of degassed 1,2-dichloroethane was added 1 mL (8 mmol) of $SnCl_4$. The mixture was refluxed under nitrogen for 3 hrs. After cooling, 4 mL of aqueous 6N HCl was added and the mixture was refluxed for another 30 min. After cooling, 100 mL of aqueous 1N HCl was added and the product was extracted with 2x 50 mL of CH_2Cl_2. The combined organic layers were washed with aqueous 1N NaOH and with water. After evaporation of the solvent, the product was purified by column chromatography (CH_2Cl_2/MeOH, 199:1 v/v). Yield 0.32 g (60%) of **17b** as a pale yellow solid. The compound was recrystallized from acetic acid: Mp 265°C. ^{1}H NMR ($CDCl_3$) *syn*-conformer (65%) δ 7.29 and 6.95 (2d, 4H, NaphtH, *J* = 9.1 Hz), 7.20-6.95 (m, 5H, ArH), 6.45 and 6.18 (2d, 4H, ArH, *J* = 7.0 Hz), 6.28 (t, 1H, ArH, *J* = 7.0 Hz), 6.15 and 5.00 (2d, 4H, NC*H*$_2$Napht, *J* = 14.5 Hz), 5.60 and 3.87 (2d, 4H, NC*H*$_2$Ph, *J* = 16.4 Hz), 4.27 and 3.98 (2s, 12H, OCH_3); *anti*-conformer (35%) δ 7.69 and 7.16 (2d, 4H, NaphtH, *J* = 9.1 Hz), 7.20-6.95 (m, 10H, ArH), 5.93 and 4.11 (2d, 4H, NC*H*$_2$Napht, *J* = 16.4 Hz), 5.41 and 3.78 (2d, 4H, NC*H*$_2$Ph, *J* = 16.4 Hz), 4.04 and 3.89 (2s, 12H, OCH_3); FAB-MS *m/z* 759 $(M+H)^+$. Anal. Calcd. for $C_{40}H_{34}N_6O_{10}$.(CH_3COOH): C, 61.61; H, 4.68; N, 10.26. Found: C, 61.71; H, 4.64; N, 10.20.

Diamino compound 17c. Compound **17b** (0.26 g, 0.34 mmol) was suspended in a degassed mixture of 10 mL of THF and 10 mL of methanol. Palladium on carbon (200 mg) and 1 mL (6.8 mmol) of triethylammonium formate were added. The mixture was stirred under nitrogen for 24 hrs, filtered under nitrogen and the residue was washed with 10 mL of CH_2Cl_2. The filtrate was evaporated to dryness to yield 0.24 g (100%) of **17c** as a pale yellow very hygroscopic solid: ^{1}H NMR ($CDCl_3$) *syn*-conformer (approx. 70%) δ 7.30-6.80 (m, 5H, ArH), 7.10 and 6.88 (2d, 4H, NaphtH, *J* = 9.0 Hz), 6.45 and 6.18 (2d, 4H, ArH, *J* = 7.3 Hz), 6.28 (t, 1H, ArH, *J* = 7.3 Hz), 6.16 and 4.98 (2d, 4H, NC*H*$_2$Napht, *J* = 14.5 Hz), 5.46 and 3.80 (2d, 4H, NC*H*$_2$Ph, *J* = 15.9 Hz), 4.01 and 3.96 (2s, 12H, OCH_3); *anti*-conformer (approx 30%) δ 7.30-6.80 (m, 10H, ArH), 7.65 and 7.16 (2d, 4H, NC*H*$_2$Napht, *J* = 9.0 Hz), 5.97 and 4.19 (2d, 4H, NC*H*$_2$Napht, *J* = 16.1 Hz), 5.38 and 3.72 (2d, 4H, NC*H*$_2$Ph, *J* = 16.1 Hz), 4.05 and 3.69 (2s, 12H, OCH_3); the signals of the amino-protons were too broad to be detected. Due to its instability, the compound was immediately used for further reaction.

Compound 18. Starting from **9** (0.20 g, 0.36 mmol) and 1,4-dimethoxynaphthalene (0.14 g, 0.72 mmol) this compound was synthesized as described for **15** (method B). Yield: 0.17 g (65%) of **18** as a white solid: Mp 322°C (dec); IR 1711 (C=O); ^{1}H NMR ($CDCl_3$) see Table I; FAB-MS *m/z* 719 $(M+H)^+$. Anal. Calcd. for $C_{44}H_{38}N_4O_6$: C, 73.52; H, 5.33; N, 7.79. Found: C, 73.87; H, 5.29; N, 7.72.

Mono-walled phenanthroline compound 19. Compound **11b** (90 mg, 0.15 mmol) was reduced to **11c** as described above. To a solution of **11c** in a mixture of 5 mL of methanol, 5 mL of THF, and 5 mL of CH_2Cl_2 was added 56 mg (0.27 mmol) of 1,10-phenanthroline-5,6-quinone. The mixture was refluxed under nitrogen for 16 hrs, the condensed solvent running back over Mol Sieves 3 Å. CH_2Cl_2 was added (25 mL) and the organic layer was washed with aqueous 1N NaOH, water, and concentrated *in vacuo*. After purification by column chromatography (CH_2Cl_2/EtOH, 93:7 v/v), 84 mg (78%, based on **11b**) of **19** could be obtained as a yellow solid: Mp > 400°C ; ^{1}H NMR ($CDCl_3$) δ 9.60 (dd, 2H, PhenH, *J* = 8.0 Hz, *J* = 2.0 Hz), 9.27 (dd, 2H, PhenH, *J* = 4.7 Hz, *J* = 2.0 Hz), 7.81 (dd, 2H, PhenH, *J* = 8.0 Hz, *J* = 4.7 Hz), 7.36-7.03 (m, 10H, ArH), 6.03 and 4.09 (2d, 4H, NCH_2Ar, *J* = 15.8 Hz), 5.53 and 4.45 (2d, 4H, NCH_2O, *J* = 11.3 Hz), 4.64 (s, 6H, OCH_3); FAB-MS *m/z* 703 $(M+H)^+$. Anal. Calcd. for $C_{40}H_{30}N_8O_5$·(CH3COOH): C, 66.14; H, 4.46; N, 14.70. Found: C, 66.39; H, 4.64; N, 14.57.

Di-phenanthroline clip 20. Compound **16c** (0.53 g, 0.66 mmol) was reduced to **16d** as described above. To a solution of **16d** in a mixture of 20 mL of methanol, 20 mL of THF and 20 mL of CH_2Cl_2, was added 0.33 g (1.6 mmol) of 1,10-phenanthroline-5,6-quinone. The mixture was refluxed under nitrogen for 16 hrs, the condensed solvent running back over Mol Sieves 3 Å. CH_2Cl_2 was added (100 mL) and the organic layer was washed with aqueous 1N NaOH, water, and concentrated *in vacuo*. After purification by column chromatography ($CHCl_3$/MeOH, 9:1 v/v), 0.45 g (66% based on **16c**) of **20** was obtained as a yellow solid: Mp > 400°C; ^{1}H NMR ($CDCl_3$) δ 9.29 (dd, 4H, PhenH, *J* = 8.2 Hz, *J* = 2.0 Hz), 9.08 (dd, 4H, PhenH, *J* = 4.5 Hz, *J* = 2.0 Hz), 7.52 (dd, 4H, PhenH, *J* = 8.2 Hz, *J* = 4.5 Hz), 7.45-7.11 (m, 10H, ArH), 6.03 and 4.05 (2d, 8H, NCH_2Ar, *J* = 16.0 Hz), 4.47 (s, 12H, OCH_3); FAB-MS *m/z* 1027 $(M+H)^+$. Anal. Calcd. for $C_{60}H_{42}N_{12}O_6$·$CHCl_3$: C, 63.91; H, 3.78; N, 14.66. Found: C, 63.81; H, 3.92; N, 14.62.

Mono-phenanthroline clip 21. Compound **16a** (0.56 g, 0.79 mmol) was reduced to **16b** as described above. To a solution of **16b** in a mixture of 20 mL of methanol, 20 mL of THF, and 20 mL of CH_2Cl_2, was added 0.25 g (1.2 mmol) of 1,10-phenanthroline-5,6-quinone. The mixture was refluxed under nitrogen for 16 hrs, the condensed solvent running back over Mol Sieves 3 Å. CH_2Cl_2 was added (100 mL) and the organic layer was washed with aqueous 1N NaOH, with water, and concentrated *in vacuo*. After purification by column chromatography (CH_2Cl_2/EtOH, 93:7, v/v), 0.49 g (75% based

on **16a**) of **21** was obtained as a yellow solid: Mp 392°C (dec); IR 1714 (C=O); ^{1}H NMR ($CDCl_3$) δ 9.49 (dd, 2H, PhenH, *J* = 7.9 Hz, *J* = 2.0 Hz), 9.20 (dd, 2H, PhenH, *J* = 7.9 Hz, *J* = 4.6 Hz), 7.65 (dd, *J* = 7.9 Hz, *J* = 4.6 Hz), 7.32-7.08 (m, 10H, ArH), 6.57 (s, 2H, ArH), 5.99, 5.62, 4.02 and 3.84 (4d, 8H, NCH_2Ar, J = 15.8 Hz), 4.55 and 3.72 (2s, 12H, OCH_3); FAB-MS *m/z* 823 $(M+H)^+$. Anal. Calcd. for $C_{48}H_{38}N_8O_6.CH_2Cl_2$: C, 64.34; H, 4.44; N, 12.34. Found: C, 64.96; H, 4.47; N, 12.18.

Mono-dipyridine clip 22. Compound **16a** (0.19 g, 0.27 mmol) was reduced to **16b** as described above. To a solution of **16b** in a mixture of 10 mL of methanol, 10 mL of THF, and 10 mL of CH_2Cl_2, was added 0.11 g (0.89 mmol) of 2,2'-pyridil. The mixture was refluxed under nitrogen for 16 hrs, the condensed solvent running back over Mol Sieves 3 Å. CH_2Cl_2 was added (50 mL) and the organic layer was washed with aqueous 1N NaOH, water, and concentrated *in vacuo*. After purification by column chromatography ($CHCl_3$/MeOH, 197:3 v/v), 69 mg (31% based on **16a**) of **22** was obtained as a yellow solid: Mp 365 °C (dec); ^{1}H NMR ($CDCl_3$) δ 8.28-8.05 (m, 4H, PyH), 7.91-7.75 (m, 2H, PyH), 7.45-6.95 (m, 12H, PyH and ArH), 6.65 (s, 2H, ArH), 5.88, 5.56, 3.96 and 3.80 (4d, 8H, NCH_2Ar, *J* = 15.8 Hz), 4.34 and 3.75 (OCH_3); FAB-MS *m/z* 825 $(M+H)^+$. Anal. Calcd. for $C_{48}H_{40}N_8O_6$: C, 69.89; H, 4.89; N, 13.58. Found: C, 70.14; H, 4.97; N, 13.24.

Mono-porphyrin clip 23a. Compound **16a** (0.18 g, 0.25 mmol) was reduced to **16b** as described above. The methanol and the THF was evaporated *in vacuo*. To a solution of **16b** in 10 mL of CH_2Cl_2 was added 0.10 g (0.16 mmol) of **24a**. The mixture was refluxed under nitrogen for 16 hrs over Mol Sieves 3 Å. CH_2Cl_2 was added (50 mL) and the organic layer was washed with aqueous 1N NaOH, with water, and concentrated *in vacuo*. After purification by column chromatography (CH_2Cl_2), 180 mg (92% based on **24a**) of **23a** was obtained as a purple solid: Mp 262°C (dec); ^{1}H NMR ($CDCl_3$) δ 8.85 and 8.69 (2d, 4H, β pyrrole, *J* = 5 Hz), 8.68 (s, 2H, β pyrrole), 8.21 (m, 8H, Ar H-2,6 Porphyrin), 7.84 (m, 8H, Ar H-3,5 Porphyrin), 7.76 (m, 4H, Ar H-4 Porphyrin), 7.15 and 7.12 (2s, 10H, ArH), 6.62 (s, 2H, ArH), 5.90, 5.57, 3.89 and 3.80 (4d, 8H, NCH_2Ar, *J* = 15.8 Hz), 3.86 and 3.75 (2s, 12H, OCH_3), -2.53 (br s, 2H, NH); FAB-MS (*m*-nitrobenzylalcohol) *m/z* 1257 $(M+H)^+$.

Mono-porphyrin clip 23b: This molecule was synthesized in an analogous manner to **23a** using **24b** instead of **24a**. ^{1}H NMR ($CDCl_3$) ∂ 8.91 and 8.54 (ABq, 4 H, *J* = 5 Hz, ß pyrrolic H), 8.65 (s, 2 H, ß pyrrolic H), 8.12 (s, 2 H, ArH porphyrin), 8.08 (s, 2 H, ArH porphyrin), 8.01 (s, 2 H, ArH porphyrin), 7.86 (s, 2 H, ArH porphyrin), 7.85 (s, 2 H, ArH porphyrin), 7.77 (s, 2 H, ArH porphyrin), 7.10 (m, 10 H, ArH diphenylglycoluril), 6.46 (s, 2 H, ArH), 5.90 and 3.93 (ABq, 4 H, *J* = 15.8 Hz, NC*H*HAr), 5.44 and 3.69 (ABq, 4 H, *J* =

15.8 Hz, NC*H*HAr) 3.73 (s, 6 H, OMe) 3.62 (s, 6 H, OMe), 1.52, 1.50, 1.41 and 1.26 (4s, 72 H, CCH_3), -2.50 (br s, 2H, NH); FAB-MS (*m*-nitrobenzylalcohol) *m/z* 1706 $(M)^+$.

Nickel salophen compound 25. To a solution of 0.43 g (0.66 mmol) of **16b** in a mixture of 20 mL of THF and 20 mL of methanol were added 0.24 g (1.97 mmol) of 2-hydroxybenzaldehyde and a solution of 0.25 g $Ni(OAc)_2 \cdot 4H_2O$ in 2 mL of methanol. The mixture was stirred under nitrogen for 64 hrs. The solvent was removed *in vacuo* and the residue was suspended in 150 mL of methanol. After filtration, the residue was redissolved in 100 mL of $CHCl_3$. The organic layer was washed with water (3x), dried ($MgSO_4$), and concentrated *in vacuo* to yield 0.40 g (66%) of **25** as a red solid. A sample was recrystallized by slow diffusion of n-hexane in a solution of **25** in $CHCl_3$: Mp 382°C (dec); ^1H NMR ($CDCl_3$) δ 9.15 (s, 2H, NC*H*Ar), 7.32-7.03 (m, 16H, ArH), 6.70 (s, 2H, ArH), 6.62 (t, 2H, ArH, *J* = 7.6 Hz), 5.62, 5.57, 3.86 and 3.77 (4d, 8H, NCH_2Ar, *J* = 15.8 Hz), 3.79 and 3.68 (2s, 12H, OCH_3); FAB-MS *m/z* 913 $(M+H)^+$. Anal. Calcd. for $C_{50}H_{42}N_6O_8Ni \cdot (CHCl_3)$: C, 59.30; H, 4.20; N, 8.14. Found: C, 59.33; H, 4.29; N, 8.01.

Nickel salophen compound 26. To a solution of compound **17c** (0.24 g, 0.34 mmol) in a mixture of 10 mL of THF and 10 mL of methanol, were added 125 mg (1.02 mmol) of 2-hydroxybenzaldehyde and a solution of 127 mg (0.51 mmol) of $Ni(OAc)_2 \cdot 4H_20$ in 1 mL of methanol. The mixture was stirred under nitrogen for 64 hrs. The solvent was removed *in vacuo* and the residue was suspended in 75 mL of methanol. After filtration, the residue was redissolved in 50 mL of $CHCl_3$. The organic layer was washed with water (3x), dried ($MgSO_4$) and concentrated *in vacuo* to yield 0.10 g (31%) of **26** as a red solid: Mp 373°C (dec); ^1H NMR ($CDCl_3$) *syn*-conformer (68%) δ 9.26 (s, 2H NC*H*Ar), 7.36-6.95 (m, 11H, ArH), 7.28 and 6.89 (2d, 4H, NaphtH, *J* = 9.0 Hz),), 6.66 (t, 2H, ArH, *J* = 7.6 Hz), 6.49 and 6.19 (2d, 4H, ArH, *J* = 7.3 Hz), 6.29 (t, 1H, ArH, *J* = 7.3 Hz), 6.15 and 4.98 (2d, 4H, NCH_2Napht, *J* = 14.7 Hz), 5.65 and 3.86 (2d, 4H, NCH_2Ph, *J* = 15.8 Hz), 3.97 and 3.81 (2s, 12H, OCH_3); *anti*-conformer (32%) δ 9.04 (s, 2H, NC*H*Ar), 7.59 and 7.17 (2d, 4H, NaphtH, *J* = 9.0 Hz), 7.36-6.95 (m, 16H, ArH), 6.60 (t, 2H, ArH, *J* = 7.6 Hz), 5.98 and 4.09 (2d, 4H, NCH_2Napht, *J* = 15.9 Hz), 5.50 and 3.88 (2d, 4H, NCH_2Ph, *J* = 15.9 Hz), 4.03 and 3.52 (2s, 12H, OCH_3). see Table II. FAB-MS *m/z* 963 $(M+H)^+$; HRMS (field desorption) calculated for $C_{54}H_{44}N_6O_8Ni$ 962.257, found 962.253.

Mono-phenanthroline compound 27. To a solution of 0.11 g (0.16 mmol) of **17c** in a mixture of 7 mL of THF and 7 mL of methanol, was added 60 mg (0.29 mmol) of 1,10-phenathroline-5,6-quinone. The mixture was refluxed under nitrogen for 64 hrs over Mol Sieves 3Å. After cooling, the precipitate was filtered off and washed with diethyl ether. The product was purified by column chromatography (CH_2Cl_2/MeOH, 93:7 *v/v*) to yield 0.11 g (80%) of **27** as a yellow solid: Mp>400°C; ^1H NMR ($CDCl_3$) *syn*-conformer (68%) δ 9.67 (dd, 2H, PhenH, *J* = 1.5, *J* = 8.2 Hz), 9.29 (dd, 2H, PhenH, *J* = 1.5, *J*

= 4.5 Hz), 7.84 (dd, 2H, PhenH, *J* = 4.5, *J* = 8.2 Hz), 7.32-6.98 (m, 5H, ArH), 7.28 and 6.90 (2d, 4H, NaphtH, *J* = 9.0 Hz), 6.54 and 6.25 (2d, 4H, ArH, *J* = 7.3 Hz), 6.30 (t, 1H, ArH, *J* = 7.3 Hz), 6.17 and 4.98 (2d, 4H, NC*H*$_2$Napht, *J* = 14.9 Hz), 6.08 and 4.01 (2d, 4H, NC*H*$_2$Ph, *J* = 15.9 Hz), 4.72 and 3.99 (2s, 12H, OCH_3); *anti*-conformer (32%) δ 9.50 (dd, 2H, PhenH, *J* = 1.5, *J* = 8.2 Hz), 9.22 (dd, 2H, PhenH, *J* = 1.5, *J* = 4.5 Hz), 7.72 (dd, 2H, PhenH, *J* = 4.5, *J* = 8.2 Hz), 7.47 and 7.02 (2d, 4H, NaphtH, *J* = 8.8 Hz), 7.32-6.98 (m, 10H, ArH), 6.04 and 4.12 (2d, 4H, NC*H*$_2$Napht, *J* = 16.4 Hz), 5.89 and 3.96 (2d, 4H, NC*H*$_2$Ph, *J* = 16.4 Hz), 4.34 and 4.05 (2s, 12H, OCH_3); see Table II. FAB-MS *m/z* 873 $(M+H)^+$; Anal. Calcd. for $C_{52}H_{40}N_6O_8.(CH_2Cl_2)$: C, 66.46; H, 4.42; N, 11.70. Found: C, 66.45; H, 4.45; N, 11.34.

Mono-porphyrin compound 28. To a solution of 0.10 g (0.15 mmol) of **17c** in 7 mL of CH_2Cl_2 was added 250 mg **24b** (0.27 mmol). The mixture was refluxed over Mol Sieves 3Å under nitrogen for 48 hrs. After cooling, the solvent was evaporated and the product was purified by column chromatography (CH_2Cl_2) to yield 70 mg (26%) of **28** as a purple solid: Mp>400°C; ^1H NMR see Table II; FAB-MS *m/z* 1760 $(M+4H)^+$.

References

1 Feiters, M. C. "*Supramolecular Catalysis*" in "*Comprehensive Supramolecular Chemistry*," **1995**, Vol 10, Lehn, J. M. ed., in press.

2 (a) Breslow, R. *Isr. J. of Chem.* **1992**, *32*, 23. (b) Breslow, R. *Recl. Trav. Chim. Pays Bas*, **1994**, *113*, 493. (c) Akkaya, E.U; Czarnik, A.W. *J .Am. Chem. Soc.* **1988**, *110*, 8553. (d) Menger, F.M.; Ladika, M. *J. Am. Chem. Soc.* **1987**, *109*, 3145. (e) Bender, M.L.; Komiyama, M. "*Cyclodextrin Chemistry;*" Springer; Berlin, **1978**. (f) Breslow, R. *Science*, **1982**, *218*, 532. (g) Tabushi, I. *Pure Appl. Chem.*, **1986**, *58*, 1529. (h) Weber, L.; Hommel, R.; Behling, J.; Haufe, G.; Hennig, H. *J. Am. Chem. Soc.* **1994**, *116*, 2400. (i) Kuroda, Y.; Hiroshige, T.; Sera, T; Shirolwa, Y.; Tanaka, H, Ogoshi, H., *J. Am. Chem. Soc.* **1989**, *111*, 1912.

3 Cramer, F. "*Einschlußverbindungen*," Springer, Berlin, **1954**.

4 Anslyn, E.; Breslow, R. *J. Am. Chem. Soc.* **1989**, *111*, 8931.

5 Diederich, F. "*Cyclophanes*," Royal Society of Chemistry; Cambridge, **1991**.

6 Diederich, F.; Lutter, H.-D., *J. Am. Chem. Soc.* **1989**, *111*, 8438.

7 (a) Benson, D. R., Valentekovich, R.; Diederich, F. *Angew. Chem.* **1990**, *102*, 213. (b) Benson, D. R., Valentekovich, R.; Knobler, C.B.; Diederich, F. *Tetrahedron* **1991**, *47*, 2401.

8 (a) Zimmerman, S. C. "*Bioorganic Chemistry Fontriers 2*," **1991**, Springer-Verlag, Berlin. 33-74 and references cited therein (b) Zimmerman, S. C.; Vanzyl, C. M. *J. Am. Chem. Soc.* **1987**, *109*, 7894. (c) Zimmerman, S. C.; Vanzyl, C. M.; Hamilton, G. S. *J. Am. Chem. Soc.* **1989**, *111*, 1373.

9 (a) Whitlock B. J.; Whitlock, H. W. *J. Am. Chem. Soc.* **1994**, *116*, 2301-2311. (b) Whitlock B. J.; Whitlock, H. W. *J. Am. Chem. Soc.* **1990**, *112*, 3910-3915.

10 Collman. J. P.; Zhang, X.; Lee, V. J.; Uifelman, E. S.; Brauman, J. I., *Science* **1993**, *261*, 1404. and references cited therein.

11 (a) Nagasaki, T.; Fujisima, H.; Shinkai, S. *Chem. Lett.* **1994**, 989. (b) Gunter, M. J.; Johnston, M. R.; Skelton, B. W.; White, A. H., *J. Chem. Perkin Trans. I*, **1994**, 1009. (c) Gunter, M. J.; Hockless, D. C. R.; Johnston, M. R.; Skelton, B. W.; White, A. H., *J. Am. Chem. Soc.* **1994**, *116*, 4810. (d) Collman. J. P.; Zhang, X.; Herrmann, P. C.; Uffelman, E. S.; Boitrel, B.; Straumanis, A.; Brauman, J. I. *J. Am. Chem. Soc.* **1994**, *116*, 2681. (e) Kuroda, Y.; Kato, Y.; Ito, M.; Hasegawa, J-y.; Ogoshi, H. *J. Am. Chem. Soc.* **1994**, *116*, 10338. (f) Bonar-Law, R. P.; Mackay, L. G.; Sanders, J. K. M. *J. Chem. Soc. Chem. Commun.* **1993**, 456.

12 (a) Anderson, H. L.; Bashall, A.; Henrick, K.; McPartlin, M.; Sanders, J. K. M., *Angew. Chem.* **1994**, *106*, 445. (b) Walter, C. J.; Anderson, H. L.; Sanders, J. K. M., *J. Chem. Soc. Chem. Commun.* **1993**, 458. (c) Mackay, L. G.; Wylie, R. S.; Sanders, J. K. M., *J. Am. Chem. Soc.* **1994**, *116*, 3141.

13 Cacciapaglia, B.; Casnati, A.; Mandolini, L.; Ungaro, R. *J. Am. Chem. Soc.* **1992**, *114*, 10956.

14 (a) Sijbesma, R. P.; Wijmenga, S. S.; Nolte, R. J. M. *J. Am. Chem. Soc.* **1992**, *114*, 9807. (b) Smeets, J. W. H; Sijbesma, R. P.; van Dalen, L.; Spek, A. L.; Smeets, W. J. J.; Nolte, R. J. M. *J. Org. Chem.* **1989**, *54*, 3710. (c) Sijbesma, R.P.; Kentgens, A.P.M.; Nolte, R.J.M.; *J. Org. Chem*, **1991**, *56*, 3199. (d) Sijbesma, R. P.; Kentgens, A. P. M.; Lutz, E. T. G.; van der Maas, J. H.; Nolte, R. J. M. *J. Am. Chem. Soc.* **1993**, *115*, 8999.

15 Sijbesma, R. P.; Kentgens, A. P. M.; Nolte, R. J. M. *J. Org. Chem.* **1991**, *56*, 3122.

16 (a) Coolen, H. K. A. C.; van Leeuwen, P. W. N. M.; Nolte R. J. M. *Angew. Chem.* **1992**, *31*, 905. (b) Coolen, H. K. A. C.; Meeuwis, J. A. M.; van Leeuwen, P. W. N. M.; Nolte R. J. M *J. Am. Chem. Soc.* **1995**, *117*, 11906.

17 Martens, C. F.; Klein Gebbink, R. J. M.; Feiters, M. C.; Nolte, R. J. M. *J. Am. Chem. Soc.* **1994**, *116*, 5667.

18 Gosling, P. A.; Sijbesma, R. P.; Spek, A. L.; Nolte, R. J. M. *Recl. Trav. Chim. Pays-Bas* **1993**, *112*, 404.

19 Cortese, N.A.; Heck, R.F. *J. Org. Chem.*, **1977**, *42*, 3491, and references cited therein.

20 (a) Smith, G.; Cagle, Jr., F.W. *J. Org. Chem.* **1947**, *12*, 781. (b) Koft, E.; Case, F. H. *J. Org. Chem.* **1962**, *27*, 865. (c) Dickeson, J.; Summers, L. *Aust. J. Chem.* **1970**, *23*, 1023.

21 Crossley, M.J.; King, L.J. *J. Chem Soc., Chem. Commun.* **1984**, 920.

22 Johnson, C. S., Jr.; Bovey, F. A. *J. Chem. Phys.* **1958**, *29*, 1012.

23 Hunter, C. A.; Sanders, J. K. M. *J. Am, Chem. Soc.* **1990**, *112*, 5525.

Chapter 3

Binding Features of Molecular Clips. Separation of the Effects of Hydrogen Bonding and π-π Interactions

3.1 INTRODUCTION

Molecular recognition continues to be a topic of great interest in supramolecular and biomimetic chemistry.[1,2] Depending upon the function and the need of selectivity in the process of molecular recognition, several types of interactions can play a role. In aqueous solution the hydrophobic effect often is the main driving force for host-guest complex formation,[3] which can lead to very high association constants for natural as well as synthetic systems. The selectivity of the binding can be improved if additional interactions are involved, such as hydrogen bonding, electrostatic interactions, Van der Waals forces, and π-π stacking interactions. When these interactions are highly complementary and directional, the binding process will be completely selective as in the case of the mutual recognition of DNA base pairs, which has served as an example for the design of many synthetic hosts capable of binding guests according to the same complementarity principles.[4] The approach of using a combination of interactions is particularly important for receptors in organic solvents, because here the hydrophobic effect is lacking. Rebek et al. have used this approach to develop host systems that can bind guests based on hydrogen bonding and π-π stacking.[5] The latter interaction is possible because of the presence of an adjacent aromatic surface, which also induces a higher degree of preorganization. An even higher degree of preorganization is achieved with two aromatic surfaces adjacent to the hydrogen bonding site resulting in tweezer type receptor molecules, as synthesized by Zimmerman.[6] Whitlock et al. have shown that by carefully tuning the cavity size, very high association constants in chloroform can be achieved.[7]

A general thorough understanding of the mechanism of complex formation in organic solvents is important for future development and design of host-guest systems and supramolecular devices. Towards this goal we have been designing and studying receptor molecules based on diphenylglycoluril (DPG) which are capable of binding

dihydroxybenzenes.[8] Clip molecule **1** has a preorganized cleft, which can bind a guest by hydrogen bonding with the urea carbonyl groups and π-π stacking interactions with the aromatic walls. Clip molecule **2** is capable of complexing aromatic guests by π-π interactions only.[9] To examine the binding forces in our host-guest complexes more precisely, we have synthesized a series of new receptor molecules based on the diphenylglycoluril building block (see Chart I). Here we present binding studies and computational investigations, that allow us to more fully understand and quantify the contributions of the different intermolecular interactions that play a role in host-guest binding with these systems.

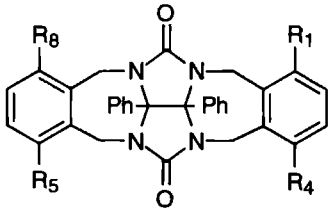

1

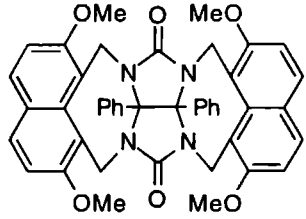

2

3.2 RESULTS AND DISCUSSION

3.2.1 Hydrogen bonding, π-π interactions and cavity effects

As depicted in Figure 1, clip molecules of type **1** contain a cleft with a cavity size of approximately 6.4 Å (center-to-center distance) which is ideal to sandwich aromatic guest molecules in between. From our earlier studies[8] it is known that the main binding interactions in the formation of complexes of dihydroxybenzenes with

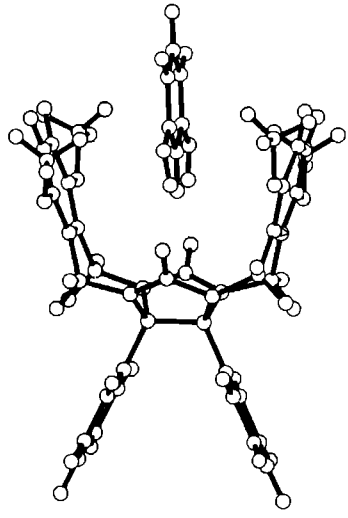

Figure 1. *Binding of an 1,3-dihydroxybenzene guest molecule between the aromatic side-walls of clip* ***1a****, due to hydrogen bond formation and π-π stacking interactions.*

molecular clip **1a** in chloroform are: *(i)* hydrogen bonding between the OH groups of the guest and the urea carbonyl functions of the host; *(ii)* π-π interactions between the aromatic surfaces of the guest and the host. It is of use to be able to manipulate the strength of complexation and to thoroughly understand the processes involved in binding. Towards this goal the complex formation between a series of receptor molecules (Chart I) and guest molecules (see Table 1) were studied. The influence of the hydrogen bond donor (guest), the hydrogen bond acceptor (host), the presence and size of the cavity wall of the host, and the substituents on the host and guest upon binding will be discussed. Binding affinities are calculated from ^{1}H NMR titrations experiments, which provide association constants (K_a's) and Complex Induced Shift (CIS) values, the latter being the maximum shift for a given proton of the host or guest, when the complex is completely formed. In addition IR studies and calculations have been performed. Some clip molecules formed dimers by self-complexation in solution (*vide infra*), which is a possible competition for the guest complexation. The self-complexation constants in general were so low, that the guest complexation was not influenced. It was not necessary therefore, to take this self-complexation into account in the calculations of the association constants.

Influence of the hydrogen bond donor on binding

In previous work it was shown from binding studies of clip molecules with 1,2-dihydroxybenzene, 1,3-dihydroxybenzene and 2,7-dihydroxynaphthalene that the O-H-O angle of the hydrogen bond has a substantial influence on the strength of the bond and hence on the association constant.[8] The strength of this hydrogen bond is also expected to be depend upon the type of donor, e.g. in the series 1,3-dihydroxybenzene > 1,3-diaminobenzene > 1,3-dithiohydroxybenzene. It has been reported by Abraham[11] that for complexes, purely based on hydrogen bonding, the strength is proportional to the hydrogen bond acidity of the donor. In line with this work, we measured the binding strength of complexes between **1a** and the above mentioned guests and found that the strength drops with decreasing acidity of the guest molecule, *viz.* from K_a = 2600 M^{-1} (1,3-dihydroxybenzene) to K_a = 65 M^{-1} (1,3-diaminobenzene) to K_a = 0 M^{-1} (1,3-dithiohydroxybenzene). The acidity of the OH groups of 1,3-dihydroxybenzenes can simply be varied by using different substituents on the 5-position of the guest molecule (Table 1). The strength of the complexation with clip **1a** was found to change significantly when the substituent was varied (Table 2). 3,5-Dihydroxypentylbenzene (**G1**), which has a slightly electron releasing substituent, has a K_a = 1500 M^{-1} and a binding energy ΔG_b = -18.1 kJ/mol which is about 10 kJ/mol lower than that of 3,5-dihydroxycyanobenzene (**G8**, K_a = 10^5 M^{-1}, ΔG_b = -28.5 kJ/mol) which contains an electron withdrawing substituent.

Chart I

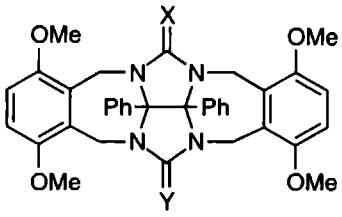

1a X,Y=O
1b X=S Y=O
1c X,Y =S

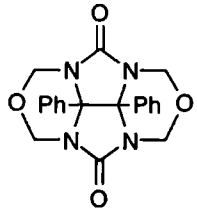

3

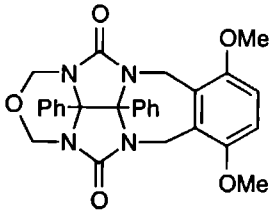

4

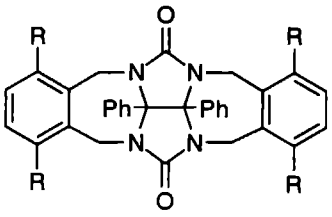

5a R=Me
5b R=H

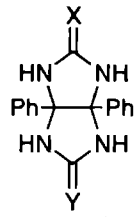

6a X,Y=O
6b X=S Y=O
6c X,Y =S

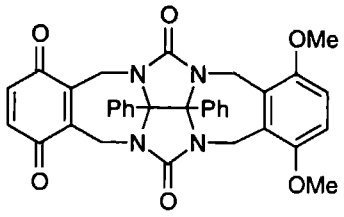

7

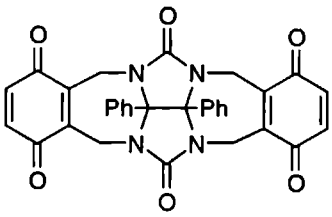

8

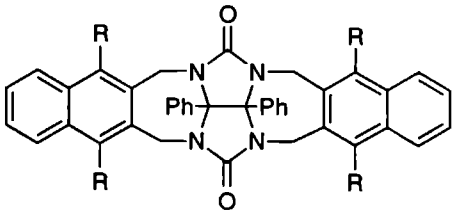

9a R = OMe
9b R = H

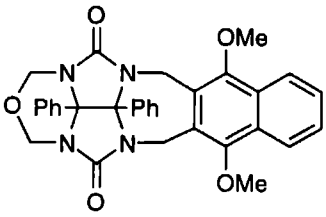

10

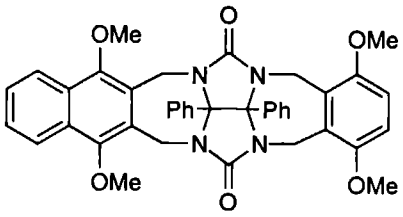

11

Table 1 *The substituted (R) 1,3-dihydroxybenzene guest molecules used for binding studies with the clip molecules in chloroform and the Hammett substituent constants (σ_m (R))*

	guest	R	σ_m (R)[a]
G	G1	C_5H_{11}	-0 08
R	G2	CH_3	-0 07
	G3	H	0 00
	G4	$CHCH_2$	0 06
	G5	OCH_3	0 12
	G6	$COOCH_3$	0 37
	G7	Cl	0 37
	G8	CN	0 56

[a] Values are taken from ref 10

A plot of the binding energy as function of the Hammett constant (σ_m (R)) of the substituent of the guest, which in turn is related to the acidity of the OH groups, gives a good linear correlation (Figure 2) An identical binding study was carried out with substituted phenols as guest molecules In the case of these guests only one hydrogen bond can be formed with the urea carbonyls of the host As seen for the 1,3-dihydroxybenzene derivatives an increase in binding was observed as the substituent became more electron withdrawing (Table 2) The binding strength of the phenolic

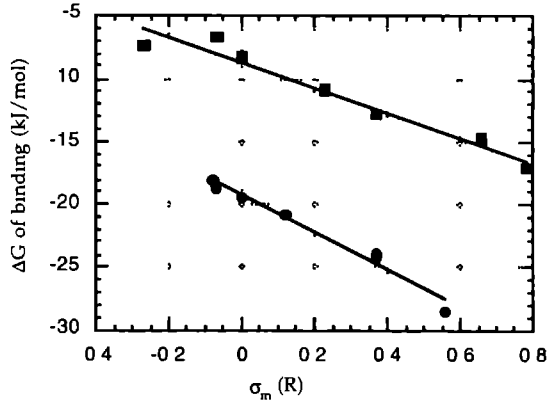

Figure 2. *Binding free energies of various 1,3-dihydroxybenzene (•) and hydroxybenzene (■) guest molecules in clip* ***1a****, plotted as function of the Hammett parameter (σ_m (R)) of the guest substituent*

guests, however, was found to be less dependent upon the substituent when compared to the binding strength of 1,3-dihydroxybenzene guests (see Figure 2, gradient being -10 0 compared to -14 7) This is a result of the fact that the substituent on the guest changes the strength of only one hydrogen bond in the case of the phenolic guest molecule

Table 2: *Association constants measured for receptor* ***1a*** *and different substituted phenols and 1,3-dihydroxybenzenes in chloroform.*[a]

Guest	Ka (M^{-1})	Guest	Ka (M^{-1})
4-Methoxyphenol	20 (15)	**G1**	1500 (200)
3-Methylphenol	15 (10)	**G2**	1900 (75)
Phenol	29 (5)	**G3**	2600 (200)
4-Chlorophenol	80 (10)	**G5**	4400 (300)
Methyl-3-		**G6**	16500 (2000)
hydroxybenzoaat	160 (15)	**G7**	16000 (2000)
4-Cyanophenol	415 (50)	**G8**	$1*10^5$ ($5*10^4$)
4-Nitrophenol	1200 (60)		

[a]Errors are given in parenthesis.

Influence of the hydrogen bond acceptor on binding

If one or two of the carbonyl oxygen atoms of **1a** are replaced by sulphur atoms (**1b** and **1c**, respectively), which are known to be very poor hydrogen bond acceptors,[11] the observed complexes formed with 1,3-dihydroxybenzenes are much weaker (Table 3). Again, however, a linear correlation was found, between the Hammett constant and the strength of binding (Figure 3a). Examination of the plots for each series reveals that the average binding strength in clip **1b**, which possesses one carbonyl and one thiocarbonyl group, is not exactly midway between those for **1a** and **1c**. This is due to the fact that when only one hydrogen bond is formed, a more optimal geometry is possible, resulting in a stronger bond (the single OH-O hydrogen bond in the complexes formed with **1b** is stronger than each of the hydrogen bonds formed with **1a**). The optimal geometry of complexation to two carbonyl functions appears to be slightly different from that to one carbonyl function. This is confirmed by the ^1H NMR CIS values of the different side-wall protons of clip **1b**, which indicate that the guest is unsymmetrically bound within the cleft, shifted towards the single carbonyl group (see Figure 4). This offset geometry is also predicted by Molecular Mechanics calculations.[12] The slope in the plot of the binding energy (ΔG_b) as function of the Hammett constant (σ_m (R)) decreases when the two carbonyls are replaced by thiocarbonyl groups (Figure 3A), but is not zero. As will be shown below, the contribution of hydrogen bonding to the binding can be neglected in the case of complexation of guest molecules in clip **1c**. In this host, binding is solely based upon interactions between the aromatic walls of the cleft and the aromatic guest.

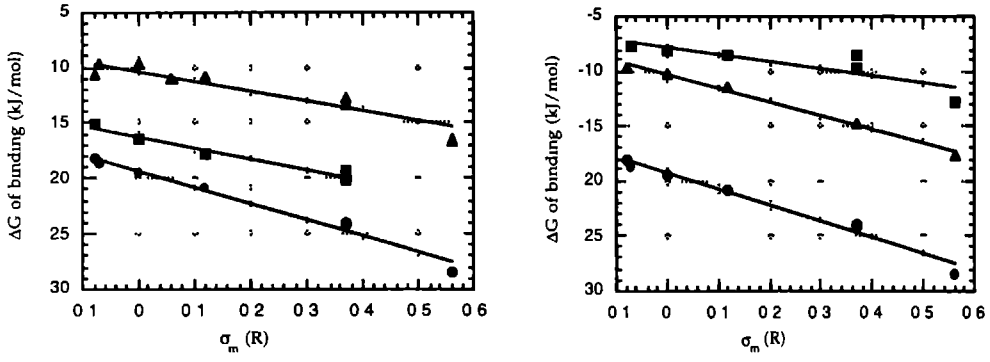

Figure 3. Binding free energies of various guest molecules (see Table 1) in clip molecules containing different hydrogen bond acceptors sites (Figure A, **1a**, •, **1b**, ■, **1c**, ▲) and a different number of side-walls (Figure B, **1a**, •; **3**, ■, **4**, ▲) plotted as a function of the Hammett constant (σ_m (R)) of the guest substituent (R)

Table 3 *Association constants and binding free energies (in kJ/mol) for host molecules containing different hydrogen bond acceptors sites with different 1,3-dihydroxybenzene guest molecules* [a]

Guest	Host **1a**			Host **1b**			Host **1c**		
	Ka	ΔG	CIS[b]	Ka	ΔG	CIS[b]	Ka	ΔG	CIS[b]
G1	1500 (200)	-18 1 (0 2)	-2 45	c	c	c	74 (15)	-10 7 (0 7)	-1 79
G2	1900 (75)	-18 7 (0 1)	-2 48	450 (40)	-15 1 (0 2)	-2 40	56 (10)	-9 8 (0 4)	-1 79
G3	2600 (200)	-19 5 (0 2)	-2 61	750 (100)	-16 4 (0 3)	-2 40	51 (4)	-9 7 (0 2)	-2 10
G4	c	c	c	c	c	c	86 (5)	-11 0 (0 1)	-2 16
G5	4400 (300)	-20 8 (0 2)	-2 56	1300 (230)	-17 8 (0 5)	-2 30	82 (15)	-10 9 (0 5)	-1 95
G6	16500 (2000)	-24 1 (0 3)	-2 75	2500 (200)	-19 4 (0 2)	-2 76	177 (12)	-12 8 (0 2)	-2 32
G7	16000 (2000)	-24 0 (0 3)	-2 82	3500 (180)	-20 2 (0 1)	-2 67	225 (15)	-13 4 (0 2)	-2 52
G8	$1*10^5$ ($5*10^4$)	-28 5 (2 2)	-2 95	c	c	c	772 (75)	-16 5 (0 2)	-2 46

[a]Errors are given in parenthesis [b]Complexation Induced Shift (CIS) values for the H^2 proton of the guest molecules [c]Not determined

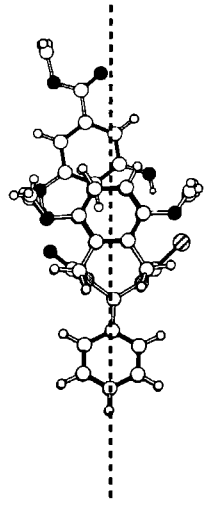

Figure 4. *Binding geometry of guest molecule G6 in clip 1b, as determined by Molecular Mechanics calculations (CHARMm Force Field) which is in agreement with the experimentally determined CIS values*

Influence of the cavity wall on binding

The substituent dependency observed for the binding strength in clip **1c**, suggests that other factors than hydrogen bonding are influenced when the substituent on the guest is changed The electron density on the aromatic ring of the guest, and therefore the interaction of this ring with the π-systems of the walls of the host, is also dependent upon the substrate substituent To examine the factors involved in the π-π interactions, binding affinities of the guests were measured with clip molecules possessing no, one or two cavity walls (**3**, **4**, **1a**, Figure 5) Comparison between the

Table 4 *Association constants and binding free energies (in kJ/mol) for host molecules with a different number of aromatic side-walls* [a]

Guest	Host **1a**			Host **3**			Host **4**		
	Ka	ΔG	CIS[b]	Ka	ΔG	CIS[c]	Ka	ΔG	CIS[b]
G1	1500	-18 1	-2 45	23	-7 8	1 47	50	-9 7	-0 96
	(200)	(0 2)		(5)	(0 4)		(10)	(0 5)	
G3	2600	-19 5	-2 61	25	-8 0	1 59	65	-10 3	-1 09
	(200)	(0 2)		(10)	(1 2)		(10)	(0 4)	
G5	4400	-20 8	-2 56	32	-8 6	1 51	105	-11 5	-1 20
	(300)	(0 2)		(12)	(1 1)		(15)	(0 4)	
G6	16500	-24 1	-2 75	30	-8 4	1 72	d	d	d
	(2000)	(0 3)		(15)	(1 7)				
G7	16000	-24 0	-2 82	52	9 8	1 85	385	-14 7	-1 24
	(2000)	(0 3)		(20)	(1 2)		(25)	(0 2)	
G8	$1*10^5$	-28 5	-2 95	175	12 8	1 88	1250	-17 7	-1 34
	($5*10^4$)	(2 2)		(30)	(0 5)		(100)	(0 2)	

[a]Errors are given in parenthesis [b]Complexation Induced Shift (CIS) values for the H^2 proton of the guest molecules [c] (CIS) values for the OH protons of the guest molecules [d]Not determined

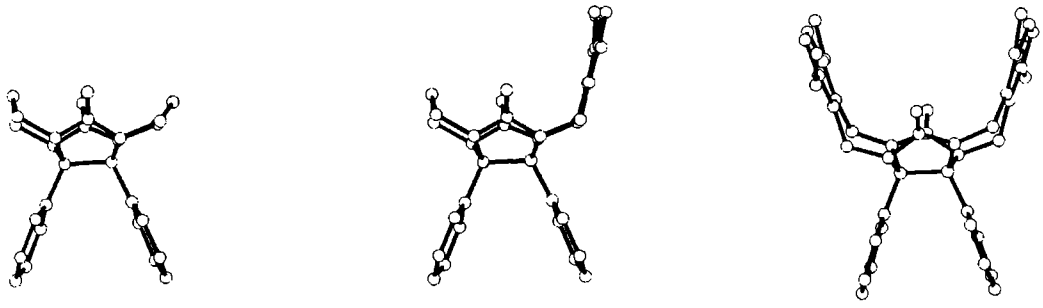

3 **4** **1a**

Figure 5. *X-ray structures showing the difference between a clip-shaped molecule* **1a** *and molecules in which binding is based upon hydrogen bonding only (***3***) and hydrogen bonding assisted by an aromatic moiety (***4***). Hydrogens have been omitted for clarity. The X-ray structures of* **3** *and* **1a** *have been published,[8,13] that of* **4** *will be published elsewhere.[14]*

three structures indicates that in case of **3** the binding can only be based upon hydrogen bonding. In the case of **4** this hydrogen bonding can be assisted by a single π-π interaction between the guest and one side-wall, and in the case of **1a** by π-π interactions with two side-walls. From the X-ray structures it is clear that there are no geometric differences in the diphenylglycoluril frame work of the molecules. Any difference in the binding properties between **1a** and **4**, therefore, must be a result of the specific cleft-shape of **1a**. The results of the binding studies with molecules **3**, **4** and **1a** and different guests are summarized in Table 4 and Figure 3b. In general the binding constants of guest molecules to host **4** are only slightly higher than those to molecule **3**. Figure 3b shows that the slope of the curve of the binding energy versus the Hammett constant for complexation to compound **4** is larger (-12.5) than that for complexation to compound **3** (-6.3). From this result we can conclude that there is a π-π interaction between the guest molecule and the side-wall of **4**, since binding to **4** is much more substituent dependent than the binding to **3**. Comparison of these data with those obtained for clip **1a**, clearly reveals that the addition of a second side-wall to the host, which result in the formation of a cleft, significantly increases the association constants. Zimmerman has observed a similar increase in binding for his molecular tweezers[6] when a second aromatic surface was added. In the case of the receptor with only one wall, **4**, the translational and rotational entropy effects are cancelled out by the favourable enthalpic effect. This entropy effect is already accounted for when the second wall is added. A guest bound to this receptor has an extra π-stacking interaction which is free from loss in entropy, resulting in a higher binding constants. Whitlock[7], Cram[15] and Collet[16] have all shown that the 'snugness' of fit between the host and guest plays a significant role in the binding. The better the fit, the larger the Van der

Waals contact. Collet[16] and Still[17] observed an additional solvation effect for their cavity containing hosts. In solvents that fitted poorly within the cavities, the binding constants of the host-guest complexes were significantly higher. In our case, chloroform molecules are too big to solvate the cavity, and upon complexation of the guest the cleft is favourably filled. The overall complex is much better solvated than the two individual components. We believe that when the second wall is added to our host molecule, the three above mentioned effects play a role: *(i)* the second π-π interaction in the case of binding to **1a** is free from entropy losses *(ii)* a larger Van der Waals contact between the host and the guest molecule occurs as a result of the guest being sandwiched between two aromatic side-walls of the host *(iii)* a favourable solvation effect arises because the cavity is too small to be solvated by the solvent molecules. The combined features *(i)* and *(iii)* can be described as the 'the cavity effect'. This effect together with *(ii)* makes that **1a** is a better receptor molecule than **4**.

Effects of substituents on the cavity wall

As outlined above the electron density on the aromatic ring of the guest influences the π-π interaction between the host and the guest. In a similar manner substituents on the aromatic walls of the host can affect the π-π interaction. In order to investigate this in more detail clips **5a** and **5b**, having different substituents on the aromatic wall, were compared to **1a**. The binding affinities of **1a**, **5a** and **5b** for different guest molecules are presented in Figure 6 and Table 5. Changing the methoxy groups of clip **1a** for methyl groups (**5a**) decreases the binding strength significantly. The clip molecule with simple unsubstituted benzene rings as side-walls (**5b**), has an even lower affinity for the dihydroxybenzene guest molecules. These differences are mainly due to changes in the strength of the π-π interactions and the size of the cavity. A stronger π-π interaction between the host and the guest results in a larger dependency of the ΔG of binding on the Hammett parameter σ_m (R)), giving a larger slope for **1a** compared to **5a** and **5b** in the plot of the binding energy versus σ_m (R). The 'cavity effect' will also be slightly different for clips **1a**, **5a** and **5b**, since the size of the cavity increases when the substituents on the side-walls are larger. It should be noted that the side-wall substituent may also change the solvation of the urea carbonyl groups and in this way affect the binding affinity, but since the difference in the hydrogen bonding properties between **1a** and **3** is small, this effect is not expected to contribute significantly.

Separation of the factors determining the binding affinities

The results of the binding studies allow us to estimate what contribution each of the different interactions has on the binding of 1,3-dihydroxybenzene derivatives in the clip molecules. This can be done by examining the fitted curves of the binding energy

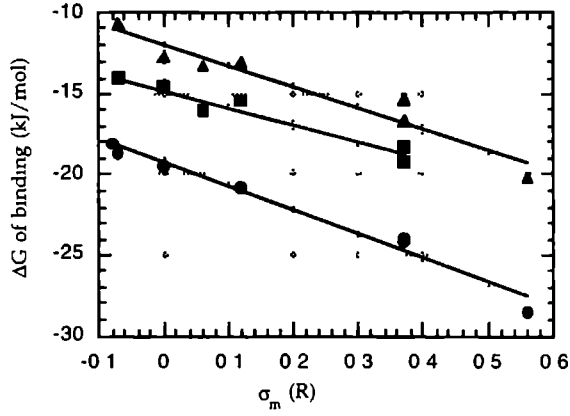

Figure 6 *Binding free energies of various guests in clip molecules having different substituents on their side-walls (**1a**, •, **5a**, ■, **5b**, ▲),plotted as function of the Hammett constant (σ_m (R)) of the guest substituent (R)*

Table 5 *Association constants and binding free energies (in kJ/mol) for host molecules with different aromatic walls* [a]

Guest	Host **1a**			Host **5a**			Host **5b**		
	Ka	ΔG	CIS[b]	Ka	ΔG	CIS[b]	Ka	ΔG	CIS[b]
G2	1900 (75)	-18 7 (0 1)	-2 48	290 (30)	-14 1 (0 3)	-2 63	74 (15)	-10 7 (0 5)	-1 97
G3	2600 (200)	-19 5 (0 2)	-2 61	360 (20)	-14 6 (0 1)	-2 93	175 (15)	-12 8 (0 2)	-2 33
G4	c	c	c	670 (30)	-16 1 (0 1)	-2 85	215 (20)	-13 3 (0 2)	-2 41
G5	4400 (300)	-20 8 (0 2)	-2 56	510 (20)	-15 4 (0 1)	-2 84	195 (20)	-13 1 (0 3)	2 37
G6	16500 (2000)	-24 1 (0 3)	-2 75	1600 (250)	-18 3 (1 3)	-3 41	475 (30)	-15 3 (0 2)	-2 97
G7	16000 (2000)	-24 0 (0 3)	-2 82	2400 (200)	-19 3 (0 2)	-3 02	850 (50)	16 7 (0 2)	-2 88
G8	$1*10^5$ ($5*10^4$)	-28 5 (2 2)	-2 95	c	c	c	3500 (400)	-20 2 (0 3)	-3 07

[a]Errors are given in parenthesis [b]Complexation Induced Shift (CIS) values for the H^2 proton of the guest molecules [c] Not determined

versus the Hammett constant for the different clips (equations 1-5) Assuming that hydrogen bonding to the thiocarbonyl groups has a negligible contribution to the binding energy,[18] equation (1) for clip **1c** gives the contribution of the two walls to the binding free energy Equation (2) obtained for clip molecule **3** describes the contribution of the hydrogen bonding to this energy (it is assumed that there is no difference in solvation of the carbonyl groups in the case of **1a** compared to **3**) The

sum of equations (1) and (2) (see equation 3) must be equal to the equation for binding to clip molecule **1a** (equation 4). It can be seen that a reasonable agreement is obtained.

Clip **1c** (2 x π-π interaction + cavity effect)	$-\Delta G = 10.4 + 9.1\sigma$	(kJ/mol)	(1)
Clip **3** (hydrogen bonding)	$-\Delta G = 7.8 + 6.3\sigma$	(kJ/mol)	(2)
Equation (1) + (2)	$-\Delta G = 18.1 + 15.4\sigma$	(kJ/mol)	(3)
Clip **1a**	$-\Delta G = 19.3 + 14.7\sigma$	(kJ/mol)	(4)
Clip **4** - clip **3** (1x π-π interaction)	$-\Delta G = 2.5 + 6.3\sigma$	(kJ/mol)	(5)

Since molecule **4** has only one aromatic wall and hence does not possess a cavity, the π-π interaction energy for one wall can be obtained by subtracting the equation for **3** from the one for **4**, giving equation (5). The cavity effect, which can be considered to be independent of the substituent of the guest, can then be estimated by subtracting twice the π-π interaction of one wall (equation 5) and the hydrogen bond contribution (equation 2) from the equation for **1a**. This gives a value of approximately 6 kJ/mol.†

ΔH and ΔS of binding

The thermodynamic parameters ΔH and ΔS for the binding of the guest 1,3-dihydroxybenzene in a series of clips were determined by ^{1}H NMR titrations at six different temperatures (270, 280, 298, 305, 318 and 328K). The results are presented in Table 6. It can be concluded that the binding is enthalpy driven. Examination of the values reveals that on going from clip **1a** to **1c**, both ΔH and ΔS decrease by a factor of 2, which is in line with the linear relation between ΔH and ΔS reported in the literature for hydrogen bond formation.[19] The increases in ΔH and ΔS for binding to **1a** as compared to **4** are both quite large as expected, indicating that the cavity effect involved in the binding to **1a** consists of both an enthalpic as well as an entropic term.

Table 6: *ΔH and ΔS of binding for complexes between 1,3-dihydroxybenzene and different clip molecules in chloroform.*[a]

	1a	**1a**[b]	**1c**	**4**	**7**
ΔH (kJ/mol)	-38	-10	-20	-17	-31
ΔS (J/mol·K)	-63	0.6	-31	-27	-53

[a]Estimated error 20%. [b]Measured in chloroform/acetonitrile (1:1 v/v).

† The fact that the π-π interaction between the guest and the second side-wall might not be optimal is neglected.

The ΔS value for binding in **1a** is approximately zero in the solvent mixture acetonitrile/chloroform (1:10, v/v) (Table 6), and binding is determined by a small negative enthalpy factor only. This is because acetonitrile solvent molecules are small enough to fit into the cleft of **1a**, resulting in a better solvation of the cleft and hence in a smaller cavity effect.

Geometry of the complexes

From the ^{1}H NMR experiments the Complex Induced Shift (CIS) values can be determined, which are the differences in chemical shifts between the fully bound and the unbound species. The CIS value is dependent upon the complex geometry. A computer program was written, based on the Johnson and Bovey tables, which calculates using ring current shifts, the approximate CIS values of certain protons in the host-guest complex.[8,20] The CIS values for the H2 proton of the 1,3-dihydroxybenzene guest molecules were calculated to increase if the guests are bound more deeply in the cleft of the clips. The CIS values also increased if the side-walls of the clip are positioned closer together.

Using this program and the experimentally obtained CIS values, the insertion depth of the guest within the cavity of the clip was calculated. The general trend for all clips of type **1** was that guest molecules with more electron rich aromatic rings, are bound less deeply within the cleft of the host molecule. The maximum difference in binding depth for the different guests was 0.3-0.4 Å for clip **1a**. In the case of clip **1c** a similar variation in binding depth was observed. The guests, however, were generally bound more deeply in clip **1a** than in **1c**, which resulted in a smaller variation of the CIS values for complexes with the former host. It should be noted that the CIS values do not vary linearly with the depth of binding. In clip **1c** the binding is based on π-π interactions and the cavity effect, whereas in clip **1a** hydrogen bonding is also a very important factor. The results obtained with **1a** and **1c** suggest that the optimal distance for π-π interaction is further out of the cavity than the optimal distance for hydrogen bonding. Thus, when a guest is bound in clip **1a** the hydrogen bonds are pulling it inside the cleft. In order to achieve an optimum π-π interaction the cavity walls are pushing the guest slightly out of the cavity. The resulting complex geometry with the host is a compromise between these two forces.

The complexes formed between the different 1,3-dihydroxybenzenes and the clip molecules were also studied by IR spectroscopy measurements in $CHCl_3$ solution. In an earlier study we showed that the hydrogen bonds of the guest are directed towards the π electrons of the urea carbonyl functions.[8] In the present study we looked at the

influence of the guest substituent on the difference in the OH stretching frequency of the bound and the unbound guest ($\Delta\nu = \nu_{unbound} - \nu_{bound}$, Figure 7) In the case of

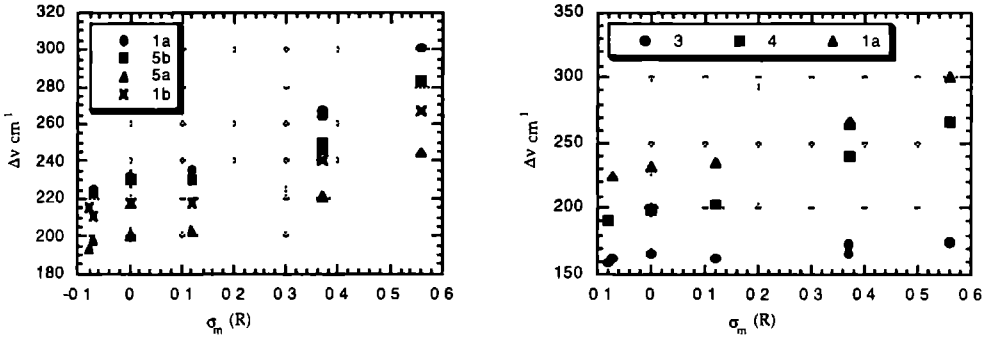

Figure 7 *Difference in OH stretching frequency between the bound and the unbound guest as function of the Hammett constant (σ_m (R)) of the guest substituent (R) for various clip molecules*

molecule **3**, which binds substrates by means of hydrogen bonds exclusively, the OH stretching frequency was only very slightly substituent dependent[21] ($\Delta\nu$ = 162-174 cm^{-1}) This suggests that a stronger hydrogen bond to the π-electrons of the urea carbonyl functions, as observed for guests with an electron withdrawing group, does not result in a larger difference in OH stretching frequency For clip molecules **1a**, **1b**, **5a**, and **5b**, the differences in OH stretching frequencies varied significantly (e g $\Delta\nu$ = 225-301 cm^{-1} for clip **1a**) This can be explained in terms of hydrogen bond length This length will be optimal for complexes formed with **3**, since hydrogen bonding is the only force holding the complex together, and this length does not vary significantly for the different substrate molecules When aromatic side-walls are involved in binding, π-π effects influence the depth of binding An electron releasing group on the dihydroxybenzene guest, forces the molecules to be bound slightly further outside the cleft, which makes the distance between the OH function and the urea carbonyl function longer This results in a smaller $\Delta\nu$ for the OH stretching frequency between the bound and unbound species In the case of clips **5a** and **5b** the π-π interaction was observed to be smaller, resulting in smaller binding constants, which is also reflected in a smaller difference in the OH stretching frequency ($\Delta\nu$ = 194-245 cm^{-1} for clip **5a** and $\Delta\nu$ = 223-283 cm^{-1} for clip **5b**) Remarkably, the variation in $\Delta\nu$ values for complexes with molecule **4** ($\Delta\nu$ = 191-266 cm^{-1}) were similar to those found for clip **1a** This suggests that for a clip with one side-wall the complex geometry alters in the same way as for a clip with two side-walls This is in agreement with the above calculated contribution of one wall to the π-π interaction energy and the relatively

large difference in CIS value for the different complexes formed with **4**. Clip **1b** also showed a large variation in the OH stretching frequencies. The results for this compound, however, cannot be compared directly with the other clips, since the guests in **1b** are bound unsymmetrically, and are shifted towards the oxygen carbonyl function. In addition, the influence of the substrate substituent on the π-π interaction will be different in **1b**, since the location of the guest between the two aromatic surfaces is different than that in clip **1a**. One can conclude, however, that the one hydrogen bond formed in **1b**, varies in a similar way to the two bonds formed in **1a** ($\Delta\nu$ = 216-267 cm^{-1} for clip **1b**).

Calculations

We performed computational studies on the host-guest complexes using the semi-empirical method† AM1.[22] The interaction energies were calculated by subtracting the energies of the host and guest from the minimum complex energy. The results for a series of host-guest combinations are summarized in Table 7 and in Figure 8. From these computational results several conclusions can be drawn. As in the experiments, a correlation is found between the interaction energy and the substituent R of the guest. The calculated interaction energies of the different complexes are larger than the experimentally observed ones, since no entropy factors are taken into account in the calculations. The calculated interaction energies of the guest **G3** with **1a** and **1c** are, however, in good agreement with the experimentally found ΔH values (Table 6). In line with the experiments, the clip molecules containing thiocarbonyl groups were calculated to have a lower affinity for the substrates than the clip molecules having carbonyl groups. According to the calculations, however, this effect is not as important as the effect of changing the 1,4-dimethoxybenzene side-wall for a benzene or xylene side-wall (see Table 7; compounds **1a**, **5a**, **5b**). The difference between calculated and observed complex stability can be explained by solvent effects, which are expected to affect the binding to a greater extent when the size of the cavity changes.

The calculated geometry of the different complexes, follows the same trend as that observed experimentally. The more electron withdrawing the substituent on the guest, the deeper it is bound in the cleft. The variation in binding depth, however, was calculated to be only ca. 0.03 Å for clip **1a** (0.3 Å was concluded from the NMR experiments). Clip **1a** binds guest molecules more deeply than **1c** according to the AM1 calculations, in agreement with the experimental results. The calculated minimum energy for the complex between **1b** and 1,3-dihydroxybenzene indicates that the

† Preliminary calculations performed with CHARMm indicated that this force field was not suitable for calculating aromatic interactions.

substrate is not symmetrically bound in the cavity but that it is shifted towards the oxygen atom of the carbonyl group of the DPG frame work (see Figure 4), in line with the experimental data

Table 7 *Calculated (AM1) interaction energies (in kJ/mol) for different combinations of clips and guest molecules*

Guest	1a	1b	1c	5a	5b	6a	6b	6c
G2	-30 250	-25 238	-17 387	-5 5976	-11 050	-9 6202	-7 0814	-4 2166
G3	-30 559	-25 493	-17 654	-6 1545	-11 585	-9 7086	-7 2320	-4 6743
G5	-30 733	-26 037	-17 834	-6 3277	-11 817	-10 134	-7 6094	-4 9806
G6	-32 617	-27 434	-19 668	-9 2495	-14 583	-10 172	-8 1144	-5 9768
G7	-33 550	-28 179	-20 413	-10 363	-15 517	-10 477	-8 2358	-6 0166
G8	-33 667	-28 468	-20 865	-11 552	-16 843	-10 924	-8 9006	-6 9582

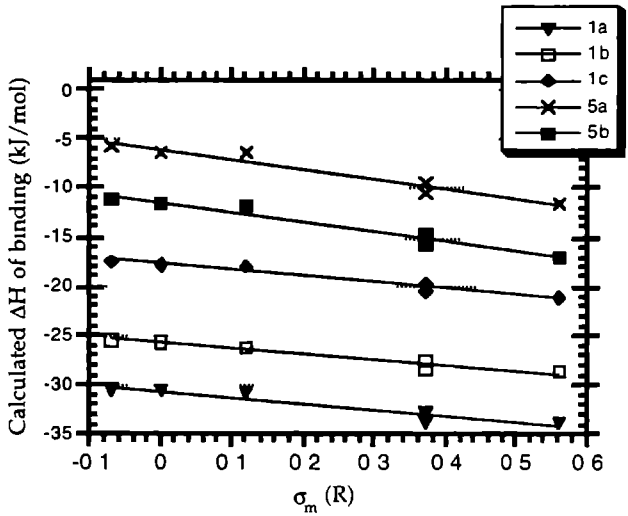

Figure 8 *Calculated interaction energies (AM1) for different combinations of clips and guest molecules*

In order to separate the hydrogen bond interactions from the other binding interactions, calculations were carried out on complexes between different guest molecules and the naked glycoluril frame work Calculations with the thioglycoluril molecule were also performed, resulting in the interaction energies plotted in Figure 9 These results indicate that again there is a correlation between the binding energy and the substrate substituent R The slopes of the fitted lines are smaller and the total interaction energies are lower, than those calculated for the complete clip molecules, suggesting that there is a significant contribution to the overall binding from the interaction between the aromatic rings of the side-walls and the guest The interaction

between the OH of the guest and the thiocarbonyl function is weaker than the interaction of this group with the carbonyl function, but is more substituent dependent. The optimal distance between the hydrogen bond donor and acceptor is approximately constant with the different guests (contrary to the calculations carried out on the complete clip molecules), which is in agreement with the experimental results.

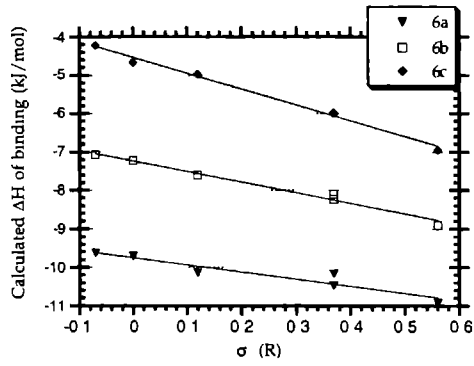

Figure 9. *Calculated interaction energies (AM1) for complexes of glycoluril and thioglycoluril, with the different 1,3-dihydroxybenzene guest molecules.*

AM1 calculations require a relatively large amount of computer time. We, therefore, decided to use a simpler model to calculate the interactions between the aromatic rings of the clip and the guests. The model of Hunter and Sanders has proven to be useful in predicting the geometric features of interacting aromatic rings.[23] The charges on the carbon atoms and the densities of the π-orbitals were calculated using AM1 and these data in turn were used as an input for a computer program based on the Hunter and Sanders model.[23] The interaction energy between the aromatic guests and the two side-walls of the clips were calculated using the geometries obtained from the previously experimental and computational results. For different guest molecules (Table 1) and different types of clip side-walls the interaction energies were calculated as a function of the guest binding depth (Figure 10). At the origin of the figure, the binding depth equals zero, the H2 proton of the guest is defined to be in line with the highest carbon atom at the top of the cleft. A number of trends can be predicted using this model, which are in agreement with the experimental data. The different aromatic side-walls have different interactions with the guest molecules. The more electron deficient the aromatic ring of the guest is, the smaller the repulsive electrostatic interaction becomes resulting in a larger overall interaction energy with

the electron rich side-walls. In the case that the repulsive electrostatic interaction decreases, the optimum π-π interaction is calculated to be located more deeply within the cavity. The bigger the side-wall is (compounds **1a** and **5a** versus **5b**), the more favourable the interaction is between the aromatic rings. The dominant force in the π-π interaction is a large Van der Waals attraction. This attractive force is large but relatively insensitive to the host-guest geometry. The electrostatic repulsive interaction, however, is very geometry dependent and dominates the complexation geometry. The optimal Van der Waals interaction generally is a complete overlap of the aromatic rings, whilst the optimum electrostatic interaction is an offset arrangement of these rings. The overall geometry of the complex is a compromise between these two forces. When the guest molecules become more electron deficient, the electrostatic repulsion decreases whilst the Van der Waals attraction remains constant. As a result the calculated minimum moves to the left in Figure 10, meaning that the guest is bound deeper in the cleft, which is in line with experimental results.

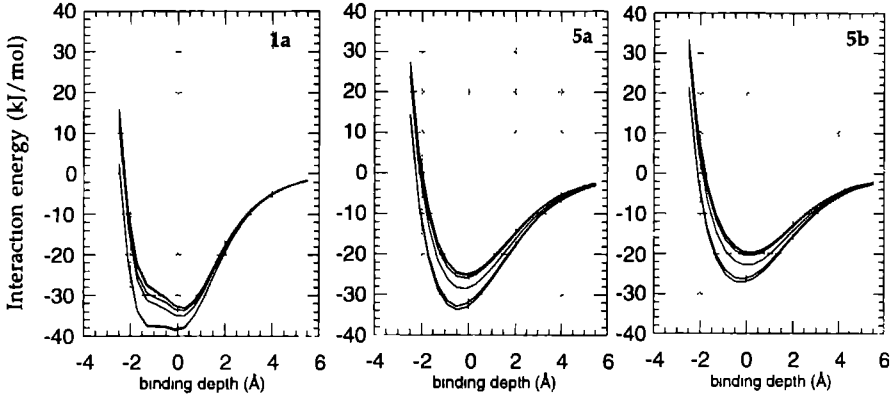

Figure 10. *Calculated interaction energy profiles, using the Hunter and Sander model, of guest molecules docked in between the two aromatic side-walls of* ***1a***, ***5a*** *and* ***5b****. The more electron withdrawing substituents on the guests give the lower binding curves.*

3.2.2 Variation of the aromatic side-wall to enlarge the π-π interaction

The calculations presented above indicate that the interactions between the aromatic rings of the clips and the guests can be divided into an attractive Van der Waals force and a repulsive electrostatic force. It was of interest to investigate whether the guest binding could be fine-tuned by using more electron deficient side-walls in order to decrease the electrostatic repulsion, or by using larger aromatic surfaces in order to

increase the Van der Waals attraction. In the following, both approaches will be discussed.

Binding to benzoquinone-walled clips

Benzoquinone is known to form strong donor-acceptor complexes with dihydroxybenzenes.[24] In order to increase the host-guest binding affinities by reducing the electrostatic repulsion, clip molecules with benzoquinone side-walls were synthesized (compounds **7** and **8**). Surprisingly, it was found that the binding of 1,3-dihydroxybenzenes to clips **7** and **8** was significantly less than that to clip **1a**. The association constants of the complexes with olivetol (**G1**) dropped from K_a = 1500 M^{-1} to K_a = 465 M^{-1} to K_a = 85 M^{-1}, respectively, when going from two 1,4-dimethoxybenzene (DMB) side-walls (**1a**) to one 1,4-DMB wall and one benzoquinone wall (**7**), to two benzoquinone side-walls (**8**). The interaction between the electron rich olivetol guest and the electron poor benzoquinone is less favourable than the interaction between the electron rich 1,4-DMB and olivetol, which is remarkable. Calculations using the Hunter and Sanders model,[23] suggested that the geometries of the complex formed between the benzoquinone clips and olivetol, which are defined by the formation of two hydrogen bonds with the carbonyl groups of the DPG framework, are not optimal for large favourable π-π interactions. According to these calculations the electrostatic repulsion between the side-walls and the aromatic guest decreases, as is expected, but the Van der Waals attraction also decreases. The latter effect is larger than the former one, resulting in an overall decrease in π-π interaction, and consequently in a lower binding constant. The calculations, however, predict a smaller decrease (only 1 kJ/mol) in binding than that experimentally observed (3.5 kJ/mol). This difference could be due to a solvation effect. This is also reflected in the thermodynamic parameters ΔH and ΔS for clip **7** compared with those for clip **1a** (Table 6). A decrease in both enthalpy and entropy was observed for clip **7**, which suggests that a combination of a smaller π-π interaction between the host and the guest, together with a change in entropy effect results in a lower binding constant.

Binding to clips with large aromatic side-walls

To enlarge the Van der Waals contact and hence to increase the binding between host and guest, we synthesized clip molecules with naphthalene side-walls. The naphthalene rings were connected at the 2,3 position (compounds **9**, **10**, and **11**, Chart I), resulting in 'high' side-walls, and at the 1,8 position (compounds **2**, **12**, **13**, and **14** *vide infra*, see also Chart II) resulting in 'broad' side-walls. Clip **9a** appeared to be unable to bind 1,3-dihydroxybenzene, which was thought to be due to the methoxy groups blocking the cleft.[8] The binding properties of the unsubstituted naphthalene

derivative (clip **9b**) were, therefore, studied. The X-ray structures of **9a** and **9b** showed that apart from the presence or absence of the methoxy groups, the cavities of the

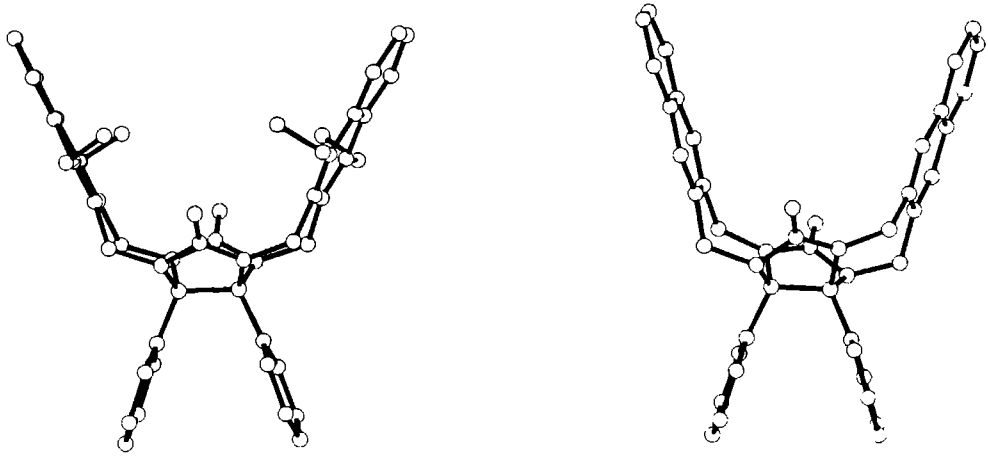

Figure 11. *X-ray structures of* ***9a***[8] *and* ***9b****. Hydrogen atoms have been omitted for clarity.*

compounds were similar (Figure 11). In **9a** the methoxy groups indeed point toward the cleft, which prevent the carbonyl functions from forming a hydrogen bond with a guest. If the presence of the methoxy groups are the only reason for the inability of **9a** to bind dihydroxybenzenes, then **9b** was expected to bind these guest molecules more strongly. Clip **9b** indeed was able to bind resorcinol, however, the association constant was low (K_a = 70 M^{-1}, Table 8). Remarkably, **9b** binds the guest less strongly than the benzene-walled clip **5b** (K_a = 175 M^{-1}, Table 5). Apparently, the enlarged π-system in the former compound is disadvantageous for host-guest complexation. This result suggests that the inability of **9a** to bind guest molecules is not solely due to steric hindrance of the methoxy groups, but also to an unfavourable π-π interaction. Calculations using the Hunter and Sanders model, confirmed that there is indeed a very large electrostatic repulsion (27.5 kJ/mol) between the naphthalene moiety and the aromatic ring of the guest when the latter is forced into the cleft in order to form hydrogen bonds with the urea carbonyl functions. The advantage of a larger Van der Waals surface (-25 kJ/mol), in this case, does not result in an increase in interaction energy (2.5 kJ/mol). This Van der Waals attraction is cancelled out by a larger electrostatic repulsion between the guest and the naphthalene side-walls. If the methoxy groups are removed, the electron density on the side-walls is smaller and the repulsion is partially reduced which enables **9b** to weakly bind dihydroxybenzenes. Comparison of the binding of olivetol to **3** and **4** with that to the naphthyl analogue of the latter compound (**10**) also reveals the negative influence of systematically enlarging the aromatic π-surface. The binding to **4** (K_a = 50 M^{-1}, Table 4) is somewhat higher than to **3** (K_a = 23 M^{-1}, Table 4) as discussed before. Enlarging the side-wall with

a larger π surface, i.e. the naphthalene moiety in **10**, decreases the binding dramatically (K_a (**10**) < 1 M^{-1}, Table 8). This is in line with the trend found for **4**, **1a** and **9a** and the above mentioned calculations which predict an unfavourable electrostatic interaction between the large naphthalene surface and the aromatic ring of the guest. Rebek et al. studied the binding of 9-ethyladenine to receptor molecules based on Kemps acid having different assisting π surfaces.[5a, 25] They found a correlation between the binding energy and the size of the π surface. In their case each benzene increased the binding energy by a 1.6 kJ/mol (see Chapter 1). Although their and our approaches are the same, *viz.* binding based on hydrogen bonding which is assisted by a side-wall for stacking interactions, the results are opposite. This shows clearly that each new host-guest system has to be analyzed carefully.

Table 8: *Association constants of olivetol in clips with different side-walls.*[a]

clip	K_a M^{-1}
1a	1500 (300)[b]
2	1400 (100)[c]
9a	<1 (5)[b]
9b[d]	70 (20)[b]
10	<1 (5)[b]
11	55 (20)[b]
12	20 (10)[c]
13	1060 (100)[c]
14	90 (10)[c]

[a]Errors are given in parenthesis. [b]Association constants were determined by following the chemical shift of the side-walls protons as a function of the guest concentration. [c]Association constants were determined by integration of the signals of the different conformers. dAssociation constant with resorcinol.

A previous binding study[9] of 1,3-dihydroxybenzene with **2**, a clip with two 2,7-dimethoxynaphthalene (2,7-DMN) side-walls, failed due to precipitation of the complex, however, the better solubility of the complex between **2** and olivetol (**G1**), allowed us to study the effect of a 'broad' aromatic side-wall (Table 8). When the naphthalene moiety is attached at the 1,8 position the geometry of the π-π interaction is altered, and the electrostatic repulsive component will be significantly reduced. A complication is that the connection between the side-wall and the glycoluril frame work in **2**, is no longer a 7-membered ring but an 8-membered ring. This results in a side-wall which flips slowly on the NMR time scale from an *anti* to a *syn* orientation with respect to the phenyl rings on the convex side of the DPG frame work (Figure 12). Clip **2** therefore can adopt three conformations *aa*, *as* and *ss*. In chloroform these ratios

are 2.7%, 89% and 8.5% respectively.[9] Molecules with only one 1,8-connected naphthalene side-wall (compounds **12-14** Chart II) consequently have two conformations in solution, *viz. anti* and *syn* (see Chapter 2). The association constants for binding of guests to the *aa* or *anti* conformers were calculated by the determination of the conformer ratio of the host as a function of the guest concentration, assuming that the clips do not bind guest molecules in the other conformers.[9]

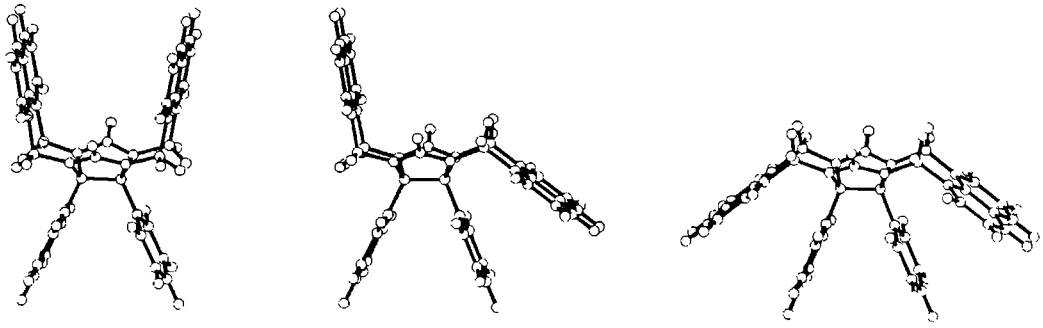

Figure 12. *The three conformations of clip* **2** *which interconvert slowly on the NMR time scale (left anti-anti (aa); middle anti-syn (as); and right syn-syn (ss)).*

This assumption is justified, since mono walled clips **12, 4** and **10** showed a very low affinity towards guest molecules. As can be seen in Table 8 the binding affinities of olivetol towards clip molecules containing 2,7-DMN side-walls are in the same range as those to clip molecules with 1,4-dimethoxybenzene (1,4-DMB) side-walls. Different factors, however, play a role in the binding to these two type of clips. The Van der Waals interaction between the aromatic ring of the guest and the naphthalene moiety

Chart II

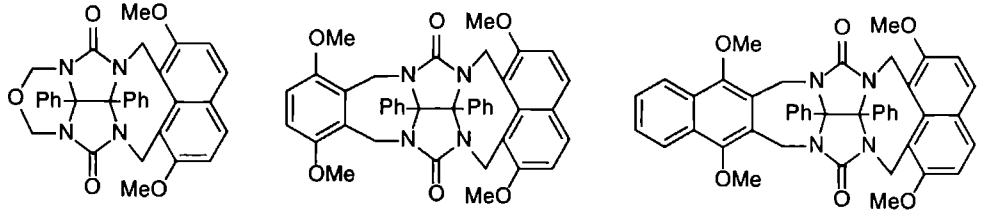

12 **13** **14**

is much larger. Other effects cancel out this favourable effect which results in an overall similar binding strength for an 1,4-DMB and a 2,7-DMN side-wall. Calculations using the Hunter and Sanders model confirmed that there is a large Van der Waals attraction (-22.5 kJ/mol) without a significantly larger electrostatic repulsion (10 kJ/mol) between the 1,8-connected naphthalene side-walls and the ring of the guest, as

compared to the 2,3-connected naphthalenes **9a** and **9b**. Comparison between the binding affinities of clip **1a** and **13** (Table 8) indicate that the substitution of one 1,4-DMB wall by a 2,7-DMN wall reduces the binding. Replacing the second 1,4-DMB wall by another 2,7-DMN wall (from **13** to **2**), slightly increases the binding. These small effects are probably due to a slightly different complex geometry and the 'cavity effect' when the side-wall is enlarged. From the X-ray structures of **2** and **12** it is known that these clip molecules have a slightly different distances and angles between the carbonyl oxygen atoms which in turn has an influence on the hydrogen bond formation between the host and the guest. More detailed studies of clip molecules which adopt different conformations are discussed in Chapter 4.

3.2.3 Self-association behaviour of clip molecules

While studying the binding properties of our clip molecules, we discovered that for some of these molecules the ^{1}H NMR spectra were concentration dependent. For example it was found that the ^{1}H NMR signal of the protons of the side-walls of clip **1a** shifted to higher field at higher concentrations. This suggests a structure in which these protons are now in the shielding zone of another aromatic ring, e.g. a dimeric structure. The advantage of forming a dimer is that two clefts can be filled at the same time. In this dimeric geometry there are 3 interactions between the aromatic side-walls. The 'cavity effect' can also make a favourable contribution to the formation of the dimeric species. ^{1}H NMR dilution experiments were performed to determine the self-association constants (K_s) of the clips (see Chapter 5). Not all clip molecules showed this kind of dimerization behaviour. Clip molecule **1a**, containing two 1,4-DMB walls, showed a self-association constant of K_s = 16 M^{-1}. The self-aggregation of clip **1b** was somewhat lower, probably because of the larger thiocarbonyl group (K_s = 8 M^{-1}). At the highest concentrations of **1b** the singlet signal of the side-wall protons, split up to form an AB pattern, indicating that the protons were no longer equivalent. Apparently, the clip molecule with one carbonyl and one thiocarbonyl group forms a non-symmetrical dimeric structure. The side-wall protons of clip **1c**, shifted only slightly suggesting that the self-association constant of this clip is low. Due to the low solubility of this clip no K_s value could be determined. The molecule containing only one 1,4-DMB side-wall (**4**) and the benzene-walled clip **5b** both did not show any measurable self-association, whereas clip **5a** showed a low self-association (K_s = 7 M^{-1}).

Applying donor-acceptor theory,[24] one would expect the unsymmetrical clip with one benzoquinone and one 1,4-dimethoxybenzene side-wall (**7**) to form much stronger dimeric complexes than clip **1a**. It was found, however, that clip **7** in solution did not dimerize. The 'cavity effect' is expected to be approximately the same for **1a** and **7** and therefore the difference has to be due to the interactions between the aromatic side-

walls of the clip molecules, leading one to conclude that the interaction between two 1,4-DMB rings is more favourable than between an 1,4-DMB ring and a benzoquinone ring. Calculations using the Hunter and Sanders model and the X-ray structure (Figure 13) confirmed this. The X-ray structure of **7** showed that in the solid state this molecule adopts a dimeric form with one side-wall of one clip filling the cleft of another one. The geometry of the dimeric is such that the major interaction is between two electron rich 1,4-DMB side-walls, and not between an electron rich 1,4-DMB side-wall and an electron poor benzoquinone side-wall. The aromatic 1,4-DMB rings of the different clips are parallel and have an offset geometry (0.60 Å, 2.05 Å) with an interplanar distance of 3.43 Å. The calculations predict that the interaction between two 1,4-DMB rings is optimal at this particular geometry and is more favourable than the interaction between two benzoquinone rings or between a benzoquinone and an 1,4-DMB ring. There is a much larger Van der Waals interaction between two 1,4-DMB rings than between a benzoquinone and an 1,4-DMB ring (Chapter 5). It is this larger Van der Waals contact which is the main reason for the favourable interaction between the two 1,4-DMB side-walls.

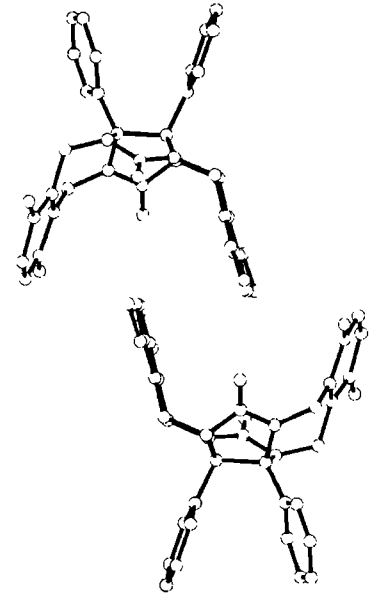

Figure 13. *X-ray structure of clip molecule 7. Hydrogen atoms have been omitted for clarity.*

Clip molecule **2**, which has two 2,7-DMN side-walls, shows the largest dimerization constant (K_s = 60 M^{-1}). Here two large cavities are simultaneously filled, and three 2,7-DMN contacts are involved. Clip molecules containing 1,4-DMN side-walls do not dimerize, because of the same unfavourable electrostatic interaction which inhibits guest complexation. The 'cavity effect' and a favourable π-π interaction are responsible for both the higher complexation of dihydroxybenzene guest molecules as well as for

the dimerization. A more detailed study concerning interactions between clip molecules in solution and the solid state will be discussed in Chapter 5.

3.3 CONCLUSIONS

Analysis of a series of complexes between a variety of clip molecules and guests by ^1H NMR and IR spectroscopy, in combination with theoretical calculations, has enabled us to get detailed insight into the binding mechanism of aromatic molecules in cleft-type host molecules. By studying a variety of complexes and by varying different parameters, we have been able to separate the contribution of the different effects involved in the binding of 1,3-dihydroxybenzenes to clip **1a**. The complexation strength between clip molecules of type **1** and 1,3-dihydroxybenzenes is a combination of a 'cavity effect', hydrogen bonding and π-π stacking interactions between the host and the guest. The cavity effect, which is a result of an entropy effect and a solvation effect, is responsible for approximately 6 kJ/mol of the binding energy. The large difference in binding affinity towards dihydroxybenzene guest molecules observed for the mono-side-walled clip **4** and clip molecule **1a** is mainly based on this effect. The hydrogen bond formation between the OH groups of the guest and the urea carbonyl functions of the glycoluril frame work, as well as the π-π interactions are dependent upon the type of substituent on the guest molecule. The contribution of the hydrogen bonding to the binding energy is given by the equation

$$-\Delta G = 8 + 6\sigma \quad \text{(kJ/mol)}.$$

The π-π interaction between one aromatic 1,4-dimethoxybenzene side-wall and the aromatic guest contributes

$$-\Delta G = 2.5 + 6\sigma \quad \text{(kJ/mol)}$$

to the overall binding energy. This interaction is based on an attractive Van der Waals force, and a repulsive electrostatic force, the latter being the dominant factor in determining the geometry of the complex. The electrostatic repulsion pushes the guest out of the cavity of the clip, whereas the hydrogen bonding pulls it into the cleft. The effect of enlarging the aromatic side-walls by using naphthalene rings, in order to increase the Van der Waals attraction, and in turn to obtain higher association constants, was more complex than expected. When the naphthalene wall is pointing upwards (1,4-DMN) the electrostatic repulsion between host and guest significantly increases, cancelling out the increase in Van der Waals attraction. In the case, however, of the 1,8-connected side-wall (2,7-DMN) a larger Van der Waals attraction is combined with only a slight increase in electrostatic repulsion between the host and the guest. This does not result, however, in larger association constants because the

clip molecule can adopt different conformations. It has been shown that the binding strength of complexes between our clips and aromatic guests can span a wide range (K_a = 0 to 10^5 M^{-1}), by simply small modifications in the host or the guest molecule. This ability to vary the binding strength will be used in future applications of these systems.

3.4 EXPERIMENTAL SECTION

The syntheses of compounds **1a, 5a, 5b, 3, 8** and **9a** have been described elswhere.[8] The syntheses of **1b** and **1c** will be described in a separate paper[18] and the syntheses of **5, 7, 9b, 10, 11, 12, 13** and **14** are described in Chapter 2. The hydroxy and dihydroxybenzene guest molecules were commercially available products except for chloro-3,5-dihydroxybenzene, which was synthesized as described in the literature.[27] $CDCl_3$ was dried on P_2O_5 and distilled before use. Binding constants were determined by ^1H NMR titration experiments on Bruker AM 500, AM 400 and AM 200 instruments, using optimal concentrations to minimize errors in the fit procedure, see ref 8.

IR spectra were recorded on a Perkin Elmer FTIR 1720-X spectrometer, with a resolution of 2.0 cm^{-1}. For each spectrum 64 scans were taken. The interferometer was flushed with nitrogen.

Dimerization constants were determined by diluting the samples from maximum solubility (varying from 10 mM - 40 mM) to a minimum concentration for detection with ^1H-NMR (approximately 0.1 mM), and following the chemical shifts of the side-wall protons of the clip molecules (Bruker AM 400 and AM 200). The obtained curves were fitted using the following equation (see also Chapter 5):

$$\partial_{obs} = \partial_m + (\partial_d + \partial_m)[1 + 4aK - (1 + 8aK)^{1/2}]/4aK$$

X-ray structures

Crystal data of **4**:

$C_{28}H_{26}N_4O_5$, Mr =498.5, T = 293 K, triclinic, space group P-1, a = 8.2849(15), b = 12.525(2), c = 13.438(4) Å, α = 116.83(2), β = 105.17(3), γ = 90.07(2)°, V = 1189 $Å^3$, Z = 2, Dx = 1.392 g/cm^3, Mo $K\alpha$ radiation, μ = 0.91 cm^{-1}.

Crystal data of **7**:

$C_{35}H_{29}N_4O_6Cl_3$, Mr = 708.0, T = 293 K, monoclinic, space group $P2_1/c$, a = 13.0326(6), b = 18.858(2), c = 13.5561(11) Å, β = 100.800(7)°, V = 3273 $Å^3$, Z = 4, Dx = 1.437 g/cm^3, Mo $K\alpha$ radiation, μ = 3.30 cm^{-1}.

Crystal data of **9b**:

$C_{40}H_{30}N_4O_2.HCCl_3$, *Mr* =718.05, *T* = 208 K, triclinic, space group P-1, *a* = 9.302(2), *b* = 12.981(2), *c* = 15.765(2) Å, α = 65.92(2), ß = 76.40(2), γ = 80.15(1)°, *V* = 1682.9 $Å^3$, *Z* = 2, *Dx* = 1.417 g/cm^3, Mo *K*α radiation, μ = 3.17 cm^{-1}.

Detailed crystallographic data will be published elsewhere.[14,28,29]

Calculations.

Calculations were performed on Silicon Graphics Challenge and Silicon Graphics Indigo II work stations. For the calculations using the Hunter and Sanders model the following procedure was used: the aromatic structures were generated with the Sybyl program and optimized by calculations with the MOPAC program using the ESP option for the charges. The charges and coordinates were taken from the output file of this program. By using the keyword PI in MOPAC the final density matrix was split into π and s contributions. The π densities at the diagonal of the density matrix were used as the π charges above and below the plane of the aromatic molecule in the calculations using the Hunter and Sanders model. For comparison the interaction between two 1,4-dimethoxybenzene molecules was also calculated with this model using the π densities extracted from the z-orbitals. The differences between the two calculations were small, and only significant when the distance between the aromatic surface was small at direct overlap. This is a result of the larger π densities in the oxygen atoms, used during this calculation. Energy surfaces were calculated, using an electrostatic and a Van der Waals potential, by stepwise changing the x and y coordinates of one of the two surfaces. For the energy profiles shown in Figure 11 the following procedure was used: a guest molecule was placed between two side-walls at the distance of minimum energy calculated with AM1. The interaction energy was then calculated as function of the x coordinate (binding depth). The AM1 calculations were carried out as follows: the complex and the free components were minimized, and the interaction energies were calculated by subtracting the heats of formation of the free components from the complex.

References

1 Recent reviews: (a) Cram, D. J. *Top. Curr. Chem.* **1981**, *98*, 43. (b) Schneider, H-J.; *Angew.Chem.* **1991**, *103*, 1419. (c) Diederich, F. *Angew. Chem.* **1988**, *100*, 372. (d) Seel, C.; Vögtle, F. *Angew. Chem.* **1992**, *104*, 542. (d) Izatt, *Chem. Rev.* **1995**, *95*, and references cited therein (e) Izatt, R. M.; Bradshaw, J. S.; Pawlak, K.; Bruening, R. L.; Tarbet, B. J. *Chem. Rev.* **1992**, *92*, 1261, and references cited therein (f) Various authors in *Tetrahedron*, **1995**, *51*, vol. 2, topic molecular recognition. (g) Cram, D. J. *Nature* **1992**, *356*, 29. (h) Zimmerman, S. C. Bioorganic Chemistry Frontiers 2, **1991**,

Springer-Verlag Berlin heidelberg, 33. (i) Hamilton, A. D. Bioorganic Chemistry Frontiers 2, **1991**, Springer-Verlag Berlin heidelberg, 115. (j) Cram, D.J. *Angew. Chem.* **1988**, *100*, 1041 (k) Lehn, J-M. *Angew. Chem.* **1988**, *100*, 92.

2 (a) Burley, S. K.; Petsko, G. A. *Science* **1985**, *229*, 23. (b) Serrano, L.; Bycroft, M.; Fersht, A. R. *J. Mol. Biol.* **1991**, *218*, 465. (c) Fersht, A. R.; Shi, J.-P.; Knill-Jones, J.; Lowe, D. M.; Wilkinson, A. j.; Blow, D. M.; Brick, P.; Carter, C.; Waye, M. M. Y.; Winter, G. *Nature* **1985**, *314*, 235. (d) Schweitzer, B. A.; Kool, E. T. *J. Am. Chem. Soc.* **1995**, *117*, 1863.

3 Tanford, C. "*The Hydrophobic Effect*", **1973**, Wiley Interscience, New york.

4 (a) Conn, M. M.; Deslongchamps, G.; de Mendoza, J.; Rebek, Jr., J. *J. Am. Chem. Soc.* **1993**, *115*, 3548. (b) Blake, J. F.; Jorgensen, W. L. *J. Am. Chem. Soc.* **1990**, *112*, 7269. (c) Hamilton, A. D.; Little, D. *J. Chem. Soc., Chem. Commun.* **1990**, 297. (d) Goswami, S.; Hamilton, A. D. *J. Am. Chem. Soc.* **1989**, *111*, 3425. (e) Zerkowski, J. A.; MacDonald, J. C.; Seto, C. T.; Wierda, D. A.; Whitesides, G. M. *J. Am. Chem. Soc.* **1994**, *116*, 2382-2391. (f) Zerkowski, J. A.; Whitesides, G. M. *J. Am. Chem. Soc.* **1994**, *116*, 4298-4304. (g) Mathias, J. P.; Seto, C. T.; Simanek, E. E.; Whitesides, G. M. *J. Am. Chem. Soc.* **1994**, *116*, 1725-1736. (h) Mathias, J. P.; Simanek, E. E.; Zerkowski, J. A.; Seto, C. T.; Whitesides, G. M. *J. Am. Chem. Soc.* **1994**, *116*, 4316-4325. (i) Mathias, J. P.; Simanek, E. E.; Whitesides, G. M. *J. Am. Chem. Soc.* **1994**, *116*, 4326-4320. (j) Chang, S.-K.; Van Engen, D.; Fan, E.; Hamilton, A. D. *J. Am. Chem. Soc.* **1991**, *113*, 7640. (k) Fan, E.; Van Arman, S. A.; Kincaid, S.; Hamilton, A. D. *J. Am. Chem. Soc.* **1993**, *115*, 369. (l) Hayashi, T.; Miyahara, T.; Hashizume, N.; Ogoshi, H. *J. Am. Chem. Soc.* **1993**, *115*, 2049. (m) Murray, T. J.; Zimmerman, S. C. *J. Am. Chem. Soc.* **1992**, *114*, 4010. (n) Bell, T. W.; Liu, J. *J. Am. Chem. Soc.* **1988**, *110*, 3673. (o) Adrian, Jr., J. C.; Wilcox, C. S. *J. Am. Chem. Soc.* **1991**, *113*, 678. (p) Kelly-Rowley, A. M.; Cabell, L. A.; Anslyn, E. V. *J. Am. Chem. Soc.* **1991**, *113*, 9687.

5 (a) Rebek, Jr., J. *Angew. Chem.* **1990**, *102*, 261. (b) Rotello, V. M.; Viani, E. A.; Deslongchamps, G.; Murray, B. A.; Rebek, Jr., J. *J. Am. Chem. Soc.* **1993**, *115*, 797.

6 (a) Zimmerman, S.C. Bioorganic Chemistry Fontriers 2, **1991**, Springer-Verlag, Berlin. 33-74 and references cited therein. (b) Zimmerman, S. C.; Vanzyl, C. M.*J. Am. Chem. Soc.* **1987**, *109*, 7894. (c) Zimmerman, S. C.; Vanzyl, C. M.; Hamilton, G. S.*J. Am. Chem. Soc.* **1989**, *111*, 1373.

7 (a) Whitlock B. J.; Whitlock, H. W. *J. Am. Chem. Soc.* **1994**, *116*, 2301-2311.
(b) Whitlock B. J.; Whitlock, H. W. *J. Am. Chem. Soc.* **1990**, *112*, 3910-3915.

8 Sijbesma, R. P.; Kentgens, A. P. M.; Lutz, E. T. G.; Van der Maas, J. H.; Nolte, R. J. M. *J. Am. Chem. Soc.* **1993**, *115*, 8999.

9 Sijbesma, R. P.; Wijmenga, S. S,; Nolte, R. J. M. *J. Am. Chem. Soc.* **1992**, *114*, 9807-9813.

10 Hansch, C.; Leo, A.; Taft, R. W. *Chem. Rev.* **1991**, *91*, 165.

11 (a) Abraham, M. H.; Grellier, P. L.; Prior, D. V.; Duce, P. P.; Morris, J. J.; Taylor, P. J. *J. Chem, Soc. Perkin Trans. II*, **1989**, 699. (b) Abraham, M. H.; Duce, P. P.; Prior, D. V.; Barratt, D. G. ; Morris, J. J.; Taylor, P. J. *J. Chem, Soc. Perkin Trans. II*, **1989**, 1355. (c) Abraham, M. H. *Chem. Soc. Rev.* **1993**, 73.

12 The average structure determined by Molecular Dynamics calculation using the CHARMm Force Field gave approximately the same complex geometry as a minimalization (ABNR; CHARMm Force Field), i.e. the guest molecule shifted towards the oxygen carbonyl atom.

13 Niele F. Thesis Utrecht, **1987**.

14 Reek, J. N. H.; Elemans, J. A. A. W.; de Gelder, R.; Rowan, A. E.; Nolte, R. J. M. to be published.

15 Cram, D. J. *Angew. Chem., Int. Ed. Engl.* **1986**, *25*, 1039.

16 (a) Canceill, J.; Lacombe, L.; Collet, A. *J. Am. Chem. Soc.* **1986**, *108*, 4230. (b) Canceill, J.; Cesario, M.; Collet, A.; Guilhem, J.; Lacombe, L.; Lozach, B.; Pascard, C. *Angew. Chem.* **1989**, *101*, 1249.

17 Chapman, K. T.; Still, W. C.*J. Am. Chem. Soc.* **1989**, *111*, 3075.

18 In a forthcomming paper it will be shown that clip **1b** binds with approximately the same affinity as a clip in which one carbonyl group is reduced to a CH_2 group. This is additional prove for the fact that the thiocarbonyl groups are not involved in hydrogen bonding. Gieling, G.; Scheeren, H.; Nolte, R. J. M. to be published.

19 Vrolix, E.; Zeegers-Huyskens, Th. *Vibrational Spectroscopy*, **1993**, *5*, 227.

20 Johnson, C. S. Jr.; Bovey, F. A. *J. Chem. Phys.* **1958**, *29*, 1012.

21 Stymme et al. have found a much stronger substituent dependency of the OH stretching frequency for substituted phenols which were complexed to dimethylacetamide. The OH bond in these complexes, however, was directed to the n-electrons and not towards the π electrons which is the case in our complexes. Stymne, B.; Stymne, H.; Wettermark, G. *J. Am. Chem. Soc.*, **1973**, *95*, 3490.

22 Dewar, M. J. S.; Zoebisch, E. G.; Healy, E. F.; Stewart, J. J. P. *J. Am. Chem. Soc.* **1985**, *107*, 3902.

23 (a) Hunter, C. A.; Sanders, J. K. M. *J. Am. Chem. Soc.* **1990**, *112*, 5525. (b) Hunter, C. A.; Singh, J.; Thornton, J. M. *J. Mol. Biol.* **1991**, *218*, 837.

24 Eggins, B. R.; Chambers,,, J. Q. *J. Electrochem. Soc.* **1970**, *117*, 186.

25 Huc, I.; Rebek Jr., J. *Tetrahedron Lett.*, **1994**, *35*, 1035.

26 (a) Briegleb, G. "*Electronen-Donator-Acceptor-Komplexe*" **1961**, Sprongler-Verlag, Berlin. (b) Morakuma, K. *Acc. Chem. Res.* **1977**, *10*, 294.

27 Hodgson, H. H.; Wignall, J. S. *J. Chem. Soc.* **1926**, 2826.

28 Reek, J. N. H.; de Gelder, R.; Rowan, A. E.; Nolte, R. J. M. to be published.

29 Reek, J. N. H.; Elemans, J. A. A. W.; de Gelder, R.; Rowan, A. E.; Nolte, R. J. M. to be published.

Chapter 4

Conformational Behaviour and Binding Properties of Naphthalene-walled Clips

4.1 INTRODUCTION

Two models are frequently used to describe the binding of a substrate molecule in the site of a receptor molecule: the 'lock-and-key' model and the 'induced fit' model. Fischer used the term 'lock and key' 100 years ago,[1] and it was Cram who combined it with the ideas of preorganisation.[2] Many host-guest complexes have been designed using Fischer and Cram's principles,[3] leading to very high association constants even in chloroform.[4] The 'induced fit' model[5a] was proposed by Koshland and is more related to binding processes in biological systems. According to Koshland the substrate induces a reorganisation of the receptor, or the substrate molecule changes its conformation upon binding. This induced fit mechanism is clearly demonstrated by the binding of nicotinamide nucleotides in the enzyme oxidoreductase,[5b] where the reorganisation activates certain functions of the enzyme. A better understanding of the way the induced fit type of receptors work, is of great use for the future design of synthetic receptors capable of performing certain tasks or functions.

We have previously reported on the conformational properties of clip molecules of type **1**.[6a] In solution these compounds, exist in three conformations *aa*, *as* and *ss* (Figure 1), of which the *as* conformation is the predominant one (ca. 90%). Binding of aromatic guest molecules occurs only in the minor *aa* conformer, where the guest is sandwiched between the two aromatic cavity walls and hold by π-π stacking interactions. Upon the addition of an excess of guest molecules, the two other conformers disappear completely. Although the binding mechanism has been studied in detail and now is reasonably well understood, some questions still remained, the most important one being, why is the clip molecule initially present as the *as* conformer? Another question is related to the binding interactions in the host-guest complex which are different from those known for donor-acceptor complexes, e.g. complexes between hexamethylbenzene and electron poor aromatic compounds.[7] In

this chapter we present additional conformational studies and binding data as well as X-ray structures of new clip molecules, which are compared with those of **1**, in order to answer these questions.

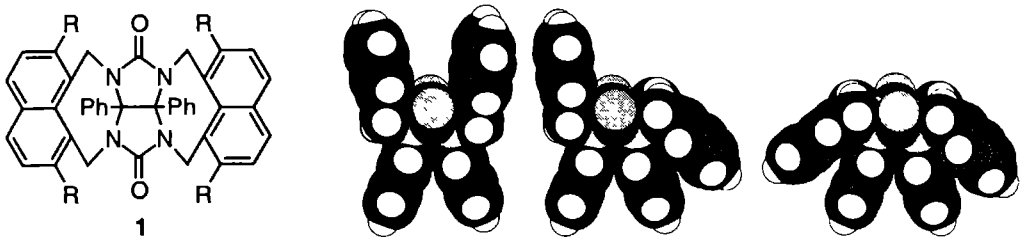

Figure 1. *The different possible orientations of the 1,8-connected naphthalene sidewalls in clip* **1**, *which result in three conformations interconverting slowly on the NMR time scale: anti-anti (aa), anti-syn (as), and syn-syn (ss).*

4.2 RESULTS AND DISCUSSION

4.2.1 Synthesis

The syntheses of clip **1a**[6] and **2-8** (Chart I, Chapter 2) have been described elsewhere. We initially tried to synthesize **1b** by reacting naphthalene with the tetrachloroderivative **6** in the presence of a Lewis acid. This, however, resulted in a mixture of isomers, which could not be separated. Another route, therefore, was developed in which 1,8-dimethylnaphthalene was brominated to yield 1,8-bis(bromo methyl)naphthalene, which was subsequently reacted with diphenylglycoluril **7** in DMSO/KOH to yield **1b** (34 %).

4.2.2 Conformational behaviour

In order to get insight in the conformational behaviour of our clip molecules ^{1}H NMR studies were carried out in $CDCl_3$. The different sets of ^{1}H NMR signals for each conformer of a clip molecule could be assigned with the help of 2D COSY NMR. For clips **1a**,[6] **2-5** this assignment is described elsewhere (Chapter 2). Clip **1b** displayed two sets of signals by ^{1}H NMR, suggesting that only two of the three possible conformers were present in solution (Figure 2). The main conformer was either the *ss* or the *aa*, since only one set of AB signals was found for the NCH_2 protons. By comparing the spectra of **1b** with the spectra of **1a** and **2-5** and by using Johnson-Bovey[8] tables in order to calculate ring current contributions, it was clear that both walls of **1b** were in the anti position with respect to the phenyl rings on the convex side of the DPG framework. Consequently, the main conformer was the *aa* one. The minor species,

displaying two sets of AB signals for the NCH_2, protons, was assigned to be the *as* conformer.

Chart I

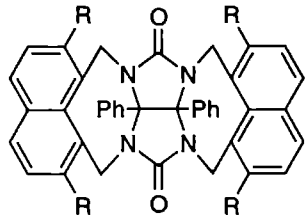

1a: R=OMe
1b: R=H

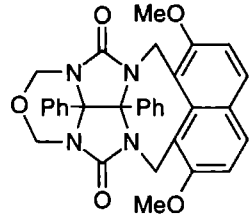

2

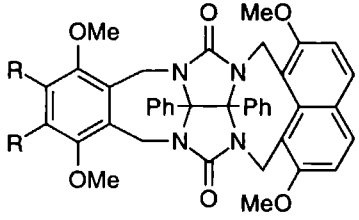

3 R=H
4 R=NO_2

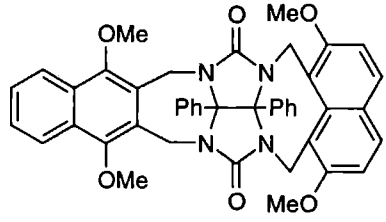

5

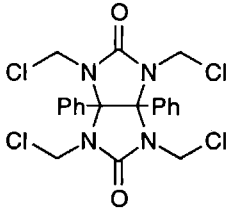

6

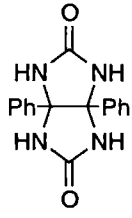

7

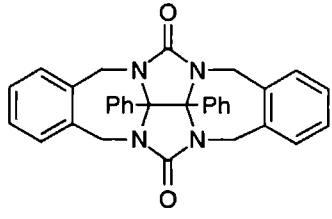

8

The naphthalene moiety which is in the *syn* orientation in **1b**, induces a large high field shift of the proton signals of the phenyl ring which are in its shielding zone. Upon heating ,these and other ^1H NMR signals of the *sa* conformer became broader, suggesting that the two conformers were interconverting faster on the NMR-time scale. At 330 K the ^1H NMR resonances of the *aa* conformer, however, were not significantly broadened, implying that coalescence was not yet reached. The rate of interconversion between the two conformations could not be determined using this technique since experiments at higher temperature could not be carried out.

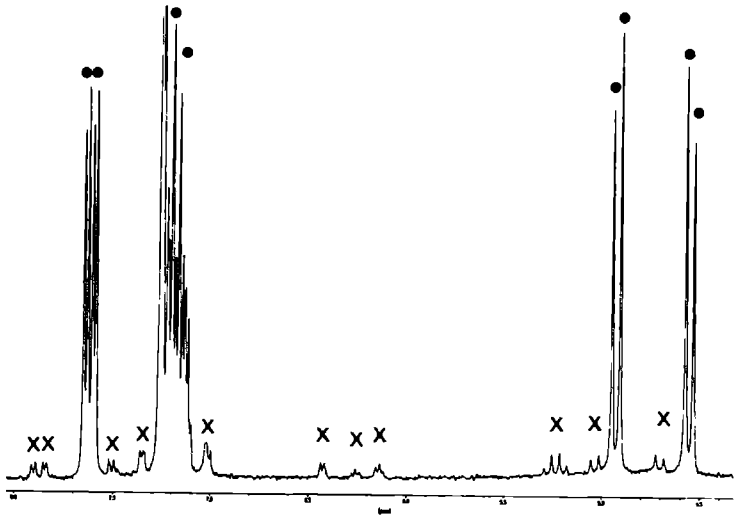

Figure 2. *^1H NMR spectrum of* ***1b****, showing two conformers: the major one is aa (•) and the minor one is as (x).*

The ratios in which the different conformers of clips **1-5** occur in chloroform solution are presented in Table 1. They give useful information about the conformational behaviour of these molecules. The large difference between the conformational ratios measured for **1a** and **1b** indicates that the methoxy groups attached at the 2,7 position of the naphthalene moieties have an enormous influence on the conformation of the clip molecules. The distance between the methoxy group and the oxygen atom of the carbonyl function is 2.96 Å for the *anti* and 4.09 Å for the *syn* conformer (calculated from the X-ray structure of **1a** and **2** (*vide infra*) and modelled structures). When the methoxy group is in the plane of the aromatic ring, which is the case in the solid state (*vide infra*), the lone pairs of the methoxy oxygen atoms point towards the oxygen atoms of the carbonyl functions. It is likely, therefore, that oxygen-oxygen repulsion plays a dominant role in the conformational behaviour of **1a**. This was further confirmed by examining the conformation of a clip molecule derived from **1a** in which one of the carbonyl groups was reduced to a CH_2 group.[9] This latter molecule was found to exist in a higher proportion in the *aa* conformation (ca. 20%).

Despite the unfavourable oxygen-oxygen repulsion compound **1a** apparently prefers to be in a conformation with one side-wall *anti* and one side-wall *syn*. This indicates that other factors must play a role, otherwise the *ss* form would be the dominant conformer. We believe that solvation effects are also very important. When clip **1a** is in the *aa* conformation the cavity will be poorly solvated since chloroform solvent molecules are too large to fit in the cavity. If the molecule is in the *as* conformation the aromatic walls will be more fully exposed to solvent molecules. The ratio of the two conformations of the mono side-walled clip **2** (Table 2) is in line with this idea: for

this compound the *anti* conformer is more favourable than the *syn* conformer. The *anti* conformer of **2** was also found in the solid state structure (*vide infra*). This preference for the anti conformation suggests that it is more favourable for the wall to be in the 'up' position. In the case of the di-walled species **1a** the enthalpic gain is less than the loss of solvation that occurs when the cavity is formed, hence, the *as* conformer is preferred.

Table 1: *Ratio of conformers of molecular clips in chloroform solution and the energy differences between them*

Clip	Conformational ratio	$K_{(as/aa)}$[a]	ΔG (kJ/mol)
1a	*aa:as:ss* = 2.7:89.6:7.7	33	-8.66
1b	*a:s* = 93:7	0.075	6.41
2	*a:s* = 77:23	0.30	2.98
3	*a:s* = 15:85	5.67	-4.29
4	*a:s* = 35:65	1.86	-1.53
5	*a:s* = 24:76	3.17	-2.85

[a] Based on the equilibrium *aa* $\rightleftharpoons$ *as*.

When the solvent was stepwise changed from chloroform to pure methanol, the percentage of *aa* conformer for **1a** increased gradually from ca. 2 to 15%. Methanol molecules fit better in the cavity of the *aa* conformer than chloroform and hence this better solvation leads to a higher percentage of *aa* conformer. The electrostatic repulsion between the oxygen atoms of the side-wall and the carbonyl oxygen atoms will also decrease as the percentage of methanol increases, which further stabilizes the *aa* conformer.

The conformational behaviour of **3**, **4** and **5** is in line with the results discussed above. The benzene side-wall and the 1,4-dimethoxynaphthalene side-wall are both observed to be in the *anti* conformation. The opposite 2,7-dimethoxynaphthalene side-wall in **3**, **4** and **5**, therefore, prefers to be in the *syn* orientation, in order to form the *as* conformation. The small energy differences between the conformations of the clips **1a**, **3**, **4**, and **5**, are probably an effect of different cavity sizes and substituents on the side-walls.

A computational study was carried out to support the experimental studies on the conformational behaviour of the clip molecules. The heats of formation of the different conformers of **1b** and the di-benzene-walled clip **8** were calculated using various force fields (see Table 2). In all cases the *aa* conformer of **1b** was calculated to

have a lower energy than the *as* conformer, which is in line with that observed experimentally For **8** the CHARMm, Model and AMBER force fields and AM1 all calculated the *aa* conformer to be more favourable than the *as* conformer, which again is in line with the experimental results The semi-empirical method AM1 was the only method which calculated a smaller energy difference between the *as* and the *aa* conformations of clip **1b** than between the *as* and the *aa* conformations of clip **8** (see Table 2) Since this result more fully agrees with the experimental data, further computational studies were carried out using the semi-empirical method AM1

As mentioned above solvation effects probably play a role in determining the conformations of the clip molecules. Calculations were, therefore, carried using solvent models (AM1-SM2 for example, see Table 2) These calculations did not give a result which was more in line with the observed data This could be possibly due to the fact that these models used a solvent potential function instead of real solvent molecules

Table 2 *Calculated enthalpies and enthalpy differences (kJ/mol) and estimated equilibrium constants for the aa and as conformers of the naphthalene-walled clip* ***1b*** *and the benzene-walled clip* ***8***

	8				**1b**			
Method	$\Delta H aa$	$\Delta H as$	$\Delta\Delta H$[a]	$K_{(as/aa)}$	$\Delta H aa$	$\Delta H as$	$\Delta\Delta H$[a]	$K_{(as/aa)}$
Experiment	—	—	—	<0 01	—	—	—	0 075
CHARMm[b]	67 32	86 53	19 20	$8\ 65 \times 10^{-4}$	245 27	272 17	26 90	$3\ 72 \times 10^{-5}$
Tripos[c]	3 10	-9 00	-12 47	$3\ 06 \times 10^{2}$	56 11	63 55	7 44	$9\ 92 \times 10^{-2}$
Tripos[d]	42 84	37 24	-5 61	$1\ 92 \times 10^{1}$	93 81	110 25	16 44	$2\ 63 \times 10^{-3}$
Model[e]	271 37	287 98	16 61	$2\ 46 \times 10^{-3}$	414 51	441 79	27 28	$3\ 33 \times 10^{5}$
MM2[f]	-111 55	-114 52	-2 97	6 63	-41 42	-33 89	7 53	$9\ 59 \times 10^{-2}$
MM2[g]	-667 39	-669 52	-2 13	4 73	-617 93	-611 16	6 78	$1\ 30 \times 10^{-1}$
MM2[h]	-667 85	-670 07	-2 22	4 90	-618 81	-612 12	6 69	$1\ 34 \times 10^{-1}$
AMBER[i]	117 40	134 85	17 45	$1\ 76 \times 10^{-3}$	194 35	215 77	21 42	$3\ 53 \times 10^{-4}$
AMBER[g]	11 13	36 28	25 15	$7\ 87 \times 10^{-5}$	67 57	102 59	36 28	$1\ 47 \times 10^{-6}$
AMBER[h]	16 48	35 69	19 20	$8\ 64 \times 10^{-4}$	66 68	89 20	22 34	$2\ 44 \times 10^{-4}$
AM1[j]	516 77	537 27	20 50	$5\ 12 \times 10^{-4}$	758 06	772 74	14 69	$5\ 35 \times 10^{3}$
AM1-SM2[k]	454 34	479 78	25 44	$6\ 99 \times 10^{-5}$	693 46	714 54	21 09	$4\ 04 \times 10^{-4}$

[a] $\Delta Has - \Delta Haa$ [b] See ref 10 [c] Including electrostatics see ref 11 [d] Excluding electrostatics [e] See ref 12 [f] In vacuum, see ref 13 [g] In $CHCl_3$ [h] In $CHCl_3$, with extended Van der Waals, electrostatic cut-off 20Å [i] In vacuum [j] See ref 14 [k] Using AMPAC s solvent model 2

The heats of formation of the different conformations of the tetramethoxy clip **1a**, calculated using AM1, were not in agreement with the experimental results. The *aa* conformer was calculated to be more favourable than the *as* conformer. The difference in enthalpy between the two conformers, however, was calculated to be 3.8 kJ/mol smaller for **1a** than for **1b**. This would be in line with the proposal that the preference of **1a** to be in the *as* conformation is partially due to methoxy-carbonyl repulsion and partially due to solvation effects.

The process of interconverting one clip conformer to another was also calculated, using AM1[15] and the CHARMm[16] force field. In the case of CHARMm, the flipping process involving one benzene side-wall of **8**, was calculated to be an one step mechanism, with both methylene bridges rotating simultaneously. The calculations using AM1 indicated that these rotations were not synchronous. The second methylene group rotated somewhat later than the first one. The flipping of each of the naphthalene walls of **1b** was calculated to be a two step mechanism by both the AM1 and the CHARMm force field. The flipping process occurred via a stable intermediate which has only one methylene group rotated (see Figure 3). The energy required to convert one wall from the *anti* to the *syn* form was calculated to be significantly smaller for the benzene clip **8** (35 kJ/mol) than for the naphthalene clip **1b** (62 kJ/mol).

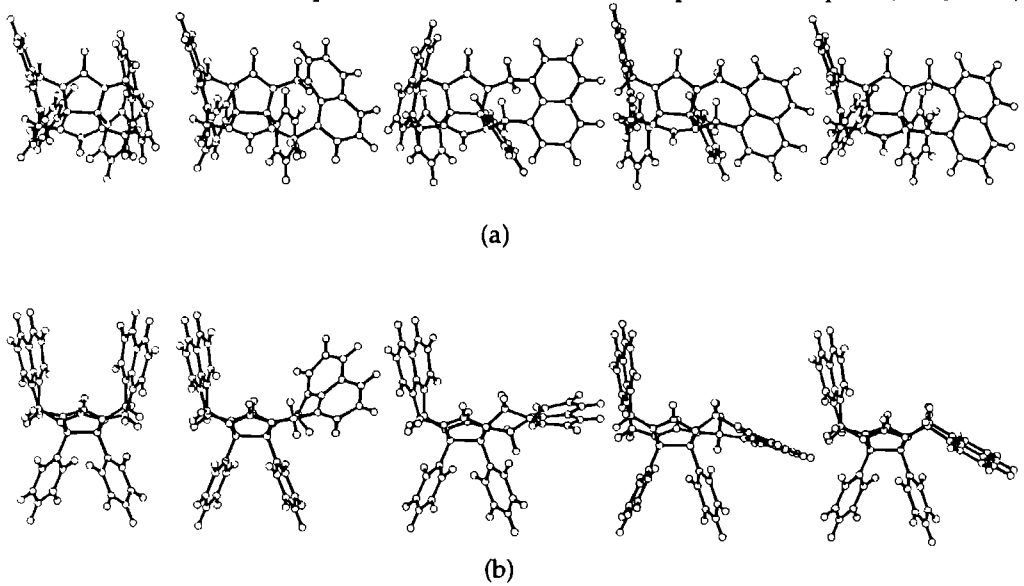

Figure 3. *The calculated mechanism (from left to right, AM1) of the flipping of an 1,8-connected naphthalene side-wall in clip* ***1b*** *(view from above (a) and front view (b)).*

This is due to greater strain present in molecule **1b** during the flipping process. One can tentatively conclude that the benzene-walled clips are more flexible than the

naphthalene-walled clips. The *aa* conformer of the benzene clip, however, is energetically much more favourable. The result is a very fast flipping process, 10^6-10^9 s^{-1} for the conversion from *aa* to *as* and 10^9-10^{12} s^{-1} from *as* to *aa* (using the Arrhenius equation), with the *aa* conformer being the only structure observed. This is in line with the ^1H NMR studies on **8**, which showed that only one conformer is present, even upon heating or cooling. As shown above, the flipping of the naphthalene walls of clip **1a** is a slow (1-10^3 s^{-1} using the Arrhenius equation) two step process. The electrostatic repulsions between the oxygen atoms of the methoxy groups and the carbonyl functions as well as solvation effects make the *as* conformer of this compound slightly more favourable than the *aa* conformer. Our experimental results and theoretical calculations are in agreement with calculations carried out by Sygula and Rabideau on the ring inversion of 9,10-dihydroanthracene and 7,12 dihydropleiadene.[17] They calculated that the benzene derivative was more flexible than the naphthalene derivative, and that the flipping process was an one step mechanism in the case of the benzene compound and a two step mechanism in the case of the naphthalene compound.

4.2.3 X-ray structures.

We were able to crystallize **2** (only the anti conformer) by slow diffusion of diethyl ether in a chloroform solution of this compound. The X-ray structure of **2** is presented in Figure 4. As can be seen the methoxy groups are in the plane of the naphthalene ring, with the lone pairs of the oxygen atoms pointing towards the carbonyl oxygen atoms of the glycoluril unit. The distance between the two oxygens is only 3Å. There is almost no twist in the diphenylglycoluril framework of the molecule which is contrary to the twist found for a clip with two 1,4-dimethoxybenzene side-walls[6b]

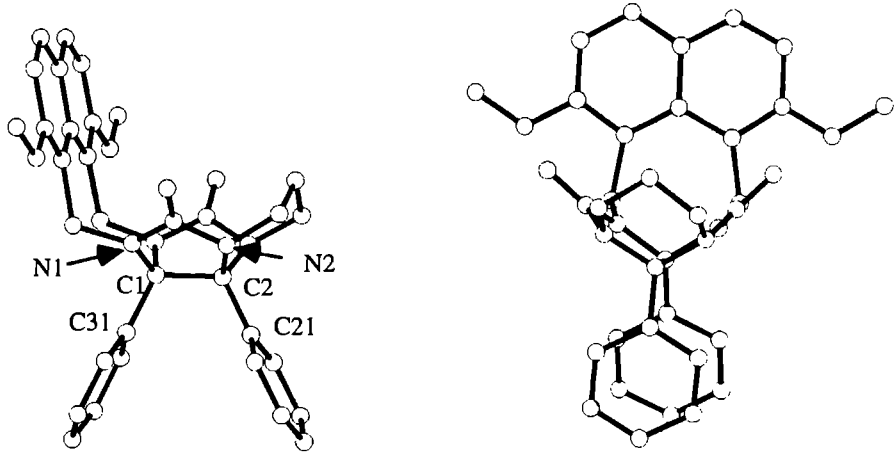

Figure 4. *X-Ray structure of* **2**; *left front view, right side view. Hydrogen atoms have been omitted for clarity.*

(torsion angle C31-C1-C2-C21 is 0.4°, torsion angle N1-C1-C2-N2 is 0.7°). The angle between the lines through the carbonyl groups (44.5°) in **2** is somewhat larger than the same angle in the above mentioned 1,4-dimethoxybenzene clip (39°). The distance between the two carbonyl oxygen atoms is somewhat smaller (5.34 Å compared to 5.52 Å). These small differences are a result of the larger 8-membered ring, which is formed by connecting the naphthalene moiety to the diphenylglycoluril part as compared to the 7-membered ring which is present in the 1,4-dimethoxybenzene clip. This larger ring makes molecule **2** more rigid. Interactions which are present between molecules of **2** within the crystal are discussed in Chapter 5.

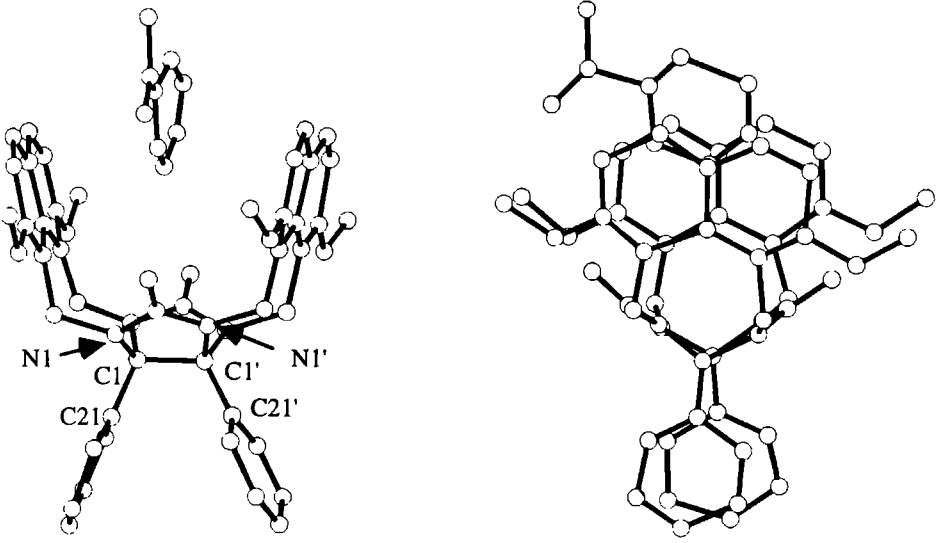

Figure 5. *Front view (left) and side view (right) of the X-ray structure of a complex of nitrobenzene with clip* ***1a****. Hydrogen atoms have been omitted for clarity.*

Attempts to crystallize **1a** failed, probably because the different conformations precipitated together, not forming a single crystalline product. This molecule therefore was crystallized in the presence of a guest molecule. Several crystals of **1a** were obtained with silver perchlorate and silver tetrafluoroborate as the guest molecules (*vide infra*). These crystals, however, were unstable under the X-ray conditions. Finally nitrobenzene was used as a guest molecule. From a mixture of chloroform and nitrobenzene, a single brown crystal was slowly grown (three months), which was suitable for X-ray analysis. The structure is shown in Figure 5. The nitrobenzene guest molecule is sandwiched between the two naphthalene rings in an offset manner. As expected the nitro group of the guest is pointing out of the cleft. The guest molecule is not symmetrically bound in the cleft, but prefers to be approximately parallel with one of the aromatic surfaces. The angle between the planes of the aromatic guest and the naphthalene rings, is approximately 5.39° for one side-wall and 16° for the other side-

wall. The center-to-center distance between the aromatic side-walls is 6.8 Å. The distance between the aromatic ring of the guest and the host side-wall is 3.4 Å, which is ideal for π-π stacking interactions. As in the case of **2** the twist in the diphenylglycoluril framework is small (torsion angle C21-C1-C1'-C21' is 2.1°, torsion angle N1-C1-C1'-N1' is 13.7°). The distance between the carbonyl oxygens atoms is 5.67 Å, and the angle between the lines through the carbonyl groups is 37.9°. As in the structure of **2**, the methoxy groups of the side-walls are in the plane of the naphthalene rings. For a discussion of the interactions between molecules within the crystal, see Chapter 5.

4.2.4 Binding properties

Binding of aromatic guest molecules

Depending on the type of guest molecule, binding in our clips can be achieved by means of π-π interactions only or by a combination of π-π interactions and hydrogen bonding. In the former case the geometry of the host-guest complex is determined completely by the most optimal π-π interaction, whereas in the latter case the geometry is mainly determined by the most optimal hydrogen bonding interaction (see Chapter 3). In Table 3 the association constants of complexes between aromatic guest molecules and clip molecules **1a**, **1b** and **2** are presented. Examination of Table 3 reveals that the binding of guest molecules in host molecule **1b** is much weaker than in **1a**. This implies that the presence of the methoxy groups, which make the naphthalene moieties more electron rich, significantly enhances the binding. In the case of clip **1b** the binding constants were, unfortunately, too low to enable a good comparison with

Table 3: *Association constants (K_a) of complexes between aromatic guest molecules and the aa conformers of different host molecules in $CDCl_3$ at 298 K.*

Guest	K_a (M^{-1}) **1a**[a]	K_a (M^{-1}) **1b**[b]	K_a (M^{-1}) **2**
1,3-dinitrobenzene	115[c]	20	< 2
1,4-dicyanobenzene	178[c]	5	< 2
1,3-dihydroxy-5-pentylbenzene	1400	45	20[a]
hexyl 3,5-dihydroxy benzoate	9000	300	-

[a] Calculated from the change in ratio of the conformers as a function of the guest concentration (estimated errors 10-15%), see ref 6. [b] Calculated by fitting the ^1H NMR chemical shifts of the naphthalene protons as function of the guest concentration The calculated CIS value for proton H4 of the naphthalene side-wall (-0.36 ppm) is comparable with the CIS value calculated for clip **8** (see Chapter 3) [c] Values taken from ref 6

the binding constants of **1a**. The results, however, suggest that the two clips display an opposite trend in the complexation of aromatic guest molecules that are bound by π-π interactions only. Clip molecule **2**, which has only one side-wall, has a negligible interaction with guest molecules that are unable to form hydrogen bonds. The presence of the second side-wall apparently is necessary to form a host-guest complex of sufficient stability (see Chapter 3). The complexation of 1,3-dihydroxybenzenes to **1a** and **1b**, follows the same pattern as found for the benzene-walled clip molecules (see Chapter 3). The complexation to **1a** is much more favourable than to either **1b** or **2**, because of the absence of the methoxy groups in **1b** and because of the fact that only one side-wall is present in **2**.

In an earlier paper we proposed that aromatic guest molecules are bound between the walls of clip **1a** in an offset geometry.[6a] The crystal structure of the complex between nitrobenzene and **1a** shows that this proposal is correct (Figure 5).[18] The nitro group of the guest points out of the cleft. The distance between the aromatic ring of the guest and the side-wall is 3.4 Å, which is ideal for π-stacking interactions. It was of interest to calculate the optimal geometry for this complex and to compare it with the experimentally determined one. The calculations were carried out using the Hunter and Sanders model.[19] The energy profile for the interaction of a nitrobenzene molecule with a 2,7-dimethoxynaphthalene molecule was determined in the following way. The nitrobenzene molecule was moved in a grid (8Åx8Å) over the naphthalene molecule at a Z displacement (face-to-face distance) of 3.4 Å. The former molecule was subsequently rotated 5° and the grid search was carried out again. This procedure was repeated until the nitro function had been rotated through 180°. The calculated energy minimum (optimum π-π interaction) was found at the same offset geometry as in the X-ray structure, with the guest molecule rotated approximately 25° with respect to the naphthalene C9-C10 bond (Figure 6).

An important consideration is the steepness of the calculated energy minimum. This gives information about how rigid the guest molecule is bound in a specific geometry in the cleft of the clip. In order to study this, the interaction energy was plotted as a function of the rotation of the guest with respect to the naphthalene ring, and as function of its displacement in horizontal (x) and vertical (y) direction (Figure 6). From Figure 6 it can be seen that the minima are relatively shallow, and that the bound guest molecule has a high degree of rotational and translational freedom. Within 1 kJ/mol range of the minima the guest molecule can shift approximately 1 Å in the x and y direction, and rotate ca. 50°. The results of these calculations lead to the same conclusion as made in Chapter 3: the Van der Waals interaction dominates the overall

attraction energy between the host and guest, while the electrostatic interaction accounts for the geometry of the complex.

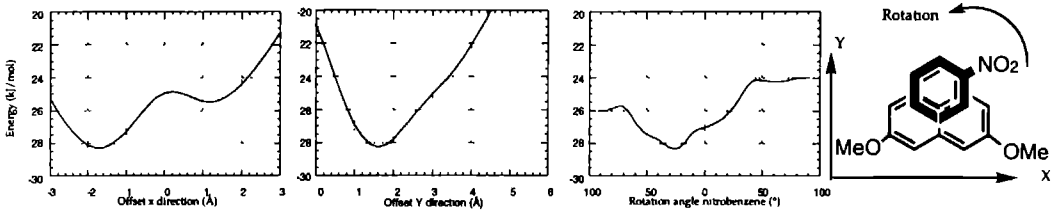

(a) (b) (c)

Figure 6: *The calculated interaction energy between a nitrobenzene and a 2,7-dimethoxynaphthalene molecule as a function of the offset in horizontal (x) and vertical (y) direction (a,b) and as function of the rotation of the nitrobenzene molecule with respect to the naphthalene ring (c).*

Binding of silver ions

It is known in the literature that silver ions can form complexes with carbon-carbon double bonds and with aromatic surfaces.[20] X-ray structures of silver ions complexed to benzene molecules show that the binding is towards one of the double bonds of the aromatic ring, with an Ag-benzene distance of approximately 2.5 Å.[21] When the sparingly soluble salt $AgClO_4$ was added to a solution of **1a** in $CDCl_3$ a decrease in the *sa* and an increase in the *aa* conformer was observed by ^1H NMR. Subsequent titrations of this host with various silver salts in $CD_3OD/CDCl_3$ (1:9, v/v, to increase the solubilty of the salts) revealed that the proportion of the *ss* conformer also increased, indicating that the latter is also capable of binding a silver ion more strongly than the *sa* conformer (Figure 7). From the changes in the conformational ratios relative binding constants for silver ions to the different conformers were calculated (Table 4). The *aa* conformer appeared to give the strongest complexes with the silver salts. In the case of this conformer a sandwich complex can be formed, with the silver ion having interactions with both aromatic side-walls. Shifts in the ^1H NMR signals of the aromatic protons of the *aa* and *ss* conformers were also observed, but these shifts could not be used to calculate the geometries of the complexes. The equilibria in these systems are too complex to be interpreted due to silver ions being bound to different conformations, whose ratios change upon increasing the silver concentration. As can be seen in Table 4 the values of K_{aa} and K_{ss} strongly depend upon the type of silver salt. The stronger the interaction is between the anion and silver ion, the weaker the complex between the silver salt and the clip molecule. A similar observation was

made by Crookes et al. in their studies on the complexation of different silver salts to ethene.[22] They explained the observed anion dependencies as a result of competition between the anion and the ethene for the Ag^+-cation.

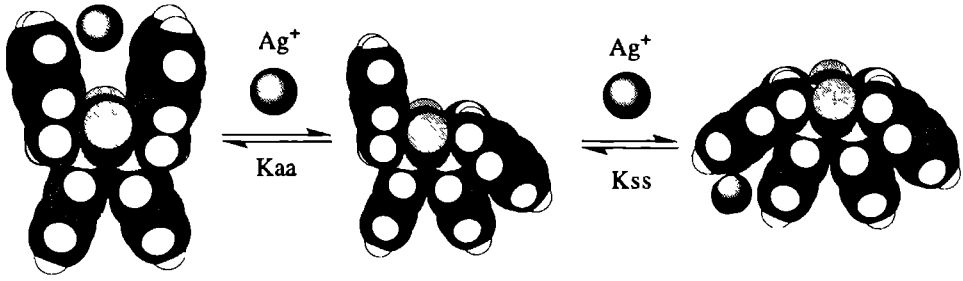

aa *sa* *ss*

Figure 7: *Binding of Ag^+ ions by the aa and the ss conformers of clip* **1a**. *Methoxy groups have been omitted.*

The relative binding constant of the *ss* conformer (K_{ss}) of **1a** is approximately half that of the *aa* conformer (Table 4). When clip **9**, in which the phenyl groups of the glycoluril unit are replaced by methyl groups, was titrated with $AgClO_4$, only a change in the amount of *aa* conformer was observed. This implies that the phenyl groups of clip **1a** are involved in the binding of Ag^+ to the *ss* conformer. The association constant of the complex between $AgClO_4$ and the *aa* conformer of **9** (K_{aa} = 44 M^{-1}) was smaller than that observed for the complex of this salt with the *aa* conformer of **1a** (K_{aa} = 149 M^{-1},Table 4). This is the result of a larger energy difference between the *aa* and the *sa* conformers of clip **9**. When no guest was present the amount of *aa* conformer of **9** was almost zero.

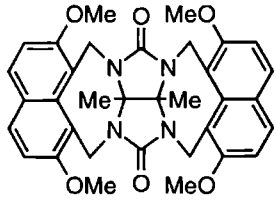

9

Table 4: *Relative association constants (M^{-1}) for the complexation of silver salts to the aa and ss conformers of* **1a**.[a]

Silver salt	K_{aa}	K_{ss}	Silver salt	K_{aa}	K_{ss}
$AgClO_4$	149	53	Ag_2SO_4	0	0
$AgBF_4$	98	37	$AgNO_3$	0	0
CF_3SO_3Ag	50	25	Ag_2CO_3	0	0
$AgPF_6$	10	10	$C_6H_5CO_2Ag$	0	0
CH_3SO_2Ag	0	0	CH_3CO_2Ag	0	0

[a]Estimated error 15%.

To locate the binding site of the silver ion, ^{13}C-NMR experiments were carried out. ^{13}C DEPT and 2-D HETCOR (HMQC) spectra were recorded in order to assign the ^{13}C-NMR signals of clip **1a**. Only those of the *sa* conformer could be completely assigned. The signals of the other conformers had intensities too low to give cross peaks in the 2-D spectra. When $AgClO_4$ was added to a solution of **1a** in $CD_3OD/CDCl_3$ (1:9, v/v), the aromatic region of the ^{13}C spectrum became extremely complex. This suggests that the aromatic rings of **1a** are involved in the process of complexation. This is in agreement with the observed shifts of the aromatic protons in the ^{1}H NMR spectrum upon the addition of silver salts. No large shifts were seen for the carbonyl or the methoxy groups, indicating that these groups do not bind the silver ions. If this indeed is the case, clip **1b** should be able to bind Ag^+ cations as well. A titration experiment with $AgBF_4$ showed that binding to **1b** does take place, but that the complex was significantly weaker (K_{aa} = 20 M^{-1}) than that found for **1a**. This is probably due to the lower electron density on the aromatic side-walls of **1b**.

To further determine the most favourable binding site for the silver ion, AM1 calculations were performed. The sites with the highest π-electron density can be expected to bind the silver ion. In Figure 8a the calculated electron distribution in the naphthalene rings of **1a** is depicted. A likely position of the silver ion is shown in Figure 8b.

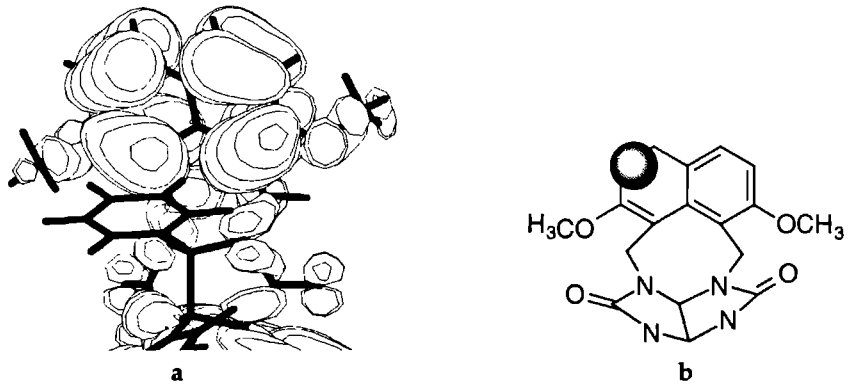

a **b**

Figure 8: *The highest occupied π-orbitals of* ***1a*** *according to AM1 calculations (a) and the predicted binding geometry of the silver ion with the aa conformer of clip* ***1a*** *(b).*

The binding of a silver ion to the *ss* conformer of clip **1a** can occur at three possible sites; *i*) between the two phenyl rings, *ii*) between a phenyl and a naphthalene ring, and *iii*) on the top of one of the naphthalene walls (see Figure 9). Although naphthalene is known to bind silver ions in the solid state,[21] binding studies with 2,7-dimethoxynaphthalene revealed that this compound does not form a complex with Ag^+ in methanol/chloroform solution at concentrations between 2 and 20 mmol. As the *as* conformer of **9** does not bind silver either, the binding of Ag^+ to the top of a

naphthalene ring (Figure 9c) can be rejected. From separate binding experiments with a diphenylglycoluril molecule without any side-walls we concluded that the silver ion is not bound between the phenyl groups of the diphenylglycoluril unit, hence Figure 9a can be rejected. The most likely place for the silver ion, therefore, is between a naphthalene and a phenyl ring (Figure 9b). Again, the most electron rich sites of the naphthalene moiety will be involved. Another possibility is that the silver ion is not complexed to the aromatic part of the *ss* conformation of **1a**, but to concave side of the diphenylglycoluril part of the molecule as depicted in Figure 9d. The inner pocket of a glycoluril molecule was recently calculated to be negatively charged,[26] which would make it favourable for the silver ion to be bound at this position. No experimental evidence, however, was found for this particular binding geometry.

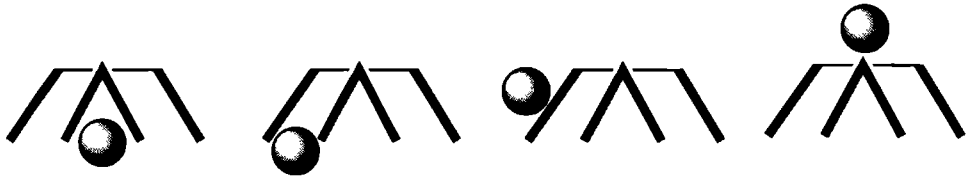

Figure 9. *Schematic representation of the four possible binding places of the silver ion in the aa conformer of* ***1a****. The second mode of complexation (b) is the proposed complex geometry.*

In a previous paper we showed that receptor molecules of type **1** functionalized with two azacrown ether rings can display cooperative and allosteric binding.[23] Attempts to achieve allosteric binding with **1a**, a silver ion and an aromatic guest (dinitrobenzene), unfortunately, were not successful: the addition of the silver salt led to competition with the aromatic guest, instead of an increased binding of the latter molecule due to a preorganizing of the host.

4.3 CONCLUSIONS

These studies have shown that the methoxy groups on the side-wall of clip **1a**, play an important role, both in determining the conformation of the host and in promoting the complexation of guest molecules. Clip molecule **1b**, which does not have methoxy groups, mainly exists in the *aa* conformation in contrast to **1a** which exists mainly in the *as* conformation. The former compound shows a significant lower affinity for aromatic guest molecules and silver ions. The lower complexation ability of **1b** compared to **1a**, is due to weaker π-π interactions with the guest molecules. This follows from experimental data as well as calculations using the Hunter and Sanders model. Solvation effects also play a role in the conformational behaviour of the clip

molecules. A molecule with only one 2,7-dimethoxynaphthalene side-wall (**2**), prefers to be in the *anti* conformation rather than in the *syn* conformation due to this solvation effect. The weaker complexes formed between aromatic guests and **2** compared to **1a**, is a result of the fact that this host molecule has only one side-wall, and is in line with the results shown in Chapter 3. The X-ray structure of a complex between nitrobenzene and **1a** showed clearly that the guest molecule is bound in an offset geometry. This geometry was also calculated to be the most favourable one. A computational study of the conversion of the side-walls of clip molecules from *anti* to *syn* with respect to the phenyl groups of the diphenylglycoluril framework, revealed that the naphthalene walls flip according to a two step mechanism and the benzene walls according to an one step mechanism. The latter process is much faster than the former, which leads to the conclusion that benzene-walled molecules are much more flexible. The *aa* conformer of benzene-walled clips is much more favourable than the *as* and *ss*, and therefore this is the only conformation observed in solution and the solid state.

4.4 EXPERIMENTAL SECTION

4.4.1 General

DMSO was distilled and stored over Mol Sieves 3Å before use. All other chemicals were commercial samples and used without further purification. For column chromatography, Merck silica gel (60H) was used. Melting points were determined on a Jeneval polarization microscope THMS 600 hot stage and are reported uncorrected. ^{1}H NMR and ^{13}C NMR spectra were recorded on a Bruker AM 400 MHz instrument. Chemical shifts are reported downfield from internal TMS (δ=0.0 ppm). Abbreviations used are d = doublet, dd = doublet of doublets and m = multiplet. FAB mass spectra were recorded on a VG 7070E instrument. IR spectra were recorded on a BioRad FTS-25 spectrometer. Elemental analyses were determined with a Carbo Erba Ea 1108 instrument.

4.4.2 Compounds

Diphenylglycoluril (7). This compound was synthesized from urea and benzil according to a literature procedure.[6]

1,8-Bis(bromomethyl)naphthalene. This compound was synthesized by bromination of 1,8-dimethylnaphthalene with N-bromosuccinimide according to a standard procedure.[27]

17b, 17c-Dihydro-17b, 17c-diphenyl-7H, 8H, 9H, 16H, 17H, 18H-7a, 8a, 16a, 17a-tetraazapentaleno[1", 6":5, 6, 7; 3", 4": 5', 6', 7'] dicycloocta[1, 2, 3-de: 1', 2', 3'd'e'] dinaphthalene-8, 17-dione (1b). A suspension of 110 mg (1.96 mmol) of powdered KOH in 2 mL of degassed DMSO was stirred under nitrogen for 30 min. Compound **7** (142 mg, 0.483 mmol) and 1,8-bis(bromomethyl)naphthalene (307 mg, 0.977 mmol) were added and the mixture was cooled whilst stirring. After 3 hrs, the mixture was poured into 50 mL of water and the product extracted twice with CH_2Cl_2. The combined organic layers were washed with water, dried ($MgSO_4$) and concentrated *in vacuo*. Purification by column chromatography (1% EtOH in CH_2Cl_2) gave 98 mg (34%) of **1b** as a white solid. A sample was recrystallized from $CHCl_3$/diethylether for analysis: Mp>400°C (dec); IR (KBr) ν 1719, 1699 (C=O); ^{1}H NMR ($CDCl_3$: *aa* conformer: δ 7.66 (d, 4H, Napht H-4, J=8.0 Hz), 7.61 (d, 4H, Napht H-2, J=7.0 Hz), 7.24 (dd, 4H, Napht H3, J=8.0 Hz J=7.0 Hz), 7.35-7.10 (m, 10H, ArH), 4.98 (d, 4H, NCH_2Napht, J= 16.2 Hz), 4.56 (d, 4H, NCH_2Napht, J= 16.1 Hz); *as* conformer: d 7.91 (d, 2H, Napht H-4 a, J=8.2 Hz), 7.85 (d, 2H, Napht H-2 a, J=6.7 Hz), 7.50 (m, 2H, Napht H3 a,), 7.38-6.98 (m, 11H, ArH a Napht-H s), 6.43 (d, 2H, Ar-H s, J=7.7 Hz), 6.30 (d, 1H, Ar-H s, J=7 Hz), 6.14 (dd, 2H, Ar-H s, J=7 Hz J=7.7 Hz), 5.27 (d, 2H, NCH_2Napht s, J= 14.6 Hz), 5.20 (d, 2H, NCH_2Napht s, J= 14.7 Hz), 5.07 (d, 2H, NCH_2Napht a, J= 16.2 Hz), 4.71 (d, 2H, NCH_2Napht a, J= 16.1 Hz). ^{13}C-NMR ($CDCl_3$) d 157.23 (urea C=O), 135.79, 135.28, 133.49, 131.06, 130.62, 130.16, 128.85, 128.60, 124.82 (Napht-C and Ph-C), 84.00 (PhCN), 47.60 (NaphtCH_2N). FAB-MS (m-nitrobenzylalcohol) m/z 599 $(M+H)^+$. Anal. Calcd. for $C_{40}H_{30}N_4O_2.CHCl_3$: C, 68.58; H, 4.35; N, 7.80. Found: C, 68.65; H, 4.42; N, 7.66.

17b, 17c-Dihydro-1, 6, 10, 15,- tetramethoxy-17b, 17c-dimethyl-7H, 8H, 9H, 16H, 17H, 18H-7a, 8a, 16a, 17a-tetraazapentaleno[1", 6":5, 6, 7; 3", 4": 5', 6', 7'] dicycloocta[1, 2, 3-de: 1', 2', 3'd'e'] dinaphthalene-8, 17-dione (9): This compound was synthesized as described elsewere.[24]

Determination of association constants by ^{1}H NMR

Two general methods were used to measure the binding constants. When possible, a signal in the ^{1}H NMR spectrum of the host was followed as function of the guest concentration (or vice versa), obtaining a curve which was fitted using the procedure described in Chapter 3. In the case of clips displaying more that one conformation the ratio between the different conformers was measured as function of the guest concentration, by integrating appropriate signals in the ^{1}H NMR spectra. More accurate results were obtained when the peak areas were determined by fitting the peaks with Lorentz curves (WIN-NMR). When only the *aa* conformer was able to bind a guest molecule the Ka was calculated by using the following equations:[6a]

$$K_a = \frac{[aa \cdot G]}{[aa] \times [G]} \quad (1)$$

$$[aa] = \frac{[sa]}{K_{sa/aa}} \quad (2)$$

$$K_{sa/aa} = \frac{[sa]}{[aa]} \quad (3)$$

$$[aa \cdot G] = [aa]_{tot} - [aa] \quad (4)$$

$$[G] = [G]_{tot} - [aa \cdot G] \quad (5)$$

In the case of the silver ions, which also bind to the ss conformer, different equations were used:

$$K_{aa} = \frac{[aa \cdot G]}{[aa] \times [G]} \qquad K_{ss} = \frac{[ss \cdot G]}{[ss] \times [G]} \quad (6)$$

$$[aa] = \frac{[sa]}{K_{sa/aa}} \qquad [ss] = \frac{[sa]}{K_{sa/aa}} \quad (7)$$

$$K_{sa/aa} = \frac{[sa]}{[aa]} \qquad K_{sa/ss} = \frac{[sa]}{[ss]} \quad (8)$$

$$[aa \cdot G] = [aa]_{tot} - [aa] \qquad [ss \cdot G] = [ss]_{tot} - [ss] \quad (9)$$

$$[G] = [G]_{tot} - [aa \cdot G] - [ss \cdot G] \quad (10)$$

The binding to the *sa* conformer was neglected. Typical concentrations for **1a** and for the silver salts were 2mM and 1 to 20 mM, respectively.

Crystal data of the ***1a****-nitrobenzene complex:*

$C_{50}H_{43}N_5O_8$, Mr = 842.9, T = 293 K, triclinic, space group P1, a = 12.188(9), b = 12.161(12), c = 17.756(13) Å, α = 103.33(13), ß = 104.74(*), γ = 107.70(*)°, V = 2285 $Å^3$, Z = 2, Dx = 1.224 g/cm^3, Mo Kα radiation, μ = 0.78 cm^{-1}.

Crystal data of **2***:*

$C_{32}H_{28}N_4O_5$, Mr = 548.6, T = 208 K, orthorombic, space group Pbca, a = 12.3332(16), b = 27.874(2), c = 15.1246(15) Å, V = 5199 $Å^3$, Z = 8, Dx = 1.402 g/cm^3, Mo Kα radiation, μ = 0.90 cm^{-1}.

More detailed crystallographic data will be published in a separate paper.[25]

References

1 Fischer, E. *Ber. Dtsch. Chem. Ges.* **1894**, *27*, 2985-2993.

2 Cram, D.J. *Angew. Chem.* **1988**, *100*, 1041.

3 Recent reviews: (a) Cram, D. J. *Top. Curr. Chem.* **1981**, *98*, 43. (b) Schneider, H-J. *Angew. Chem.* **1991**, *103*, 1419. (c) Diederich, F. *Angew. Chem.* **1988**, *100*, 372. (d) Seel, C.; Vögtle, F. *Angew. Chem.* **1992**, *104*, 542. (d) Rebek, Jr., J. *Angew. Chem.* **1990**, *102*, 261. (e) Izatt, R. M.; Bradshaw, J. S.; Pawlak. K.; Bruening, R. L.; Tarbet, B. J. *Chem. Rev.* **1992**, *92*, 1261. (f) various authors in *Tetrahedron*, **1995**, *51*, vol. 2 topic molecular recognition. (g) Cram, D. J. *Nature*, **1992**, *356*, 29. (h) Zimmerman, S. C. "*Bioorganic Chemistry Frontiers 2*," **1991**, Springer-Verlag Berlin heidelber, 33. (i) Hamilton, A. D. "*Bioorganic Chemistry Frontiers 2*," **1991**, Springer-Verlag Berlin heidelber, 115.

4 Whitlock B. J.; Whitlock, H. W. *J. Am. Chem. Soc.* **1994**, *116*, 2301-2311.

5 (a) Koshland, D. E., Jr. *Proc. Natl. Acad. Sci. U.S.A.* **1958**, *44*, 98. (b) Birktoft, J. J.; Banazak, L. J. in "*Peptide and Protein Reviews*," Hearn, M. T. W. Ed. Dekker, New York, **1984**, vol 4, 1-46.

6 (a) Sijbesma, R. P.; Wijmenga, S. S,; Nolte, R. J. M. *J. Am. Chem. Soc.*, **1992**, *114*, 9807-9813. (b) Sijbesma, R. P.; Kentgens, A. P. M.; Lutz, E. T. G.; Van der Maas, J. H.; Nolte, R. J. M. *J. Am. Chem. Soc.* **1993**, *115*, 8999.

7 (a) Perrin, C. L.; Gipe, R. K.; *J. Am. Chem. Soc.*, **1984**, *106*, 4036. (b) Abel, E. A.; Coston, T. P. J.; Orrell, K. G.; Sik, V.; Stephenson, D. *J. Magn. Reson.*, **1986**, *70*, 34. (c) Jorgensen, W. L.; Severance, D. L. *J. Am. Chem. Soc.*, **1990**, *112*, 4768.

8 Johnson, C. S., Jr.; Bovey, F. A. *J. Chem. Phys.* **1958**, *29*, 1012.

9 Compound **1a** was reduced by a procedure developed by G. Gieling (Thesis, Nijmegen 1996). The ^{1}H NMR (1-D, and 2-D COSY), ^{13}C-NMR spectra and FAB-MS of the compound indicated that it was the mono-reduced 2,7-dimethoxynaphthalene clip.

10 CHARMm Version 22.0, Revision 92.0911, Resident and Fellows of Harvard College ©1984, 1992, using template charges.

11 Sybyl Molecular Modeling Software, Version 6.0, TRIPOS Associates, Inc. **1992**.

12 Allinger, N.L.; Tribble, M.T.; Miller, M.A.; Wertz, D.H. *J. Am. Chem. Soc.* **1971**, *93*, 1637.

13 Mohamadi, F.; Richards, N.G.J; Guida, W.C.; Liskamp, R.; Lipton, M.; Caufield, C.; Chang, G.; Hendrickson, T.; Still, W.C. *J. Comp. Chem.* **1990**, *11*, 440.

14 Dewar, M.J.S.; Zoebisch, E.G.; Healy, E.F.; Stewart, J.J.P. *J. Am. Chem. Soc.* **1985**, *107*, 3902.

15 The conformation of the clip was forced to change and the transition structures were refined using the TS algorithm of ampac, see Dewar, M.J.S.; Healy, E.F.; Steward, J.J.P., *J. Chem. Soc., Faraday Trans. 2*, **1984**, *80*, 227.

16 The travel algorithm of CHARMm was used, see Fischer, S.; Karplus, M. *Chem. Phys. Lett.* **1992**, *194(3)*, 252.

17 Sygula, A.; Rabideau, P.W. *J. Comp. Chem.* **1992**, *13*, 633.

18 For other complexes with nitrobenzene guest molecules see: (a) Harmata, M. Barnes, C. L. *J. Am. Chem. Soc.* **1990**, *112*, 5655. (b) Harmata, M. Barnes, C. L.; Karra, S. R.; Elahmad, S. *J. Am. Chem. Soc.* **1994**, *116*, 8392. Whitlock, B. J. ; Whitlock, H. W. *J. Am. Chem. Soc.* **1990**, *112*, 3910.

19 Hunter, C. A.; Sanders, J. K. M. *J. Am. Chem. Soc.* **1990**, *112*, 5525.

20 (a) Lewandos, G. S.; Gregston, D. K.; Nelson, F. R. *J. Organmetal. Chem.* **1976**, *118*, 363. (b) Andrews, L. J. *Chem. Revs.* **1954**, *54*, 713. (c) Griffith, E. A. H.; Amma, E. L. *J. Am. Chem. Soc.* **1974**, *96*, 5407. (d) Griffith, E. A. H.; Amma, E. L. *J. Am. Chem. Soc.* **1971**, *93*, 3167. (e) Kang, H. C.; Hanson, A. W.; Eaton, B.; Boekelheide, V. *J. Am. Chem. Soc.* **1985**, *107*, 1979. (f) Pierre, J-L.; Baret, P.; Chautemps, P.; Armand, M. *J. Am. Chem. Soc.* **1982**, *103*, 2986. (g) Komfort, M.; Rohne, B.; Dreeskamp, H.; Zander, Z. *J. Photochem. Photobiol. A: Chem.* **1993**, *71*, 39.

21 (a) Rodesiler, P. F.; Griffith, E. A. H.; Amma, E. L. *J. Am. Chem. Soc.* **1972**, *94*, 761. (b) Taylor, Jr., I. F.; Hall, E. A.; Amma, E. L. .*J Am. Chem. Soc.* **1969**, *91*, 5745. (c) Griffith, E. A. H.; Amma, E. L. *J. Am. Chem. Soc.* **1974**, *96*, 743.

22 Crookes, J.V.; Woolf, A.A. *J. Chem. Soc. Dalton* **1973**, 1241-1247.

23 Sijbesma, R. P.; Nolte, R. J. M. *J. Phys. Org. Chem.* **1992**, *5*, 649.

24 van Nunen, H. L. M., Thesis **1995**, Nijmegen.

25 de Gelder, R.; Beurskens, P. T.; Reek, J. N. H.; Nolte, R. J. M. to be published.

26 Li, N.; Maluendes, S.; Blessing, R. H.; Dupuis, M.; Moss, G. R.; DeTitta, G. T. *J. Am. Chem. Soc.* **1994**,*116*, 6494.

27 Sisti, A. J.; Meyers, M. *J. Org. Chem.* **1973**, *38*, 4431.

Chapter 5

Self-Association and Self-Assembly of Molecular Clips in Solution and in the Solid State

5.1 INTRODUCTION

In our group we have synthesized clip-shaped molecules of type **1** (Chart I) which are able to selectively bind dihydroxybenzenes.[1] This binding is based upon hydrogen bonding, π-π interactions and a so-called 'cavity effect'. After detailed investigations we were able to separate the contribution of each factor involved in this complexation process (see Chapter 3). Enlarging the side-walls of **1** resulted in a clip (**2**) which was able to bind aromatic guest molecules by π-π interactions only.[2] During these binding studies we observed that some of our clips underwent self-association in solution. In this chapter we describe this self-association process in more detail. We also discuss the solid state structures of a series of clip molecules, which -as will be shown- are generated by self-association and self-assembly processes involving π-π interactions.

5.2 RESULTS AND DISCUSSION

5.2.1 Self-association in solution

Careful study of the ^{1}H NMR spectra of a series of molecular clips related to **1** has revealed that upon dilution or temperature variation the ^{1}H NMR resonances changed. Since in most of these clip molecules no conformational changes were expected and since the shifted signals were mainly those of the side-walls and the methoxy groups, a dimerization process was proposed (Chapter 3). In order to study this dimerization in more detail the ^{1}H NMR chemical shifts of the clips were followed upon stepwise dilution of the compounds (Figure 1). Dilution curves were fitted using the standard equation[3] for the equilibrium:

$$2A \rightleftharpoons A_2 \qquad (1)$$

From these fits values for the self-association constant (K_{self}) and the complex induced shifts (CIS)† were obtained. These CIS values can be used to obtain information about the geometry of the complex, as in the case of the host-guest complexes (see Chapter 3). A program based on the Johnson and Bovey[4] tables was used to calculate the approximate geometries of the complexes. According to this method compound **1a** dimerized symmetrically, with one side-wall of a clip filling the cavity of the other (Figure 1). The influence of the depth of binding on the CIS values was calculated. The X-ray structure of dimeric **3** (*vide infra*) was used as a reference point. The geometry of this dimer was calculated to induce an average shift of the side-wall protons of 1.8 ppm. Since this value was more than the observed shift for **1a**, the molecules of the dimer were pulled stepwise apart, and the CIS values were calculated at each point. These CIS values decreased linearly with increasing clip distance, see Figure 2. From this figure we concluded that the molecules of the dimer of **1a** in solution are approximately 1.5 Å further apart than those of **3** in the solid state.

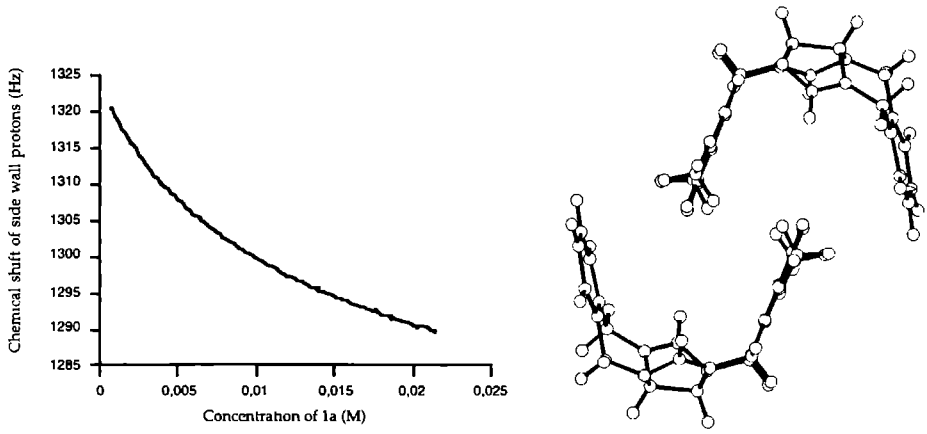

Figure 1: *The ^1H NMR (200 MHz) chemical shift of the side-wall protons of clip* ***1a*** *which vary as a function of the concentration (left). The dimeric structure of clip* ***1a****, based on the calculated CIS value and the Johnson and Bovey tables (right). Phenyl groups of the diphenylglycoluril unit have been omitted.*

At room temperature, the self-association constant of **1a** was found to be low (K_{self} = 16 M^{-1}). The basis underlying the self-association was thought to be due to two factors; (i) π-π interactions between the two sets of 1,4-dimethoxybenzene side-walls (which is calculated to be favourable using the Hunter and Sanders model, *vide infra*) and (ii) a 'cavity effect'. The latter effect can be considered to consist of two components: a

† CIS predicted shift ($\partial_s = \partial_{dimer} - \partial_{monomer}$) upon full dimerization.

solvation effect and an entropy effect. The initial π-π interaction between two walls reduces the rotational freedom of the clip molecules. This reduction in rotational freedom is entropically unfavourable. The π-π interactions between the third and fourth side-wall are 'free' of this loss in entropy. The cavity effect in the dimerization process is expected to be of the same order of magnitude as the cavity effect observed for the formation of a host-guest complex (see Chapter 3). The addition of methanol to a concentrated sample of clip **1a** in chloroform, caused a large downfield shift of the ^{1}H NMR signals of the side-wall protons. This suggests that methanol molecules break up the dimer, probably because they solvate the cavity of the clip to a greater extent than chloroform molecules do. A part of this solvent effect may also be due to an increase in the dielectric constant.

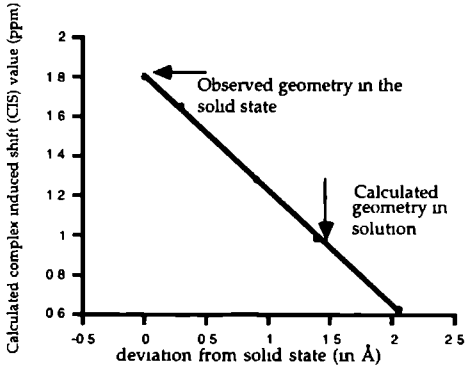

Figure 2: *The calculated complex induced shift (CIS) values of the side-wall protons of two clips* ***1a****, forming a dimer, as function of the distance between them. As reference point the the geometry of the X-ray structure of* ***3*** *was taken.*

In order to obtain more insight into the factors determining the dimerization process, the self-association behaviour of a series of different clip molecules was studied in detail (Table 1). From these studies several trends were derived. Methoxy groups attached to the aromatic side-walls of the clips appeared to enhance the dimerization. Substituting the methoxy groups of clip **1a** for methyl groups (**1c**) reduced the self-association. Clip molecules with unsubstituted benzene side-walls (**1b** and **4b**) did not self-associate at all. In the case of these clips the cavity effect and the π-π interactions (which is reduced due to a smaller Van der Waals interaction) are decreased to such an extent that no gain in free energy is obtained by dimerization.

Enlarging the aromatic ring of **1a** to a 2,7-dimethoxynaphthalene ring (clip **2**), increased the self-association significantly (for the *aa* conformer: K_{self} = 60 M^{-1}, Table 1). This increase is due to a larger contribution of both the π-π interaction and the

cavity effect. We expected that dimers between two *aa* conformers of clip **2**† would be more easily formed than between an *aa* conformer and an other conformer of **2**, since in the former case two cavity effects and three 'side-wall'-'side-wall' interactions are involved. Theoretically the *as* and *ss* conformer could also participate in the dimerization process, however, in the concentration range studied no change in conformational ratios were observed. In addition, the shifts of the protons of the *as* and *ss* conformations did not vary upon dilution, suggesting that the role of the *as* and *ss* conformer in the association process is negligible. At much higher concentrations these dimerization equilibria can perhaps be present, however, the solubility of the compound was too low to prove this.

Chart I

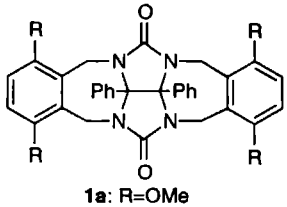

1a: R=OMe
1b: R=H
1c: R=Me

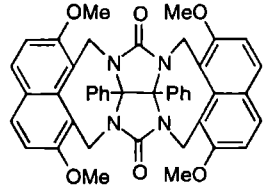

2

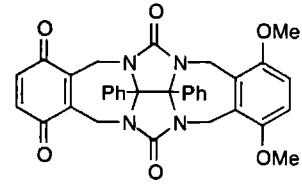

3

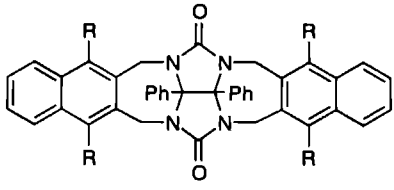

4a R=OMe
4b R=H

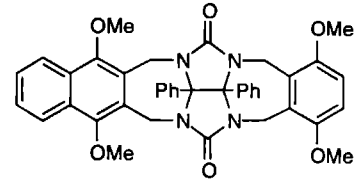

5

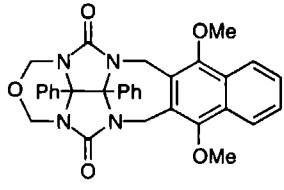

6

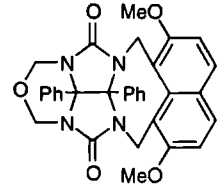

7

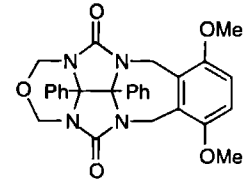

8

† For a discussion of the various conformers of this clip, see Chapter 4.

Table 1: *Dimerization constants of clip molecules as measured by ^1H NMR dilution studies.*[a]

Clip	K_{self} (M^{-1})	Clip	K_{self} (M^{-1})
1a	16	**6**	0
1b	0	**7**	10[c]
1c	7	**8**	0
2	60[b]	**9**	95
3	<5	**10**	35
4a	0	**11**	0
4b	0	**12a**	<5
5	<5	**12b**	10

[a]Estimated error 15-50%. [b]Only the self-association constant of the *aa* conformer was determined. [c]Only the self-association constant of the *anti* conformer was determined.

Clip molecules with 2,3-connected naphthalene side-walls (**4**) did not show any self-complexation behaviour. Although the cavity effect in these molecules is larger, no dimeric structure was found in solution. The geometry of the aromatic rings in the dimer leads to an unfavourable π-π interaction. According to calculations using the Hunter and Sanders[5] model, the electrostatic contribution to the π-π interaction in dimeric structure of **4** is very repulsive and prohibits complexation of either another clip molecules **4** or a guest molecule (see Chapter 2 and 3).

Clips **6** and **8**, having only one side-wall, did not show any self-association either. Apparently, one π-π interaction without any cavity effect is not large enough to allow dimeric species in solution to be formed. In the case of clip **7**, however, the π-π interaction between two 2,7-dimethoxynaphthalene rings was large enough to give self-association (Table 1). This self-association was relatively small when compared to that measured for clip **2**. Since there is no cavity effect involved in the dimerization of **7**, different geometries are possible. From the NMR data we were unable to distinguish between these geometries, however, we believe that the dimer geometry will be similar to that found in the X-ray structure of this compound (*vide infra*). In the case of **7** the geometry of dimerization will be completely dominated by the optimal π-π interaction.

Clip molecules **3** and **5** have one dimethoxybenzene side-wall and a second different aromatic side-wall. This means that there are three possible dimeric structures. In solution, however, only very small shifts in the ^1H-NMR were observed upon dilution of the samples, indicating that the K_{self} values are low (Table 1). Apparently, the combination of a cavity effect and only one favourable *p*-dimethoxybenzene π-π

interaction is not enough to result in significant self-association in solution. In the case of clip **3** the interaction between the quinone side-wall and the *p*-dimethoxybenzene side-wall was calculated to be less favourable than between two *p*-dimethoxybenzene walls (*vide infra*), which explains the lower self-association.

Chart II

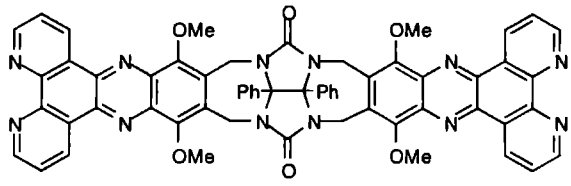

9

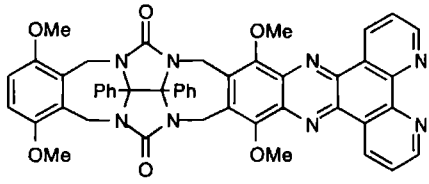

10

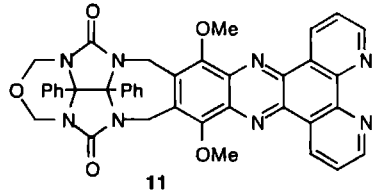

11

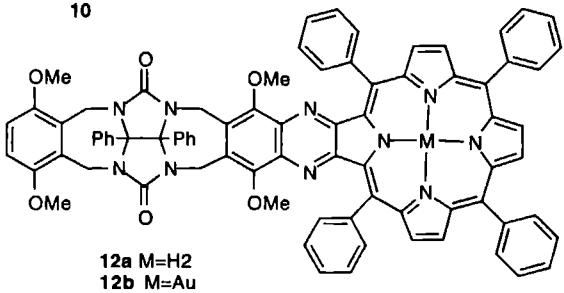

12a M=H2
12b M=Au

Enlarging the aromatic side-walls of the clips further to dipyrido[3,2-a : 2'3'-c]phenazine (phenazino-bpy)[6] (**9**, Chart II), resulted in an increase in dimer formation (Table 1). It is known that hexaazatriphenylene (HAT) derivatives can display π-complexation in the solid state.[6] The interplanar distance of the HAT rings in the solid state structure is 3.32 Å, which is approximately the distance between the side-walls of a dimeric complex of **9**. The fact that molecule **11** does not show any self-association, suggests that the π-π interaction itself is not large. The driving force behind the dimerization of **9** is an entropic effect due to the large cavity (*vide infra*). Clip **10**, however, displayed a relatively large self-association constant when compared with **1**, **3** and **5** (Table 1). This molecule can form dimeric species with different geometries (Figure 3), *i.e.* with the two *p*-methoxybenzene rings overlapping (A), with the two phenanthroline rings overlapping (B) or with the phenanthroline overlapping with a *p*-methoxybenzene ring (C). This third dimeric structure is thought not to be very

likely since it is not compact and only one cavity is filled. A geometry in which the π-π interactions occur at the outside of the clip can be excluded on the fact that clip **11** does not show dimerization.

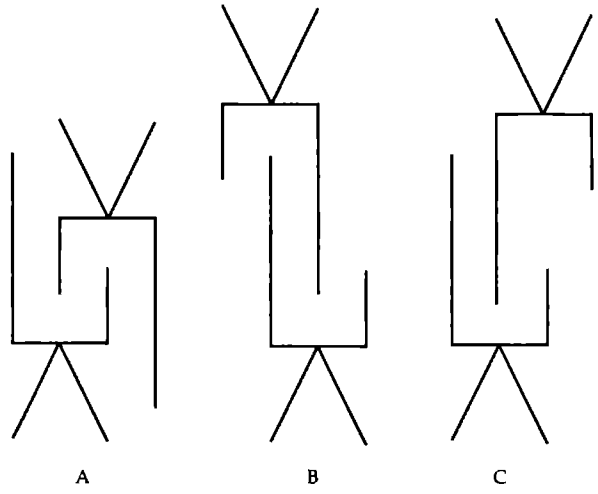

Figure 3: *The three possible geometries for the dimeric structure of clip* ***10****.*

The dimerization properties of clip molecules **1a**, **9**, **10** and **11** were further studied by temperature dependent ^{1}H NMR experiments. The spectra were recorded at a constant concentration and the temperature was varied over a wide range. The side-wall protons of clip **1a**, shifted to higher field at lower temperatures suggesting that more dimeric complex was formed. At very low temperatures (230 K), the ^{1}H NMR signal for the side-wall protons broadened, which indicated that the equilibrium is slow on the NMR time scale. The observation that the shifts of the side-walls protons were much larger than the shifts of the other protons and the fact that the temperature at which the signals of the side-wall protons started to broaden was concentration dependent, indicated that the observed effects were the result of a dimerization process and not of conformational effects (see Chapter 4).

Clip **10** showed almost the same ^{1}H NMR behaviour as clip **1a**. All the signals of the side-walls moved to higher field at lower temperatures, except the methoxy signal of the quinoxaline part, again pointing to an enhanced dimerization upon lowering the temperature. When the concentration of the sample was increased the signal of the methoxy groups attached to the quinoxaline ring moved to lower field, in contrast with the other signals. This suggests that the methoxy groups have to rotate out of the cavity in order for a dimeric species to be formed. Broadening of the phenanthroline protons, the *p*-dimethoxybenzene protons, and the methoxy protons was observed at 220 K ($CDCl_3$), suggesting that exchange between the monomeric and dimeric species was slow on the ^{1}H NMR time scale at this temperature.

The signals of clip **9** moved to lower field when the temperature was decreased suggesting that the dimer complex becomes weaker at lower temperature. Only a small broadening of the ^1H NMR signals was observed, indicating that the exchange was still fast on the NMR time scale. To confirm that indeed the association constants are changing at different temperatures, and not the geometry of the dimer structures, some self-association constants were determined at various temperatures. From these data the thermodynamic parameters were calculated (Table 2).

Table 2: *Self-association constants of clips 9 and 10 at different temperatures, and the calculated thermodynamic parameters*

T (K)	K_{self} (**9**)	CIS (ppm)	K_{self} (**10**)	CIS (ppm)
253	50 (±5)	1.39[a]/0.84[a]	105 (±15)	0.37[b]/1.03[a]/0.74[a]
273	90 (±10)	1.30[a]/----[c]	72 (±10)	0.37[b]/1.01[a]/0.69[a]
298	95 (±15)	1.48[a]/0.90[a]	35 (±5)	0.38[b]/1.02[a]/----[c]
318	100 (±15)	1.31[a]/0.86[a]	28 (±5)	0.39[b]/0.92[a]/0.57[a]
	9		**10**	
ΔH	7 kJ/mol		-14 kJ/mol	
ΔS	60 J/mol·K		-17 J/mol·K	

[a]CIS values for the protons next to the nitrogen atoms of the phenanthroline ring. [b]CIS values for the p-dimethoxybenzene side-wall protons. [c]Signal could not be followed.

Table 2 shows that the dimerization of **9** is entropy driven, whereas it is enthalpy driven for **10**. This difference suggests that the driving force for the self-association of **9** is different from that of **10**. In the case of clip molecule **9**, all four large rigid surfaces are involved in the association. These surfaces are rigid, and therfore the amount of vibrational and rotational entropy which is lost during the dimerization is small. A considerably entropy is gained upon desolvation of these four large surfaces. This is in line with the dimerization of kite-type molecules found by Cram et al., which also appeared to be entropically favourable.[16] The dimerization of **10**, apparently, is based on favourable Van der Waals interactions between the two monomeric species of the complex, and therefore is found to be enthalpy driven. The CIS values of the 1,4-dimethoxybenzene side-wall protons of **10** were different from the CIS values of the corresponding protons of **1a**. The CIS values of the phenanthroline wall protons of this compound differed from those of the wall protons of **9**, consequently it was difficult to obtain any information about the actual dimeric structure of **10** in solution. The CIS values, however, were approximately constant over the temperature range studied, which means that the geometries of the dimeric complexes formed by **9** and **10** are not temperature dependent. This means that clip **10** exists only in one form,

since it is unlikely that dimers of type A and B (Figure 3) will have the same thermodynamic parameters.

^{1}H NOE NMR studies were carried out in order to elucidate the dimeric structure of **10**. These experiments were unsuccessful because of the low association constant of **10** and the fact that the exchange between the monomeric and dimeric species was fast on the NMR time scale. Since the temperature dependent behaviour of the dimeric species of **1a** and **10** is the same, we tentatively propose that structure A is the most likely structure.

5.2.2 Self-association and self-assembly in the solid state

A topic of current interest in supramolecular chemistry, is the use of molecular recognition to construct well-defined and predictable structures in the solid state (crystal engineering).[7,8] In general hydrogen bonding is the predominant tool used,[9] however, in some cases π-π interactions are used as well.[10] During our studies the question was raised whether it would be possible to use the knowledge obtained from experiments carried out in solution, to construct structures in the solid state. In other words, would the interactions involved in the self-association behaviour of our clips in solution be sufficiently large and geometrically selective, to influence the molecular packing in the solid state? The main problem, of course, is that in the crystallization process packing forces are involved, which can not be easily quantified. In general, one of the driving forces in the case of crystal packing is the necessity to have a minimum volume and a maximum density. We were able to crystallize clips **1a**, **3**, **4a**, **4b**, **5**, **7**, **8**, **11** and **2**, the latter clip in the presence of nitrobenzene as a guest molecule. In the following we will compare the solid state structures of these compounds with those found in solution. Interactions between the aromatic rings of the clips were calculated using the Hunter and Sanders[5] model and were used to obtain insight into the packing geometries observed in the crystals.

From the dimerization studies in solution, it can be concluded that the interaction between two dimethoxy-substituted aromatic rings is very favourable. In order to get an idea of the interaction energies as a function of the geometry, energy profiles were calculated for the π-π interaction between different aromatic moieties, *viz.* the combinations *p*-dimethoxybenzene-*p*-dimethoxybenzene, 1,4-dimethoxynaphthalene-1,4-dimethoxynaphthalene, 2,7-dimethoxynaphthalene-2,7-dimethoxynaphthalene, and naphthalene-naphthalene. In Figure 4 the interactions between two planar *p*-dimethoxybenzene rings at a distance of 3.4 Å are shown. The energy surface was calculated for rings with their methoxy groups pointing in the same direction, resulting in a symmetric profile, and for rings with their methoxy groups pointing in

opposite direction. Each surface shows three large energy maxima, which are the result of the direct overlap of the methoxy groups giving a large Van der Waals repulsion (Figure 4). Direct overlap is also disfavoured by repulsive electrostatic interactions between the aromatic rings. In the symmetric case (Figure 4, left), it is evident that an

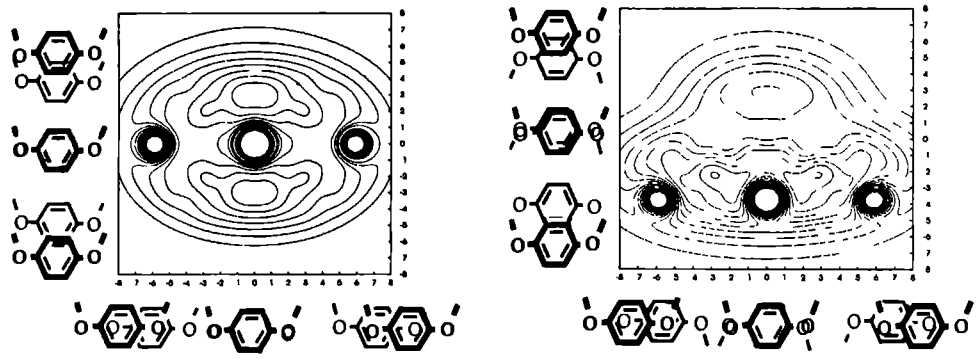

Figure 4: *The energy surfaces for two interacting p-dimethoxybenzene rings; left figure symmetric overlap of rings, right figure asymmetric overlap of rings.*

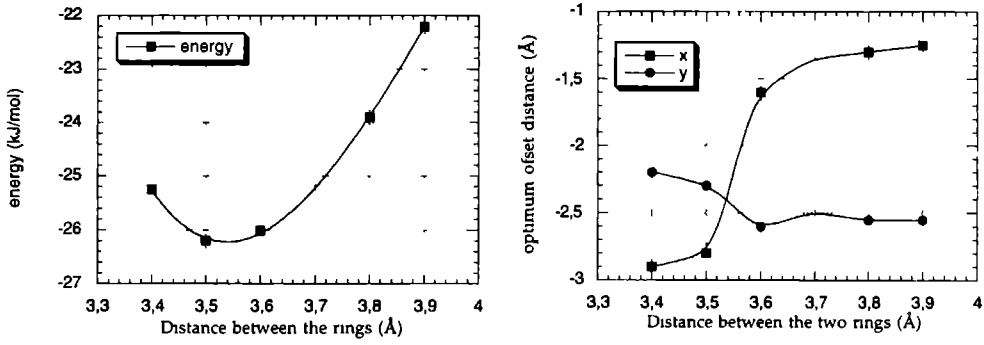

Figure 5: *The energy minimum (left) and the position (x and y offset) of the energy minimum (right) as a function of the distance between the two p-dimethoxybenzene rings. The curves correspond to the minimum of Figure 4, right.*

offset geometry is more favourable than direct overlap. In the unsymmetrical case (Figure 4, right) two energy minima are observed both having an offset geometry. The direct overlap again is unfavourable, but now only due to an electrostatic repulsion between the aromatic rings. It can be concluded that the geometry of the *p*-dimethoxybenzene rings in the dimeric structure of **1a** in solution (Figure 1) is very similar to the calculated minimum (Figure 4).

The offset for the minima in Figure 4 (right) is ±3, -2 Å (x,y). These minima are dependent on the distance between the aromatic rings, see Figure 5. The optimum x-offset distance is shifted by approximately 1.6 Å, if the aromatic rings are pulled apart 0.3 Å. The energy minimum is relatively constant when rings are between 3.4 and 3.8 Å apart. Once fixed at a certain distance, it is of interest to know how the energy changes when the geometry of the rings is varied. As can been seen in Figure 6, the energy minima are relatively global. Within the range of 2 kJ/mol the aromatic ring can move approximately 1.5 Å in both directions.

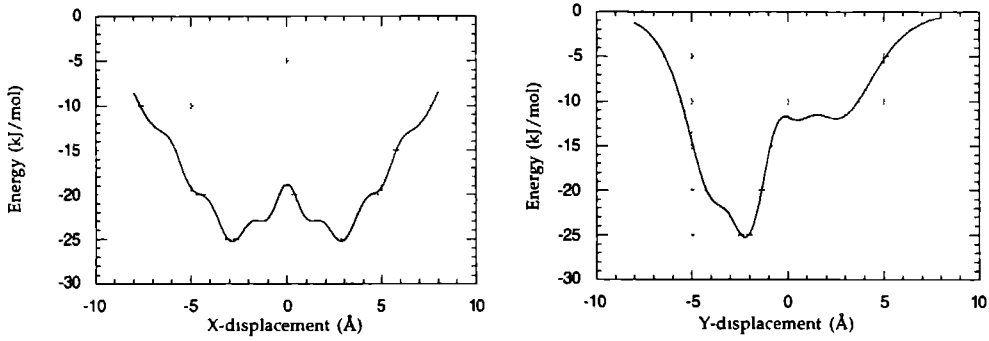

Figure 6: *The interaction energy between two p-dimethoxybenzene rings kept at 3.4 Å distance, as a function of the movement of one ring from the energy minimum in the x and y direction.*

The solution and X-ray structures of the five clip molecules having *p*-dimethoxybenzene side-walls, showed great similarity with the calculated minimum geometries. For clips **3** and **12a** the observed crystal geometry (Figure 7, for **12a** see also Chapter 7) is identical to the geometry derived from the ^{1}H NMR studies in solution. Well defined dimers are formed, in which a strong interaction between the *p*-dimethoxybenzene rings is present. The geometry in both cases is an offset one, similar to the geometry predicted by the calculations (Figure 7). The distances between the planes of the dimethoxybenzene rings is approximately 3.4 Å. Somewhat surprising is that the interaction between the *p*-dimethoxybenzene rings is more favourable than between an electron poor quinone and an electron rich *p*-dimethoxybenzene ring. This is contrary to what is expected on the basis of the donor-acceptor theory.[11] Calculations which were performed using the Hunter and Sanders model (a similar energy surface was calculated as between two *p*- dimethoxybenzene rings) predicted that the interaction between a quinone ring and a *p*-dimethoxybenzene ring indeed is less favourable by 4 kJ/mol at the geometry found in

the X-ray structure. If the interactions are examined more closely one calculates that the electrostatic interaction between a quinone and a *p*-dimethoxybenzene ring is actually 1 kJ/mol more favourable than the interaction between two *p*-dimethoxybenzene rings, as would be expected. This electrostatic interaction, however, is not large enough to overcome the drop in Van der Waals interaction energy, which is 5 kJ/mol less favourable in the case of the quinone-*p*-dimethoxybenzene interaction. Consequently, the overall interaction between two *p*-dimethoxybenzene moieties is more favourable.

The mono-walled clip **8** also showed an ordered packing in the solid state with noticeable *p*-dimethoxybenzene interactions. Dimeric structures are formed, which also have favourable interactions with neighbouring dimers (Figure 8). The molecules are arranged in such a way that each molecule has two offset *p*-dimethoxybenzene interactions with its neighbours. These offset interactions are calculated to be favourable, although the distance between the aromatic surfaces is relatively large (3.9 Å for the interaction at the inside of the clip and 4.2 Å at the outside, see Figure 8). It can be seen in Figure 5, however, that even at a distance of 3.9 Å there is still a significant π-π interaction.

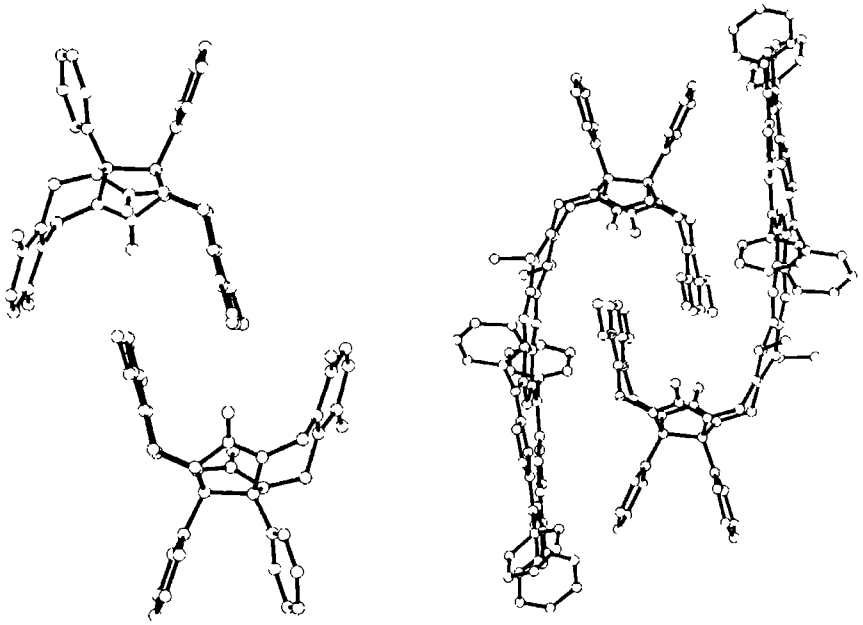

Figure 7: *X-ray structures of clip molecules* **3** *(left) and* **12a** *(right).*

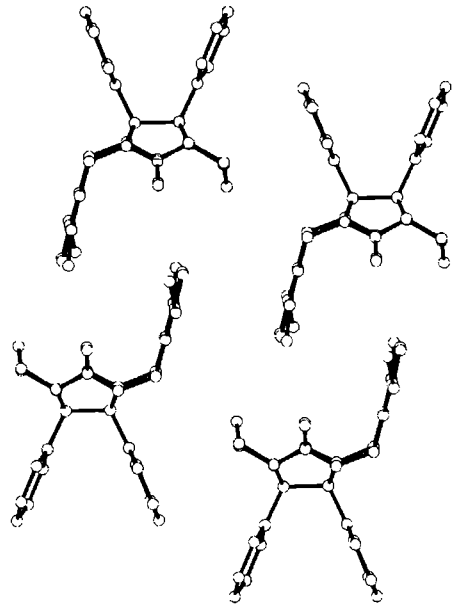

Figure 8: *X-ray structure of clip molecule* ***8***.

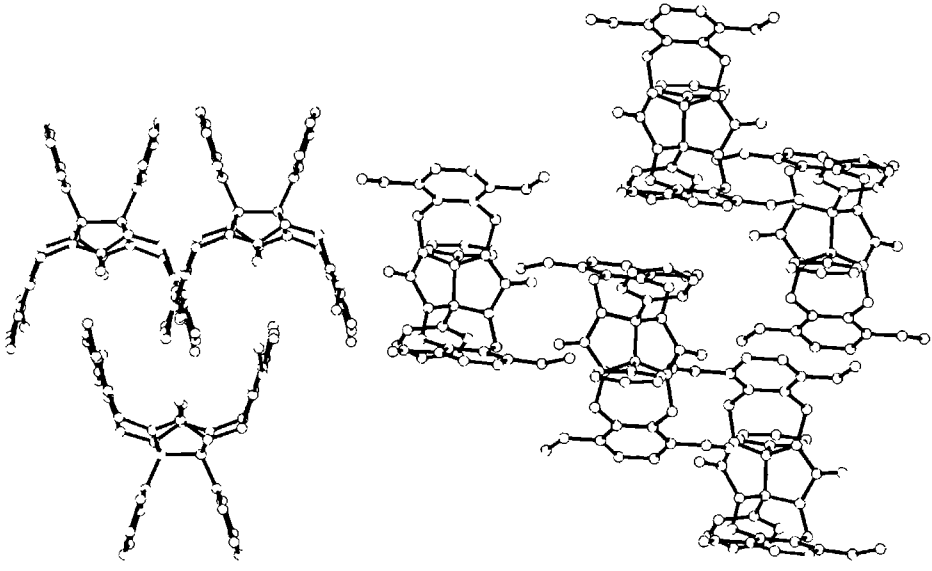

Figure 9: *X-ray structure of clip molecule* ***1a****, frontview left, topview right.*

The X-ray structure of **1a**,[1] the clip with the strongest self-association behaviour in solution, revealed that the clip molecules are not in a dimeric geometry, but form rows in which each molecule has an interaction with four neighbouring molecules (Figure 9). One clip molecule forms an offset dimer (x=1.6; y=4.6 Å) with two other clip molecules. In this way a more favourable packing arrangement can be obtained, in

which the cleft of a molecule is half occupied by two walls from adjacent molecules in the row. The next row of clip molecules is inverted with respect to the first row. Each molecule in a row has an interaction with molecules from the rows on either side. These four interactions, apparently are more favourable than a simple dimeric structure. According to our calculations the *p*-dimethoxybenzene interactions do not have a specific minimum energy, but rather a region in which the energy is low. Hydrogen bonds, in contrast, have a very specific geometry and hence are more angle and distance dependent. The solid state structure of clip **1a** is the result of π-π interactions which are still significantly attractive even at large offsets and z-displacements.

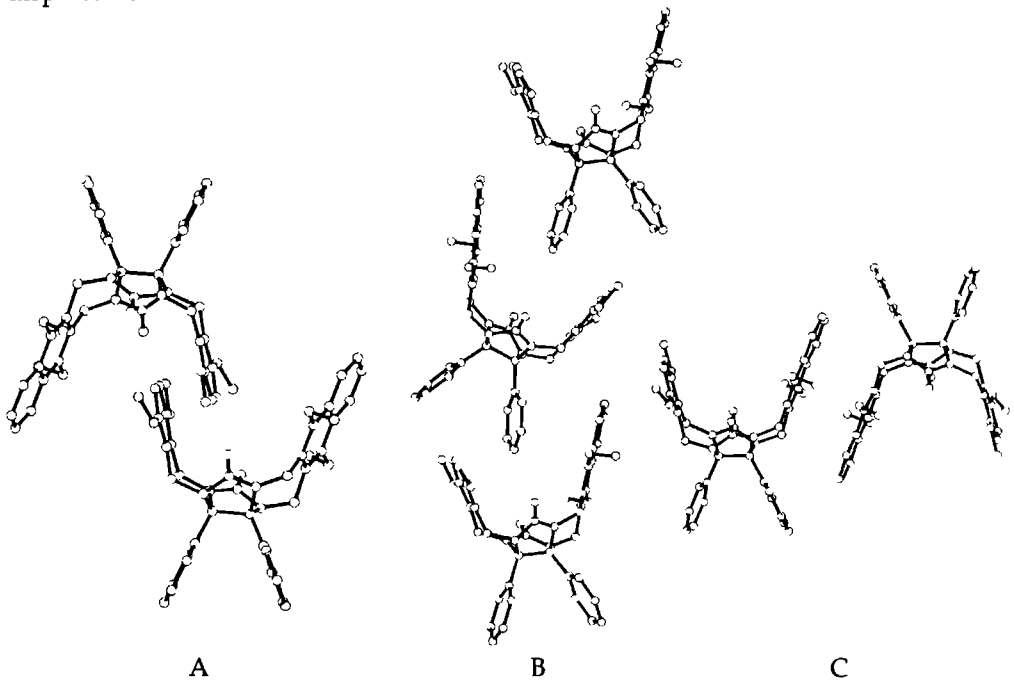

Figure 10: *The three types of interactions observed in the crystal structure of clip* **5**. *For discussion see text.*

Clip molecule **5** has two different side-walls which both can have favourable π-π interactions. The larger aromatic naphthalene surfaces were expected to dominate the geometry of the crystal structure. This indeed was found to be the case (Figure 10C). The distance between two 1,4-dimethoxynaphthalene rings of adjacent molecules is 3.64 Å. The observed offset geometry between these rings (x=1.795; y=2.450 Å) is very favourable according to calculations. The geometry for the optimal interaction between the 1,4-dimethoxynaphthalene rings can not be achieved if the molecules form a dimeric structure, in which the cleft of one molecule is filled with the side-wall

of another molecule, because of steric hindrance (note that in solution no dimerization was observed). The methoxy groups of the naphthalene side-walls are pointing in opposite directions. A relatively small interaction between two *p*-dimethoxybenzene rings having a large offset (x=1.8; y=5.7Å) is observed in the X-ray structure. In order to obtain a better packing arrangement the cleft of one clip molecule is filled by a phenyl group of the diphenylglycoluril unit of another molecule. This phenyl group has an interaction with the naphthalene side-walls (distance is ca. 3.6 Å). Due to this interaction each molecule located above is twisted, resulting in row of molecules. In Figure 10 the interactions observed in the crystal structure of **5** are shown separately, *viz.* the naphthalene-naphthalene interactions (Figure 10C), the phenyl-naphthalene interaction generating a row of clip molecules (Figure 10B) and the offset *p*-dimethoxybenzene-*p*-dimethoxybenzene interaction (Figure 10A).

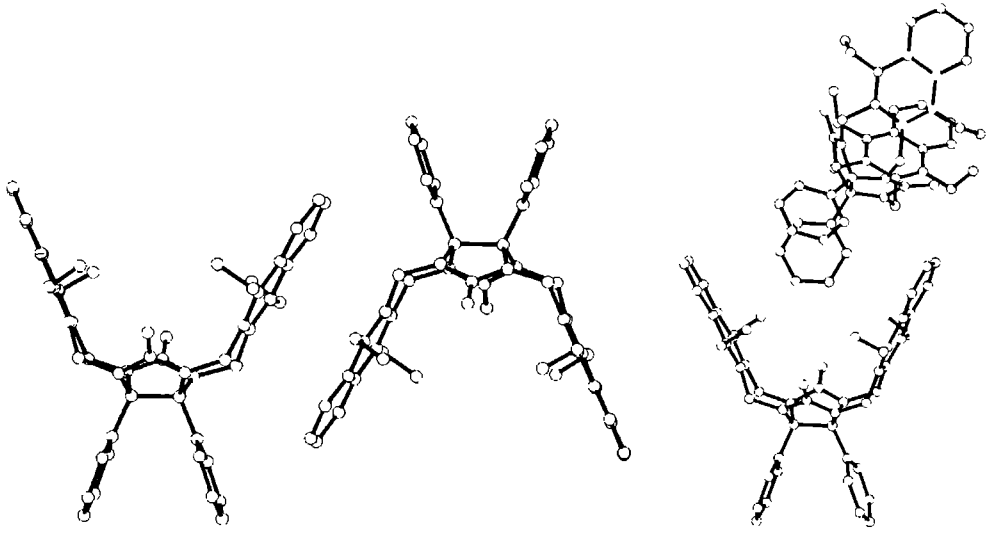

Figure 11: *The solid state structure of* ***4a****, showing the interaction between two 1,4-dimethoxynaphthalene moieties, and the face-to-edge interaction between the phenyl groups and the naphthalene side-walls (see text).*

The above described geometric packing of the 1,4-dimethoxynaphthalene moieties is also found in the solid state structure of clip **4a** (Figure 11).[12] The outside distance between two aromatic surfaces is 3.60 Å, with an offset of x=1.43 and y=2.73 Å. In the case of this clip the methoxy groups point into the cavity, unlike in the X-ray structure of **5** where these groups were pointing in opposite directions. Clip molecule **4a** has two identical side-walls and hence two favourable side-wall interactions. The molecules contain a large cavity, which must be filled in order to achieve a good packing. In the solid state this cavity is filled by the phenyl group of the diphenylglycoluril unit of a neighbouring molecule, as was seen in the X-ray structure of **5** (Figure 11). In this case

the molecule is more twisted, with the phenyl group having a face-to-edge interaction with each of the naphthalene side-walls of the underlying clip molecule.

One may ask the question how important are the methoxy groups in the interactions between the aromatic rings? According to our calculations with the Hunter and Sanders model, the Van der Waals energy is optimal when the aromatic rings are totally overlapping. In the case of dimethoxynaphthalene, however, a large Van der Waals repulsion is observed as a result of the protons of the methoxy groups, making close contact with each other. The Van der Waals attraction is slightly smaller when the displacement increases. The electrostatic contribution, which is repulsive at direct overlap, is in contrast to the Van der Waals energy very sensitive to the geometric arrangement and falls off rapidly as the displacement increases. In the case of the electrostatic interaction, the methoxy groups play a significant role, making some of the carbon atoms of the ring more electron rich and others electron poor (Hammett values for the para and meta position are 0.12 and -0.27 respectively!)[13] As a result, the overall energy surface of the interaction between two 1,4-dimethoxynaphthalene rings is less smooth than the energy surface of the interaction between two naphthalene rings (Figure 12). This, of course, leads to a different optimal offset geometry, and thus different interactions in the solid state.

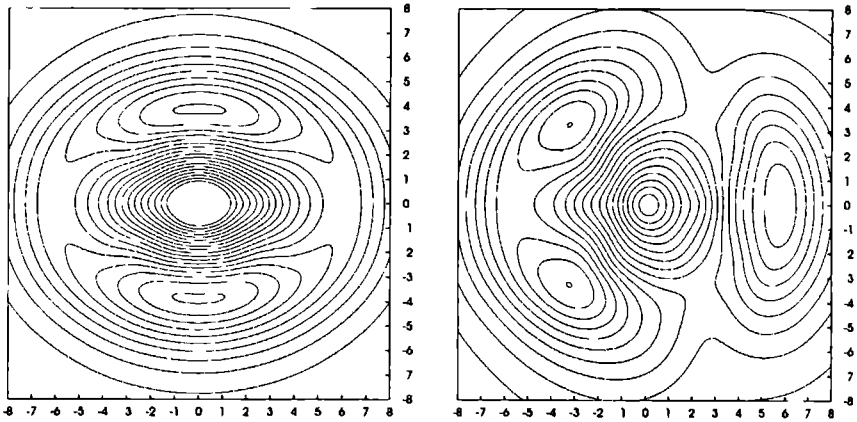

Figure 12: *The interaction energy surfaces between two naphthalene rings and two 1,4-dimethoxynaphthalene rings as calculated with the Hunter and Sanders model.*

Two main offset interactions between the side-walls are found in the X-ray structure of **4b** (Figure 13). The first one involves two side-walls that are partly filling the clefts of two opposing clip molecules (Figure 13A). The two aromatic rings have a distance of 3.53 Å, and an offset of x=1.09 and y=2.45 Å. The second interaction is at the outside of the clip molecule and is similar to the interaction observed for **4a**, *viz.* phenyl rings

that partly fill the cavity of another clip molecule (Figure 13B). The distance between the rings is 3.56 Å, and the offset is x=1.02 and y=2.96 Å. A chloroform molecule is incorporated in the crystal, forming a weak hydrogen bond with the carbonyl group of the diphenylglycoluril unit (CCl_3H--OC distance is 2.19Å).

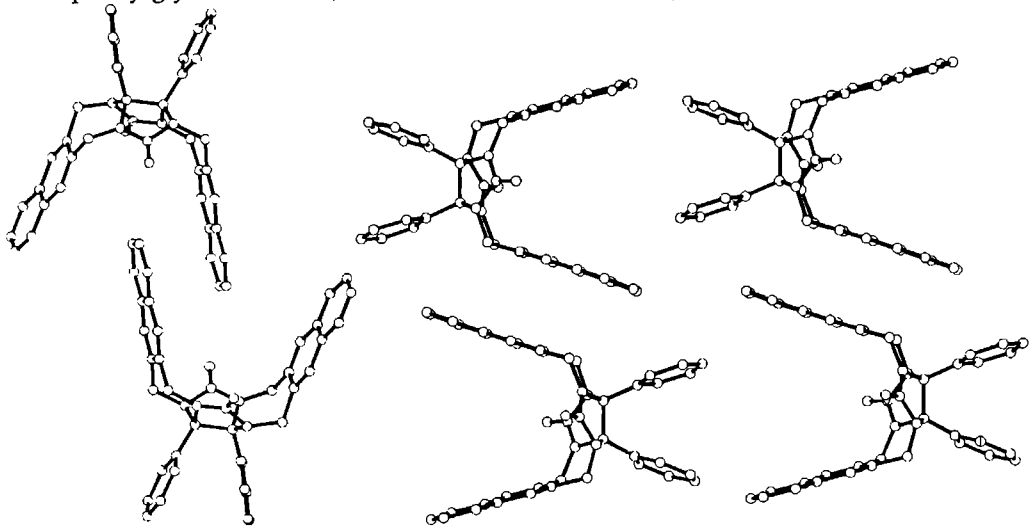

Figure 13: *The two interactions observed in the crystal packing of clip* ***4b****.*

In solution clip molecules **2** and **7** both show self-association, due to a favourable interaction between the 2,7-dimethoxynaphthalene side-walls (*vide supra*). Calculations which were carried out revealed that there are two regions of optimal geometry, differing in energy by 2.5 kJ/mol (Figure 14). In the X-ray structure of clip **7**, the geometry with the lowest calculated energy is observed (Figure 15). The interaction takes place at the outside of the clip. The distance between the aromatic surfaces is 3.42 Å, and the offset x=0.51 and y=3.46 Å. The molecules are packed in dimers, with a small interaction between neighbouring dimers. A CH_3 - aromatic interaction is observed (distance is approximately 3.04 Å, see Figure 15), however, this is not expected to contribute much to the overall interaction energy.[14]

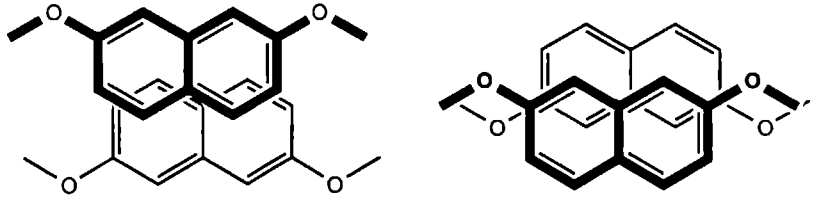

Figure 14: *The two optimum interactions between two 2,7-dimethoxynaphthalene rings according to calculations using the Hunter and Sanders model. The geometry on the right is 2.5 kJ/mol more favourable than the one on the left.*

Clip molecule **2**, in contrast to **7**, has two naphthalene side-walls that can interact. This molecule, unfortunately, could not be crystallized, despite numerous attempts. Crystallization, however, could be induced in the presence of a guest molecule (nitrobenzene). The presence of a co-crystallizing guest molecule means that the cavity of the clip is already filled and that a dimeric structure cannot be adopted. Using previous information obtained from calculations and X-ray data we predicted that the major interaction in the X-ray structure of **2**, would be between the side-walls of adjacent clip molecules. Figure 14 shows that the most favoured interaction is at an inverted offset geometry. Since clip molecule **2** has two side-walls, an interaction on both sides can be expected, resulting in long arrays of stacked molecules. This is indeed what was found in the X-ray structure of **2** (Figure 16). Neighbouring molecules are pointing in opposite direction and stack with their side-walls at exactly the calculated optimum offset distance, which is 3.45 Å. All the stacked rows are independent of each other. The cleft of each molecule is occupied by a nitrobenzene molecule, which has an optimal stacking geometry with the 2,7-dimethoxynaphthalene side-walls (see Chapter 4).

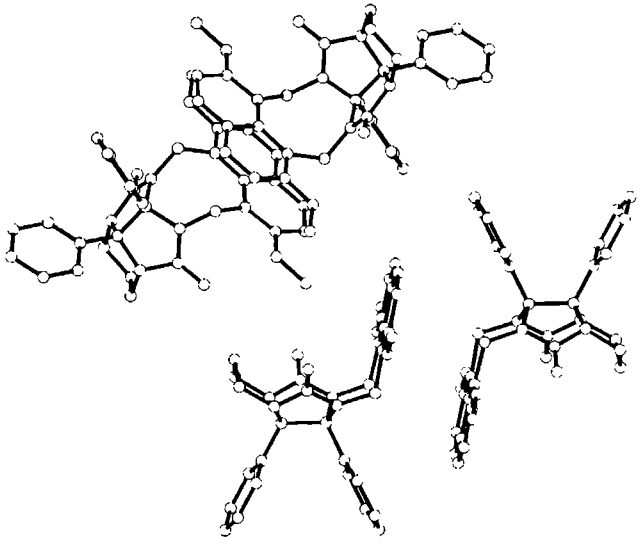

Figure 15: *The crystal structure of* **7**.

In the solid state structures of the different clip molecules, the phenyl groups of the diphenylglycoluril unit are often observed to be within close proximity of an aromatic side-wall. It is obvious that this geometry leads to a favourable interaction, particularly in the case of clip **12**, which has a large porphyrin unit nearby these phenyl group. In all examples the distances between the above mentioned phenyl groups and the aromatic side-walls were between 3.5 and 3.6 Å. These obviously, are important

interactions in the solid state structure, but they are not expected to determine the geometry of the structures in solution.

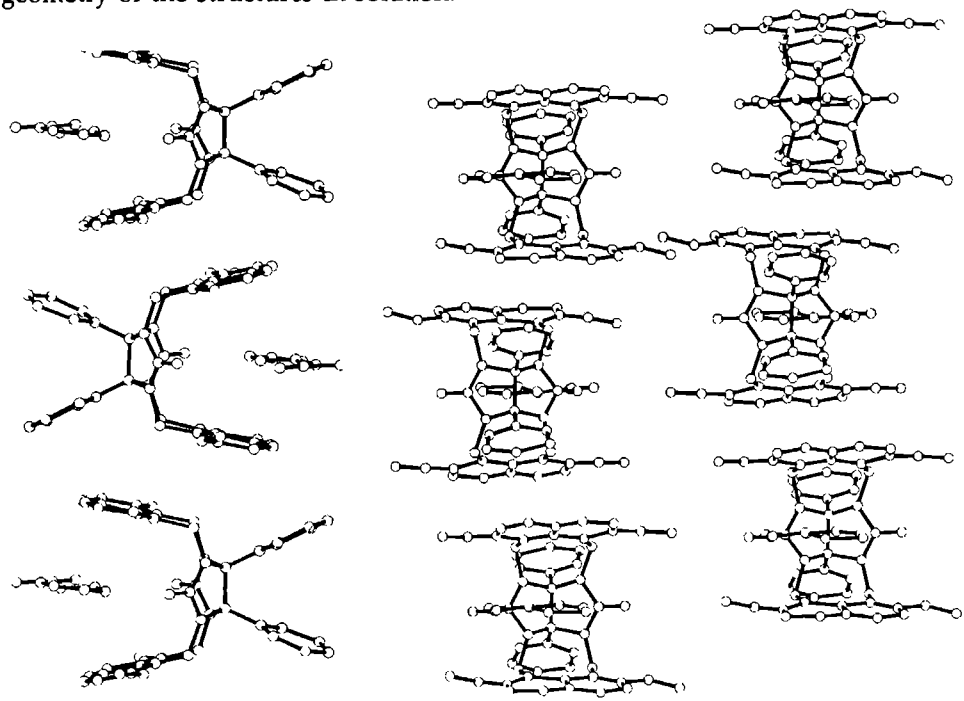

Figure 16: *The crystal structure of* **2** *in the presence of nitrobenzene as guest molecule, sideview left, topview right.*

5.3 CONCLUSIONS

In Table 3 we have summarized the important distances and offsets between aromatic rings found in the solid state structures of clip molecules. Comparison of the X-ray geometries with the optimal geometries calculated using the Hunter and Sanders model, shows that there is relatively good agreement between calculations and experimental result. Although the Hunter and Sanders model is relatively simple it is useful in calculating the optimum geometries and relative interaction energies between aromatic molecules. Using this computational tool, we have been able to interpret structures in solution and in the solid state. In solution the poor solvation of the cavity by solvent molecules and favourable π-π stacking interactions play an important role in the dimer formation of the clip molecules. In the solid state these π-π interactions together with crystal packing forces determine the structures. The π-π interactions direct the packing arrangement, but they are not as geometrically stringent as hydrogen bonds. In the systems described here, an approximate region of favourable interaction between aromatic rings was observed. The optimum calculated interaction

geometry, therefore, is not always exactly the one found in the X-ray structure. A crystal packing which results in four weaker interactions is more favourable than one

Table 3: *Summary of the aromate-aromate interactions observed in the solid state structures of different clip molecules*

Clip	Type of interaction	Z-distance (Å)	Y-distance (Å)	X-distance (Å)	Calculated Energy (kJ/mol)[b]
1a	B[a]	4.23	1.72	4.66	-16
	B	3.73	3.14	2.16	-16
2	N	3.45	3.46	1.56	
3	B	3.43	2.05	0.60	-22
4a	N	3.60	2.73	1.43	
4b	N	3.53	2.45	1.09	
	N	3.57	2.96	1.02	
5	B	2.99	1.81	5.71	-17
	N	3.64	2.45	1.80	
7	N	3.43	3.46	0.51	
8	B	4.20	2.06	1.64	-21
	B	3.97	1.32	1.68	-20
11a	B	3.31	1.89	0.15	-21

[a] B = between two benzene rings, N = between two naphthalene rings

[b] According to the Hunter and Sanders model.

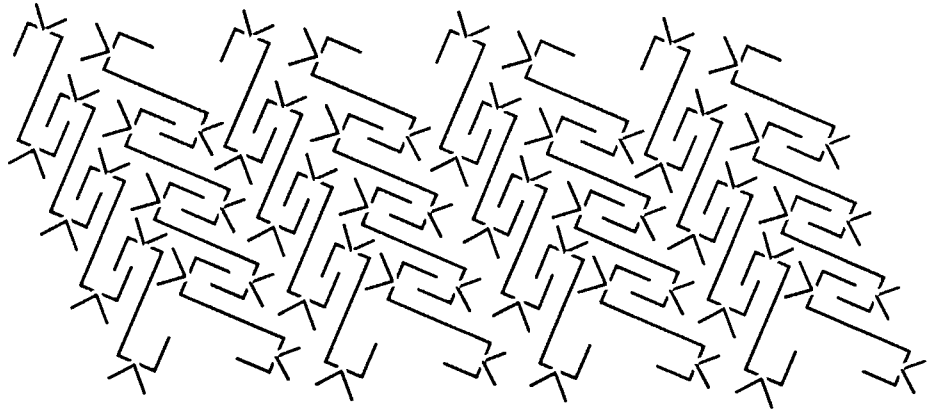

Figure 17: *Schematic picture of the possible crystal packing of a dimeric clip-shaped molecule.*

stronger interaction as was seen in the case of clip **1a**. Using the knowledge obtained from interactions in solution and in the solid state, we may be able in the near future to predict with some confidence the most dominant aromatic interaction and hence

the probable crystal packing arrangements. Although the present study is only a very first step towards the use of clip molecules in the rational design of organic solid state lattices, we feel that we already have a reasonable understanding of the packing forces involved in the crystallization of this type of molecules. Further work will be focused on the synthesis and crystallization of dimeric clip molecules, which are expected to form long arrays in the solid state (see Figure 17).

5.4 EXPERIMENTAL SECTION

5.4.1 general

The synthesis of the molecules discussed in this chapter are described in Chapter 2, and in references cited therein. Dimerization constants were determined by diluting the samples from their maximum solubilities (varying from 10 mM - 40 mM) to their minimum concentrations required for detection of signals by ^{1}H-NMR (approximately 0.1 mM). In general the chemical shifts of the side-wall protons were followed as function of the concentration of the clips. The obtained curves were fitted using the following equation:

$$\partial_{obs} = \partial_m + (\partial_d + \partial_m)[1 + 4aK - (1 + 8aK)^{1/2}]/4aK$$

∂_{obs} = the observed chemical shift

∂_m = the chemical shift of the monomer

∂_d = the chemical shift of the dimer

a = the total concentration

The ^{1}H-NMR measurements were carried out on Bruker AM 400 MHz and 200 MHz instruments.

5.4.2 X-ray structures

The X-ray structures of **1a** and **4a** were taken from ref. 1 and 12. The X-ray data of the **2**-nitrobenzene complex and of **7** are given in Chapter 4.

Crystal data **3**:
$C_{35}H_{29}N_4O_6Cl_3$, *Mr* = 708.0, *T* = 293 K, monoclinic, space group $P2_1/c$, *a* = 13.0326(6), *b* = 18.858(2), *c* = 13.5561(11) Å, ß = 100.800(7)°, *V* = 3273 Å^3, *Z* = 4, *Dx* = 1.437 g/cm^3, Mo *K*α radiation, μ = 3.30 cm^{-1}.

Crystal data **4b**:
$C_{40}H_{30}N_4O_2.CHCl_3$, *Mr* =718.05, *T* = 208 K, triclinic, space group P-1, *a* = 9.302(2), *b* = 12.981(2), *c* = 15.765(2) Å, α = 65.91(2), ß = 76.40(2), γ = 80.15(1)°, *V* = 1682.9 Å^3, *Z* = 2, *Dx* = 1.417 g/cm^3, Mo *K*α radiation, μ =3.17 cm^{-1}.

Crystal data **5**:
$C_{42}H_{38}N_4O_6Cl_6$, *Mr* = 907.5, *T* = 208 K, monoclinic, space group $P2_1/n$, *a* = 12.5667(9), *b* = 19.1713(12), *c* = 17.4311(11) Å, ß = 91.676(6)°, *V* = 4198 $Å^3$, *Z* = 4, *Dx* = 1.436 g/cm^3, Mo *Kα* radiation, μ = 4.61 cm^{-1}.

Crystal data **8**:
$C_{28}H_{26}N_4O_5$, *Mr* =498.5, *T* = 293 K, triclinic, space group P-1, *a* = 8.2849(15), *b* = 12.525(2), *c* = 13.438(4) Å, α = 116.83(2), ß = 105.17(3), γ = 90.07(2)°, *V* = 1189 $Å^3$, *Z* = 2, *Dx* = 1.392 g/cm^3, Mo *Kα* radiation, μ = 0.91 cm^{-1}.

Crystal data for **12a**:
$C_{80}H_{60}N_{10}O_6.C_2OC_2$ *Mr* = 1321.46, *T* = 173 K, monoclinic, space group $P2_1/n$, *a* = 14.8272(12), *b* = 24.0148(25), *c* = 19.1212(13) Å, ß = 99.048(69)°, *V* = 6724 $Å^3$, *Z* = 4, D_x =1.305 g/cm^3, Mo *Ka* radiation, μ = 0.791cm^{-1}

Detailed crystallograpic data will be published elsewere.[15]

5.4.3 Calculations.

Calculations were performed on Silicon Graphics Challenge and Silicon Graphics Indigo II work stations. The molecular structures were generated with the Sybyl program, and optimized by calculations using the MOPAC program and the ESP option for the charges. The charges and coordinates were taken from the output file of this program. The keyword PI in MOPAC splits the final density matrix into π and σ contributions. The π densities at the diagonal of the density matrix were used as the π charges above and below the plane of the aromatic molecule in the case of the calculations using the Hunter and Sanders model. Energy surfaces were calculated, using an electrostatic and a Van der Waals potential, by stepwize changing the x and y coordinates of one of the two surfaces.

References

1 Sijbesma, R. P.; Kentgens, A. P. M.; Lutz, E. T. G.; van der Maas, J. H.; Nolte, R. J. M. *J. Am. Chem. Soc.* **1993**, *115*, 8999.
2 Sijbesma, R. P.; Wijmenga, S. S,; Nolte, R. J. M. *J. Am. Chem. Soc.*, **1992**, *114*, 9807-9813.
3 Abraham, R. J.; Rowan, A. E.; Mansfield, K. E.; Smith, K. M. *J. Chem. Soc., Perkin Trans. 2* **1991**, 515.
4 Johnson, C. S., Jr.; Bovey, F. A. *J. Chem. Phys.* **1958**, *29*, 1012.
5 Hunter, C. A.; Sanders, J. K. M. *J. Am. Chem. Soc.*, **1990**, *112*, 5525.

6 Beeson, J. C.; Fitzgerald, L. J.; Gallucci, J. C.; Gerkin, R. E.; Rademacher, J. T.; Czarnik, A. W. *J. Am. Chem. Soc.*, **1994**, *116*, 4621.

7 (a) Service, R.F.*Science*, **1994**, *265*, 316. (b) Whitesides, G.M.; Mathias, J.P.; Seto, C.T. *Science*, **1991**, *254*, 1312. For good approaches in predicting packing of organic molecules: (a) Perlstein, J. *J. Am. Chem. Soc.*, **1992**, *114*, 1955-1963. (b) Gavezzotti, A. *J. Am. Chem. Soc.*, **1991**, *113*, 4622-4629.

8 (a) Lawrence, D. S.; Jiang, T.; Levette, M. *Chem. Rev.* **1995**, *95*, 2229-2260. (b) Hanessian, S.; Simard, Roelens, S, *J. Am. Chem. Soc.*, **1995**, *117*, 7630-7645. (c) Ochiai, K.; Mazaki, Y.; Kobayashi, K.; *Tetrahedron lett.*, **1995**, *36*, 5947. (d) Sugiura, K.; Toyoda, J.; Yoon, J-W.; Mitani, T.; Nakasuji, K. *Tetrahedron lett.*, **1995**, *36*, 5535. (e) Thalladi, V. R.; Panneerselvam, K.; Carrell, C. J.; Carrell, H. L.; Desiraju, G. R.; *J. Chem. Soc., Chem. Commun.*, **1995**, 341. (f) Kane, J. J.; Liao, R.-F.; Lauher, J. W.; Fowler, F. W. *J. Am. Chem. Soc.*, **1995**, *117*, 12003. (g) Kimizuka, N.; Fujikawa, S.; Kuwahara, H.; Kunitake, T.; Marsh, A.; Lehn, J.-M. *J. Chem. Soc., Chem. Commun.*, **1995**, 2103. (h) Bernstein, J.; Davis, R. E.; Shimoni, L.; Chang, N.-L.; *Angew. Chem.* **1995**, *107*, 1689. Including inorganic compounds: (i) McCullough, R. D.; Belot, J. A.; Rheingold, A. L.; Yap, G. P. A. *J. Am. Chem. Soc.*, **1995**,*117*, 9913. (j) Van Calcar, P. M.; Olmstead, M. M.; Balch, A. L. *J. Chem. Soc., Chem. Commun.*, **1995**, 1773. (k) Yaghi, O. M.; Li, H. *J. Am. Chem. Soc.*, **1995**, *117*, 10401.

9 (a) Zerkowski, J. A.; MacDonald, J. C.; Seto, C. T.; Wierda, D. A.; Whitesides, G. M. *J. Am. Chem. Soc.*, **1994**, *116*, 2382-2391. (b) Zerkowski, J. A.; Whitesides, G. M. *J. Am. Chem. Soc.*, **1994**, *116*, 4298-4304. (c) Mathias, J. P.; Seto, C. T.; Simanek, E. E.; Whitesides, G. M. *J. Am. Chem. Soc.*, **1994**, *116*, 1725-1736. (d) Mathias, J. P.; Simanek, E. E.; Zerkowski, J. A.; Seto, C. T.; Whitesides, G. M. *J. Am. Chem. Soc.*, **1994**, *116*, 4316-4325. (e) Mathias, J. P.; Simanek, E. E.; Whitesides, G. M. *J. Am. Chem. Soc.*, **1994**, *116*, 4326-4320. (f) Endo, K.; Sawaki, T.; Koyanagi, M.; Kobayashi, K.; Masuda, H.; Aoyama, Y. *J. Am. Chem. Soc.*, **1995**,*117*, 8341-8352. (g) Wang, X.; Simard, M.; Wuest, J. D. *J. Am. Chem. Soc.*, **1994**, *116*, 12119. (h) Lokey, R. S.; Iverson, B. L. *Nature*, **1995**, *375*, 303. (i) Bergeron, R. J.; Yao, G. W.; Erdos, G. W.; Milstein, S.; Gao, F.; Weimar, W. R.; Phanstiel, O. *J. Am. Chem. Soc.*, **1995**, *117*, 6658-6665. (j) Araki, K.; Abe, M.; Ishizaki, A.; Ohya, T. *Chem. Let.*, **1995**, 359. (k) Fan, E.; Yang, J.; Geib, S. J.; Stoner, T. C.; Hopkins, M. D.; Hamilton, A. D. *J. Chem. Soc., Chem. Commun.*, **1995**, 1251. (l) Yang, J.; Marendaz, J-L.; Geib, S. J.; Hamilton, A. D. *Tetrahedron Lett.* **1994**, *35*, 3665. (m) Fujita, M.; Kwon, Y. J.; Sasaki, O.; Yamaguchi, K.; Ogura, K. *J. Am. Chem. Soc.*, **1995**,*117*, 7287.

10 (a) Ashton, P. R.; Ballardini, R.; Balzani, V.; Credi, A.; Gandolfi, M. T.; Menzer, S.; Pérez-García, L.; Prodi, L.; Stoddart, J. F.; Venturi, M.; White, A. J. P.; Williams, D. J. *J. Am. Chem. Soc.*, **1995**, *117*, 11171. (b) Amabilino, D. B.; Anelli, P. R.; Ashton, P. R; Brown, G. R.; Córdova, E.; Godínez, L. A.; Hanes, W.; Kaifer, A. E.; Philp, D.;

Slawin, A. M. Z.; Spencer, N.; Stoddart, J. F.; Tolley, M. S.; Williams, D. J. *J. Am. Chem. Soc.*, **1995**, *117*, 11142. (c) P. R.; Ashton, P. R; Cleassens, C. G.; Hanes, W.; Menzer, S.; Stoddart, J. F.; White, A. J. P; Williams, D. J. *Angew. Chem.* **1995**, *107*, 1994. (d) Amabilino, D. B.; Stoddart, J. F.; Williams, D. J. *Chem. Mater.* **1994**, *6*, 1159.

11 (a) Briegleb, G. "*Electronen-Donator-Acceptor-Komplexe*" **1961**, Sprongler-Verlag, Berlin. (b) Morakuma, K. *Acc. Chem. Res.* **1977**, *10*, 294.

12 Bosman, W. P.; Beurskens, P. T.; Admiraal, G.; Sijbesma, R. P.; Nolte, R. J. M. Z. *Kristallogr.* **1991**, *197*, 305.

13 Hansch, C.; Leo, A.; Taft, R. W. *Chem. Rev.* **1991**, *91*, 165.

14 Nisio, M.; Hirota, M. *Tetrahedron* **1989**, *45*, 7201.

15 de Gelder, R.; Beurskens, P. T.; Reek, J. N. H.; Nolte, R. J. M. to be published.

16 (a) Bryant, J. A.; Knobler, C. B.; Cram, D. J.; *J. Am. Chem. Soc.* **1990**, *112*, 1254. (b) Bryant, J. A.; Ericson, J. L..; Cram, D. J.; *J. Am. Chem. Soc.* **1990**, *112*, 1255.

Chapter 6

Synthesis, Binding Studies and Aggregation Behaviour of Novel Water Soluble Molecular Clips

6.1 INTRODUCTION

The formation of host-guest complexes has been studied in both apolar solvents and water.[1] The type of solvent in which the complexes are formed, is of importance, since it governs the type of interactions present between the host and the guest. In aqueous solution, the main driving force is the hydrophobic effect.[2] The host and guest molecules form a complex in order to reduce their contact with the water molecules. In enzymes, complexation of a substrate often is driven by this hydrophobic effect. This effect is also known to induce the self-assembly of phospholipid molecules into bilayer membranes.[3] The construction of supramolecular structures by self-organization and self-assembly is currently receiving increased interest[4] since such structures are expected to have practical application in various areas *i.e.* catalysis, material science and sensor development.[5] We are interested in designing new supramolecular architectures using different types of building blocks in an aqueous environment.[6] As part of this program we decided to prepare water soluble molecular clips derived from diphenylglycoluril and to study their self-organization properties as well as their ability to bind guest molecules in water.

We previously found that diphenylglycoluril clips modified with crown ether rings and functionalized with long tails, formed vesicles and tubuli when dispersed in water.[7] As shown in Chapter 5 simple clip molecules form dimers in the solid state and in organic solvents. It therefore was of interest to see if this dimerization would also occur in water, and whether this would led to further aggregation. In this chapter studies are described which were carried out along this line.

6.2 RESULTS AND DISCUSSION

6.2.1 Synthesis

In order to keep the cavity of the water soluble clip molecule comparable with that of the chloroform soluble analogue, a strategy was developed in which only the phenyl rings on the convex side of the diphenylglycoluril framework were modified. Our first approach was to start from clips molecules with pyridyl groups, which could be subsequently protonated or methylated to generate charged, water soluble molecules. Using standard procedures,[8] dipyridyl glycoluril **1** was synthesized. Subsequent reaction with paraformaldehyde, in order to obtain the cyclic ether derivative of **1**,[8] resulted in a mixture of compounds which could not be separated. A synthetic route was, therefore, developed which yielded clip shaped molecules directly from compound **1**. 1,2-Bisbromomethyl substituted aromatic molecules were reacted with **1** in DMSO under basic conditions (KOH) to give clips **2** and **3** in 56 and 25 % yield, respectively. These clip molecules were soluble in aqueous HCl solution (pH = 1).

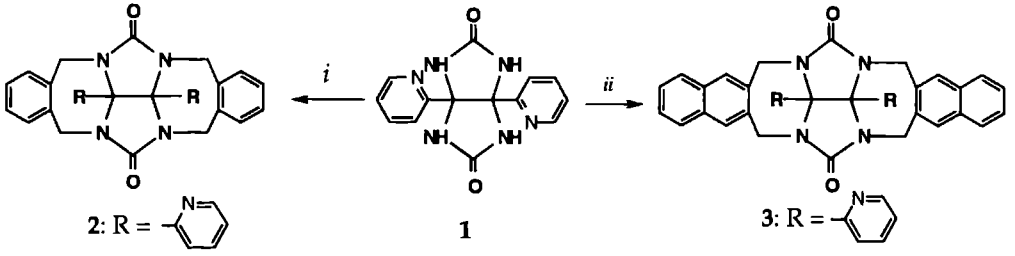

Scheme 1: *(i) KOH/DMSO, α,α'-dibromo-o-xylene; (ii) KOH/DMSO, α,α'-dibromo-2,3-dimethylnaphthalene.*

Due to the ortho positions of the nitrogen atoms the clips can exist as different conformers, *viz.* with the nitrogens pointing to the same side (*syn*) and the nitrogens pointing to opposite sides (*anti*) (see Figure 1). In both the ^{1}H NMR and the ^{13}C NMR spectrum only one set of signals was observed, indicating that the equilibrium between the two conformers is fast on the NMR timescale or that only one conformer exists in solution. Molecular modelling calculations which were carried out suggested that the *anti* conformer is approximately 12 kJ/mol more favourable than the *syn* conformer, due to an electrostatic repulsion between the nitrogens in the latter conformer.[9] This large energy difference would mean that the amount of *syn* conformer is less than 1%. The observed set of signals in the NMR spectrum, therefore, were assigned to the anti conformer.

Attempts to methylate clip molecule **2** under normal conditions (THF/CH_2Cl_2; MeI) failed. Only at higher temperature (50 °C) and pressure (16 kbar), a sparingly soluble precipitate was obtained. From the ^1H NMR spectrum (DMSO-d_6/D_2O) it was concluded that the product was the mono-methylated clip. Four AB patterns were found for the bridging methylene protons and two sets of pyridyl signals, with only one set resonance shifted significantly to lower field with respect to the non-methylated product. In the ^{13}C NMR spectrum of methylated **2**, four signals were visible for the bridging methylene

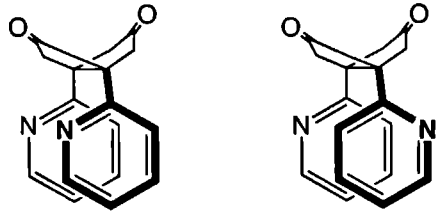

Figure 1: *Two possible conformations (syn and anti, respectively) of a dipyridyl glycoluril molecule.*

groups and four for each carbon of the side-wall whilst only one signal was observed for the methyl group. The quaternary carbons of the DPG framework, were also inequivalent and gave two signals. In the FAB-MS, the largest peak corresponded to the monomethylated clip **2**, with only a very small peak corresponding to the dimethylated product. All these data point to the fact that only one of the pyridyl nitrogens was methylated. Attempts to methylate both positions using different solvent mixtures failed. Since the monomethylated clip was only sparingly soluble in water and the synthesis of this type of clip molecules was only possible via 1,2-bisbromomethyl substituted aromatic molecules, an alternative route was developed.

The second approach used to functionalize the clip at the convex side started from 4,4'-dimethylbenzil. This molecule was converted to ditoluylglycoluril using standard procedures[8]. Reaction with paraformaldehyde gave the ether bridged compound **4** (Scheme 2). This compound was brominated using NBS in tetrachloromethane, yielding **5**. Several attempts to purify **5** by column chromatography and reverse phase HPLC, failed, the impurities being the mono- and tri-brominated derivatives. Recrystallization from acetonitrile, however, resulted in almost pure **5** (95%). Amidoalkylation[8] of **5** with 1,4-dimethoxybenzene and 1,4-dimethoxynaphthalene yielded clips **6** and **7** respectively in good yields (93 and 75 %, respectively). These compounds, however, still contained a small amount of mono- and tri-brominated product. Refluxing **6** in THF/CH_2Cl_2 (1:1, v/v) for 18 hours with an excess of pyridine gave a precipitate, which turned out to be pure compound **8**. A similar reaction yielded pure compound **9** in 50 % yield. Clip molecules with only one bromine or with three bromines also reacted with the pyridine but did not precipitate. Reaction of **6** and **7** with triethylamine instead of pyridine in order to synthesize clips with

different water soluble groups, resulted in a mixture of mono and di-substituted products

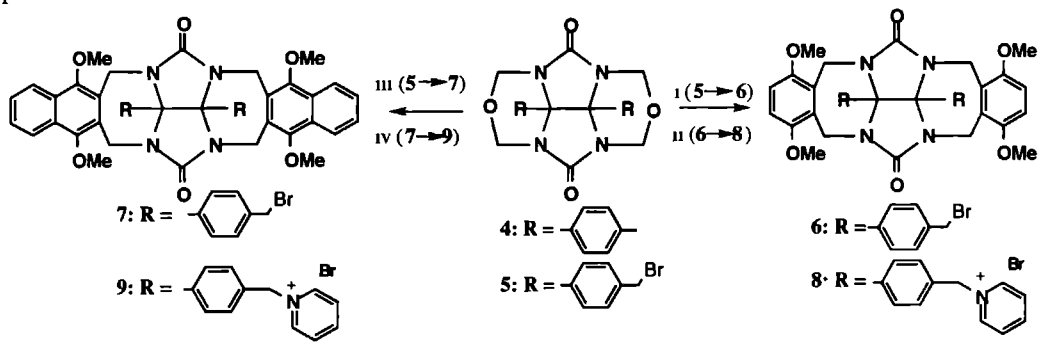

Scheme 2 *(i) 1,4-dimethoxybenzene, Ac_2O/TFA, (ii) pyridine, THF/CH_2Cl_2, (iii) 1,4-dimethoxynaphthalene Ac_2O/TFA, (iv) pyridine, THF/CH_2Cl_2*

6.2.2 Binding properties

In order to evaluate the binding properties of the new clip molecules binding studies were carried out in water with hydroxy- and dihydroxybenzene guest molecules In Chapter 3 it was shown that these guests can be bound in the cleft of the chloroform

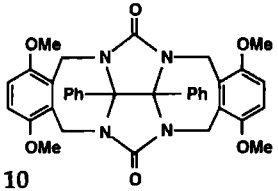

10

soluble clip **10** The binding is based on hydrogen bonding, π-π interactions and the so-called 'cavity effect The strength of the binding was dependent on the substituent of the guest molecule, *i e* more electron withdrawing substituents increase the binding ^{1}H NMR titrations with protonated **2** could not be carried out, due to rapid exchange of the protons with deuterium in D_2O This resulted in a prohibitively large water resonance Binding experiments were carried out, however, with receptor **8** These revealed that in water the affinity of this host for dihydroxybenzene guest molecules is very low (Table 1) A small shift of the side-wall protons was observed upon the addition of a dihydroxybenzene, however, it was not possible to fit the obtained data points to a curve for an 1 1 host-guest complex Upon the titration of 4-nitrophenol with **8**, small shifts of proton signals were observed the resonances of the side-walls protons, the methylene bridges and the methoxy group were all shifted Assuming the formation of an 1 1 complex the data could be fitted to give a binding constant of 4500 M^{-1} and a complex induced shift (CIS) value of 0 1 ppm for the side-wall protons of the clip The very low CIS value suggests that the complex geometry is considerably different from that of **10** in chloroform (In chloroform CIS values in the range of 0 4-0 5 ppm for the side-wall protons of **10** were measured) From ^{1}H NMR titrations in which the resonances of the guest protons were followed, it became clear that the CIS values of these protons were also very small Based on

these data we propose that the phenol guest molecule is not bound inside, but complexes to the outside of the clip (Figure 2a).

Table 1: *Binding constants of complexes between different guest molecules and clip* ***8*** *in D_2O, and between guest molecules and the chloroform soluble analogue* ***10****.*

Guest molecule	**8** (D_2O), K_a (M^{-1})	**10** ($CDCl_3$), K_a (M^{-1})[a]
Resorcinol	<10	2600
5-Chlororesorcinol	<10	16000
Methyl-3,5-dihydroxy benzoate	<10	16500
4-Nitrophenol	4500	1200
4-Cyanophenol	400	415
4-Chlorophenol	<10	80

[a] See Chapter 3.

In chloroform the guest molecule binds within the cavity, where it is sandwiched between the side-walls (see Figure 2b). In water the complexation geometry will be dominated by hydrophobic interactions, which favour direct overlap between aromatic rings. When the guest molecule is complexed to the outside of the clip, more overlap between the aromatic rings can occur, shielding one side of the aromatic wall of the clip and one side of the aromatic ring of the guest from the solvent. In this situation the hydroxyl functions and the substituents on the guest molecule can still be solvated and form hydrogen bonds with water molecules. The whole system will be in dynamic equilibrium, and no specific geometry will be enforced, hence the average distance between the clip side-wall and the guest molecule is large compared to the situation in which the guest molecule is bound in the cleft. This larger distance and more flexible geometry results in smaller CIS values. Upon changing the solvent from D_2O to D_2O/acetone (1:1 v/v) no complexation of substrate molecules was observed. This would be expected if binding occurs at the outside of the cleft and is governed by hydrophobic effects. Hydrophobic interactions are known to be significantly reduced in acetone compared to water. From the complexation geometry shown in Figure 2a it is clear that an 1:2 host-guest complex should also be possible with the second guest molecule bound to the other side of the clip. Our titration data, however, could only be fitted to the equation for 1:1 complex formation. Probably, the 1:2 complex is entropically less favourable, or the binding of the second guest is not influenced by the first bound molecule. Assuming that each clip contains two independent binding sites for guests, the experimental data can be fitted if double the host concentration is used. In that case the calculated binding constants are approximately twice as large.

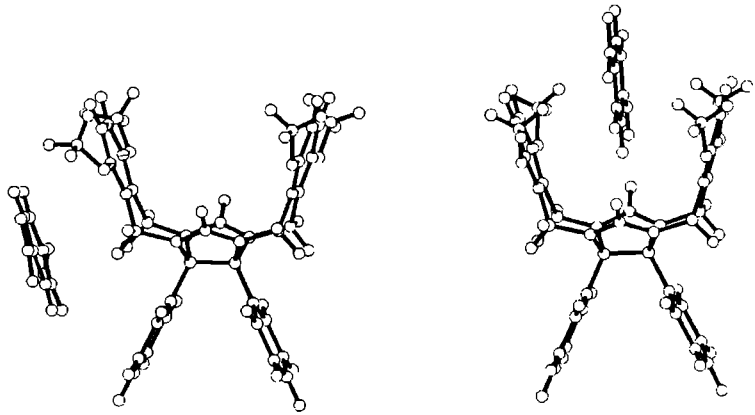

Figure 2: *The binding geometry of the complex between nitrophenol and 8 in water (left) compared to the binding geometry of the complex between nitrophenol and 10 in chloroform (right). The structures are minimized structures using the CHARMm force field, the pyridyl groups have been omitted for clarity.*

Increasing the size of the hydrophobic cavity of the clip by using 1,4-dimethoxy-naphthalene side-walls (clip **9**) instead of 1,4-dimethoxybenzene walls, did not increase the binding affinity for aromatic guests. Instead the host was more inclined to self-aggregate (*vide infra*), which prevented the guest molecule from binding in its cleft. The addition of *p*-nitrophenol or methyl 3,5-dihydroxybenzoate to **9**, resulted in a small ^{1}H NMR shift of the side-wall protons to lower field, suggesting that for these guests the self-association process is partially disrupted. Due to the complexity of the equilibria (a mixture of self-association and host-guest complexation) we were unable to fit the titration data, and hence no binding constants could be calculated.

6.2.3 Dimerization of clip molecules

In chapter 5 it was shown that our clip molecules are able to give dimeric complexes in organic solvents. This dimerization is due to a 'cavity effect' and a favourable π-π interaction between the side-walls of the clips. In aqueous solution, hydrophobic effects will enhance this dimerization behaviour. ^{1}H NMR dilution studies revealed that clips **8** and **9** indeed showed larger self-association constants in water (Table 2) than compound **10** in chloroform (16 M^{-1}).† The calculated Complex Induced Shift (CIS) values of the side-wall protons of **8** (-1.64 ppm), indicated that the side-walls are inserted more deeply (approximately 1Å) into the clefts of the dimeric partners than in the case of the dimeric complex in chloroform.

† The signal to noise ratio in the ^{1}H NMR spectrum of **9** slowly decreased in time, which is indicative of the formation of larger aggregates. This was not observed in the ^{1}H NMR of **8**.

Table 2: *Dimerization constants of clips 8 and 9 in water at different temperatures.*

Clip	Temperature (K)	Ks (M^{-1})
8	298	305
8	318	75
8	338	30
9	298	> 5000[a]

[a]Due to aggregation of the clip, no reliable value could be calculated. Assuming that only dimerization occurs, a K_S > 5000 M^{-1} was calculated.

In chapter 5, it was shown that in chloroform the dimers have an off-set geometry which is enforced by the electrostatic repulsion between the aromatic walls. This repulsion is reduced in water, since in this solvent the dielectric constant is higher. This reduction in electrostatic repulsion allows the walls to have a greater overlap of their π-systems and enables the two clips to come closer together. The temperature dependent NMR studies on **8** showed that the formation of the dimeric species in aqueous solution is an enthalpy driven process (ΔH = -48 kJ/mol, ΔS = -114 J/mol·K). Similar enthalpy driven processes have been reported for the binding of aromatic guests in cyclophanes[10] and in cyclodextrins[11] in water.

Clip molecule **9** contains a larger hydrophobic cleft than **8** and was expected to form stronger dimeric complexes. The electrostatic repulsion between the two 1,4-dimethoxynaphthalene moieties, which inhibits this clip from dimerizing in chloroform, will be reduced in water. ^{1}H NMR dilution studies (0.1-3.0 mM of **9**) confirmed the strong self-association behaviour of clip **9**, K_S > 5000 M^{-1} (due to the formation of larger aggregates (*vide infra*) this value is an estimated lower value). Surprisingly, not only the ^{1}H NMR signals of the protons of the naphthalene side-walls of **9** shifted upon dilution but also those of the pyridine protons at the convex side of the glycoluril framework. These results imply that in solution two self-association geometries are possible: a 'head-to-head' and a 'head-to-tail' geometry (Figure 3). In the latter case a favourable interaction between the electron rich 1,4-dimethoxynaphthalene side-walls of one molecule and the electron poor pyridinium group of the other can be envisaged. In the 'head-to-head' case self-association is mainly based upon hydrophobic effects. The 'head-to-tail' type of dimerization, was not observed for clip **8**, probably because the side-wall was too small for a favourable interaction between the electron rich and electron poor aromatic surfaces.

Comparison of our studies with those performed on other water soluble receptor molecules, enables us to make some general conclusions. Cyclodextrins[11], cyclophanes[10] and also basket-shaped molecules reported previously by us[7] contain a

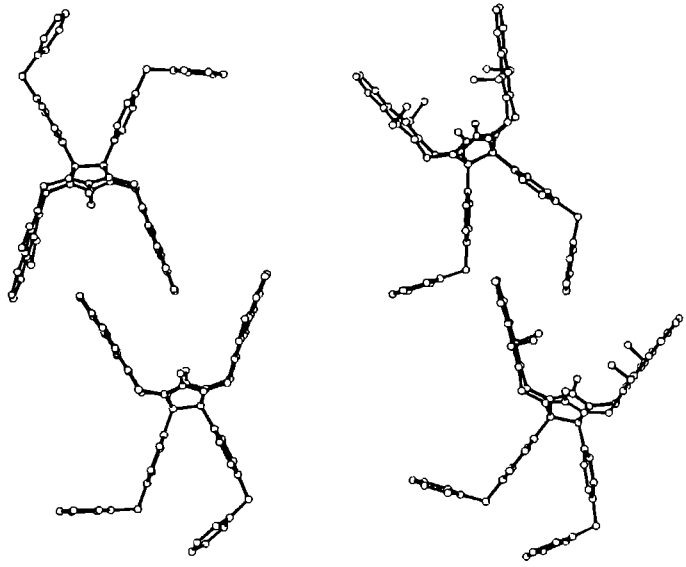

Figure 3: *Two different types of dimeric species observed for clip* **9**: *'head-to-head' (left) and 'head-to-tail' (right).*

large cavity, which is available for apolar guest molecules. Bound guests are almost completely shielded from the water solvent, resulting in very high binding constants. In the case of clip **8**, however, the cleft is too small to completely shield the guest molecule and as a result the guest prefers to bind to the outside of the cleft. In the case of a clip with a large hydrophobic surface a strong self-aggregation of the host occurs which prohibits the guest molecule from binding in the cavity. A detailed insight into the binding properties of this kind of receptor molecules is complicated by the

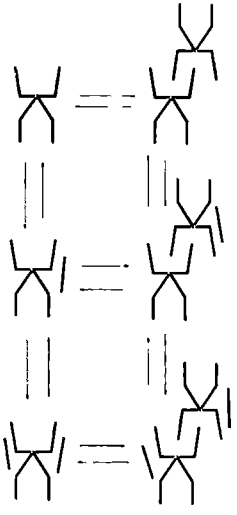

Figure 4: *Schematic overview of the host-guest binding equilibria involved in the case of clip* **8**.

numerous equilibria that are involved. An overview of these equilbria for clip **8** is presented in Figure 4. In summary we may conclude that receptor molecules which can encapsulate a guest and do not self-associate are better receptors for apolar guest molecules in water than our cleft-shaped molecules.

6.2.4 Aggregation of clip molecules

If concentrated samples (1-3 mM) of **9** were allowed to stand for several hours, a pearly, milk-like dispersion was gradually formed. This suspension is indicative of the presence of large assemblies of molecules. The addition of acetone or methanol to the suspension caused complete dissociation of the aggregates. ^{1}H NMR of the resulting clear solution showed the presence of monomeric species only. Investigation of the pearly dispersion by electron microscopy (platinum shadowing technique, Figure 5A) revealed the presence of well defined 'razor blade-like' aggregates which were stacked back-to-back to give long chains (Figure 5B). These 'razor blades' all had approximately the same dimension (1.2 x 8 μm) and rounded corners with the same curvature. Scanning electron microscopy showed that the surfaces of the superstructures were also slightly convex. According to freeze fracture electron microscopy (Figure 5C) the 'razor blades' were constructed from a limited number of layers. Electron diffraction experiments confirmed that the aggregates were not crystals. Samples of the pearly suspension were investigated by powder diffraction measurements, which revealed a strong reflection corresponding to a repeating distance of 16.8 Å. This is the distance expected for 'head-to-tail' type of dimers. From the SEM pictures the thickness of the aggregates were estimated to be approximately 90 nm. Together with the data from the powder diffraction experiment this result suggest that the 'razor blades' consist of approximately 50 layers.

As mentioned above clip **8** does not form head-to-tail dimers. The formation of larger aggregates was also not observed. Clip molecule **3** which is water soluble after protonation of the pyridine groups did form aggregates, which were studied by electron microscopy. Transmission and scanning electron micrographs showed that at pH = 1 long fibers were present, with lengths up to 10 micron (Figure 5E). The thickness of these fibers varied from approximately 65 Å, which is twice the size of a dimer, to approximately 330 Å (bundle of 5 fibers).

In order to obtain information about the size and packing ability of the clip molecules, monolayer experiments were carried out with both **3** and **9**. From the isotherm of **9** a molecular area of 42 Å^2 was calculated. This value, however, is not reliable, because the monolayer was not stable: the clip molecules appeared to be too soluble, resulting in a decrease in area at constant pressure. This was also the case for clip **3** at low pH. At

pH 6, stable monolayers were formed because **3** is less water soluble at this pH The calculated area per molecule was approximately 55Å, which indicates that the clip molecules are in an upright position, with the pyridyl groups pointing toward the water surface

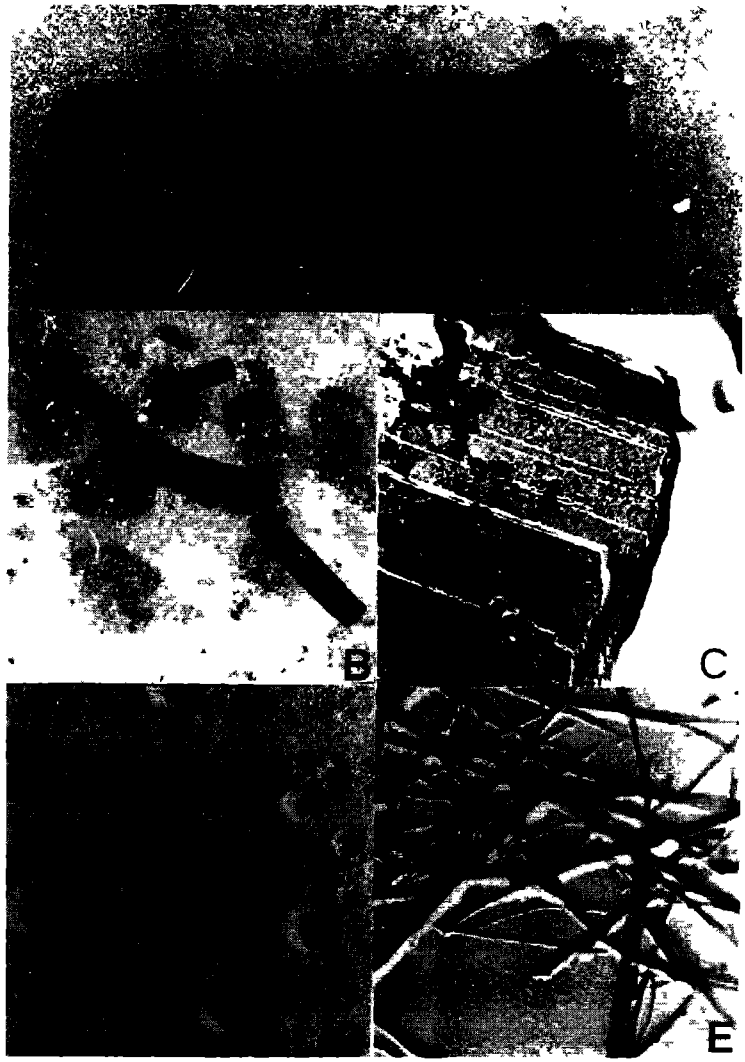

Figure 5: *Electron microscopic pictures of 'razor blade-like' aggregates formed in water by clip* **9** *(A and B, platinum shadowing technique, for A 1 cm = 0 8 μm, for B 1 cm = 3 2 μm) Freeze fracture electron micrograph of a 'razor blade-like" aggregate (C 1 cm = 0 08 μm) Sphere-like structures formed from* **9** *by the addition of the oxidized form of riboflavine (D, platinum shadowing technique, 1 cm = 0 16 μm, a similar structure is generated in the presence of caffeine) Fibers formed from* **3** *in water (E, pH = 1 platinum shadowing technique, 1 cm = 0 16 μm)*

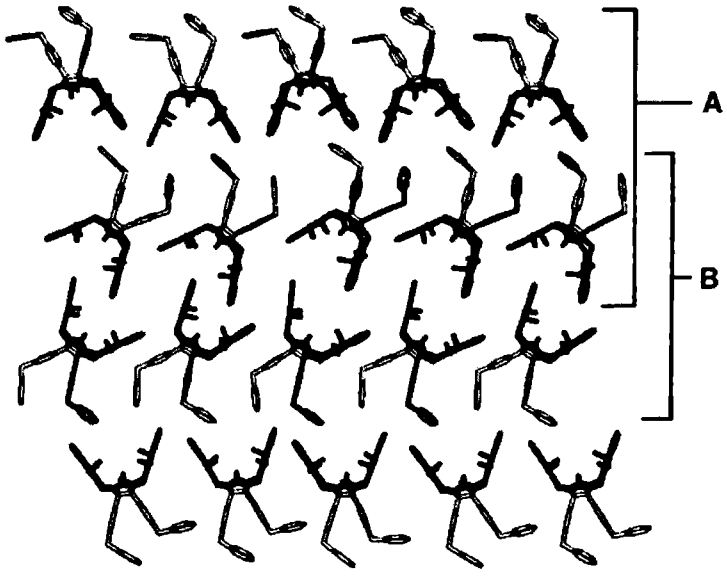

Figure 6: *Computer generated picture showing the middle section of a 'razor blade-like' aggregate of* **9**. *'Head-to-tail' dimers (A, twice the repeating unit of 17 Å). Central layer of 'head-to-head' dimers (B, thickness 32 Å).*

Based on the aforementioned ^{1}H NMR dilution experiments, the EM studies and the X-ray powder diffraction experiments, we propose that the formation of the 'razor blades' starts from head-to-head dimeric seeds of **9**, which act as initiators for further growth. These dimers are the most abundant species in solution according to ^{1}H NMR. Monomers can subsequently attach themselves onto the pyridinium units of the dimers in a head-to-tail fashion, eventually forming a multilayer structure (Figure 6) of which the outer surface is hydrophilic on all sides. Molecular modelling calculations (CHARMm force field) suggested that the head-to-tail layers had a thickness of 17 Å, which is in good agreement with the results from the X-ray powder diffraction experiment.

A very remarkable feature of the 'razor blade-like' structures is that they have such a well defined size and shape. Apparently, at a certain stage they stop growing and do not form larger aggregates. This phenomenon is of great interest since obtaining control over size and shape of aggregates[13] by using self assembly, is one of the great challenges in supramolecular chemistry.[14]

For molecules of **3** the interaction between the naphthalene moieties and the protonated pyridine groups is expected to be relatively small because of steric reasons.

Clips **3** therefore are expected to form only 'head-to-head' type of dimers as found in the X-ray structure of the diphenylglycoluril analogue (Chapter 5). These type of dimers, which can be considered to be a kind of bola-amphiphiles[12], can aggregate by sticking together forming long fibers.

6.2.5 Influence of guest molecules on the aggregation behaviour

In order to investigate the nature of the self-association of **9** in more detail, we studied the effect of guest molecules on the aggregation process. ^{1}H NMR binding studies at low concentrations of **9** were performed in water using 4-nitrophenol, 1,3-dihydroxybenzene, and caffeine as the guests. The first two molecules did not bind to **9**, probably because the host forms too strong dimeric complexes (*vide supra*). Caffeine, however, was found to bind with a binding constant of approximately K_a = 8400 M^{-1}, assuming an 1:1 complex. ^{1}H NMR showed, however, that this substrate was located between adjacent clip molecules and not in the cavities of the clips themselves. The addition of caffeine to **9** (1:1 molar ratio) resulted in a change in the shape of the aggregates: instead of 'razor blade-like' structures, spherical aggregates were formed. Powder diffraction revealed that the latter aggregates had approximately the same repeating distance as the former ones, *viz* 17.1 Å. This suggests that these spherical aggregates are still composed of the same head-to-tail type of dimers. The presence of the caffeine molecules between adjacent clips apparently induces a larger curvature and hence a more bent, *i.e.* a sphere-shaped, nanostructure (diameter 80-300 nm).

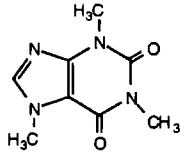

caffeine

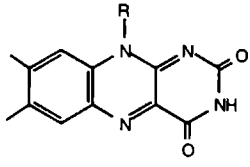

riboflavine

^{1}H NMR experiments revealed that the oxidized form of riboflavine can also be bound in aggregates of **9**. Dispersing **9** in the presence of this oxidized riboflavine, yielded spherical aggregates, comparable to those induced by caffeine (Figure 5D). The flat structure of riboflavine can be changed reversibly into a bent structure with an angle of ca. 30°, by reduction with $Na_2S_2O_4$. ^{1}H NMR data suggested that this reduced form of riboflavine was not strongly bound in the aggregate probably due to its bent structure. This opened the possibility to switch from spherical aggregates to 'razor blade-like' structures by reducing the guest (Figure 7). Experiments were carried out to test this idea. Unfortunately, in the presence of the reduced form of riboflavine compound **9** did not form 'razor-blades' but aggregates which consisted of infinite multilayer structures. A solution of **9** consisting of spherical aggregates containing the oxidized form of riboflavine, could be changed into these multilayer structures upon reducing the riboflavine, but the reversed process, *i.e.* going back to spherical structures, by re-oxidizing the reduced form of riboflavine, was unsuccessful. Very few

examples of reversibly switching of aggregate structures have been reported in the literature.[15] Attempts to synthesize clip molecules which had a flavine molecule as a side-wall in order to incorporate the switchable function in the clip itself, failed.

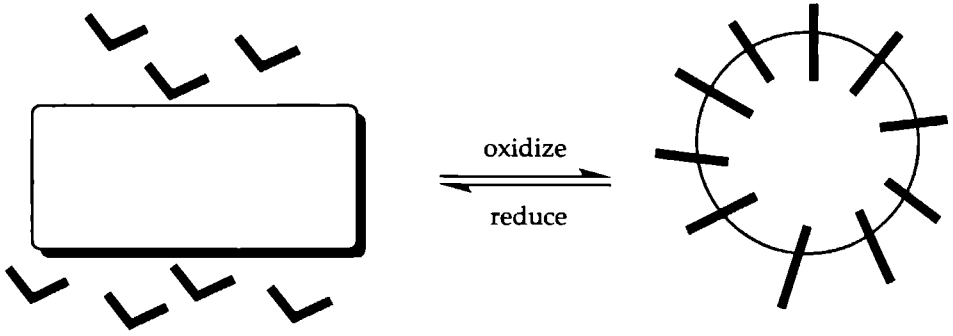

Figure 7: *Schematic picture of switching the aggregate structure by oxidizing and reducing the riboflavine guest molecule.*

In a final series of experiments we investigated the possibility to form chiral aggregates by adding a chiral guest-molecule **11**,[7b] to a dispersion of clip **9** in water. According to electron microscopy (TEM, platinum shadowing and freeze fracture technique), spherical type of aggregates were obtained, similar to those observed in the case of caffeine and riboflavine, suggesting that the molecules of **11** were complexed in between adjacent clip molecules. The aggregates, unfortunately had no chiral shapes.

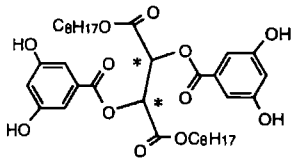

11

6.3 CONCLUSIONS

We have shown that clip molecules derived from diphenylglycoluril can be made water soluble by attaching solubilizing substituents to the convex side of these host molecules. The binding of aromatic guests to these clips turned out to be more complicated than expected. The hydrophobic effect which should induce strong guest binding, also induced self-association of the clips. The latter association was particularly strong when the clip had large aromatic side-walls. We may conclude that the water soluble clip molecules are unsuitable for host-guest chemistry because their cavities are no longer available for substrate binding. The formed aggregates, however, are of great interest, especially the 'razor blade-like' structures which are generated from clip **9**. These nanometer-sized aggregates have a well-defined size and shape, which can be modified by the addition of guest molecules. This feature can be considered as being one of the first steps towards the construction of aggregates with controlled shape and dimension.

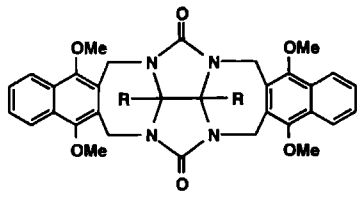

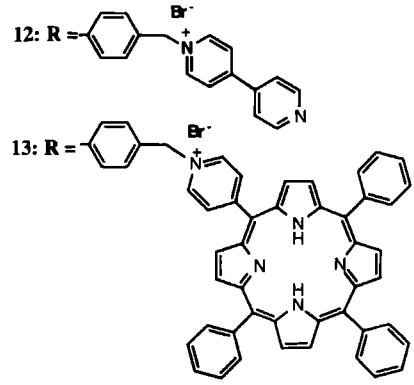

The route which we have developed for synthesizing water-soluble clips, makes it possible to easily attach other functional groups to the host molecules. Preliminary experiments have shown that clips **12** and **13**, which contain a bipyridinium and a porphyrin functional substituent, respectively, are easily accessible from **7**. These clip molecules may be of interest in the study of photoinduced electron transfer from a donor (Zn-porphyrin or free base porphyrin) to an acceptor (methyl viologen), both incorporated in an aggregate.[16]

6.4 EXPERIMENTAL SECTION

6.4.1 General

DMSO was distilled and stored over Mol Sieves (3Å) before use. Tetrachloromethane was dried over 4Å Mol Sieves. THF and CH_2Cl_2 were freshly distilled before use over sodium and $CaCl_2$, respectively. Pyridine and triethylamine were dried over CaH_2, and distilled before use. All other chemicals were commercial products and were used without further purification. For column chromatography, Merck silica gel (60H) was used. Melting points were determined on a Jeneval polarization microscope, THMS 600 hot stage, and are reported uncorrected. ^1H NMR and ^{13}C-spectra were recorded on Bruker AM-400 MHz, Bruker WM-200, and Bruker WF-90 instruments. Chemical shifts are reported downfield from internal tetramethylsilane. Abbreviations used are s = singlet, d = doublet, dd = doublet of doublets, t= triplet, b = broad, and m = multiplet. FAB mass spectra were recorded on a VG 7070E instrument, the matrix used was *m*-nitrobenzylalcohol. Elemental analyses were determined with a Carbo Erba Ea 1108 instrument. The high pressure experiments were carried out with a home-built apparatus.

6.4.2 Compounds

Dipyridylglycoluril (1). A mixture of 5.0 g (22.9 mmol) of α,α'-pyridyl, 2.8 g (45.8 mmol) of urea, and 4.6 mL of trifluoroacetic acid were refluxed in 90 mL of toluene in a Dean-Stark apparatus for 8 hrs. A brown precipitate was formed which was filtered off and washed with diethylether and ethanol to yield 4.07 g of compound **1** (60%). Mp 215°C (dec); ^{1}H NMR (d_6-DMSO) ∂ 8.27 (d, 4H, PyrH, *J* = 4.0 Hz), 7.56 (s, 4H, NH), 7.45 (t, 2H, PyrH, *J* = 6.7 Hz), 7.09 (b, 4H, PyrH, *J* = 6.7 Hz). FAB-MS *m/z* 297 $(M+H)^+$. Anal. Calcd. for $C_{14}H_{12}N_6O_2 \cdot 0.2(C_7H_8)$: C, 58.77; H, 4.36; N, 26.70. Found: C, 58.42; H, 4.32; N, 26.44.

5,7,12,13b,13c,14-Hexahydro-13b,13c-α,α'-dipyridyl-6H,13H-5a,6a,12a,13a-tetraazabenz[5,6] azuleno[2,1,8-ija]benz[f]azulene-6,13-dione (2). To a suspension of 450 mg (8.0 mmol) of KOH in 3 mL of DMSO was added 300 mg (1.0 mmol) of **1** and 528 mg (2.0 mmol) of α,α'-dibromo-o-xylene. The mixture was stirred for 16 hrs and then poured into 20 mL of water. The compound was extracted with 20 mL of CH_2Cl_2, the organic layer was washed with aqueous 1 N NaOH, water, and dried over $MgSO_4$. After evaporation of the solvent the compound was washed with diethyl ether yielding 280 mg (56%) of white powder. Further purification is possible by column chromatography (eluent 1.5% MeOH/CH_2Cl_2). Mp > 315°C; ^{1}H NMR ($CDCl_3$) ∂ 8.53 (d, 4H, PyrH, *J* = 4.09 Hz), 7.53-6.84 (m, 14H, PyrH + ArH), 4.82 (d, 4H, NCH_2Ar, *J* = 15.6 Hz), 4.11 (d, 4H, NCH_2Napht, *J* = 15.6 Hz). FAB-MS (m-nitrobenzylalcohol) m/z 501 $(M+H)^+$. Anal. Calcd. for $C_{30}H_{24}N_6O_2$: C, 71.99; H, 4.83; N, 16.79. Found: C, 72.25; H, 4.82; N, 16.53.

6,8,15,16b,16c,17-Hexahydro-16b,16c-α,α'-dipyridyl-7H,16H-6a,7a,15a,16a-tetraazanaphto[5,6] azuleno[2,1,8-ij]naphto[f]azulene-7,16-dione (3). To a suspension of 360 mg (6.4 mmol) of KOH in 3 mL of DMSO was added 236 mg (0.8 mmol) of **1** and 500 mg (1.6 mmol) of α,α'-dibromo-2,3-dimethylnaphthalene. The mixture was stirred for 16 hrs and then poured into 20 mL of water. The compound was extracted with 20 mL of CH_2Cl_2, the organic layer was washed with aqueous 1 N NaOH, water, and dried over $MgSO_4$. After evaporation of the solvent the compound was purified by column chromatography (eluent 1.5% MeOH/CH_2Cl_2) and recrystallization from $CHCl_3$ yielding 100 mg white powder (25%). Mp > 300°C; ^{1}H NMR ($CDCl_3$) δ 8.55 (d, 2H, PyrH, *J* = 5.73 Hz), 7.78-6.89 (m, 14H, ArH en PyrH), 7.67 (s, 4H, ArH), 5.05 en 4.24 (2d, 8H, NCHHAr, *J* = 16.4 Hz); FAB-MS *m/z* 601 $(M+H)^+$. Anal. Calcd. for $C_{38}H_{28}N_6O_2 \cdot (CHCl_3)$: C, 63.58; H, 3.97; N, 11.36. Found: C, 63.87; H, 4.02; N, 11.23.

Ditoluylglycoluril. A mixture of 10.0 g (42 mmol) of 4,4'-dimethylbenzil, 5 g (84 mmol) of urea and 4.2 mL of trifluoroacetic acid was refluxed in 85 mL of toluene in a Dean-

Stark apparatus for 8 hrs. A white precipitate was formed which was filtered off and washed with ethanol to give 10.82 g of product (80%). Mp > 300°C ; ^{1}H NMR (d_6-DMSO) ∂ 7.62 (s, 4H, NH), 6.91 (m, 8H, ArH), 2.11 (2, 6H, CH_3). FAB-MS *m/z* 323 $(M+H)^+$. Anal. Calcd. for $C_{18}H_{18}N_4O_2$: C, 67.07; H, 5.63; N, 17.38. Found: C, 67.64; H, 6.14; N, 15.94.

Dihydro-8b,8c-4,4'-bismethyldiphenyl-1H,3H,4H,5H,7H,8H,-2,6-dioxa-3a,4a,7a,8a-tetraazacyclopenta[def]]fluorene-4,8-dione (4). A suspension of 14.4 g of ditoluylglycoluril (45 mmol) and 6.6 g (220 mmol) of paraformaldehyde in 42 mL of DMSO was made basic (pH =9) with aqueous 1 N NaOH. After stirring for 16 hrs the mixture was acidified with aqueous 12 N HCl (pH = 1) and refluxed for 1 hr. After cooling 16 mL of water was added, a white precipitate was formed which was filtered off, washed with water and ethanol, and dried under vacuum to yield 11.5 g (65%) of compound **4**. Mp 209 °C ; ^{1}H NMR ($CDCl_3$) ∂ 6.98 (dd, 8H, ArH, *J* = 6.5 Hz), 5.64 and 4.56 (2d, 8H, NCHHAr, *J* = 10.6 Hz), 2.20 (s, 6H, CH_3). FAB-MS *m/z* 407 $(M+H)^+$. Anal. Calcd. for $C_{22}H_{22}N_4O_4(CH_3COOH)_2$: C, 59.31; H, 5.74; N, 10.64. Found: C, 59.64; H, 5.65; N, 10.94.

Dihydro-8b,8c-4,4'-bisbromodimethyldiphenyl-1H,3H,4H,5H,7H,8H,-2,6-dioxa-3a,4a,7a,8a-tetraazacyclopenta[def]]fluorene-4,8-dione (5). A mixture of 2 g (4.92 mmol) **4**, 1.77 g (9.94 mmol) *N*-Bromosuccinimide (NBS) in 200 mL of CCl_4 was refluxed for 16 hrs under nitrogen in the presence of a catalytic amount of benzoyl peroxide. After cooling the excess NBS and succinimide were filtered off, and the solution was concentrated. Recrystallization of the resulting product from acetonitrile (10 mg/mL) yielded 1.11 g (40%) of almost pure **5**. It was not possible to completely remove small amounts of tri- and mono-brominated compounds, see text. Mp 142 °C; ^{1}H NMR ($CDCl_3$) ∂ 7.13 (m, 8H, ArH), 5.66 and 4.57 (2d, 8H, NCHHAr, *J* = 11.1 Hz), 4.30 (s, 4H, CH_2Br). CI-MS *m/z* 564 $(M-H)^+$. As small amounts of mono- and tri-brominated compounds were present, no elemental analysis was performed.

5,7,12,13b,13c,14 - Hexahydro - 1,4,8,11 - tetramethoxy - 13b,13c - 4,4'-bisbromodimethyldiphenyl - 6H,13H-5a,6a,12a,13a - tetraazabenz[5,6]azuleno[2,1,8-ij]benz[f]azulene - 6,13 - dione (6). A solution of 420 mg (0.75 mmol) of **5** in 0.75 mL of acetic anhydride and 0.75 mL of trifluoroacetic acid was stirred for 30 min at 95 °C. After the addition of 204 mg (1.5 mmol) of *p*-dimethoxybenzene the solution was stirred at 95 °C for an additional 30 min. After cooling 1.5 mL of methanol was added. The formed precipitate was filtered off and washed with cold methanol to yield 550 mg (93%) of white solid **6**. Mp > 300°C; ^{1}H NMR ($CDCl_3$) ∂ 7.03 (dd, 8H, ArH, *J* = 3.92 Hz), 6.66 (s, 4H, ArH), 5.55 and 3.58 (2d, 8H, NCHHAr, *J* = 16.1 Hz), 4.30 (s, 4H, $ArCH_2Br$),

3.77 (s, 12H, OCH_3); FAB-MS *m/z* 805 $(M+H)^+$. As small amounts of mono- and tri-brominated compounds were present, no elemental analysis was performed.

6,8,15,16b,16c,17-Hexahydro-5,9,14,18 - tetramethoxy - 16b,16c - 4,4'-bisbromodimethyldiphenyl-7H,16H-6a,7a,15a,16a-tetraazanaphto[5,6]azuleno[2,1,8-ij]naphto[f]azulene-7,16-dione (7). A solution of 124 mg (0.31 mmol) of **5** in 0.35 mL of acetic anhydride and 0.35 mL of trifluoroacetic acid was stirred for 30 min at 95 °C. After the addition of 126 mg (0.63 mmol) of 1,4-dimethoxynaphthalene the solution was stirred at 95 °C for an additional 30 min. After cooling 1.5 mL of methanol was added. The formed precipitate was filtered off and washed with cold methanol, yielding 170 mg (75%) of white solid **7**. Mp 297- 300°C; ^1H NMR ($CDCl_3$) ∂ 7.97 and 7.44 (2m, 8H, NaftH), 7.16 (m, 8H, ArH), 5.74 and 3.94 (2d, 8H, NCHHAr, *J* = 14.7 Hz), 4.33 (s, 4H, $ArCH_2Br$), 4.04 (s, 12H, OCH_3); FAB-MS *m/z* 905 $(M+H)^+$. As small amounts of mono- and tri-brominated compounds were present, no elemental analysis was performed.

Compound 8. To a solution of 50 mg (0.06 mmol) of **6** in 20 mL of THF and 20 mL of CH_2Cl_2 (both freshly distilled), was added 7 drops of pyridine and the reaction mixture was refluxed for 18 hrs. A precipitate was formed which was filtered hot, washed with CH_2Cl_2 and diethylether, to give 29.0 mg (50%) of white solid **8**. Mp > 330°C; ^1H NMR (D_2O) (1.08 mM) ∂ 8.74 (d, 4H, PyrH, *J* = 5.8 Hz), 8.50 (t, 2H, PyrH, *J* = 7.0 Hz), 8.00 (t, 4H, PyrH, *J* = 5.8 Hz), 7.24 (dd, 8H, ArH), 6.19 (s, 4H, ArH), 5.59 (s, 4H, $ArCH_2Pyr$), 5.22 and 3.74 (2d, 8H, NCHHAr, *J* = 16.0 Hz), 3.54 (s, 12H, OCH_3); FAB-MS *m/z* 881 en 883 $(M-Br)^+$, 723 $(M-2Br-Pyr)^+$. Anal. Calcd. for $C_{48}H_{46}N_6O_6Br_2 \cdot (3H_2O)$: C, 56.70; H, 5.15; N, 8.27. Found: C, 56.06; H, 5.06; N, 8.39.

Compound 9. To a solution of 100 mg (0.11 mmol) of **7** in 35 mL of THF and 35 mL of CH_2Cl_2 (both freshly distilled), was added 12 drops of pyridine and the reaction mixture was refluxed for 18 hrs. A precipitate was formed which was filtered hot, washed with CH_2Cl_2 and diethylether, to give 58.5 mg (50%) of white solid **8**. Mp 278°C; ^1H NMR (D_2O) (2.8 mM) δ 8.94 (d, 4H, PyrH, *J* = 5.6 Hz), 8.66 (t, 2H, PyrH, *J* = 8.0 Hz), 8.14 (t, 4H, PyrH, *J* = 5.6 Hz), 7.58 (m, 8H, ArH), 7.50 en 6.79 (2m, 8H, NaftH), 5.89 (s, 4H, $ArCH_2Pyr$), 5.64 and 4.32 (2d, 8H, NHCHHAr, *J* = 15.6 Hz), 3.95 (s, 12H, OCH_3); FAB-MS m/z 902 $(M-2Br)^+$. Anal. Calcd. for $C_{56}H_{50}N_6O_6Br_2 \cdot (3H_2O)$: C, 60.22; H, 5.05; N, 7.52. Found: C, 59.82; H, 4.95; N, 7.57.

Association constants of complexes between clips and the guest molecules and self-association constants were determined by ^1H NMR as described in Chapters 3 and 5.

6.4.3 Electronic microscopy studies

Sample preparation: aqueous solutions of the clip molecules were heated, sonificated and allowed stand for several hours to a few of days (the aggregates were stable for several days). A drop of the resulting suspension was placed on a Formvar-coated copper grid. After 1 min. the excess dispersion was removed, and the samples were shaded with Pt (layer thickness 2nm, sputter angle 45°).

Samples for freeze-fracturing were prepared by bringing a drop of a dispersion of clip onto a golden microscope grid (300 mesh), which was subsequently placed between two copper plates and fixated in supercooled liquid nitrogen. Sample holders were placed in a Balzers Freeze Etching System BAF 400 D at 10^{-7} Torr and warmed to -130°C. After fracturing, the samples were etched for 1 min., and shaded with Pt (layer thickness 2nm, sputter angle 45°) and 20 nm carbon. The replicas were allowed to warm up to room temperature, left on 20% chromic acid for 16 hours and washed with water.

The SEM samples were prepared by placing a drop of a dispersion of a clip on a Formfar-coated copper grid. After 1 min the excess dispersion was removed, and the samples were shaded with a layer of gold.

The TEM studies were carried out on a Philips TEM 201 (60kV) instrument, and the SEM studies on a JEOL JSM-T300 instrument.

6.4.4 Powder diffraction

Samples were prepared in a desiccator, by placing a drop of a suspension of a clip on a silicon single crystal. Evacuation resulted in the freezing of the sample. After sublimation of the ice the sample was placed in a Philips PW1710 diffractometer, which was equipped with a Cu LFF X-ray tube operating at 40 kV and 55 mA (wavelengths (a1,a2): 1.54060, 1.54438).

References

1 (a) Smithruth, D.B.; Diedrich, F. *J. Am. Chem. Soc.* **1990**, *112*, 339. (b) Ferguson, S. B.; Sanford, E. M.; Seward, E. M.; Diedrich, F. *J. Am. Chem. Soc.* **1991**, *113*, 5410. (c) Smithruth, D.B.; Wyman, T. B.; Diedrich, F. *J. Am. Chem. Soc.* **1991**, *113*, 5420. (d) Schneider, H. J. *Angew. Chem.* **1991**, *103*, 1419. see also ref 10 and 11.

2 Tanford, C. "*The Hydrophobic Effect*", **1973**, Wiley Interscience, New York.

3 (a) Fendler, J. H. "*Membrame mimetic chemistry*," wily, New York **1982**. (b) Ringsdorf, H.; Schlarb, B.; Venzmer, J. *Angew. Chem.* **1988**,*100*, 117.

4 Whitesides, G.M.; Mathias, J.P.; Seto, C.T. *Science*, **1991**, *254*, 1312. For recent reviews see: (a) Lawrence, D. S.; Jiang, T.; Levette, M. *Chem. Rev.* **1995**, *95*, 2229-2260. (b) Bernstein, J.; Davis, R. E.; Shimoni, L.; Chang, N.-L. *Angew. Chem.* **1995**,*107*, 1689. (c) Percec, V.; Heck, J.; Johansson, G.; Tomazos, D.; Kawasumi, M.; Chu, P.; Ungar, G. *Pure Appl. Chem.* **1994**, 1719.

5 Service, R.F. *Science*, **1994**, *265*, 316.

6 (a) van Esch, J. H. Thesis, Nijmegen, **1993**. (b) Sommerdijk, N. A. J. M. Thesis, Nijmegen, **1995**. (c) Hafkamp, R. Thesis, Nijmegen, **1996**.

7 (a) Schenning, A. P. H. J.; de Bruin, B.; Feiters, M. C.; Nolte, R. J. M. *Angew. Chem. Int. Ed. Engl.*, **1994**,*33*, 1662. (b) Nunen, H. L. M., Thesis, Nijmegen, **1995**.

8 (a) Smeets, J.W.H; Sijbesma, R.P; van Dalen, L.; Spek, A.L.; Smeets, W.J.J.; Nolte, R.J.M. *J. Org. Chem.*, **1989**, *54*, 3710. (b) Sijbesma, R.P.; Kentgens, A.P.M.; Nolte, R.J.M.; *J. Org. Chem.*, **1991**, *56*, 3199. (c) Sijbesma, R.P.; Kentgens, A.P.M.; Lutz, E. T. G.; van der Maas, J. H.; Nolte, R.J.M. *J. Am. Chem. Soc.* **1993**, *115*, 8999.

9 Calculations were performed using the CHARMm force field.

10 Diederich, F. "*Cyclophanes*;" Royal Society of Chemistry; Cambridge, **1991.**

11 (a) Bender, M.L.; Komiyama, M. "*Cyclodextrin Chemistry*;" Springer; Berlin, **1978**. (b) Wenz, G. *Angew. Chem.* **1994**,*106*, 851, and references cited therein.

12 Okahata, Y.; Kunitake, J. *J. Am. Chem. Soc.* **1979**, *101*, 5231.

13 For other examples in which control over the shape of aggregates is obtained see: (a) Menger, F.M.; Lee, S.E. *J. Am. Chem. Soc.* **1994**, *116*, 5987. (b) Ghadiri, M.R.; Granja, J.R.; Milligan, R.A.; McRee, D.E.; Khazanovich, N. *Nature*, **1993**, *366*, 324. (c) Lhotak, P.; Shinkai, S. *Tetrahedron Lett.*, **1995**, *36*, 4829. (d) Arimori, S.; Nagasaki, T.; Shinkai, S. *J. Chem. Soc. Perkin Trans. 2*, **1995**, 679. (e) Muñoz, S.; Abel, E.; Wang, K.; Gokel, G.W.*Tetrahedron*, **1995**, *51*, 423 (f) Mathias, J.P.; Simanek, E.E.; Zerkowski, J.A.; Seto, C.T.; Whitesides, G.M. *J. Am. Chem. Soc.* **1994**, *116*, 4316. (g) Mathias, J.P.; Simanek, E.E.; Whitesides, G.M. *J. Am. Chem. Soc.* **1994**, 116, 4326. (h) Mathias, J.P.; Seto, C.T.; Simanek, E.E.; Whitesides, G.M. *J. Am. Chem. Soc.* **1994**, *116*, 1725.

14 Mann, S. *Nature*, **1993**, *365*, 499.

15 (a) Sayi, T;, Hoshino, K.; Aoyagai, S. J. *J. Chem. Soc. Chem. Commun.*, **1985**, 865. (b) Munoz, S.; Gokel, G. W. *J. Am. Chem. Soc.* **1993**, *115*, 4899.

16 Kuhn, H. *Pure & Appl. Chem.*, **1979**, *51*, 341.

Chapter 7

Novel Cleft Containing Porphyrins as Model Systems for Studying Electron Transfer Processes

7.1 INTRODUCTION

Green plants and photosynthetic bacteria have the ability to convert sunlight into chemical energy which is subsequently used for all other biological reactions. This process is of enormous importance, since all energy used by living systems is derived from this photosynthesis. The very high quantum efficiency of this process is the result of a very fast electron transfer over a long distance, via a very complicated cascade of chromophores, and a very slow backtransfer of the electron. Both the importance and the high efficiency of the process, makes the understanding of the underlying mechanism one of the biggest challenges in science.

A great deal of progress has been made in the understanding of the molecular structure and function of the relatively simple photosynthetic system in bacteria. A knowledge of how this system functions is expected to aid in the understanding of the more complicated photosynthetic reaction centers in green plants. The structures of reaction centers of the purple photosynthetic bacteria *Rhodopseudomonas viridis*[1] and *Rhodobacter sphaeroides*.[2] have been elucidated and in combination with detailed spectroscopic[3] studies a detailed insight into the mechanism of charge separation in these systems has been obtained. Very recently the crystal structure of an integral membrane light-harvesting antenna complex (LH2) from the purple non-sulfur photosynthetic bacterium *Rhodopseudomonas acidphila* was solved.[4] LH2 consists of two concentric cylinders of helical protein subunits, which enclose pigment molecules, *viz.* eighteen bacteriochlorophyll *a* molecules, which form a continuous overlapping ring, and an additional nine bacteriochlorophylls which are perpendicular to this ring. These latter rings are very efficient in absorbing light energy, which in turn is passed -via other rings- to the special pair in the photosynthetic reaction center, where the initial electron transfer takes place.[5]

Although considerable progress has been made in solving the mechanism which plays a role in the photosynthetic reaction center, still a detailed understanding is lacking. Many model systems have been synthesized and their photochemical properties studied in order to get a better understanding.[6] These studies are mainly directed towards the charge separating electron transfer steps. Synthetic systems possessing covalently linked donor and acceptor sites have been designed and synthesized in order to get insight into the influence of distance and orientation between donor and acceptor upon the rate of electron transfer,[7] and on the influence of the driving force,[8] the temperature, and the solvent.[9] These investigations have led to systems which show relatively fast electron transfer over large distances. The charge recombination in all synthetic systems developed so far is very fast compared to the natural systems. The complicated structures of the chromophores and the surrounding proteins in nature are involved in the generation of the long lived charge separated state. Covalently linked synthetic models designed to mimic these structural influences are of course extremely difficult and time consuming to synthesize. Consequently, non-covalently linked systems have more recently been described in the literature as model systems for the study of electron transfer processes.[10] Although this supramolecular approach is novel, it is already very promising.

In this chapter we describe novel porphyrin systems (**1-3** see chart I) containing a cleft based on diphenylglycoluril which have been designed in order to study the effect of aromatic ring systems bound in the cleft on the electron transfer properties of the porphyrin. Molecule **2** is of special interest since it contains both a donor and an acceptor site and is able to bind aromatic guest molecules. Using this molecule we have been able to study the role in the electron transfer processes, of aromatic molecules intervening between the donor and the acceptor. In the biological systems aromatic side chains of amino acids are thought to enhance the electron transfer rate,[11] whereas their role in the life time of the charge separated state is not known. Our systems were designed and synthesized to study these problems.

7.2 RESULTS AND DISCUSSION

7.2.1 Synthesis

Compounds **1a**, **1e** and **3a** were synthesized by a condensation reaction of diamino clip **4b** with porphyrin-2,3-dione **5** (see Chapter 2) and porphyrin 2,3,7,8-tetraone **8**, respectively (Scheme 1). In the latter reaction two isomers were formed, *viz* the C-shaped and the S-shaped isomer, which could not be separated by chromatography.

After metallation to the zinc porphyrin, however, the two isomers could be separated by flash chromatography.

Chart I

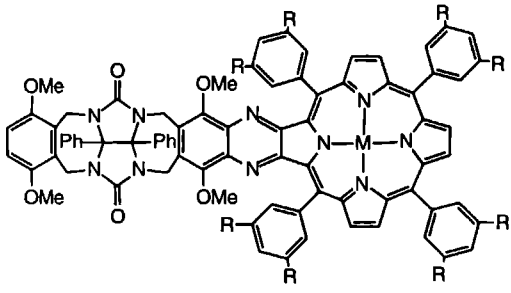

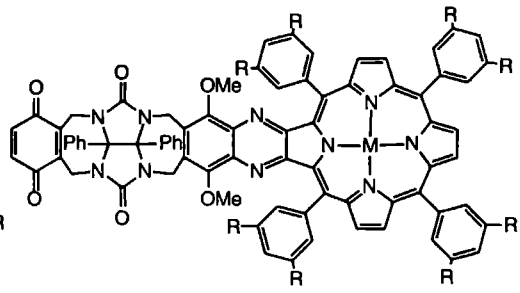

1a: R=H, M=2H
1b: R=H, M=Zn
1c: R=H, M=Cu
1d: R=H, M=Au

1e: R=^{t}Bu, M=2H
1f: R=^{t}Bu, M=Zn

2a: R=^{t}Bu, M=2H
2b: R=^{t}Bu, M=Zn

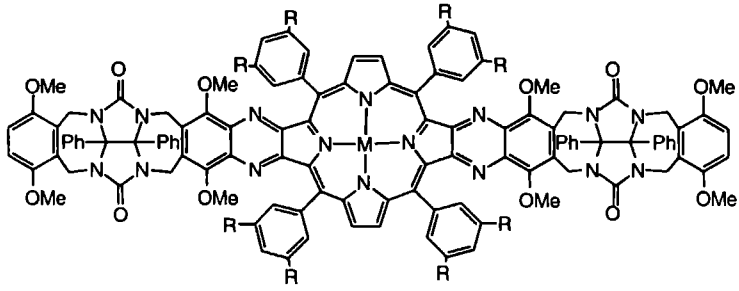

3a: R=^{t}Bu, M=2H
3b: R=^{t}Bu, M=Zn

The synthesis of **2** started from the dinitro half-clip **6**, which was described in Chapter 2. The second side-wall is a hydroquinone ring which was attached in the presence of *p*-toluenesulfonic acid in 1,2-dichloroethane. This hydroquinone ring was subsequently oxidized by bubbling air through a solution of the compound in DMSO/pyridine, which contained Cu_2Cl_2. After the reduction of the nitro groups with Pd/carbon and triethylammonium formiate in THF/MeOH, the condensation reaction with porphyrin-2,3-dione **5** was carried out. The yield of **2a** was 20% with respect to **7a**.

During the reduction of the nitro groups the benzoquinone ring was partly reduced to the hydroquinone and a new compound was also obtained. This compound (**9**) had a quinone-like side-wall, with double bonds between the side-wall and the methylene bridges. This same side reaction was also observed during the oxidation of the 1,4-

dimethoxybenzene/hydroquinone clip **10** (Scheme 2) yielding **12** as a side product. The two AX patterns observed in the ^1H NMR spectrum for the CH_2N protons, which are characteristic for a clip molecule with two different side-walls, were altered and now only one AX pattern and one singlet at low field (8.1 ppm) was observed. The latter signal had the intensity of two protons, and is due to the doubly bonded bridge between the diphenylglycoluril unit and the side-wall.

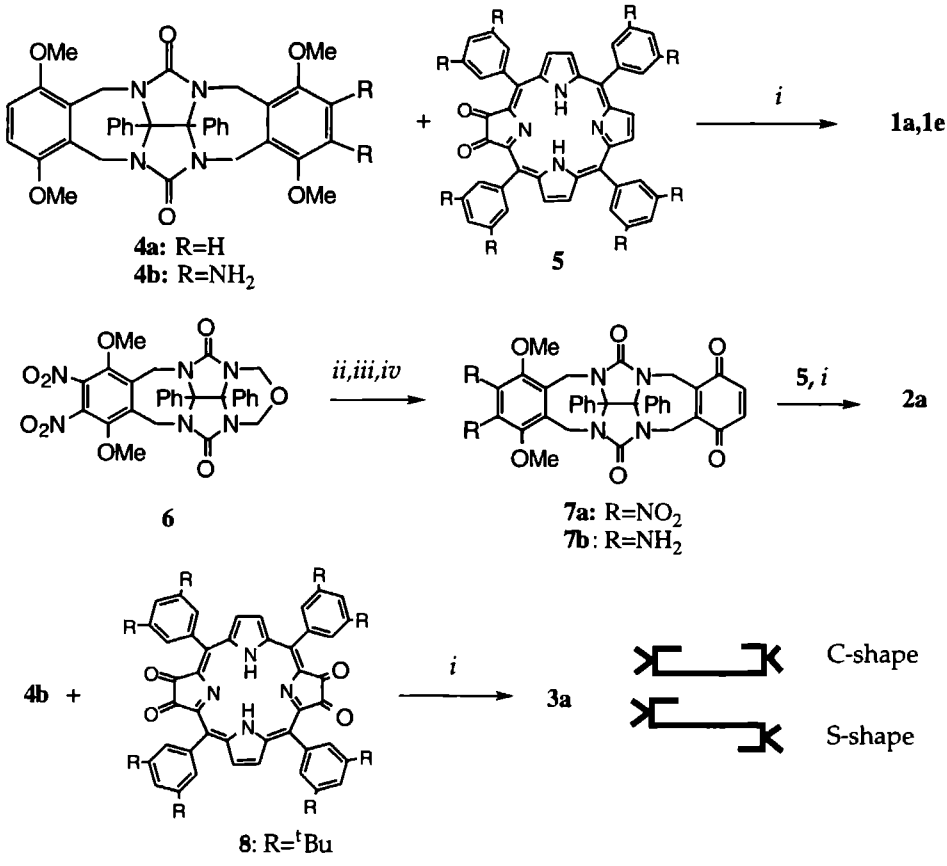

Scheme 1: *(i) Reflux over mol. sieves in CH_2Cl_2 under N_2; (ii) hydroquinone, p-toluenesulfonic acid, 1,2-dichloroethane, reflux over mol. sieves; (iii) Cu_2Cl_2, pyridine, DMSO, oxygen; (iv) Pd/C, TEAF, THF/MeOH (1:1, v/v).*

Metallation of the porphyrin ring to give the zinc derivative was carried out in boiling DMF/toluene by treatment with an excess of zinc acetate (90% yield). The copper metallated derivative **1c**, was synthesized by refluxing **1a** in DMF/toluene in the presence of an excess of $Cu(OAc)_2$. The gold porphyrin **1d**, was obtained after refluxing **1a** in acetic acid in the presence of $KAuCl_4$ and NaOAc for two days.

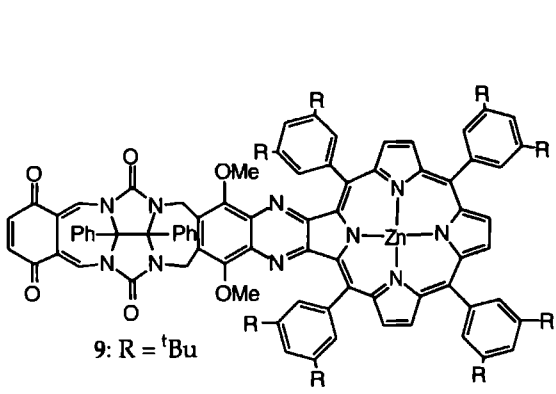

9: R = ^{t}Bu

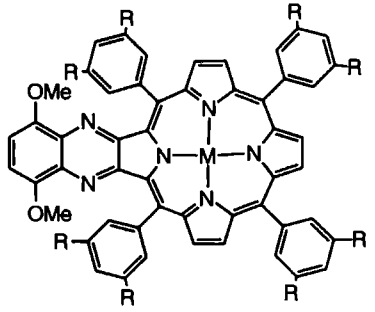

13a: R = ^{t}Bu M = 2H
13b: R = ^{t}Bu M = Zn

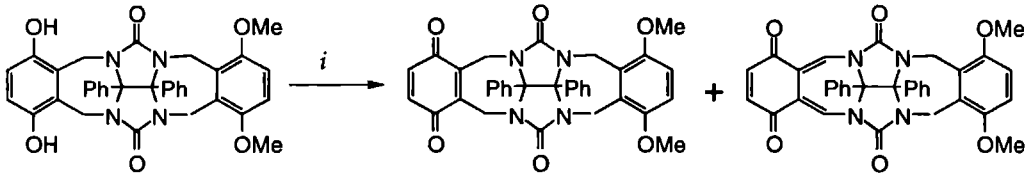

10 11 12

Scheme 2: *(i) Cu_2Cl_2, pyridine, DMSO, oxygen.*

Reference compounds **13a** and **13b** were synthesized in order to study the influence of the dimethoxyquinoxaline unit attached to the porphyrin upon the electronic properties of the latter ring. These derivatives were synthesized by a condensation reaction of 1,4-dimethoxy-2,3-diaminobenzene with **5**, yielding **13a** in 80%. The zinc compound **13b** was synthesized under the same conditions as mentioned above, giving **13b** in 95% yield.

7.2.2 Structures

Purple crystals of **1a** suitable for a X-ray structure analysis, were grown by slow diffusion of diethyl ether into a chloroform solution of this compound. The crystal structure of **1a** is monoclinic. The unit cell contains 4 clip-shaped molecules, which are packed in dimeric pairs perpendicular to each other. A drawing of a clip dimer is shown in Figure 1.

The diphenylglycoluril unit in the X-ray structure of **1a** is quite similar to that in the X-ray structure of **4a**.[12] The twist in the diphenylglycoluril framework of molecule **1a** is very small, unlike that observed in molecular clip **4a**. This is most clearly seen in the dihedral angle C21-C9-C9'-C21' (Figure 1), which is 5.5° as compared to 22° in clip **4a**. The methoxy groups of the 1,4-dimethoxybenzene side-wall point upwards in the

same way as in the crystal structure of **4a**, whereas the methoxy groups of the porphyrin wall point outwards

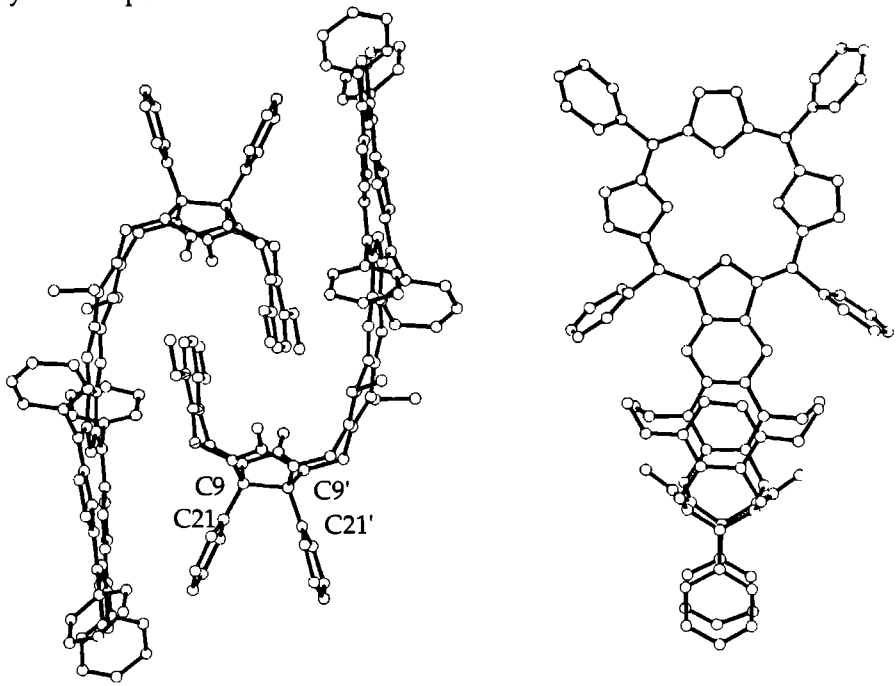

Figure 1 *X-ray structure of* ***1a*** *A side-view of the dimeric complex (left) and the front-view of the monomer are shown (right) Hydrogen atoms have been omitted for clarity*

The two dimethoxybenzene groups attached to the diphenylglycoluril unit define a tapering cleft, with a center-to-center distance of 6 28 Å The carbonyl groups make the same angle (37°) as in **4a** (39°), with the distances between the oxygen atoms of the carbonyl groups almost equal (5 58 Å, as compared to 5 52 Å in **4a**) The porphyrin wall of **1a** is non-planar and bends towards the cavity with an out of plane angle of 15°, resulting in the porphyrin unit and the opposite dimethoxybenzene wall being parallel This bending can be attributed to favourable stacking interactions between two molecules in the solid state (Figure 1) The dimethoxybenzene wall of one molecule occupies the cleft of its dimeric partner, forming a structure which is also found in other clip molecules in both solution and the solid state (Chapter 5) The large porphyrin wall wraps around the back of the diphenylglycoluril part of its partner, and interacts with a phenyl group on the convex side Although no crystals suitable for X-ray analysis could be grown from **2**, we expect that a single molecule of **2** will have approximately the same structure as a single molecule of **1a**, since the structures of **4a** and **11** were found to be similar (Chapter 5) The edge-to-edge distance

between the electron donor (zinc porphyrin) and the electron acceptor (benzoquinone) in **2** therefore will be approximately 6.5 Å, with a center-to-center distance of 9 Å.

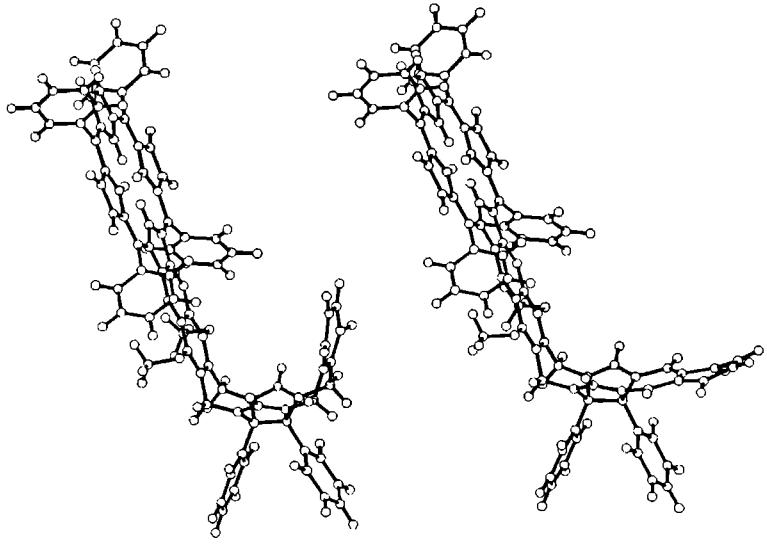

Figure 2: *Calculated structures (CHARMm force field) of* **2** *and* **9**. *t-Butyl groups have been omitted for clarity.*

Molecules **9** and **12**, which have a doubly bonded connection between the side-wall and the diphenylglycoluril frame work, are expected to have a different geometry than **1a** and **2**. The conformations of **2b** and **9** were derived from molecular mechanics calculations, performed using the CHARMm force field in the QUANTA modelling package.[13] The structure of **2b** was found to be very similar to the X-ray structure of **1a**, the main difference being the bent form of the porphyrin in the latter molecule. This bend is thought to be the result of the interactions between the two clip molecules in the dimeric structure of **1a** (*vide supra*). According to the calculations the doubly bonded connection in **9** results in a side-wall which is perpendicular to the other aromatic moiety, hence the molecule does not possess a cleft. The center-to-center distance between the porphyrin unit and the quinone-like moiety in **9** is 15 Å, and the planes make an angle of 101°.

As mentioned above the S-shaped and the C-shaped isomers of clip molecule **3b** could be separated by column chromatography. We were unable, unfortunately, to grow crystals suitable for X-ray diffraction of either the C-shaped or the S-shaped species. All spectroscopic data for the two structures were very similar. In order to distinguish between the two species, host-guest binding experiments were carried out by ^{1}H NMR.

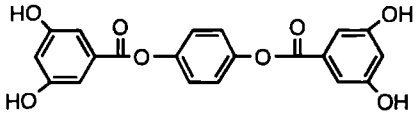

14

A dimeric resorcinol guest molecule (**14**),[14] which was insoluble in chloroform, was added to solutions of both the S-shaped and the C-shaped species and sonicated. One of the isomers was able to bind the guest very strongly and formed a complex which was soluble in chloroform. Large ^{1}H NMR shifts were observed for both the guest molecule and the host molecule, indicating that the former molecule was bound in the clefts of the latter. The other isomer was unable to increase the solubility of **14**, and no complex formation was observed by ^{1}H NMR. Molecular modelling calculations indicated that **14** fits nicely into the C-shaped structure of **3b**, forming hydrogen bonds with the two diphenylglycoluril parts of the molecule (Figure 3). From this calculation and the fact that clip molecule **1f** is unable to bind guest molecule **14** resulting in a soluble complex, we were able to distinguish between the two forms of **3b**. An experiment to confirm the shapes of the two structures, was carried out using the bulky *trans*-pyridyl-porphyrin **15**. This porphyrin molecule was added stepwise to a

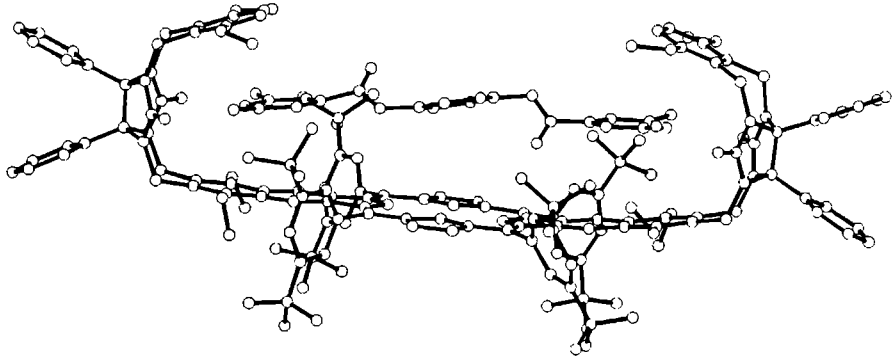

Figure 3: *Computer modelled structure of the complex between the C-shaped structure of* **3b** *and the guest* **14**.

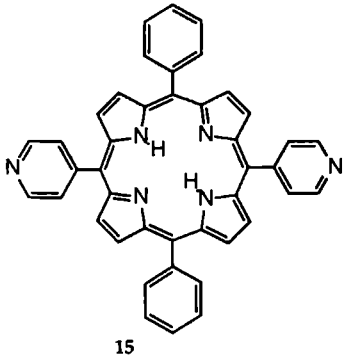

15

solution of the S-shaped isomer **3b** and to a solution of the C-shaped isomer **3b**. These additions were followed by ^{1}H NMR and UV-VIS spectroscopy. Upon the addition of **15** in both cases the Q-bands of the zinc-porphyrin **3b** shifted to the red, indicating that the pyridine ligands were complexed to the zinc.[15] This complexation was confirmed by ^{1}H NMR, since the signals of the zinc porphyrin shifted to lower field. When **15** was

complexed to the S-shaped isomer, a shift of the protons of the *p*-dimethoxybenzene side-walls of the latter molecule was observed, indicating that these protons were in the shielding zone of the complexed porphyrin ligand. In the complex with the C-shaped isomer, no shifts of the side-wall protons of **3b** were observed. In this case the complexation was at the outside of the molecule (Figure 4, right).

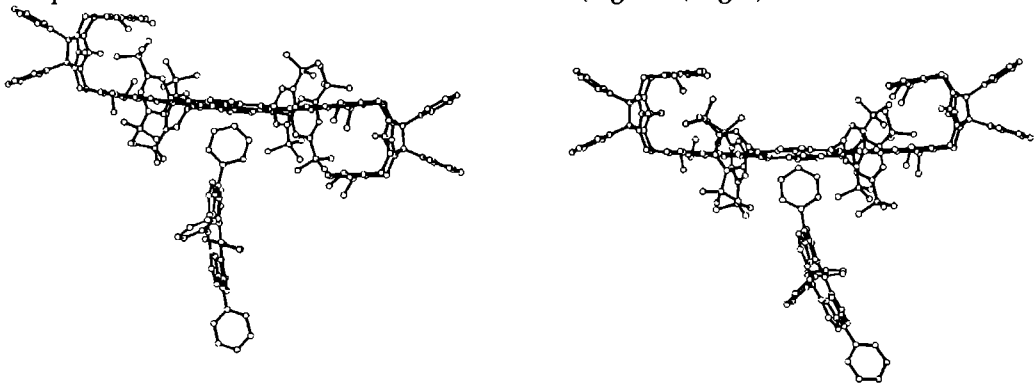

Figure 4: *Complexation of trans-bipyridyl-porphyrin* **15** *to the S-shaped isomer (left) and the C-shaped isomer (right) of* **3b**.

7.2.3 Binding properties

In Chapter 3 we showed that molecular clips of type **4a** bind dihydroxybenzene guests by hydrogen bonding with the carbonyl functions of the diphenylglycoluril unit and π-π stacking interactions with the aromatic walls of the clip (K_a resorcinol = 2600 M^{-1}). ^1H NMR titration experiments with **1a** and the guest 5-pentylresorcinol (olivetol) in $CDCl_3$ revealed that the latter molecule is bound weakly in the cleft of **1a** (K_a = 25 M^{-1}). The more electron poor guest, hexyl 3,5-dihydroxybenzoate, formed a stronger complex with host molecule **1a** (K_a = 120 M^{-1}). From the calculated complex induced shift values it followed that the guest was bound in an slightly off-center position between the xylylene walls of **1a**, as was found for complexes with other clip molecules. The complexation of dihydroxybenzenes in zinc porphyrin clip **1f** was somewhat stronger (hexyl 3,5-dihydroxybenzoate: K_a = 540 M^{-1}). This feature was also observed for other metal functionalized clip molecules (see Chapter 2). It is known that the incorporation of metals into porphyrins increases the π-π stacking interactions of the latter molecules.[15a] The binding constants were expected to be much larger in CCl_4 - which is the solvent used for the fluorescence studies (*vide infra*)- since in this solvent hydrogen bonding is stronger (estimated increase is 5 kJ/mol per hydrogen bond). Binding studies in CCl_4 using an external solvent as the lock signal and the reference, revealed that the association constant between hexyl 3,5-dihydroxybenzoate and **1f** is indeed much stronger (K_a = 2x10^3 M^{-1}). The binding affinities of **2** are

expected to be somewhat lower: on the basis of the difference between **4a** and **12** 3 kJ/mol. The geometry of the complex will be similar to that of the complex of **1f** *i.e.* the guest being located between the zinc porphyrin and the quinone function. This host-guest complex, therefore, was felt to be an interesting model for studying the influence of an intervening aromatic molecule upon the electron transfer process between a porphyrin donor and a quinone acceptor (*vide infra*).

7.2.4 Self-association

As shown in Chapter 5, some clip molecules are able to dimerize in solution. The porphyrin functionalized molecules also formed dimers in solution, with a geometry similar to that found in the X-ray structure of **1a**. Upon diluting a concentrated solution of **1a** in $CDCl_3$ the signals of the aromatic walls in the ^1H NMR spectrum shifted downfield, indicating that the dimeric complex of **1a** dissociated. The shifts were not large enough for a self-association constant to be calculated. The metal functionalized porphyrin clip molecules, as expected, showed a stronger self-association behaviour, probably due to a decrease in electron density on the porphyrin side-wall. As was found for the binding of dihydroxybenzene guest molecules, a decrease in electron density and hence a decrease in electrostatic repulsion between aromatic rings leads to higher association constants. In the case of molecular clips **1b**, **1d** and **1f** the shifts were large enough to calculate the self association constant: K_{as} = 18 M^{-1} for **1b** and **1f**, and K_{as} = 12 M^{-1} for **1d**.

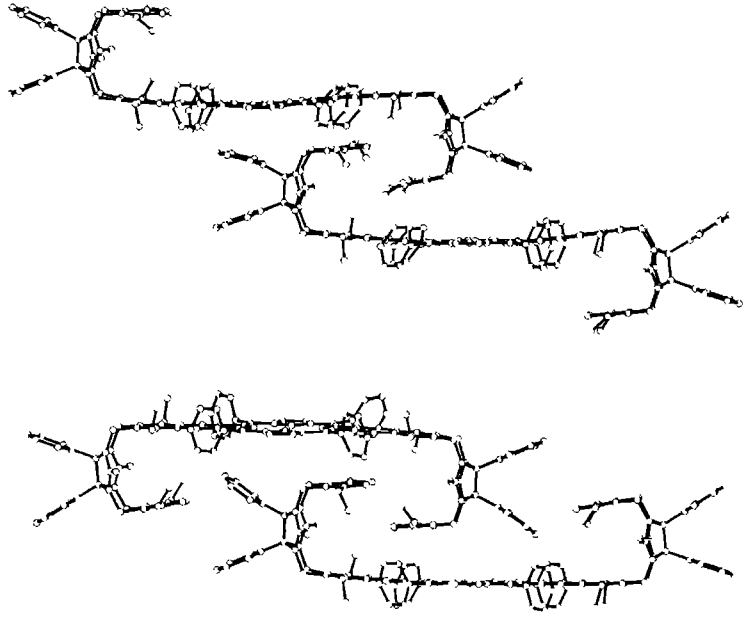

Figure 5: *Structure of the dimers of the C-shaped (under) and S-shaped (above) isomers of* ***3b****.*

The *p*-dimethoxybenzene side-wall and the methylene bridges to which the porphyrin ring is attached, showed -together with the methoxy groups- the largest shifts upon dilution, indicating that the dimeric complex had a similar geometry to that in the crystal structure (Figure 1). The self-assocation of **1d** was measured at various temperatures. At lower temperatures the dimeric complex was found to be more stable, indicating that the process of dimerization is enthalpy driven (a similar observation was made for clip molecules which were monofunctionalized with a phenanthroline ring, see Chapter 5). At very low temperatures larger aggregates were formed in CCl_4. For instance, the UV-VIS spectra of **1f** broadend upon cooling the solution to -200°C, to such an extent that no Q-bands could be distinguished. At room temperature the spectrum very slowly (±15 min) returned to the normal spectrum. The fluorescence intensity also decreased when larger aggregates were formed, *i.e.* at low temperature.

^{1}H NMR dilution studies of the S-shaped isomer of **3b** revealed that this molecule formed dimers as well, however, the observed shifts were small suggesting that the strength of the dimeric complex was also small. This is probably due to the steric hindrance caused by the phenyl groups on the porphyrin ring. The ^{1}H NMR signals of the C-shaped isomer of **3b** not only shifted upon an increase in concentration, but also broadend. This suggests that the rate of exchange between the monomeric and dimeric species is slow. The higher energy barrier in the case of the dimerization of the C-shaped isomer of **3b** is not unexpected since in the dimer the molecules fit tightly together, and two large surfaces have to be solvated upon breaking apart. In Figure 5 the dimeric species of both S- and C-shaped isomers of **3b** are shown. The dimer of S-shaped **3b** is of interest because it has two clefts which can further interact with other molecules of **3b** to form a long chain of organized porphyrins. Preliminary studies on the aggregation behaviour of the two isomeric forms of **3b**, revealed that they self-assemble upon evaporation of a chloroform solution to give ring-shaped structures.[16] From a mixture of chloroform/methanol, block-shaped aggregates were formed. A detailed study, however, is necessary to get insight into how these aggregates are constructed.

Upon diluting a concentrated solution of the reference compound **13b**, no ^{1}H NMR shifts were observed, indicating that this compound does not self-associate, besides the normal aggregation behaviour known for porphyrin molecules.[15] The propensity of our porphyrin containing clip molecules to self-associate, makes them ideal models for studying tandem electron transfer and tandem energy transfer processes.

7.2.5 Electrochemistry

In order to investigate the redox properties of porphyrin clip molecules **1** and **2** cyclic voltammetry (CV) and differential pulse voltammetry (DPV) measurements were carried out. In Table 1 the reduction potentials of the different porphyrins are given. All first reductions of the porphyrin π-systems were reversible or nearly reversible,

Table 1. *Halfwave potentials (from CV and DPV) for the reduction and oxidation of different porphyrin clip molecules in dichloromethane.* [a]

	Reduction potentials		Oxidation potentials	
Porphyrin	$E_{1/2}$ (V)	ΔEp (mV)	$E_{1/2}$ (V)	ΔEp (mV)
1a	-1.61	60	0.40	62
	-1.79	63		
1b	-1.69	42	0.30	70
	-2.02	69		
1c	-1.62	52	0.52	70
	-2.00	54		
1d	-0.91	66	-	-
	-1.44	57		
1e	-1.67	70	0.42	56
	-1.86	80		
1f	-1.78	70	0.30	76
	-2.04	90	0.56	80
1f + guest			0.29	80
			0.58	125
13a	-1.67	70		
	-1.86	80		
13b	-1.75	65		
	-2.04	70		
Porphyrin-quinone				
2b	-0.93[b]	74	0.30	68
	-1.77	70	0.56	98
	-2.06			
2b + guest	-0.78[b]	-	0.28	69
9	-1.45[b]	55	0.32	73
			0.57	107

[a] Measured in CH_2Cl_2 with 0.1 M tetrabutylammonium hexafluorophosphate (TBAH) as supporting electrolyte. A Pt working electrode, a Pt auxiliary electrode and a Ag/AgI (0.1 M^{-1} TBAH, 0.02 TBAI) were used. Potentials are reported vs. Fc/Fc^+ in CH_2Cl_2. [b]These values are for the quinone side-wall

except the reduction of the π-system of porphyrin clip **2**. This, however, is due to the quasi-reversible reduction of the quinone unit of the molecule (*vide infra*), which leads to absorption on the electrode.[17] As expected, metallation of the porphyrin

resulted in a change in the reduction potential. The second reduction of **1b** and **1c** is shifted approximately 200 mV to lower potential. The charged Au(III) porphyrin clip **1d** displayed a reduction at higher potential -0.91 V (vs Fc/Fc^+), which is comparable with the reduction potential of quinone (-0.93 V). This Au(III) porphyrin, therefore, can be used as an electron acceptor in electron transfer processes.

More important with respect to the photoinduced electron transfer processes presented below, are the oxidation potentials of the electron donating group (zinc porphyrin) and the reduction potential of the electron accepting group (quinone) (see Table 1). The first oxidation potentials of the zinc porphyrins in **1b**, **1f**, **2b**, and **9** were all reversible and at approximately 0.3 V vs Fc/Fc^+, which is similar to potentials found for comparable systems in the literature.[15] The free base and the copper porphyrins were somewhat harder to oxidize than the zinc porphyrin molecules (0.4 and 0.5 V respectively). No oxidation of the gold porphyrin **1d** was observed. The reduction of the quinone group of clip **2b** occurred at -0.93 V and was quasi-reversible. The latter was confirmed by scan rate studies. It is known that quinone groups can polymerize and interact with the electrode.[17]

The presence of an excess of hexyl 3,5-dihydroxybenzoate guest had a small influence on the oxidation potential of **1f** and **2b**. The reduction of the quinone group of **2b**, was found to be shifted 0.2 V to higher potential. The reduction was now chemically irreversible, resulting in a small re-oxidation current. The reduction of the quinone like side-wall in **9** was observed at -1.45 V (vs Fc/Fc^+), and found also to be quasi-reversible. This group is harder to reduce than to the quinone unit in **2b**, and hence is not as good an electron acceptor as the quinone side-wall.

7.2.6 Steady-state absorption spectroscopy

The conjugated quinoxaline group attached to the porphyrin units induces a symmetry element which is different from normal tetraphenyl porphyrin (TPP) resulting in somewhat deviating absorption spectra for our compounds. In the case of the free base porphyrins **1a**, **1e**, **2a**, and **13a** a large Soret band at approximately 440 nm was observed, as well as two Q-bands at 530 and 600 nm, and two very small Q-bands at 568 and 650 nm. The zinc porphyrin molecules **1a**, **1f**, **2b**, **9** and **13b** showed a broad solvent dependent Soret band with one or two maxima between 420 and the 450 nm, two larger Q-bands at 570 and 612 nm, and a small Q-band at 530 nm (see Figure 6A). The porphyrin unit in **3**, has a different symmetry and hence a different absorption spectrum. For the free base porphyrin **3a** the Soret band was observed at 463 nm, and the Q-bands (in decreasing intensities) at 540, 619 and 673 nm. The zinc porphyrin in **3b** gave absorption bands at 475 nm (Soret band), and at 661 nm and in addition to this

some small bands at 560, 586, 610 and 630 nm (Q-bands), similar to the pattern seen for Chlorins.[15]

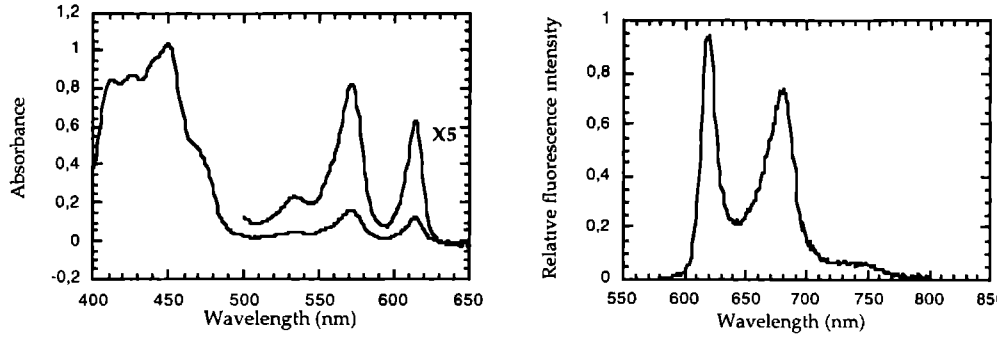

A B

Figure 6: *Typical absorption (A) and emission spectra (B) of zinc porphyrins to which the conjugated quinoxaline unit is attached.*

7.2.7 Steady-state fluorescence spectroscopy

A typical emission spectrum of a zinc porphyrin with an attached conjugated quinoxaline unit, is shown in Figure 6B. Two maxima are observed at 620 and 680 nm. Comparison of the fluorescence quantum yields of the different zinc porphyrin molecules can provide information about additional processes involved in the decay of the excited state, *i.e.* photoinduced electron transfer.

Table 2. *Fluorescence quantum yields of different porphyrins measured in various chlorinated solvents.* [a]

Porphyrin	CH_2Cl_2	$CHCl_3$	CCl_4
1b	0.016	0.016	0.022
1f	0.016	0.016	0.020
2b	0.002	0.002	0.020
13b	0.024	-	0.024
Zn(TPP)	0.025	-	0.025

[a] Excitation wavelength 572 nm.

In CCl_4 the quantum yields of **1b**, **1f**, **2b**, and **13b** were comparable to those observed for Zn(TTP) (Table 2). In the more polar solvents CH_2Cl_2 and $CHCl_3$ the fluorescence quantum yield of **2b** was approximately 10 times lower than that for the other molecules, e.g. reference compound **13b**. This suggests that in these more polar

solvents electron transfer occurs from the excited state of the zinc porphyrin to the quinone side-wall.

Table 3. *Fluorescence quantum yields of different porphyrins measured in various non-chlorinated solvents.*[a]

		1f		2b	
Solvent	ε	Φ_f	λ_{em} (max)	Φ_f	λ_{em} (max)
c-hexane	2.03	0.020	615 nm	0.018	616 nm
hexane	2.05	0.018	615 nm	0.013	616 nm
diethyl-ether	4.20	0.012	624 nm	0.004	624 nm
THF	7.58	0.018	625 nm	0.004	625 nm
dibutyl-ether	3.10	0.016	626 nm	0.004	625 nm
acetonitrile	37.50	0.0052	635 nm	0.001	633 nm

[a] Excitation wavelength 572 nm.

The quantum yields of **1f** and **2b** were also measured in a series of non-chlorinated solvents (Table 3). Again the quantum yields were very dependent upon the dielectric constant of the solvent, indicating that in the more polar solvents the fluorescence of **2b** is quenched by a photoinduced electron transfer process. For both molecules the maxima of the emission wavelengths changed to longer wavelength as the solvent polarity increased. The excited states of these molecules are stabilized by more polar solvents, which suggests that this state has a larger dipole moment than the ground state.

7.2.8 Time resolved fluorescence spectroscopy

Time-resolved, single photon counting (SPC) fluorescence studies were carried out on **1b**, **1f**, **2b** and **13b** in CH_2Cl_2 and CCl_4 (Figure 7). Global analysis of the curves of **1b**, **1f** and **13b** measured at different emission wavelengths, revealed that the fluorescence decay of these compounds is bi-exponential (Table 4). The decay times in CH_2Cl_2 are shorter (80 %) than those in the apolar solvent CCl_4 which is in agreement with the observed decreases in quantum yields. The decay times calculated for **1b**, **1f**, and **13b** are rather similar, indicating that the radiative rate constants remain fairly constant for these compounds. These values are similar to those found for other zinc porphyrin systems.[18] Compound **2b**, which has an acceptor side-wall, showed a tri-exponential decay pattern. Two of the calculated decay times were similar to those measured for the other compounds. The third very short decay time (52 ps), was the largest component (90%) in the more polar CH_2Cl_2 solvent. This again is in agreement with the observed decrease in quantum yield of **2b** going from CCl_4 to CH_2Cl_2, and is ascribed to a photoinduced electron transfer.

Table 4. *Fluorescence decay times calculated from the measured SPC spectra of different porphyrins in various chlorinated solvents.*[a]

	Decay time	
Porphyrin	CH_2Cl_2 (ns)	CCl_4 (ns)
1b	0.81; 1.15	-
1f	0.89; 1.44	0.99; 2.0
2b	0.052; 0.78; 1.47	0.21; 1.2; 2.8
13b	0.98; 1.45	-

[a] Calculated using global analysis; excitation wavelength 568 nm, detection 620, 640, 660, 680 nm.

The fluorescence decay curves of **1b**, **1f** and **13b** were expected to be mono-exponential, however, they appeared to be bi-exponential. Each contributing exponent had a large component in the decay curve (70% and 30% for **1f** in CH_2Cl_2), indicating that the bi-exponential behaviour is not due to impurities. Compounds studied in the literature having similar conjugated quinoxaline bridges, showed only mono-exponential decays.[19] These literature compounds, however, did not have methoxy groups on their quinoxaline units, as our molecules have. This difference may indicate that the methoxy groups in our molecules are responsible for the process being bi-exponential. The red shift in the emission spectra, observed in the more polar solvents, suggests that the excited state has a larger dipole moment than the ground state. The methoxy groups can have their dipole moments either in the same direction or in opposite direction to the dipole of the excited state. This canceling or enhancement of dipoles might be the origin of the bi-exponential behaviour.

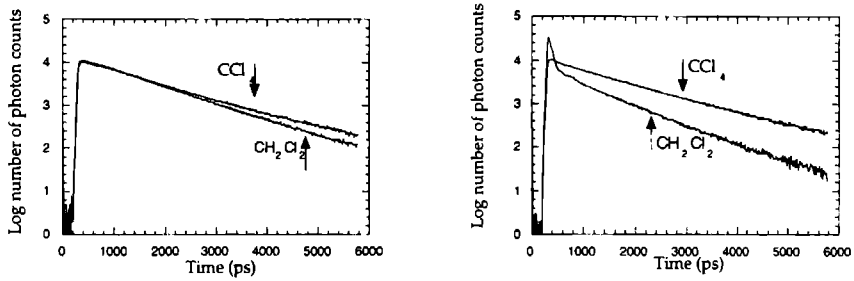

Figure 7: *Fluorescence decay curves, as measured by picosecond time correlated single photon counting, for* ***1f*** *(left) and* ***2b*** *(right) in* CH_2Cl_2 *and* CCl_4. *Excitation 568 nm, detection at 640 nm; channel time is 11.3 ps.*

7.2.9 Transient absorption spectroscopy.

Transient absorption spectroscopy, which gives information about the absorption spectrum of the excited state of the molecules, was carried out for the porphyrin molecules **1f, 2b , 9** and **13b** in hexane and acetonitrile. In hexane all the spectra were similar, having maxima around 500 and 600 nm (Table 5). These maxima are due to triplet-triplet (T(1)-T(n)) absorptions. The exact maximum of the absorption bands can not be determined due to groundstate depletion (Figure 8), however, the spectra are similar to other Zn porphyrin containing systems.[18,10k] In the more polar solvent acetonitrile, the absorption maxima were red shifted (Table 5), indicating that the excited triplet state (T(n)) is more polar than T(1). For clip molecule **2b** no transient absorption was observed in acetonitrile, indicating that the electron transfer process in this solvent occurs in preference to the triplet formation. This is in line with the low fluorescence quantum yields observed in the more polar solvents, and the SPC measurements. According to the latter, the fluorescence decay time was only 52 ps, whereas the transient absorption was measured after 100 ns. The rapid electron transfer results in a charge separated state in which radical ions are formed. The transient absorption measurements were unable to detect these radical ions, suggesting that the charge recombination process is faster than 100 ns.

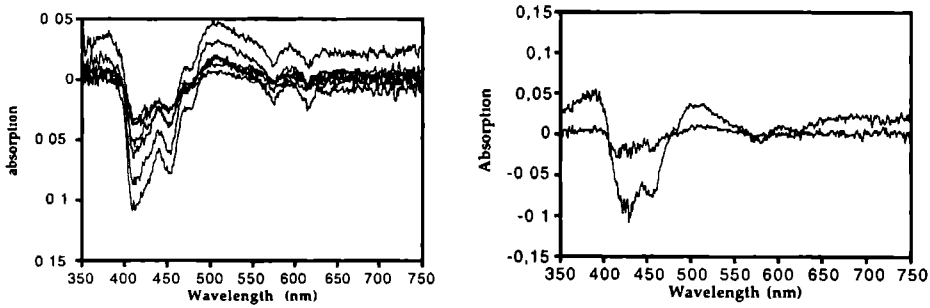

Figure 8· *Transient absorption spectra of compound 9 (left) and 2b (right) in hexane, measured 100 ns after excitation (400 nm)*

Due to the low solubility and photo-instability of our compounds and because of the low intensity of the laser at the measured wavelength no quantitative conclusions about the triplet lifetimes can be made. Some trends, however, were observed The triplet lifetimes of **1f** and **9** were longer in the more apolar solvent hexane. In contrast

to data for the reference compound **13b**, the triplet lifetime was longer in the more polar solvent acetonitrile. The reason for this different behaviour is unclear.

Table 5. *Maxima observed with transient absorption spectroscopy.*[a]

Porphyrin	Hexane	Acetonitrile
1f	509; 428[b]	513; 602; 433[b]
2b	508; 602; 428[b]	none
9	508; 593; 411[b]	513; 602; 445[b]
13b	490; 589; 440[b]	503; 601; 442[b]

[a]Excitation wavelength 400 nm; absorption measured 100 ns after excitation.
[b]Groundstate depletion.

7.2.10 Photoinduced charge separation

Within the framework of the Marcus theory,[20] the energy barrier $\Delta G^{\#}$ for electron transfer can be expressed by equation (2):

$$\Delta G^{\#} = (\Delta G^{\circ} + \lambda)^2 / 4\lambda \qquad (2)$$

where ΔG° is the driving force and λ is the overall reorganization energy. The driving force for photoinduced electron transfer ΔG° can be calculated using equation (3):

$$\Delta G^{\circ} = e[E_{OX} - E_{RED}] - E_S - (e^2/4\pi\varepsilon_s\varepsilon_0 R_{cc}) = e[E_{OX} - E_{RED}] - E_S - (14.4/\varepsilon_s R_{cc}) \qquad (3)$$

where E_{OX} refers to the redox potential for one-electron oxidation of the Zn porphyrin (0.30 V vs Fc/Fc^+ for **2b**), E_{RED} refers to the redox potential for one-electron reduction of the quinone (-0.93 V vs Fc/Fc^+ for **2b**), E_S is the singlet excitation energy of the porphyrin unit (2.18 eV for **2b**), and R_{cc} is the center-to-center distance between the porphyrin and the quinone. When the distance is large and/or the solvent is polar the last term of equation (3) equals zero. In the case of **2b**, however, the distance is 9Å which means that the driving force for the electron transfer will be solvent dependent. The reorganization energy λ for similar systems has been estimated to be as large as 0.9-1 eV.[7a,19] Assuming a similar reorganization energy in our systems we can calculate the driving force and estimate the energy barrier for electron transfer in **2b** in the different solvents (Table 6). It is clear from Table 6 that there is a significant barrier to the electron transfer process in the apolar solvents CCl_4 and hexane. In these apolar solvents indeed no photoinduced electron transfer occurred, as was concluded from the fluorescence quantum yields, the SPC data and the transient absorption measurements. In the more polar solvents, however, photoinduced electron transfer was observed for **2b**.

The calculated driving force for photoinduced electron transfer in molecule **9** (-0 41 eV, using eq. 3), indicates that for this molecule in polar solvents rather high energy barriers (0 09 eV) are expected In agreement with theory, no electron transfer processes were observed for this molecule

Table 6 *Calculated driving force and estimated energy barrier for photoinduced electron transfer in* ***2b***

Solvent	$\Delta G°$ (eV)	$\Delta G^{\#}$ (eV)
CCl_4	-1 81	0 16
$CHCl_3$	-1 28	0 02
CH_2Cl_2	-1 13	0 004
hexane	-1 75	0 14
ether	-1 33	0 03
THF	-1 16	0 006
acetonitrile	-0 95	0 0006

7.2.11 Influence of guest molecules on the electron transfer

We showed (*vide supra*) that dihydroxybenzene guest molecules can be bound in the cleft of molecules **1** and **2** The addition of hexyl 3,5-dihydroxybenzoate or olivetol to a solution of **2b** in CCl_4, resulted in a decrease in fluorescence intensity (Figure 9) This

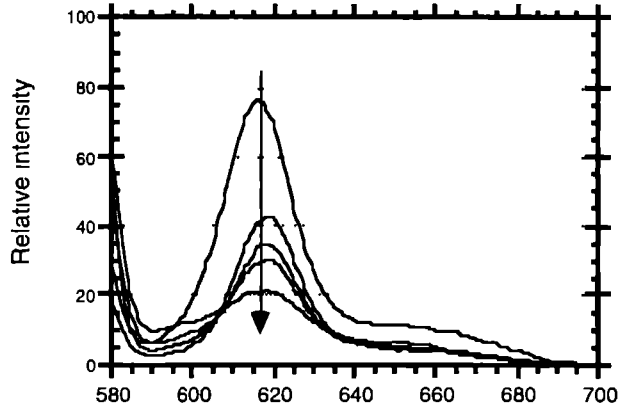

Figure 9 *Fluorescence intensity of* ***2b*** *as a function of the guest concentration measured in CCl_4 Excitation wavelength 570 nm*

decrease in fluorescence intensity was not observed for either Zn(TPP), **1f** or **13b** (Table 7), and hence is likely to be the result of a photoinduced electron transfer process SPC

time resolved fluorescence measurements suggest that the electron transfer between the porphyrin and the quinone became faster than 3 ps when an aromatic guest was bound between the donor and the acceptor. The addition of hexyl 3,5-dihydroxybenzoate to a CCl_4 solution of **1f** resulted in the appearance of an extra emission band, indicating that the emission process was altered by the binding of the guest molecule. This emission is ascribed to an exciplex (excited complex) between the bound guest molecule and the porphyrin in **1f**. SPC measurements revealed that the

Table 7. *Fluorescence quantum yields of different porphyrins measured in CCl_4 in the presence of a guest molecule.*[a]

Porphyrin	CCl_4	CCl_4 +guest[b]
1f	0.020	red-shift[c]
2b	0.020	0.004
13b	0.024	0.024
Zn(TPP)	0.025	0.025

[a] Excitation wavelength 572 nm.[b] Addition of an excess of hexyl 3,5dihydroxybenzoate.[c] An additional emission band appeared at 680 nm.

fluorescence decay curve of the exciplex was mono-exponential with a calculated lifetime (1.75 ns) similar to that of the free **1f**. This result is in line with the idea that the bi-exponential behaviour of our clip porphyrins is due to the orientation of the methoxy groups: when a guest molecule is bound these methoxy groups are all pointing outwards, leading to one type of excited state.

The significant enhancement of the electron transfer upon complexation of a guest molecule, is of great interest since in the photosynthetic reaction center intervening aromatic residues are thought to play a role in the electron transfer process.[11] Studies on a variety of covalently linked donor acceptor systems, which were shown to have through bond electron transfer, have supported this suggestion of aromatic mediation.[18] It was suggested that a super exchange mechanism was responsible for the enhancement in electron transfer. Recently, a super exchange pathway was also suggested for the solvent mediated electron transfer in a donor-acceptor system.[21] This solvent mediated transfer can be seen as a non-covalent way of coupling the two components. In our case the aromatic guest is selectively bound in between the donor and the acceptor. It is of course of interest to know the mechanism of the electron transfer process when the guest molecule is bound between the porphyrin and the quinone. Is the electron transferred via an exchange mechanism, or is the bound guest molecule just creating a local polarity effect which enhances the electron transfer? From our CV measurements, it is clear that the guest molecule changes the redox

potentials of both the donor and the acceptor species, and hence the driving force is also modified. In CCl_4 this would result in a driving force of -1.98 eV, and in polar solvents of -1.12 eV. It is not likely that the guest molecule changes the local polarity to such an extent that this driving force is approximately -1.12 eV. We believe, therefore, that the electron transfer enhancement is partly due to an exchange mechanism. The exciplex formed between the aromatic guest molecule and the porphyrin unit of **1f**, also suggests that an exchange mechanism is likely.

7.3 CONCLUSIONS

A series of novel porphyrin containing clip molecules has been synthesized and characterized. These molecules contain a binding site for dihydroxybenzene guest molecules nearby a porphyrin ring. Besides the binding of guests, these molecules are able to form dimers in solution and in the solid state. Although the self-association constants of these molecules are low, the observed type of dimeric complex is of interest for the study of tandem electron and energy transfer processes. Clip molecule **2** is of great interest for studying electron transfer reactions, since in this molecule the binding site for dihydroxybenzene guests is located exactly between a donor and an acceptor group. The photoinduced electron transfer from the zinc porphyrin in **2** to the quinone site, appears to be dependent on the solvent polarity. In CCl_4 and hexane no photoinduced electron transfer is observed. In CH_2Cl_2 a fluorescence decay time of 52 ps was measured by SPC experiments. This short lifetime is the result of photoinduced electron transfer from the zinc porphyrin to the quinone unit which is even faster when an aromatic guest molecule is bound between the donor and the acceptor group (fluorescence decay time less than 3 ps). This enhancement may be due to a change in local polarity induced by the bound guest or, more likely, by the aromatic guest acting as a mediator between the donor and the acceptor. More detailed photophysical studies on this host-guest system and the design of new host-guest systems displaying photoinduced electron transfer which is independent of the solvent polarity, are planned in the future in order to obtain a more detailed insight into the influence of bound aromatic guest molecules on the mechanism of electron transfer.

7.4 EXPERIMENTAL SECTION

7.4.1 General

Triethylammonium formate was distilled prior to use. THF and diethyl ether were distilled under nitrogen from sodium benzophenone ketyl. Dichloromethane and chloroform were distilled from $CaCl_2$. All other solvents and chemicals were

commercial materials and used as received. For column chromatography Merck Silica Gel (60H) was used and for thin layer chromatography Merck Silica Gel F_{254} plates. IR spectra were recorded on a Perkin Elmer FTIR 1720-Xspectrometer. ^1H NMR spectra were recorded on Bruker WH-90, Bruker WM-200, and Bruker AM-400 instruments. Chemical shifts (∂) are reported in ppm downfield from internal $(CH_3)_4Si$ (∂ = 0.00 ppm). Abbreviations used are s = singlet, d = doublet, m = multiplet, br = broad. FAB-MS spectra were recorded on a VG 7070E instrument, the matrix used was *m*-nitrobenzyl alcohol. FAB High Resolution Mass Spectroscopy (HRMS) was carried out using a JEOL JMS SX/SX102A four-sector mass spectrometer, coupled to a JEOL MS-MP7000 data system. The samples were loaded in a matrix solution onto a stainless steel probe and bombarded with xenon atoms with an energy of 3 KeV. During the high resolution FAB-MS measurements a resolving power of 10.000 (10% valley definition) was used. Cesium iodide and/or glycerol was used to calibrate the mass spectrometer.

7.4.2 Physical measurements

Cyclic Voltammetry (CV) and Differential Pulse Voltammetry (DPV) measurements were performed using an EG&G Princeton Applied Research Model 273 Galvanostat/Potentiostat and a PAR Model 173 potentiostat equipped with a PAR model 176 I/E converter coupled to a PAR Model 175 universal programmer. A conventional three-electrode cell, with Pt working and auxiliary electrodes and 0.1 M TBAH electrolyte was used. A Ag/AgI reference electrode was employed. Absorption spectra were recorded on a Perkin Elmer Lambda 6 UV/VIS and a Perkin Elmer Lambda 5 UV/VIS spectrometer. Fluorescence measurements were performed using a Perkin-Elmer luminescence spectrometer LS50B and a SPEX Fluorolog spectrofluorimeter. The 1.00 cm quartz cuvette was placed in a thermostated cuvette holder. Time-resolved fluorescence decay traces were obtained by excitation at 568 nm using a pyromethane dye laser, pumped by a beam locked argon ion laser at 514 nm, with a repetition frequency of 800 kHz. The fluorescence photons were detected by a multichannel plate (Hamamatsu R2809 U). Erythrosine in methanol was used as reference compound. Each decay trace had about 10000 counts in the peak channel and in all the experiments the total number of channels was 511. The decay parameters were recovered using a global analysis fitting program. The transient absorption spectra were recorded using the output of a dye laser (640 nm) which was mixed with the fundamental of a DCR3 Nd-YAG (Spectra Physics) laser in a WEX wavelength extender (Spectra Physics), in order to obtain 4 ns laser pulses at 400 nm. The analysing light was provided by a 450 W Xenon arc lamp (Müller-Elektronik-Optik) which could be pulsed (Pulseinheit MSP 05 Müller-Elektronik-Optik) to deliver an intense

analyzing beam. The spectra of the generated transients were analyzed from 350 nm up to 750 nm using an OMA III system (EG&G Instruments) capable of delivering high voltage pulses with pulse widths varying between 100 ns and 10 ms. The experimental set-up was controlled by the OMA console which delivered the output trigger pulses to a detector scan controller (model 1463 EG&G). A digital Delay Generator (model 9650 EG&G) equipped with a time base stability option was used to control the relative delays of the different trigger signals. For all experiments the detector was cooled to -5 °C. In order to increase the signal to noise ratio the signals were averaged 20 times.

7.4.3 Compounds

Compounds **1a, 1e, 4** and **6** were synthesized as described in Chapter 2. Porphyrin-2,3-dione **5** and porphyrin-2,3,7,8-tetraone **8** were kindly provided by Prof. M. J. Crossley.[22] All reactions with porphyrins were carried out under nitrogen atmosphere and with the reactions flasks covered with aluminium foil. The pyridine containing porphyrins used to determine the structure of **3b**, were synthesized as described in ref 15b.

Zn-porphyrin clip 1b: A mixture of 47 mg (0.037 mmol) of **1a** and an excess of $Zn(OAc)_2$ (50 mg) in 2 mL of toluene was refluxed for 16 hrs. After cooling 15 mL of toluene was added and the solution was washed with water (3x), with 5% Na_2CO_3 solution (2x) and again with water. The organic solution was evaporated to dryness and the green solid was purified by column chromatography (CH_2Cl_2/MeOH, 98:2 v/v) yielding 40 mg of **1b** (80%); Mp: >310 °C; ^1H NMR ($CDCl_3$) ∂ 8.89 and 8.54 (ABq, 4H, *J* = 5 Hz, ß pyrrolic H), 8.75 (s, 2H, ß pyrrolic H), 8.20-8.0 (m, 8H, 2,6-ArH porphyrin), 7.81-7.72 (m, 12H, 3,5-Ar H4-ArH porphyrin), 7.15 (s, 5 H, ArH diphenylglycoluril), 7.14 (s, 5H, ArH diphenylglycoluril), 6.62 (s, 2H, ArH), 5.92 and 3.98 (ABq, 4H, *J* = 15.8 Hz, NC*H*HAr), 5.56 and 3.82 (ABq, 4H, *J* = 15.8 Hz, NC*H*HAr) 3.86 (s, 6H, OMe) 3.72 (s, 6H, OMe); UV-vis ($CHCl_3$) λ/nm: 408, 447, 530, 570, 612; FAB-MS (*m*-nitrobenzylalcohol) *m/z* 1321 $(M+H)^+$.

Cu-porphyrin clip 1c: A mixture of 40 mg (0.032 mmol) of **1a** and an excess of $Cu(OAc)_2$ (50 mg) in 2 mL of toluene and 1 mL of DMF was refluxed for 16 hrs. After cooling 25 mL of toluene was added and the solution was washed with water (3x), with 5% Na_2CO_3 solution (2x) and again with water. The organic solution was evaporated to dryness and the green solid was purified by column chromatography (CH_2Cl_2/MeOH, 99:1 v/v) yielding 38 mg of **1c** (90%); Mp: >310 °C; UV-vis (CH_2Cl_2) λ/nm: 411, 446, 532, 564, 608; FAB-MS (*m*-nitrobenzylalcohol) *m/z* 1318 $(M+H)^+$.

Au-porphyrin clip 1d: A mixture of 40 mg (0.032 mmol) of **1a**, 30 mg (0.080 mmol) of KAuCl4 and 10 mg (0.13 mmol) of NaOAc in 15 mL of acetic acid was refluxed for 48

hrs. After cooling the solvent was evaporated and the solid dissolved in CH_2Cl_2. The reulting solution was washed with water (3x), with 5% Na_2CO_3 solution (2x) and again with water. Anion exchange was carried out by stirring the organic phase with saturated KPF_6 solution. The organic solution was washed with water and evaporated to dryness. The brown solid was purified by column chromatography (CH_2Cl_2/MeOH, 98:2 v/v) yielding 38 mg of **1c** (90%); Mp: >310 °C; ^{1}H NMR ($CDCl_3$) ∂ 8.89 and 8.54 (ABq, 4H, *J* = 5 Hz, ß pyrrolic H), 8.75 (s, 2H, ß pyrrolic H), 8.20-8.0 (m, 8H, 2,6-ArH porphyrin), 7.81-7.72 (m, 12H, 3,5-Ar H4-ArH porphyrin), 7.15 (s, 5 H, ArH diphenylglycoluril), 7.14 (s, 5H, ArH diphenylglycoluril), 6.62 (s, 2H, ArH), 5.92 and 3.98 (ABq, 4H, *J* = 15.8 Hz, NC*H*HAr), 5.56 and 3.82 (ABq, 4H, *J* = 15.8 Hz, NC*H*HAr) 3.86 (s, 6H, OMe) 3.72 (s, 6H, OMe); UV-vis (CH_2Cl_2) λ/nm: 438, 549, 593; FAB-MS (*m*-nitrobenzylalcohol) *m/z* 1451 $(M\text{-}PF_6)^+$.

Zn-porphyrin clip 1f: The same procedure was used as for **1b**. Purification was carried out by column chromatography (CH_2Cl_2), yield 90%; Mp: >310 °C; ^{1}H NMR (diluted solution) ($CDCl_3$) ∂ 8.91 and 8.54 (ABq, 4H, *J* = 5 Hz, ß pyrrolic H), 8.85 (s, 2H, ß pyrrolic H), 8.12, 8.07, 8.01, 7.86, 7.85, 7.77 (6s, 12H, ArH porphyrin), 7.15 (m, 10 H, ArH diphenylglycoluril), 6.46 (s, 2H, ArH), 5.90 and 4.01 (ABq, 4H, *J* = 15.8 Hz, NC*H*HAr), 5.44 and 3.69 (ABq, 4H, *J* = 15.8 Hz, NC*H*HAr) 3.89 (s, 6H, OMe) 3.61 (s, 6H, OMe), 1.52, 1.50, 1.48 and 1.41 (4s, 72 H, CCH_3); UV-vis ($CHCl_3$) λ/nm: 412, 447, 530, 572, 615; FAB-MS (*m*-nitrobenzylalcohol) *m/z* 1769 $(M+H)^+$. HRMS Calcd for $C_{111}{}^{13}C_1H_{122}N_{10}O_6Zn$: 1767.887; $C_{112}H_{123}N_{10}O_6Zn$: 1767.892; Found: 1767.882.

Quinone porphyrin clip 2a: Compound **7b** was obtained after reduction of 220 mg (0.32 mmol) of dinitro derivative **7a** by stirring the latter in 10 mL of THF and 10 mL of MeOH in the presence of TEAF and Pd/C (see Chapter 2). The Pd/C was filtered off under nitrogen, 10 mL of CH_2Cl_2 and 350 mg of porphyrindione **5** were added and the mixture was refluxed for 18 hrs over Mol Sieves (3Å). After cooling the solution was washed with water (3x) and the organic solvents were removed *in vacuo*. After column chromatography (CH_2Cl_2/EtOH, 99:1 v/v) 107 mg (20%) of pure **2a** was obtained; Mp >310 °C; ^{1}H NMR (diluted solution) ($CDCl_3$) ∂ 8.90 and 8.56 (ABq, 4H, *J* = 5 Hz, ß pyrrolic H), 8.73 (s, 2H, ß pyrrolic H), 8.20, 8.08, 8.04, 7.92, 7.88, 7.87 (6s, 12H, ArH porphyrin), 7.15 (m, 10 H, ArH diphenylglycoluril), 6.59 (s, 2H, Quinone-H), 5.97 and 3.95 (ABq, 4H, *J* = 15.8 Hz, NC*H*HAr), 5.50 and 3.72 (ABq, 4H, *J* = 15.8 Hz, NC*H*HAr) 3.79 (s, 6H, OMe), 1.54, 1.52, 1.50 and 1.48 (4s, 72 H, CCH_3), -2.50 (s, 2H, NH); UV-vis ($CHCl_3$) λ/nm: 441, 531, 568, 601, 650; FAB-MS (*m*-nitrobenzylalcohol) *m/z* 1678 $(M+2H)^+$.

Quinone porphyrin clip 2b: The same procedure was used as for **1b**. Purification was carried by column chromatography (CH_2Cl_2), yield 90%; Mp: >310 °C; ^{1}H NMR (diluted solution) ($CDCl_3$) ∂ 8.92 and 8.57 (ABq, 4 H, *J* = 5 Hz, ß pyrrolic H), 8.86 (s, 2 H, ß

pyrrolic H), 8.13 (s, 2 H, ArH porphyrin), 8.08 (s, 2 H, ArH porphyrin), 8.02 (s, 2 H, ArH porphyrin), 7.92 (s, 2 H, ArH porphyrin), 7.87 (s, 2 H, ArH porphyrin), 7.77 (s, 2 H, ArH porphyrin), 7.16 (m, 10 H, ArH diphenylglycoluril), 6.57 (s, 2 H, quinone), 5.99 and 3.98 (ABq, 4 H, J = 15.8 Hz, NC*H*HAr), 5.49 and 3.72 (ABq, 4 H, J = 15,8 Hz, NC*H*HAr) 3.80 (s, 6 H, OMe), 1.52, 1.50, 1.48 and 1.41 (4s, 72 H, CCH_3); UV-vis ($CHCl_3$) λ/nm: 421, 449, 530, 571, 615; FAB-MS (*m*-nitrobenzylalcohol) *m/z* 1738 $(M+H)^+$; HRMS Calcd for $C_{110}H_{117}N_{10}O_6Zn$: 1737.845; Found: 1737.840.

Bisclip-porphyrin 3a: In situ prepared compound **4b** (0.29 mmol) was refluxed with 100 mg (0.1 mmol) of porphyrintetraone **8** in CH_2Cl_2 for 36 hrs. After cooling the mixture was washed with water (3x), and the organic solvent was removed *in vacuo*.. After column chromatography (CH_2Cl_2) mono-reacted porphyrin and di-reacted porphyrin **3a** were isolated. It was not possible to separate the S-shaped isomer from the C-shaped one (see text), leaving a mixture of the two isomers (56% yield); Mp > 310 °C; ^1H NMR (diluted solution) ($CDCl_3$) ∂ 8.57 and 8.54 (2s, 4H, ß pyrrolic H), 8.18 (m, 4H, ArH porphyrin), 7.87 (m, 8H, ArH porphyrin), 7.16 (m, 20H, ArH diphenylglycoluril), 6.62 and 6.58 (2s, 4H, ArH), 5.90 and 3.93 (ABq, 8H, J = 15.8 Hz, NC*H*HAr), 5.56, 554 and 3.90, 3.88 (2 ABq, 8H, J = 15.8 Hz, NC*H*HAr) 3.75, 3.71 (2s, 24H, OMe), 1.52, 1.50, 1.48 and 1.41 (4s, 72 H, CCH_3), -2.50 (s, 2H, NH); UV-vis ($CHCl_3$) λ/nm: 463, 540, 619, 673; FAB-MS (m-nitrobenzylalcohol) m/z 2348 $(M+H)^+$. HRMS Calcd for $C_{148}H_{155}N_{16}O_{12}$: 2348.201, Found: 2348.207.

Bisclip-Znporphyrin 3b: The same procedure was used as for **1b**. Purification was carried out by column chromatography (CH_2Cl_2), total yield 60% after purification. The S-shaped and C-shaped isomers could be separated by column chromatography; Mp (both fractions): >310 °C; ^1H NMR (fraction 1, S-shape, dilute $CDCl_3$ solution) ∂ 8.57 (s, 4H, ß pyrrolic H), 8.14 (s, 4H, ArH porphyrin), 7.87, 7.84, 7.83 (3s, 8H, ArH porphyrin), 7.16 (m, 20H, ArH diphenylglycoluril), 6.52 (s, 4H, ArH), 5.92 and 3.94 (ABq, 8H, J = 16 Hz, NC*H*HAr), 5.50 and 3.75 (ABq, 8H, J = 16 Hz, NC*H*HAr) 3.74, 366 (2s, 24H, OMe), 1.52, 1.50, 1.48 and 1.41 (4s, 72 H, CCH_3).; ^1H NMR (fraction 2, C-shape, dilute $CDCl_3$ solution) ∂ 8.56 (s, 4H, ß pyrrolic H), 8.14 (s, 4H, ArH porphyrin), 7.86 (s, 8H, ArH porphyrin), 7.16 (m, 20H, ArH diphenylglycoluril), 6.52 (s, 4H, ArH), 5.91 and 3.93 (ABq, 8H, J = 16 Hz, NC*H*HAr), 5.50 and 3.78 (ABq, 8H, J = 16 Hz, NC*H*HAr) 3.74, 3.68 (2s, 24H, OMe), 1.52, 1.50, 1.48 and 1.41 (4s, 72 H, CCH_3) (peaks at 6.52, 5.50 and 3.68 are slightly broadend). UV-vis ($CHCl_3$) λ/nm: 473, 560, 586, 610, 630, 660; FAB-MS (m-nitrobenzylalcohol) m/z 2410 $(M+H)^+$. HRMS Calcd for $C_{148}H_{153}N_{16}O_{12}Zn$: 2410.115; Found: 2410.120.

Dinitro compound 7a: A mixture of 420 mg (0.714 mmol) of **6**, 300 mg (1.57 mmol) of *p*-toluene sulfonic acid in 10 mL of 1,2-dichloroethane was refluxed under nitrogen

over Mol Sieves for 10 min. To this solution was added 155 mg (1.4 mmol) of 1,4-dihydroxybenzene and refluxing was continued for 16 hrs. The solvent was removed in *vacuo*. and the solid was dissolved in 10 mL of DMSO. To this solution were added 50 mg Cu_2Cl_2 and 0.6 mL of Pyridine and air was bubbled through the solution for 2h. The suspension was poured into 50 mL of aqueous 1N HCl and the product was extracted with 50 mL of $CHCl_3$. The organic layer was washed with aqueous 1N HCl, aqueous 5% NH_3 (2x), and with water, and concentrated *in vacuo*. After purification 260 mg (54%) of pure **7a** was obtained. Mp: >310 °C; ^{1}H NMR ($CDCl_3$) ∂ 6.95-7.20 (m, 10H, ArH diphenylglycoluril), 6.75 (s, 2H, QuinoneH), 5.52 and 3.85 (ABq, 4H, *J* = 16 Hz, NC*H*HAr), 5.50 and 3.70 (ABq, 4H, *J* = 16 Hz, NC*H*HAr) 4.15 (s, 6H, OMe). This compound was directly used for further synthesis.

Dimethoxyquinoxaline porphyrin 13a: 2,3-Diamino-1,4-dimethoxybenzene was obtained after reduction of 40 mg (0.175 mmol) of 2,3-dinitro-1,4-dimethoxybenzene by stirring the latter compound in 5 mL of THF and 5 mL of MeOH in the presence of TEAF and Pd/C (see Chapter 2). The Pd/C was filtered of under nitrogen and the solvent was evaporated *in vacuo*, subsequently 10 mL of CH_2Cl_2 and 80 mg of dioneporphyrin **5** were added and the mixture was refluxed for 3 hrs over Mol Sieves (3Å). After cooling the solution was washed with water (3x) and the organic solvents were removed in *vacuo*. After column chromatography ($CHCl_3$/hexane, 1:1 v/v) 31 mg (35%) of pure **13a** was obtained; Mp >310 °C; ^{1}H NMR (diluted) ($CDCl_3$) ∂ 8.96 and 8.93 (ABq, 4H, *J* = 5 Hz, ß pyrrolic H), 8.77 (s, 2H, ß pyrrolic H), 8.04, 8.01, 7.87, 7.80 (4s, 12H, ArH porphyrin), 7.01 (s, 2H, ArH), 3.82 (s, 6H, OMe), 1.54, 1.52, 1.50 and 1.48 (4s, 72 H, CCH_3), -2.47 (s, 2H, NH); UV-vis ($CHCl_3$) λ/nm: 438, 531, 568, 600, 650; FAB-MS (*m*-nitrobenzylalcohol) *m/z* 1226 $(M+H)^+$.

Dimethoxyquinoxaline Zn-porphyrin 13b: The same procedure was used as for **1b**. Purification was carried out by column chromatography (CH_2Cl_2), yield 90%; Mp >310 °C; ^{1}H NMR (diluted) ($CDCl_3$) ∂ 8.98 and 8.82 (ABq, 4H, *J* = 5 Hz, ß pyrrolic H), 8.81 (s, 2H, ß pyrrolic H), 8.05 (d, 4H, *J* = 2 Hz, ArH porphyrin) 7.97 (d, 4H, *J* = 2 Hz, ArH porphyrin), 7.66 (t, 2H, *J* = 2 Hz, ArH porphyrin), 7.50 (t, 2H, *J* = 2 Hz, ArH porphyrin), 7.56 (s, 2H, ArH), 3.82 (s, 6H, OMe), 1.54, 1.52, 1.50 and 1.48 (4s, 72 H, CCH_3); UV-vis ($CHCl_3$) λ/nm: 412, 447, 530, 572, 615; FAB-MS (*m*-nitrobenzylalcohol) *m/z* 1289 $(M)^+$. Anal. Calcd for $C_{84}H_{100}N_6O_2$: C, 82,31; H, 8.22; N, 6.86. Found: C, 82.45; H, 8.29; N, 6.65.

The two side products with a double bond as connection between the side-wall of the clip and the diphenylglycoluril frame work had the following physical properties:
Zn porphyrin clip 9: Mp: >310 °C; ^{1}H NMR ($CDCl_3$) ∂ 8.93 and 8.58 (ABq, 4H, *J* = 5 Hz, ß pyrrolic H), 8.87 (s, 2H, ß pyrrolic H), 8.16 (s, 2H, CC*H*N), 8.13 (s, 2H, ArH porphyrin), 8.09 (s, 2H, ArH porphyrin), 8.02 (s, 2H, ArH porphyrin), 7.92 (s, 2H, ArH porphyrin),

7 87 (s, 2H, ArH porphyrin), 7 78 (s, 2H, ArH porphyrin), 7 16 (m, 5H, ArH diphenylglycoluril), 7 05 (m, 5H, ArH diphenylglycoluril), 6 67 (s, 2H, quinone-H), 6 16 and 3 98 (ABq, 4 H, J = 15 8 Hz, NC*H*HAr), 4 07 (s, 6 H, OMe), 1 52, 1 50, 1 48 and 1 41 (4s, 72 H, CCH_3), UV-vis ($CHCl_3$) λ/nm 421, 449, 530, 571, 615, Field Desorption *m/z* 1736 $(M+H)^+$, HRMS Calcd for $C_{110}H_{115}N_{10}O_6Zn$ 1735 829, Found 1735 820

Clip 12 Mp >310 °C, ^1H NMR ($CDCl_3$) ∂ 8 12 (s, 2H, CC*H*N), 7 16 (m, 5H, ArH diphenylglycoluril), 6 90-7 10 (m, 5H, ArH diphenylglycoluril), 6 87 (s, 2H, ArH), 6 69 (s, 2H, quinone-H), 5 78 and 3 84 (ABq, 4H, J = 16 Hz, NC*H*HAr), 3 89 (s, 6H, OMe) FAB-MS (m-nitrobenzylalcohol) *m/z* 587 $(M+H)^+$

References

1 (a) Deisenhofer, J , Epp, O , Mike, K , Huber, R , Michel, H *J Mol Biol* **1984**, *180*, 385 (b) Deisenhofer, J , Epp, O , Mike, K , Huber, R , Michel, H *Nature* **1985**, *318*, 618 (c) Michel, H , Epp, O , Deisenhofer, J *EMBO J* **1986**, *5*, 2445

2 Allen, J P , Feher, G , Yeates, T O , Komiya, H , Rees, D C *Proc Nat Acad Sci U S A* **1987**, *84*, 5730

3 (a) For a review see Fox, M A "*Photoinduced electron transfer*" **1988**, Chanon, M A ed Elsevier, New York (b) Barber, J *Nature* **1988**, *333*, 114 (c) Feher, G , Allen, J P , Okamura, M Y , Rees, D C *Nature* **1989**, *339*, 111 (d) Fleming, G R , Martin, J L , Breton, J *Nature* **1988**, *333*, 190 (e) Barber, J , Andersson, B *Nature* **1994**, *370*, 31

4 McDermott, G Prince, S M , Freer, A A , Hawthornthwaite-Lawless, A M , Papiz, M Z , Cogdell, R J , Isaacs, N W *Nature* **1995** *374*, 517

5 Holten, D , Windsor, M W , Parson, W W , Thornber, J P *Biochem Biophys Acta* **1978**, *501*, 112

6 For a reviews see (a) Wasielewski, M R *Chem Rev* **1992**, *92*, 435 (b) Kurreck, H Huber, M *Angew Chem* **1995**, *107*, 929

7 (a) Leland, B A , Felker, P M , Hopfield, J J , Zewail, A H , Dervan, P B *J Phys Chem* **1985**, *89*, 5571 (b) Joran, A D , Leland, B A , Geller, G G , Hopfield, J J , Dervan, P B *J Am Chem Soc* **1984**, *106*, 6090 (c) Warman, J M , de Haas, M P , Paddon-Row, M N , Cotsaris, E , Hush, N S , Oevering, H , Verhoeven, J W *Nature* **1986**, *320*, 615 (d) Staab, H A , Feurer, A , Hauck, R *Angew Chem* **1994**, *106*, 2542, *Angew Chem Int Ed Engl* 1994, *33*, 2428

8 (a) Joran, A D , Leland, B A , Felker, P M , Zewail, A H , Hopfield, J J , Dervan, P B *Nature* **1987**, *327*, 508 (b) Miller, J R , Calcaterra, L T , Close, G L *J Am Chem Soc* **1984**, *106*, 3047 (c) Wasielewski, M R , Niemczyk, M P , Svec, W A , Pewitt, E B *J Am Chem Soc* **1985**, *107*, 1080 (d) Kundkar, L R , Perry, J W , Hanson, J E , Dervan, P B *J Am Chem Soc* **1994**, *116*, 9700

9 (a) Pasman, P.; Mes, G. F.; Koper, N. W.; Verhoeven, J. W. *J. Am. Chem. Soc.* **1985**, *107*, 5839. (b) Schmidt, J. A.; Siemiarczuk, A.; Weedon, A. C.; Bolton, J. R. *J. Am. Chem. Soc.* **1985**, *107*, 6112.

10 (a) Sessler, J. L.; Wang, B.; Harriman, A. *J. Am. Chem. Soc.* **1995**,*117*, 704. (b) Harriman, A.; Magda, D. J.; Sessler, J. L. *J. Phys. Chem.* **1991**, *95*, 1530. (c) Collin, J. -P.; Harriman, A.; Heitz, V.; Odobel, F.; Sauvage, J. -P. *J. Am. Chem. Soc.* **1994**, *116*, 5679. (d) Tecilla, P.; Dixon, R. P.; Slobodkin, G.; Alavi, D. S.; Waldeck, D. H. *J. Am. Chem. Soc.* **1990**, *112*, 9408. (e) Harriman, A.; Magda, D. J.; Sessler, J. L. *J. Chem. Soc.,Chem. Commun.* **1991**, 345. (f) Harriman, Kubo, Y.; Sessler, J. L. *J. Am. Chem. Soc.* **1992**, *114*, 388. (g) Turro, C.; Chang, C. K.; Leroi, G. E.; Cukier, R. I.; Nocera, D. G. *J. Am. Chem. Soc.* **1992**, *114*, 4013. (h) Aoyama, Y.; Asakawa, M.; Matsui, Y.; Ogoshi, H. *J. Am. Chem. Soc.* **1991**, *113*, 6233. (i) Hayashi, T.; Miyahara, T.; Hashizume, N.; Ogoshi, H. J. *J. Am. Chem. Soc.* **1993**, *115*, 2049. (j) D'Souza, F. *J. Am. Chem. Soc.* **1996**, *118*, 923. (k) Harriman, A.; Odobel, F.; Sauvage, J.-P. *J. Am. Chem. Soc.* **1995**, *117*, 9461.

11 Several authors in: "*Reaction Centers of Photosynthetic Bacteria*" **1990**, Michel-Beyerle, M. -E. (ed.), Springer-Verlag, Berlin.

12 Sijbesma, R. P.; Kentgens, A. P. M.; Lutz, E. T. G.; van der Maas, J. H.; Nolte, R. J. M. *J. Am. Chem. Soc.* **1993**, *115*, 8999.

13 The structures were generated by changing the X-ray structure of **1a** in the molecular editor of the Quanta packages. Minimizations were carried out using the CHARMm Force Field (NABR; CHARMm Force Field).

14 Nunen, van H. L. M., Thesis, **1995**, Nijmegen.

15 (a) Dolphin, D. Ed. "*The Porphyrins*", Academic, 1978, New York. (b) Fleischer, E. B.; Shachter, A. M. *Inorg. Chem.* **1991**, *30*, 3763.

16 Schenning, A. P. H.Thesis, Nijmegen, **1996**.

17 Lindsey, A. S. in "*Polymeric Quinones, The Chemistry of Quinoid Compounds*", Patai, S. Ed., **1974**, John Wiley and Sons, New York.

18 Wasielewski, M. R.; Niemczyk, M. P.; Johnson, D. G.; Svec, W. A.; Minsek, D. W. *Tetrahedron*, **1989**, *45*, 4785.

19 Antolovich, M.; Keyte, P. T.; Oliver, A. M.; Paddon-Row, M. N.; Kroon, J.; Verhoeven, J. W.; Jonker, S. A.; Warman, J. M. *J. Chem. Phys.* **1991**, *95*, 1933.

20 Marcus, R. A. *J. Chem. Phys.* **1965**, *43*, 679.

21 Kumar, K.; Lin, Z.; Waldeck, D. H.; Zimmt, M. B. *J. Am. Chem. Soc.* **1996**,*118*, 243.

22 (a) Crossley, M. J.; King, L. G.*J. Chem. Soc.,Chem. Commun.* **1984**, 920. (b) Crossley, M. J.; Govenlock, L. J.; Prashar, J. K. *J. Chem. Soc.,Chem. Commun.* **1995**, 2379.

Chapter 8

Monofunctionalized Molecular Clips as Supramolecular Catalysts

8.1 INTRODUCTION

An important fundamental goal in chemistry is the development of catalysts that are selective and highly efficient. Enzymes are such catalysts. They have a complex polymeric structure, containing a binding site for a substrate molecule and an active center, which are encapsulated by a hydrophobic protein membrane. The reasons for the high efficiency of enzymes are still being debated, however, entropy effects and the ability of the enzyme to stabilize the transition state are thought to play a major role.[1] Although these two factors are thought to be important, so far no enzyme reaction has been sufficiently well characterized for a detailed insight to be obtained. It is therefore of interest to study these natural systems as well as synthetic model systems, also because such studies may give insight in how to develop new catalytic systems.

The first simple enzyme mimics (synzymes) reported in the literature were functionalized cyclodextrins,[2] which turned out to be active catalysts for ester hydrolysis reactions and transesterification reactions.[3] More recent examples include Diedrich's cyclophanes,[4] which when functionalized with a thiozolium[5] or a porphyrin group[6] proved to be good enzyme mimics. Both the cyclodextrin- and the cyclophane-based catalysts contain a substrate binding site nearby a catalytically active function. Sanders et al. have synthesized a porphyrin trimer[7] in which the porphyrin units are part of the binding site. Using metal-to-ligand bonding, substrates were brought together in the trimer and induced to undergo a remarkable selective Diels Alder reaction. Rate enhancements for acyl transfer reactions, were also achieved using this porphyrin trimer.[8] These large rate enhancements were the result of reducing the entropy of the reaction.

Towards the goal of developing supramolecular catalysts, we have designed and synthesized new types of clip and basked-shaped host molecules which can be functionalized with catalytically active components.[9] These clip and basket shaped

hosts have been shown to be ideal receptors for hydroxybenzene substrates.[10] Subsequent functionalization of the baskets with metal centers which were positioned above the cavity of the molecule gave synzymes which were still able to bind dihydroxybenzene substrates but in addition behaved as catalysts. When provided with a catalytically active rhodium complex, enzyme properties such as substrate selectivity, Michaelis Menten kinetics, inhibition and rate enhancements by a co-substrate were observed.[11] In a related system, *viz.* a copper functionalized basket-shaped host molecule, a large rate enhancement (50,000x) was observed in a stochiometric oxidation reaction.[12]

In Chapter 2 we described various clip molecules which were functionalized with phenanthroline, salophen and porphyrin ligands. These ligands were part of the aromatic side-wall of the clips. It was of interest to see whether these clips with rigidly fixed ligands could be metallated and convert a substrate molecule bound in its cavity. One of the questions which we hoped to answer by the study described in this chapter was whether an approach in which the catalyst is rigidly attached to the substrate binding site would be more successful than an approach in which the catalyst is linked via a flexible spacer.

8.2 RESULTS AND DISCUSSION

8.2.1 Strategy

Several reactions were investigated, the general approach in all cases being the same: the guest molecule is bound in the cleft of the clip molecule, with its reactive group positioned near the catalytic center (Figure 1). Rate enhancements induced by binding

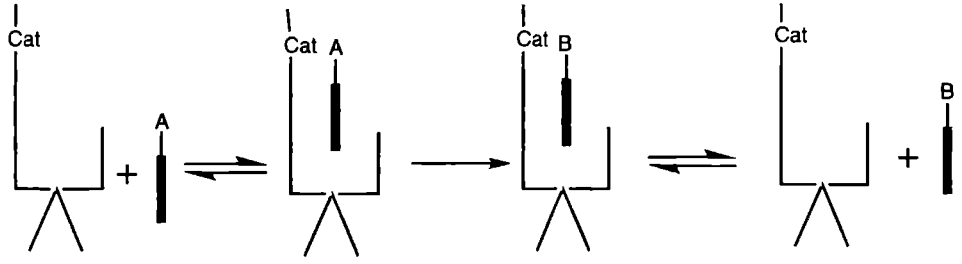

Figure 1: *Working model for a supramolecular catalyst based on a clip molecule with a rigidly attached catalytic center.*

to the clip may be due to either an entropic effect (concentration effect, in the case of a strong host-guest complex), or a stabilization of the transition state. As mentioned in the introduction, both effects are thought to be responsible for the rate enhancements

observed for enzymes. In order to test clip molecules as supramolecular catalysts, we have chosen an approach in which several reactions are screened rather than one in which one single reaction is studied in great detail. These reactions, being reductive carbonylation, epoxidation and aziridination, will be discussed in the following.

8.2.2 Reductive carbonylation

The synthesis of isocyanates and carbamates is of great industrial interest. The most common reaction route, *viz.* via amines using phosgene, has some serious environmental drawbacks, and therefore it is of commercial and environmental value to study alternative synthetic routes such as the reductive carbonylation of aromatic nitro compounds (Scheme 1). [13]

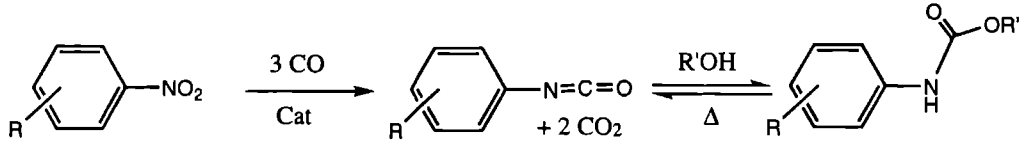

Scheme 1: *The reductive carbonylation of aromatic nitro compounds catalyzed by Pd(II) phenanthroline complexes.*

From the literature it is known that this reaction is catalyzed by complexes of Pd, Rh and Ru.[14] 1,10-Phenanthroline (Phe) has been used as a bidentate nitrogen ligand in the case of the Pd catalyst. The active species is formed by exchange of the solvent with CO (Scheme 2).[18] The actual mechanism of the reaction is still uncertain, however,

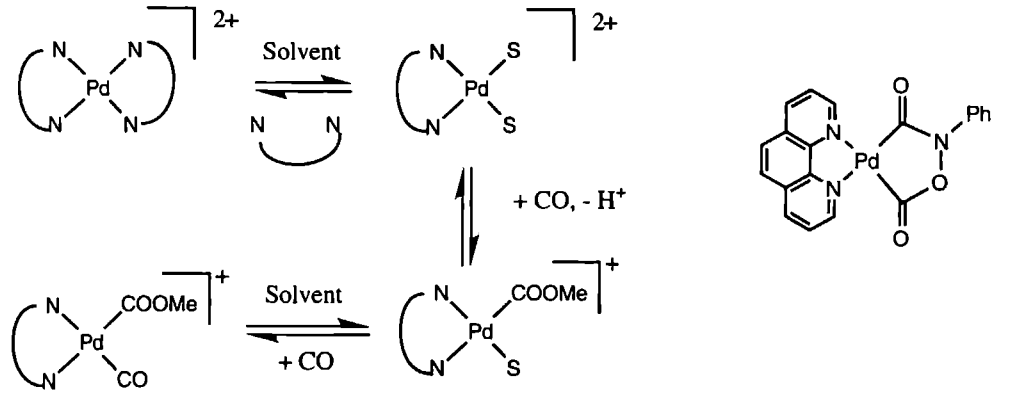

Scheme 2: *Proposed mechanism for the formation of the catalytically active species in the reductive carbonylation of aromatic nitro compounds catalyzed by $Pd(Phe)_2(PF_6)_2$ (left, S = MeOH). A proposed intermediate in the reaction (right).*

some intermediates have been proposed such as nitroso and nitrene complexes and a metallacycle (Scheme 2) The latter species was isolated from a catalyst, generated in situ from $Pd(OAc)_2$ and 1,10-phenanthroline, and was characterized by spectroscopic techniques [19]

An advantage of the carbonylation reaction is that hydroxybenzene molecules do not disturb the reaction Hydroxy groups on the aromatic ring of the guest molecule are necessary in order to obtain strong binding in the cleft of our host molecule (see Chapter 3) We chose to study the above mentioned reaction with complexes based on clip molecule **2** (see Chart I)

Chart I

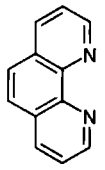

1

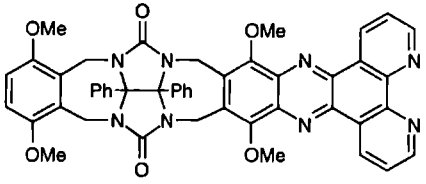

2

Synthesis of the Pd(II) complexes

The synthesis of clip **2** has been described in Chapter 2 Reference complex $Pd(\mathbf{1})_2(BF_4)_2$ was synthesized via an exchange reaction of phenanthroline with $Pd(CH_3CN)_4(BF_4)_2$ [16] Using the same procedure for the synthesis of the Pd complex of compound **2**, resulted in a mixture of products An alternative two-step route via the

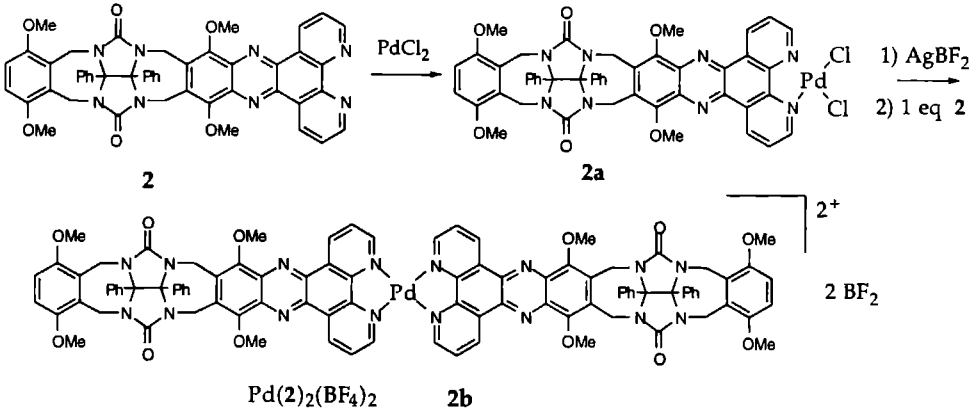

2 **2a**

$Pd(\mathbf{2})_2(BF_4)_2$ **2b**

Scheme 3: *Synthesis of the dimeric clip complex* $Pd(\mathbf{2})_2(BF_4)_2$ *(**2b**)*

monomeric $PdCl_2$ complex (**2a**, Scheme 3), however, gave a pure product, complex **2b** which was characterized by ^1H NMR, IR, UV-vis and FAB-MS (see experimental) Pd

phenanthroline complexes are known to be square planar. In the case of complex **2b** this results in two isomers, *viz.* the S-shaped and the C-shaped isomer (similar to the isomers found for the bisclip-porphyrins described in Chapter 7). These isomers were observed by ^{1}H NMR in $CDCl_3$, but no attempts were made to separated them, since the active species in the reductive carbonylation is a Pd complex with only one phenanthroline ligand attached to the metal center. For the catalytic reactions the mixture of isomers was used.

Catalysis

The reductive carbonylation reaction was performed at high CO pressure (60 bar) and elevated temperature (135 °C). Initially it was planned to use chloroform as a solvent, since binding studies had shown that host-guest complexes are formed in this solvent. The solubility of the Pd-complex, however, was very low in chloroform and test reactions, therefore, were carried out in a mixture of MeOH and $CHCl_3$. In this solvent mixture the Pd complex was found to decompose, resulting in a Pd(0) precipitate without any substrate conversion.[17] The reaction was subsequently carried out in a mixture of benzene and MeOH (9:1, v/v). In this solvent mixture the Pd complex was stable, and nitrobenzene and 4-nitrophenol were converted to a carbamate derivative. Unfortunately, in this solvent the host-guest complexation was found to be very weak since a benzene solvent molecule can complex in the cleft of the host, and therefore compete with the guest molecule. In Table 1 the results of the different catalytic reactions are given. Comparing the results for the clip catalyst ($Pd(\mathbf{2})_2(BF_4)_2$) with those for the reference phenanthroline catalyst ($Pd(\mathbf{1})_2(BF_4)_2$) (entries 1 and 2), reveals that the supramolecular clip catalyst is approximately 5 times less active than the reference catalyst, for the reaction with 4-nitrophenol. This lower catalytic activity can be ascribed to the electron donating influence of the quinoxaline side-wall in **2**. The reductive carbonylation reaction is known to be very sensitive to the substituent on the phenanthroline ligand, with electron withdrawing and strong electron releasing substituents causing a decrease in reactivity.[18] A steric effect may also be involved in the lower activity of $Pd(\mathbf{2})_2(BF_4)_2$ compared to $Pd(\mathbf{1})_2(BF_4)_2$. The reaction is known to be cocatalyzed by an organic acid,[18] however, the use of 2,4,6-trichlorobenzoic acid did not influence the yields of the reaction (entries 3 and 4), which could indicate that 4-nitrophenol itself is acting as a cocatalyst.

Reactions with nitrobenzene gave lower yields (entries 5 and 6). For the reaction catalyzed by the reference catalyst $Pd(\mathbf{1})_2(BF_4)_2$ yields of only 9% were obtained and for the clip catalyst $Pd(\mathbf{2})_2(BF_4)_2$ only a trace amount of product was observed. To investigate whether the observed increase in reactivity for the clip catalyst and 4-nitrophenol, when compared to the clip catalyst and nitrobenzene, was a result of the

guest being bound in the cleft, competition experiments were carried out with an 1:1 mixture of nitrobenzene and 4-nitrophenol. Under these conditions, the nitrobenzene substrate gave a higher yield of product than the 4-nitrophenol substrate (approximately 4 times, entry 8). The same result was obtained in a competition experiment with $Pd(\mathbf{1})_2(BF_4)_2$ as catalyst (entry 7). Apparently, the OH groups of 4-nitrophenol act as cocatalyst in the reaction of nitrobenzene. The clip catalyst $Pd(\mathbf{2})_2(BF_4)_2$ again was found to have a lower activity than the reference catalyst $Pd(\mathbf{1})_2(BF_4)_2$. Table 1 shows that the product ratio of the reactions with the mixed substrates is the same for both the reference catalyst and the clip catalyst (entries 7 and 8), suggesting that there is no effect of the cavity of the clip on the reaction.

Table 1: *Catalytic reductive carbonylation of nitrobenzene and 4-nitrophenol using different catalyst.*[a]

Entry	Catalyst	Substrate	Yield	Remarks
1	$Pd(\mathbf{1})_2(BF_4)_2$	4-nitrophenol	35%	
2	$Pd(\mathbf{2})_2(BF_4)_2$	4-nitrophenol	7%	
3	$Pd(\mathbf{1})_2(BF_4)_2$	4-nitrophenol	32%	50 equiv. cocatalyst[b]
4	$Pd(\mathbf{2})_2(BF_4)_2$	4-nitrophenol	4%	50 equiv. cocatalyst[b]
5	$Pd(\mathbf{1})_2(BF_4)_2$	nitrobenzene	9%	40% side-product[c]
6	$Pd(\mathbf{2})_2(BF_4)_2$	nitrobenzene	trace	
7	$Pd(\mathbf{1})_2(BF_4)_2$	nitrobenzene/	44%[d]	7.3 mmol of both
		4-nitrophenol	10%[e]	substrates were used
8	$Pd(\mathbf{2})_2(BF_4)_2$	nitrobenzene/	13%[d]	7.3 mmol of both
		4-nitrophenol	4%[e]	substrates were used

[a]0.02 Mmol catalyst, 0.08 mmol ligand **1** or **2**, 14.6 mmol substrate, 60 bar CO pressure, T = 135 °C; yields were determined after 2 hrs by ^1H NMR. [b]2,4,6-Trichlorobenzoic acid. [c]N,N'-Diphenylurea. [d]Based on nitrobenzene. [e]Based on 4-nitrophenol.

The disadvantage of the above described reaction is that a solvent is required (to dissolve the Pd complex) which significantly reduces the binding strength of the hydroxybenzene substrate in the clip. The entropic advantage of the substrate being bound nearby the active site consequently is very small for this system. If the presumed metallacyclic complex is an intermediate in the reaction it will prevent the substrate from being bound in the cleft because the phenyl ring of the substrate is pointing in the wrong direction (see Figure 2). Because of these reasons and since no solvent could be found which was favourable for both the binding of the substrate in the clip and the catalytic activity of the Pd complex, no further studies were carried out on the reductive carbonylation reaction.

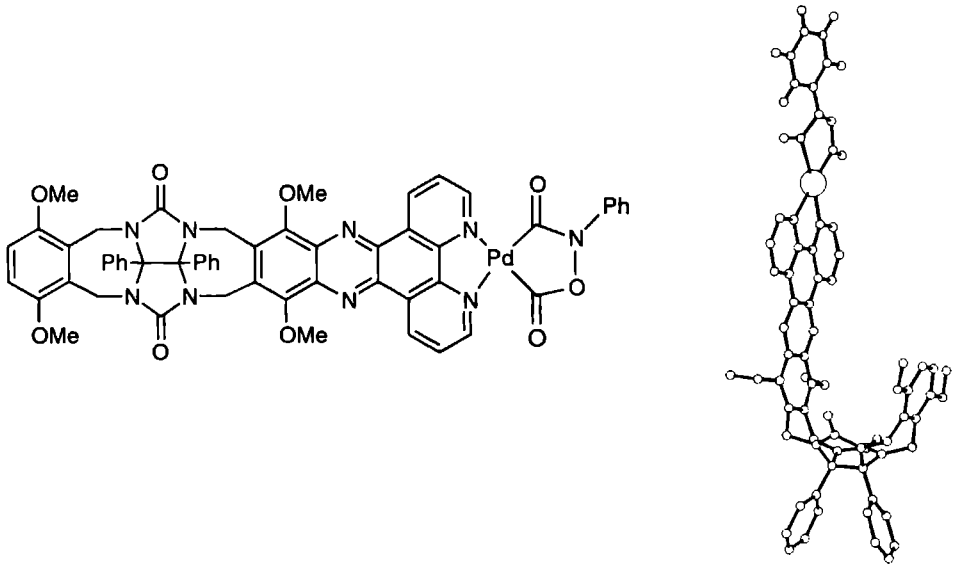

Figure 2: *Structure of the presumed intermediate in the reductive carbonylation reaction catalyzed by complex* $Pd(2)_2(BF_4)_2$.

8.2.3 Epoxidation

In an epoxidation reaction a double bond is converted into a three-membered oxygen containing ring (Scheme 4). Epoxides are important synthetic intermediates, especially if they are chiral. The development of catalysts for the conversion of alkenes to epoxides is an area of intense activity.[20] Metallo-porphyrins, metallo-salen and metallo-salophen complexes have been found to be good catalysts for this reaction, in combination with oxidants such PhIO, NaOCl, H_2O_2, $NaIO_4$ and the combination of O_2 and a reductor. The latter oxidant is of special interest for industry, since it is cheap and only gives water as a waste product.

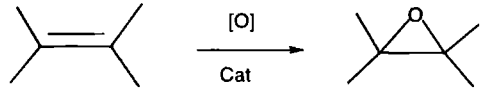

Scheme 4: *Epoxidation reaction.*

In Chapter 2 we showed that mono-salophen functionalized clip molecules **3** and **4** (Chart II) are able to bind 1,3-dihydroxybenzenes in chloroform (K_a = 920 and 1200 M^{-1}, respectively). The ideal substrate for supramolecular catalysis with these complexes was thought to be 3,5-dihydroxystyrene, which has the ability to form a complex with the clip and also contains an alkene unit which can be epoxidized. The reaction can be carried out in CH_2Cl_2, which is a good solvent for the complex formation.

Chart II

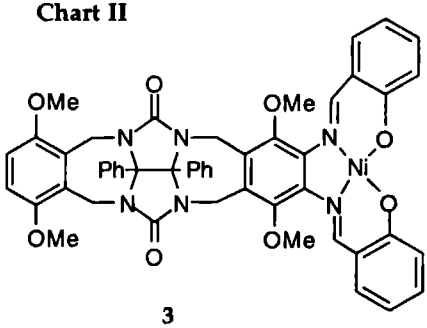

3

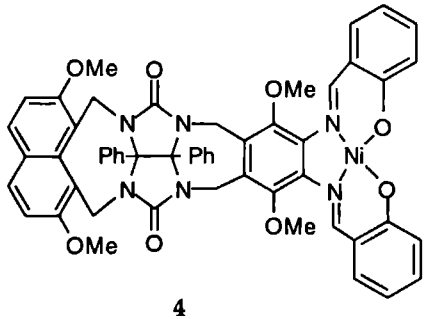

4

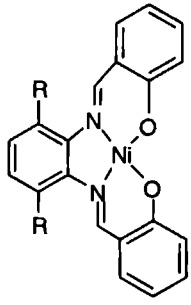

5a R = H
5b R = OMe

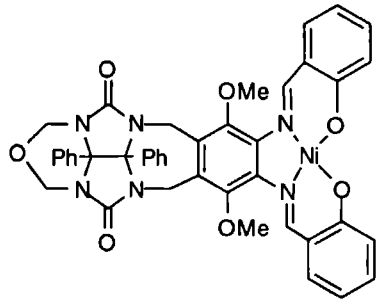

6

Recent studies in our group, however, have shown that hydroxybenzene substrates are not compatible with the reaction conditions of the epoxidation reaction.[21] Test reactions revealed that the same holds for 1,3-aminobenzene substrates. The origin of this effect is thought to be two-fold; (*i*) the hydroxyl and amino functions can be oxidized by the strong oxidants such as iodosylbenzene and (*ii*) hydroxybenzenes can act as trapping agents for radicals which probably are intermediates in the reaction.

In a first approach to cope with these problems, we generated the active species from catalyst **3** before the substrate 3,5-dihydroxystyrene was added. This, however, did not result in any detectable epoxide product.

Another approach would be to bind the guest molecules without using the OH groups, *i.e.* by π-π stacking interactions and not hydrogen bonding. Aromatic molecules without hydroxy groups can be bound in the cavity of **3**, however, with very low binding constants. Clip molecules with two 2,7-dimethoxynaphthalene side-walls e.g. **4**, are known to bind electron poor aromatic guest molecules more strongly, due to their larger π-π surface (see Chapter 4). We decided to test metallo clips **3** and **4** as catalysts for the epoxidation of different alkenes with molecular oxygen as oxidant and isobutyraldehyde as cocatalyst.[20a,21]

Catalysis

Epoxidation reactions were carried out with clip **3** and for comparison also with the reference compounds **5** and **6** Some preliminary experiments were performed with clip **4** (*vide infra*) All substrates, except α-Pinene, were aromatic compounds which can bind in the cleft of the clips The reaction conditions were the same in all experiments, and the yields were determined after 3 hours The results of the epoxidation reactions are summarized in Table 2

Examination of this table reveals that no higher yields are obtained when clip **3** is used as a catalyst (compare the results with that for the non-clip catalyst **5a**) The similar reactivity of **5a** and **5b**, implies that the methoxy groups of the side-wall do not have any significant influence on the reaction The conversion of α-pinene is somewhat lower when clip **3** is used instead of **5a** This may point to a steric effect of the diphenylglycoluril framework on the reaction of this substrate The yields of styrene-epoxide and *cis*-stilbene-epoxide for catalysts **3** and **5a** are similar, which suggests that in this case there is no steric impediment of the diphenylglycoluril framework during the reaction The styrene and stilbene substrates probably react at both faces of the catalyst, indicating that the cavity of **3** has no special effect

Table 2 *Epoxidation of various alkenes with nickel(II) salophen catalysts*[a]

Substrate	Catalyst **5a**	Catalyst **5b**	Catalyst **6**	Catalyst **3**
α-Pinene	94%	76%	95%	70%
Styrene	22%	-	-	26%
4-Methoxystyrene	< 2%	-	-	< 2%
3-Nitrostyrene	< 2%	< 2%	< 2%	< 2%
cis-Stilbene	31% [b]	25% [b]	27% [b]	30% [b]
trans-Stilbene	65% (trans)	67% (trans)	25% (trans)	35% (trans)

[a]Reaction conditions 0 6 M substrate, 1 8 M isobutyraldehyde, 1 mol% cat, 1 atm O_2, 5 ml CH_2Cl_2, T=298 °C Yields were determined after 3 hrs using GC or ^1H NMR (stilbene) [b]Cis-trans molar ratio is ca 3 7

trans-Stilbene showed a much lower reactivity towards clip catalyst **3** and **6** than towards the reference catalysts **5a** and **5b**, suggesting that this substrate experiences a steric effect of the framework of the clips during the reaction The fact that the yields with **3** and **6** are approximately half that with **5a** and **5b**, may indicate that only one face of the former catalysts, *viz* the outside, is available for reaction Based on the results obtained with *cis*-stilbene and *trans*-stilbene we propose that the substrate approaches the catalyst from above (between the two oxygen ligands) or from the side (via the carbon-nitrogen double bond) In the case of *cis*-stilbene this results in a complex geometry that is not sterically hindered by the inside of the clip, whereas in

the case of *trans*-stilbene there will be a significant steric interaction with the inside of the diphenylglycoluril framework (Figure 3). More detailed mechanistic studies, however, are needed in order to obtain the exact reason for the difference in reactivity between **3** and **5** towards the epoxidation of *trans*-stilbene.

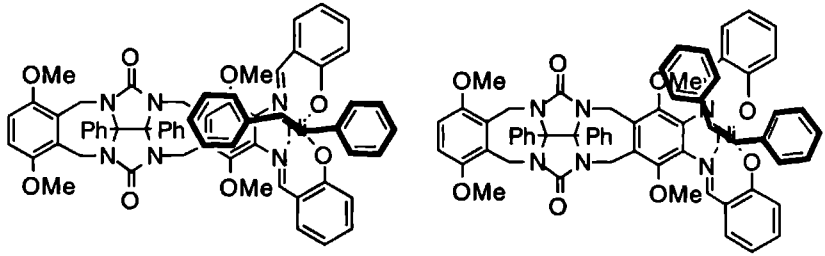

Figure 3: *Proposed geometries for reaction of trans-stilbene (left), and cis-stilbene (right) with catalyst 3. The approach of the alkene is via the cleft side of the catalyst.*

The epoxidations of α-pinene and *trans*-stilbene were followed as a function of time by monitoring the appearance of the epoxide product (Figure 4). The curves could be fitted using first order kinetics. For the combination α-pinene and **5a** a first order rate constant $k_1 = 2.3 \times 10^{-4}$ s^{-1} was calculated and for the combination α-pinene and **3** a first order rate constant $k_1 = 8.7 \times 10^{-5}$ s^{-1}. In the case of *trans*-stilbene these rate constants were $k_1 = 7.3 \times 10^{-5}$ s^{-1} for catalyst **5a** and $k_1 = 4.0 \times 10^{-5}$ s^{-1} for **3**. These results indicate that for both substrates the reaction rates are lower when clip **3** is used as catalyst, which is in line with observed lower yields (*vide supra*).

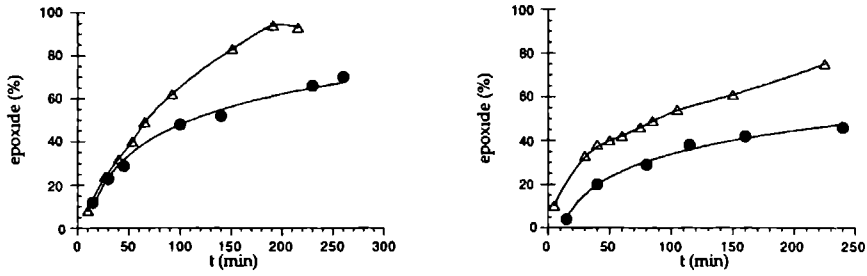

Figure 4: *Conversion of α-pinene (Δ) and trans-stilbene (•) as a function of time for catalyst 5a (left) and catalyst 3 (right).*

The conversion of *trans*-stilbene with **3** as catalyst, initially followed first order kinetics, however, after 2 hours the reaction started to deviate from first order (clearly seen from a logarithmic plot). We ascribe this effect to degradation of the catalyst. This was also evident from the observed decrease in brightness of the red catalyst solution after this period. The UV-vis spectrum of the reaction mixture was monitored during

the catalytic experiments. In the case that no substrate was present, the maxima at 378 and 478 nm, which are due to the nickel salophen complex, disappeared in approximately 10 minutes. When α-pinene was added, these maxima started to decrease after this substrate had been almost completely converted (three hours). In the presence of less reactive substrates such as styrene and *cis*-stilbene, the maxima already started to decrease slowly at the beginning of the reaction. Apparently, the catalyst starts to react with itself in the absence of active substrates.

The fact that *cis*-stilbene gives epoxide products with the same cis-trans ratios in all reactions, indicates that the isomerization process is unaffected by the steric bulk of the clip. Between the opening of the double bond, and the ring closure step, which yields the epoxide, a phenyl group must rotate from cis to trans. It was tentatively concluded above that *cis* stilbene is able to react at both faces of the catalyst, whereas *trans*-stilbene only reacts at the outside of the clip. If in the case of *cis*-stilbene the rotation around the opened double bond would take place in the clip, than an effect of the framework of the clip upon this isomerization would have been expected. Since this is not observed it is likely that this reaction does not go via a concerted mechanism.

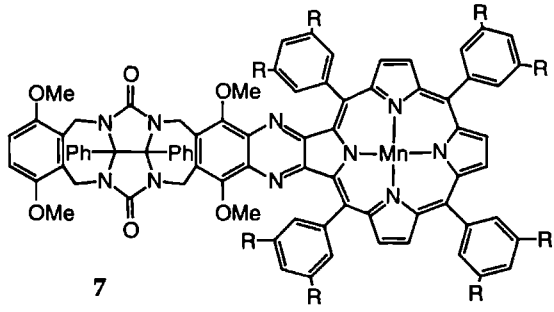

7

Some preliminary catalytic experiments were carried out with catalyst **4**, which has the larger 2,7-dimethoxynaphthalene side-wall. This catalyst, however, did not give higher yields than **3**. Test reactions with nitrostyrene, which was expected to bind more strongly in the cavity of **4** than in the cavity of **3**, gave no oxidized product, probably because the substrate molecule was too electron deficient. ^{1}H NMR experiments revealed that there was no significant binding in the cleft of **4**. In order to obtain higher binding constants, the substrate molecule needs to be even more electron deficient, e.g. dinitrostyrene would be a better guest. The reactivity, however, will also decrease further when the substrate is more electron poor. The problem is that the requirements for high binding and good catalysis in this case are opposed.

Preliminary epoxidation experiments were also performed with styrene and porphyrin clip **7** as a catalyst. The same conditions were used as for the epoxidation

reactions with the nickel catalyst. These experiments revealed that this catalyst did not give higher yields than the reference catalyst Mn(III)TPPCl (TPP = tetraphenylporphyrin).

In summary we may conclude that catalyst **3**, **4** and **7** are catalytically active, but do not behave as supramolecular catalysts under the conditions used. The main problem is that substrates which have high binding in the cleft of the clips, *viz.* substrates with hydroxyl groups, can not be used for this epoxidation reaction. Binding by π-π stacking interactions can only be enhanced by using electron poor substrates molecules, however, these substrates are not reactive towards epoxidation. We decided, therefore, to use our clip-catalysts for an other reaction (see next section).

8.2.4 Aziridination

The final type of reaction which was investigated using our clip-shaped molecules was the aziridination reaction. This reaction is similar to the epoxidation reaction, however, in this case the three membered ring is closed by a nitrogen instead of an oxygen atom (Scheme 5).[22] It was recently reported that the aziridination reaction can be carried out with PhI=NTos as reactant in a variety of organic solvents, even CH_2Cl_2, using copper(I) complexes as catalyst.[23]

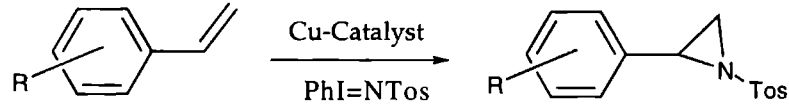

Scheme 5: *The copper(I) catalyzed aziridination reaction.*

Strong evidence has been found that the aziridination reaction occurs via a nitrene intermediate.[24] In the case of a copper(I) phenanthroline complex as catalyst the mechanism of the reaction was proposed to be as depicted in Scheme 6. The styrene derivative is expected to attack the copper at the axial position.

Complex synthesis

In order to make supramolecular catalysts for the aziridination reaction, ligands **2** (Chart I), **8**, and **9** (Chart III) were metallated with copper(I). The copper complexes were synthesized by a ligand exchange reaction, stirring $Cu(CH_3CN)_4(PF_6)$[25] in CH_2Cl_2 with two equivalents of the phenanthroline ligands **2**, **8**, and **9** yielding CuL_2PF_6 complexes. The instantaneously formed complexes were deeply red in colour, and were precipitated with hexane. The complexes were characterized with Field

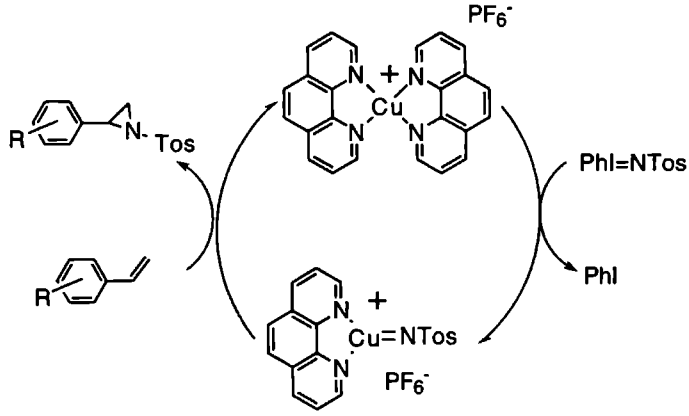

Scheme 6: *Proposed mechanism for the aziridination reaction.*

Desorption high resolution mass spectroscopy, IR-spectroscopy, and UV-vis spectroscopy (see Experimental).

Chart III

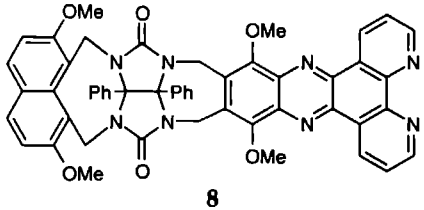

8

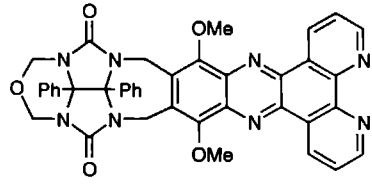

9

Catalysis

For the catalytic reactions the catalysts were prepared *in situ*, by the addition of 0.005 mmol $Cu(CH_3CN)_4(PF_6)$ and 2 equivalents of ligand **2**, **8** or **9** to 2 mL of CH_2Cl_2. The solution was stirred for 20 minutes under nitrogen, and 0.5 mmol of substrate and 0.1 mmol of PhI=NTos were added. After exactly 2 hours the reaction mixture was analyzed by HPLC. The reactions were also performed using pre-prepared complexes, which gave the same results as the reactions with the *in situ* prepared catalysts. The results of the catalytic experiments are presented in Table 3. As can be seen in this Table, substrate molecules like 3,5-dihydroxystyrene which possess hydroxyl functions, inhibit the reaction. The reaction mixture changed colour from deep red to brown upon addition of dihydroxystyrene, which is indicative of the formation of phenolate complexes (when other substrates were added in the presence of PhI=NTos, the colour of the solution changed to green). These phenolate complexes are no longer active in the aziridination reaction.

Table 3: *Aziridination of various alkenes with different copper(I) complexes.*[a]

	Catalysts		
Substrate	$Cu(\mathbf{2})_2PF_6$	$Cu(\mathbf{8})_2PF_6$	$Cu(\mathbf{9})_2PF_6$
3,5-Dihydroxystyrene	0%	0%	0%
4-Methoxystyrene	33%	36%	33%
Styrene	48%	40%	35%
3-Nitrostyrene	58%	46%	36%

[a] Reaction conditions: 0.25 M substrate, 50 mM PhI=NTos, 1 mol% catalyst, 1 atm. N_2, 2 mL CH_2Cl_2 T = 298 °C. Yields were determined after 2 hrs by HPLC.

The remaining substrate molecules of Table 3 can only be bound in the cleft of the clip catalysts by means of π-π stacking interactions. ^1H NMR experiments revealed that the binding of these substrates in clefts of the ligands **2** and **8** is very weak. Reaction enhancement on the basis of high binding affinities therefore can not be expected. ^1H NMR binding experiments with the copper-catalysts could not be carried out due to broadening of the signals because of the paramagnetic properties of the oxidized catalyst. From previous experiments with other metal containing clip molecules (Chapters 2 and 7) we know that the presence of the metal increases the binding strength of the guest, however, the binding of the substrates will still be weak.

The results in Table 3 suggest that, despite the weak binding of the substrates in the clefts of **2** and **8**, there is a positive effect of the cavity of the clip on the aziridination reaction. The copper complex prepared from the ligand without any cleft (**9**), reacts with all substrates in the same way giving similar yields. The cleft containing complexes, however, give significant higher yields of product in the case of the nitrostyrene substrate. For $Cu(\mathbf{2})_2PF_6$ the yield of the reaction with nitrostyrene is almost twice as high as that for the reaction with methoxystyrene. Apparently, reactions with electron poor substrates are enhanced by the catalysts containing a ligand with a cleft. These electron deficient substrates have a larger π-π interaction when they are sandwiched between the electron rich side-walls of the clip, which might explain their enhanced reactivity. In the case of ligand **8**, the highest substrate binding was expected, because of the large 2,7-dimethoxynaphthalene side-wall which is present in this clip molecule, and consequently also the highest substrate reactivity. This was found not to be the case (see Table 3). Clip molecule **8** adopts two conformations in solution, with only 32% of the molecules having a cleft (see Chapter 2), even in the presence of guest molecules. The remaining 68% of the molecules have not a cavity and are more similar to molecule **9**. The yields of the reactions of $Cu(\mathbf{8})_2PF_6$ with electron poor substrates are slightly less than those with catalyst $Cu(\mathbf{2})_2PF_6$, and higher than those observed for $Cu(\mathbf{9})_2PF_6$. Assuming that the 32% *aa*

conformer of **8** is responsible for the extra 10% yield in the reaction with nitrostyrene as compared with methoxystyrene, one can calculate what the yield for 3-nitrostyrene would be if all the molecules were in the *aa* conformation. This yield is 57%, which is in agreement with the 58% yield found for the reaction with $Cu(\mathbf{2})_2PF_6$ and nitrostyrene.

In order to confirm that the higher yields observed in the case of 3-nitrostyrene and complex $Cu(\mathbf{2})_2PF_6$ are a result of substrate binding within the cleft of the catalyst, competition experiments were carried out. In such an experiment with nitrostyrene and methoxystyrene using catalyst $Cu(\mathbf{9})_2PF_6$, approximately equal amounts of product were obtained (24 and 19%, respectively). In the same competition experiment using $Cu(\mathbf{2})_2PF_6$ as the catalyst, more nitrostyrene-product was obtained (36% compared to 21% methoxystyrene-product). This together with the results in Table 3 indicates that the product ratios for the competition experiment and the separated experiments are the same. This suggests that the higher yields found for the aziridination reaction of nitrostyrene in the presence of clip catalyst $Cu(\mathbf{2})_2PF_6$ are due to an enhanced reaction rate in which the cavity is involved and not to an entropy effect (concentration effect) as the result of selective binding. More experiments, however, are needed to verify this.

8.3 CONCLUSIONS

In this chapter we have shown that clip molecules with catalytically active metal centers can be prepared. These molecules are able to bind hydroxybenzene substrates as was shown previously (Chapter 2). The different catalytically active metals are active in reductive carbonylation, epoxidation, and aziridination reactions. Our studies indicate that simply combining a binding site with a catalytically active group, which should lead to a supramolecular catalyst, is not an approach which immediately leads to success. Under the conditions required for substrate molecules to be bound in the clefts of the clips, the catalytic active sites were deactivated and *vice versa*. The problems which we encountered during the reactions, are summarized in the following list:

- In solvents in which the catalyst is active, the substrate is not bound (reductive carbonylation reaction).
- The position of the cleft is such that the bound substrate can not react at the metal center (reductive carbonylation reaction).
- The hydroxyl groups which enhance the binding of the substrate in the cleft, are oxidized by the active site of the supramolecular catalyst or by the cocatalyst (epoxidation reaction).

- The hydroxyl groups disturb the reaction by acting as radical scavengers or by forming complexes with the catalyst (epoxidation reaction, aziridination reaction).
- The substrate molecule is bound too weakly in the cleft of the clip in order to give reaction enhancements due to concentration effects (reductive carbonylation reaction, epoxidation reaction, aziridination reaction).

In the copper(I) catalyzed aziridination reaction, the clip catalysts gave higher yields when they were combined with electron deficient substrates. These substrates probably are bound more strongly due to favourable interactions with the electron rich side-walls of the clips.

Comparing the approach in which the catalyst is rigidly attached to the clip with the approach in which this catalyst is linked to the binding site via flexible spacers,[11,12] one can conclude that the latter approach is a more successful one. This conclusion is also in agreement with the recently proposed idea that the activity and enantioselectivity of an enzyme are related to the flexibility of this biomolecule.[26] In the case of a rigid supramolecular catalyst, one has to know exactly the mechanism of the reaction in order to be successful, whereas in a flexibly linked system the "unknowns" can be compensated for by this flexibility.

8.4 EXPERIMENTAL SECTION

8.4.1 General.

Dichloromethane, acetone and chloroform were distilled from $CaCl_2$. Hexane and diethylether were distilled under nitrogen from sodium benzophenone ketyl. All other solvents and chemicals were commercial materials and used as received. IR spectra were recorded on a Perkin Elmer FTIR 1720-Xspectrometer. ^1H NMR spectra were recorded on Bruker WH-90, Bruker AC-100, Bruker WM-200, and Bruker AM-400 instruments. Chemical shifts are reported downfield from internal tetramethylsilane. Abbreviations used are s = singlet, d = doublet, m = multiplet, br = broad. FAB-MS spectra were recorded on a VG 7070E instrument, the matrix used was *m*-nitrobenzylalcohol. Elemental analyses were determined with a Carlo Erba Ea 1108 instrument. Field Desorption (FD) mass spectrometry was carried out using a JEOL JMS SX/SX102A four-sector mass spectrometer, coupled to a JEOL MS-MP7000 data system, 10 μm tungsten wire FD emitters containing carbon micro-needles with an average length of 30 μm were used. The samples were dissolved in methanol/water and then loaded onto the emitters with the dipping technique. An emitter current of

0-15 mA was used to desorb the samples. The ion source temperature was generally 90 °C.

8.4.2 Compounds

The syntheses of compounds **2**, **3**, **4**, **8** and **9** are described in Chapter 2. 3,5-Dihydroxystyrene was synthesized as described in ref. 21. All other compounds were commercially available products.

Nickel salophen compound 6. To a solution of the diamino-precursor (compound **11c** Chapter 2) (100 mg, 0.2 mmol) in a mixture of 7 mL of THF and 7 mL of methanol, were added 80 mg (0.65 mmol) of 2-hydroxybenzaldehyde and 85 mg (0.34 mmol) of $Ni(OAc)_2 \cdot 4H_2O$. The mixture was stirred under nitrogen for 4 days, and the precipitate was filtered off and washed with methanol. The solid was dissolved in chloroform and washed with water (2X). The solvent was concentrated *in vacuo* and purified by column chromatography (CH_2Cl_2/EtOH, 98:2 v/v) yielding 90 mg pure **6**. Mp > 350 °C; ^1H NMR ($CDCl_3$) δ 9.21 (s, 2H, NC*H*Ar), 7.39-7.03 (m, 16H, ArH), 6.62 (td, 2H, ArH, *J* = 7.6 and 1.7 Hz), 5.61 and 3.90 (2d, 4H, NCH_2Ar, *J* = 16.2 Hz), 5.51 and 4.45 (2d, 4H, NCH_2Ar, *J* = 11.2 Hz), 3.78 (s, 6H, OCH_3); FAB-MS *m/z* 793 $(M+H)^+$. Anal. Calcd for $C_{42}H_{34}N_6O_7Ni \cdot (EtOH)$: C, 62.95; H, 4.80; N, 10.01. Found: C, 63.98; H, 4.68; N, 9.83.

Pd(1)$_2$(BF$_4$)$_2$. This complex was kindly provided by Dr. P. Wehman.[16,18]

Pd(2)(Cl)$_2$ (2a). To a solution of 50.6 mg (62 mmol) of **2** in 10 mL of $CHCl_3$ was added a well-stirred suspension of 17.4 mg (88 mmol) of $PdCl_2$ in 10 mL of methanol. After 16 hrs of stirring diethyl ether was added and the precipitate was collected. Yield: 38.9 mg (39 mmol, 63%) of a green/yellow powder. Mp > 400 °C ^1H-NMR (DMSO-d_6) δ 9.44 (d, 2H, phen$H_{2,9}$, *J* = 7 Hz), 9.30 (d, 2H, phen$H_{4,7}$, *J* = 5 Hz), 7.97 (dd, 2H, phen$H_{3,8}$, *J* = 7 and 5 Hz), 7.22-7.14 (br, 10H, ArH), 6.57 (s, 2H, ArH), 5.73 and 4.13 (2d, 4H, NCH_2Quinox, *J* = 15.8 Hz), 5.42 and 3.71 (2d, 4H, NCH_2Ar, *J* = 15.8 Hz), 4.37 (s, 6H, OCH_3), 3.58 (s, 6H, Ar-OCH_3). IR (CsI) 1713 cm^{-1} (C=O), 246 cm^{-1} (Pd-Cl). FAB-MS (m-nitrobenzylalcohol) m/z 928 (Pd(**2**))$^+$.

Pd(2)$_2$(BF$_4$)$_2$ (2b). Under exclusion of light 30.5 mg (30 mmole) of **2a** was suspended in 25 mL of acetone and 35 mg (180 mmol) of $AgBF_4$ was added. The reaction mixture was stirred until the solution was clear (2 hrs). Subsequently 25.0 mg (30 mmol) of clip **2** was added and the solution was stirred for another 2 hrs. The solution was concentrated *in vacuo* to one-third of the volume. The concentrated solution was centrifuged and the resulting pale yellow solution was decanted from the grey precipitate. The solvent was evaporated and the product was washed several times

with diethyl ether yielding 37.0 mg (63%) of pale yellow **2b**. Mp > 400 °C. ^{1}H-NMR (DMSO-d$_6$) δ 9.26 (d (br), 4H, phenH$_{2,9}$), 9.04 (d (br), 4H, phenH$_{4,7}$), 7.76 (br, 4H, phenH$_{3,8}$), 7.19-7.11 (br, 20H, ArH), 6.53 (s (br), 4H, ArH), 5.68 and 4.04 (2d, 8H, NC*H*$_2$Quinox, *J* = 16 Hz), 5.39 and 3.70 (2d, 8H, NC*H*$_2$Ar, *J* = 16 Hz), 4.33 (s, 12H, OCH$_3$), 3.55 (s, 12H, Ar-OC*H*$_3$). IR: (CsI) 1713 cm^{-1} (C=O), 1075 cm^{-1} (BF$_4$)$^-$. FAB-MS (m-nitrobenzylalcohol) m/z 1750 (**Pd(2)$_2$**)$^+$, 928 (**Pd(2)**)$^+$, 823 (**2** + H)$^+$. Due to the instability of the compound no satisfactory elemental analyses could be obtained.

Cu(9)$_2$(PF$_6$). To a solution of 4.9 mg (0.013 mmol) of Cu(CH$_3$CN)$_4$(PF$_6$) in 5 ml of CH$_2$Cl$_2$ under argon, was added 18.3 mg (0.026 mmol) of clip **9**, and the mixture was stirred for 2 hrs under exclusion of light. Hexane (5 mL) was added and a brown solid was formed which was allowed to precipitate overnight. The product was recrystallized from CH$_2$Cl$_2$ several times yielding 15.3 mg (73%) of Cu(**9**)$_2$(PF$_6$) as a brown microcrystalline solid: Mp > 400 °C; IR (KBr) 1717 (C=O) 835, 555 (PF$_6^-$); UV-Vis (CH$_2$Cl$_2$) λ_{MLCT} 436 nm; High Resolution Field Desorption-MS Calcd. for C$_{80}$H$_{60}$N$_{16}$O$_{10}$Cu 1467.397, found: 1467.394.

Cu(2)$_2$(PF$_6$). This compound was synthesized as described for the complex Cu(**9**)$_2$(PF$_6$), using 9.1 mg (0.025 mmol) of Cu(CH$_3$CN)$_4$(PF$_6$) dissolved in 10 mL of CH$_2$Cl$_2$ and 41.1 mg (0.050 mmol) of clip **2**. Yield: 35 mg (0.019 mmol, 76%) of Cu(**2**)$_2$(PF$_6$) as a brown microcrystalline solid: Mp > 400 °C; IR (KBr) 1712 (C=O), 843,557 (PF$_6^-$); UV-Vis (CH$_2$Cl$_2$) λ_{MLCT} 436 nm; High Resolution Field Desorption-MS Calc. for C$_{96}$H$_{76}$N$_{16}$O$_{12}$Cu 1707.512, found: 1707.511.

Cu(8)$_2$(PF$_6$).This compound was synthesized as described for the complex Cu(**9**)$_2$(PF$_6$), using 9.1 mg (0.025 mmol) of Cu(CH$_3$CN)$_4$(PF$_6$) dissolved in 10 mL of CH$_2$Cl$_2$ and 43.6 mg (0.050 mmol) of clip **8**. Yield: 33.7 g (0.017 mmol, 69%) of Cu(**8**)$_2$(PF$_6$) as a brown microcrystalline solid: Mp > 400 °C; IR (KBr) 1712 (C=O), 846, 557 (PF$_6^-$); UV-Vis (CH$_2$Cl$_2$) λ_{MLCT} 436 nm; High Resolution Field Desorption-MS Calcd. for C$_{104}$H$_{81}$N$_{16}$O$_{12}$Cu 1808.552. Found: 1808.553.

Mn(III) porphyrin chloride clip 7. A solution of 22 mg (0.013 mmol) of free base porphyrin **7** in 2 mL of DMF was heated to reflux under N$_2$. To this solution was added 10 mg of Mn(OAc)$_2$.H$_2$O, and the mixture was refluxed until all free base porphyrin had reacted (approximately 1 hr). The solvent was evaporated *in vacuo*, the solid was dissolved in chloroform and the resulting solution was stirred in the presence of 1 equiv. of a saturated aqueous NaCl solution for one night. The organic solution was washed with water and concentrated, to give 20 mg of Mn(III) porphyrin clip **7**, yield 85%. UV-vis (CHCl$_3$) λ/nm: 382, 506, 568, 592, 657; FAB-MS (m-

nitrobenzylalcohol) m/z 1759 $(M+H-Cl)^+$. High Resolution Field Desorption-MS Calcd. for $C_{112}H_{123}N_{10}O_6Mn$: 1758.901; Found: 1758.905.

8.4.3 Catalysis

Reductive carbonylation

An autoclave was charged with 9 mL of benzene, 1 mL of MeOH, 0.02 mmol of $Pd(\mathbf{L})_2(BF_4)_2$, 0.08 mmol of ligand (**1** or **2**) (6 equivalents with respect to Pd) and 14.6 mmol of substrate. The autoclave was pressurized with 60 bar of CO and heated to 135 °C within 35 min. The initial working pressure at 135 °C was approximately 80 bar. After 2 hrs, the autoclave was rapidly cooled down and the pressure was released. The reaction mixture was analyzed by ^1H NMR.

Epoxidation reaction

In a Schlenk-vessel containing 3 mL of CH_2Cl_2 were mixed 1 mL of a 3 M substrate stock solution, 1 mL of 9 M isobutyraldehyde, and 1 mol% of Ni-catalyst (with respect to the substrate). The solution was placed under an oxygen atmosphere and stirred for 3 hrs. The reaction was monitored in time by taking samples which were analyzed by GC after adding an internal standard, or the reaction was stopped after 3 hrs and the yields of epoxide products were determined by GC or ^1H NMR.

Aziridination reaction

In a typical experiment 1.86 mg (0.005 mmol) of $Cu(CH_3CN)_4(PF_6)$ and 2 equiv. of ligand were dissolved in 2 mL of CH_2Cl_2 in a 5 mL Schlenk-vessel under an inert atmosphere. This solution was stirred for 20 min. after which the substrate (0.5 mmol) and PhI=NTos (0.1 mmol) were added. Exactly 2 hrs after the addition of the PhI=NTos, a 25 μL sample was taken. This sample was quickly dried *in vacuo* and dissolved again in 50 μL of CH_3CN containing 0.075 M of α,2,6-trichlorotoluene as a standard. The samples were analyzed by HPLC (LiChrospher 100 RP18, 5 mm, 250 x 4 mm column) using CH_3CN : H_2O (6:4, v/v) as eluent. The compounds were detected by UV-absorption at 239 nm using a KONTRON Uvikon 725 spectrophotometer coupled to a LKB 2221 Intergrator. The system was calibrated by injecting samples with different ratios of the standard and the appropriate aziridines.

References

1 Kraut, J. *Science*, **1988**, *242*, 533.

2 (a) Breslow, R. *Isr. J. of Chem.* **1992**, *32*, 23. (b) Breslow, R. *Recl. Trav. Chim. Pays Bas*, **1994**, *113*, 493. (c) Akkaya, E.U; Czarnik, A.W. *J .Am. Chem. Soc.* **1988**, *110*, 8553. (d) Menger, F.M.; Ladika, M. *J. Am. Chem. Soc.* **1987**, *109*, 3145. (e) Bender, M.L.; Komiyama, M. "*Cyclodextrin Chemistry;*" Springer; Berlin, **1978**. (f)

Breslow, R. *Science*, **1982**, *218*, 532. (g) Tabushi, I.*Pure Appl. Chem.*, **1986**, *58*, 1529. (h) Weber, L.; Hommel, R.; Behling, J.; Haufe, G.; Hennig, H. *J. Am. Chem. Soc.* **1994**, *116*, 2400. (i) Kuroda, Y.; Hiroshige, T.; Sera, T; Shirolwa, Y.; Tanaka, H, Ogoshi, H., *J. Am. Chem. Soc.* **1989**, *111*, 1912.

3 Anslyn, E.; Breslow, R. *J. Am. Chem. Soc.* **1989**, *111*, 8931.

4 Diederich, F. "*Cyclophanes;*" Royal Society of Chemistry; Cambridge, **1991**.

5 Diederich, F.; Lutter, H.-D., *J. Am. Chem. Soc.* **1989**, *111*, 8438.

6 (a) Benson, D. R., Valentekovich, R.; Diederich, F. *Angew. Chem.* **1990**, *102*, 213. (b) Benson, D. R., Valentekovich, R.; Knobler, C.B.; Diederich, F. *Tetrahedron* **1991**, *47*, 2401. (d) Benson, D. R., Valentekovich, R.; Tam, S.-W; Diederich, F. *Helv. Chim. Acta*, **1993**, *76*, 2034.

7 (a) Anderson, H. L.; Bashall, A.; Henrick, K.; McPartlin, M.; Sanders, J. K. M., *Angew. Chem.* **1994**, *106*, 445. (b) Walter, C. J.; Anderson, H. L.; Sanders, J. K. M., *J. Chem. Soc. Chem. Commun.* **1993**, 458;

8 Mackay, L. G.; Wylie, R. S.; Sanders, J. K. M., *J. Am. Chem. Soc.* **1994**, *116*, 3141.

9 (a) Smeets, J. W. H; Sijbesma, R. P.; van Dalen, L.; Spek, A. L.; Smeets, W. J. J.; Nolte, R. J. M. *J. Org. Chem.* **1989**, *54*, 3710. (b) Sijbesma, R.P.; Kentgens, A.P.M.; Nolte, R.J.M.; *J. Org. Chem*, **1991**, *56*, 3199.

10 (a) Sijbesma, R. P.; Kentgens, A. P. M.; Lutz, E. T. G.; van der Maas, J. H.; Nolte, R. J. M. *J. Am. Chem. Soc.* **1993**, *115*, 8999. (b) Sijbesma, R. P.; Kentgens, A. P. M.; Nolte, R. J. M.; *J. Org. Chem.* **1991**, *56*, 3122.

11 (a) Coolen, H. K. A. C.; van Leeuwen, P. W. N. M.; Nolte R. J. M. *Angew. Chem.* **1992**, *31*, 905. (b) Coolen, H. K. A. C.; Meeuwis, J. A. M.; van Leeuwen, P. W. N. M.; Nolte R. J. M *J. Am. Chem. Soc.* **1995**, *117*, 11906.

12 Martens, C. F.; Klein Gebbink, R. J. M.; Feiters, M. C.; Nolte, R. J. M. *J. Am. Chem. Soc.* **1994**, *116*, 5667.

13 Ugo, R.; Psaro, R.; Pizotti, M.; Nardi, P.; Dossi, C.; Andreetta A.; Capparella G. *J. of Organomet. Chem.* , **1991**, *417*, 211and references cited theirein.

14 Skoog, S.J.; Campbell, J.P.; Gladfelter, W.C. *Organometallics*; **1994**, *11*, 4137 and references cited theirein.

15 Alessio, E.; Mestroni, G.; *J. of Organomet. Chem*, **1985**, *291*, 117.

16 Wehman, P.; Kaasjager, V.E.; de Lange, W.G.J.; Hartl, F.; Kamer, P.C.J.; van Leeuwen, P.W.N.M. *Organometallics*, **1995**, *14*, 3751.

17 Decomposition of the Pd catalysator results in a black precipitate, P. Wehman, personal communication.

18 Wehman, P. Thesis Amsterdam, **1996**.

19 Leconte, P.; Metz, F.; Mortreux, A.; Osborn, J.A.; Paul, F.; Petit, F.; Pillot, A.J.; *J. Chem. Soc., Chem. Com.* **1990**, 1616.

20 (a) Katsuki, T. *Coordination Chem. Rev.* **1995**, *140*, 189. (b) Katsuki, T.; Sharpless, K. B. *J. Am. Chem. Soc.* **1980**, *102*, 5974. (c) Gao, Y.; Hanson, R. H.; Klunder, J. M.; Ko, S. Y.; Sharpless, K. B. *J. Am. Chem. Soc.* **1987**, *109*, 5765. (d) Jacobsen, E. N.; Zhang, W.; Muci, A. R.; Deng, L. Sharpless, K. B. *J. Am. Chem. Soc.* **1991**, *113*, 7063. (e) Collman, J. P.; Zhang, X.; Lee, V. J.; Uifelman, E. S.; Brasuman, J. I. *Science*, **1993**, *261*, 1404. (f) Jacobsen, E. N. in "*Catalytic Asymmetric Synthesis*" 1993, Ojima, I. Ed., VCH, New York.

21 (a) Gosling, P. A.; Sijbesma, R. P.; Spek, A. L.; Nolte, R. J. M. *Recl. Trav. Chim. Pays-Bas* **1993**, *112*, 404. (b) P. Gosling Thesis Nijmegen, **1996**.

22 (a) Mansuy, D.; Mahy, J.P.; Dureault, A.; Bedi, G.; Battioni, P. *J. Chem. Soc., Chem. Comm.* **1984**, 1161. (b) Yamada, Y.; Yamamoto, T.; Ohawara, M. *Chem. Lett.* **1975**, 361.

23 (a) Evans, D.A.; Woerpel, K.A.; Hinman, M.M.; Faul, M.M. *J. Am. Chem. Soc.*, **1991**, *113*, 726. (b) Evans, D.A.; Faul, M.M.; Bilodeau, M.T. *J. Org. Chem.* **1991**, *56*, 67. (c) Evans, D.A.; Faul, M.M.; Bilodeau, M.T. *J. Am. Chem. Soc.*, **1994**, *116*, 2742.

24 Peri, P.J.; Brookhart, M.; Templeton, J.L. *Organometallics*, **1993**, *12*, 261. (b0 Li, Z.; Quan, R.W.; Jacobsen, E.N. *J. Am. Chem. Soc.* **1995**, *117*, 5889.

25 Kubas, G. *Inorg. Synth.* **1979**, *19*, 90.

26 Broos, J.; Visser, A.. J. W. G.; Engbersen, J. F. J.; Verboom, W.; van Hoek, A.; Reinhoudt, D. N. *J. Am. Chem. Soc.* **1995**, *117*, 12657.

Summary

The synthesis, binding studies and reactivity of clip-shaped receptor molecules are described in this thesis.

In nature many processes are based on molecular recognition. Complexes of different molecules are held together by weak interactions such as hydrogen bonding, π-π stacking, electrostatic and Van der Waals interactions and hydrophobic effects. The shape and interactional complementarity results in a selective binding process. An example of such a natural system is an enzyme, in which a binding pocket is located nearby a catalytically active center. The mimicking of these natural systems is of great interest, since it may give insight in how to design synthetic systems with similar efficiency and selectivity as biological systems.

A synthetic receptor molecule **1** based on diphenylglycoluril having two side-walls, which was able to bind dihydroxybenzene guest molecules, has been described recently. In this thesis a synthetic route, which enables the construction of receptor molecules having only one side-wall (**2**) is described. Subsequent modification led to the development of an extensive array of new molecular clips and clip-shaped receptor molecules with one side-wall functionalized by an active site (**3**).

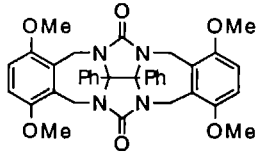

1

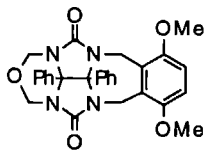

2

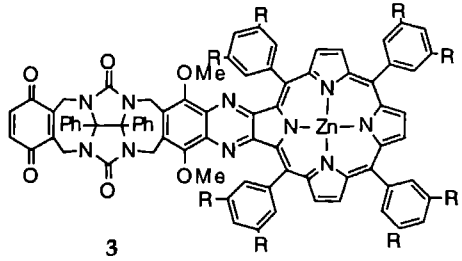

3

A detailed binding study with these new receptor molecules using ^{1}H NMR, IR, and computational methods revealed that the binding of 5-substituted 1,3-dihydroxybenzenes was based on hydrogen-bonding between the phenols of the guest and the amidic carbonyl group of the diphenylglycoluril frame work, π-π stacking interactions between the aromatic rings of the host and the guest, and a so-called 'cavity effect'. The former two interactions are dependent upon the substituent on the guest molecule, resulting in binding constants to **1** varying between K_a = 1,500 and 100,000 M^{-1}. A detailed analysis of the binding of a series of receptor molecules with a series of guests enabled the separation of the contributions of these three effects. The binding of e.g. 1,3-dihydroxybenzene in **1** is due to 8 kJ/mol hydrogen bonding, 5 kJ/mol π-π interaction and 6 kJ/mol cavity effect. Enlarging the height of the aromatic

side-wall, *viz.* a 2,3-connected naphthalene moiety, resulted in a larger clip which forms much weaker complexes with dihydroxybenzenes. This is due to an unfavourable π-π interaction between the host and the guest, which is enforced by the hydrogen bond formation. In the case of clips with 1,8-connected naphthalene side-walls, these π-π interactions are far more favourable. This does not lead, however, to significantly higher binding constants, since these molecules must change their conformation in order to form a cleft-shape which is required for complex formation. These receptor molecules are also able to bind silver ions between the two large cavity side-walls.
Several clip molecules were found to form dimers both in solution and in the solid state. This dimerization process is due to favourable π-π interactions and cavity effects. In the solid state crystal packing effects resulted in some clip molecules forming other, more favourable structures. Water soluble clip molecules, which have their water soluble groups connected to the diphenylglycoluril framework, formed more stable dimers in solution because of a large hydrophobic driving force. In the case of water soluble clips with naphthalene side-walls this dimerization also led to the formation of larger 'razor-blade' like aggregates, with a well-defined size and shape. These 'razor-blade' like structures formed upon self-aggregation could be modified by the addition of guest molecules resulting in spherical aggregates.

The receptor molecule **3** was synthesized in order to study photo-induced electron transfer processes, since one side-wall is known to act as an electron donor (Zn porphyrin), and the other as an electron acceptor (quinone). A spectroscopic study revealed that after excitation of the porphyrin ring, an electron was transferred to the quinone side-wall. This electron transfer was enhanced when an aromatic guest molecule was bound in between the donor and the acceptor. The study of these electron transfer processes being enhanced by aromatic mediation is of great interest, in particular in the investigation of biological photosynthetic reaction centers, where the electron transfer processes are also thought to be enhanced by intervening aromatic moieties.
Preliminary reactions were performed, with the different monofunctionalized clip molecules as catalysts in efforts to obtain enzyme mimics. These molecules were considered to be ideal synzymes since guest molecules are bound in a cavity nearby the catalytically active site. The conditions in which both strong binding of the guest and catalyst activity occur, were difficult to optimize. The best result obtained with the clip-shaped supramolecular catalysts, was a two fold increase in reactivity in the aziridination reaction of a bound nitrostyrene compared to a methoxystyrene.

Samenvatting

In dit proefschrift worden de synthese, de complexeringseigenschappen en de reactiviteit van receptormoleculen beschreven.

In de natuur zijn veel processen gebaseerd op moleculaire herkenning. Zwakke interacties tussen moleculen, zoals waterstofbruggen, hydrofobe effecten, π-π interacties en elektrostatische en van-der-waals-interacties, zijn bij deze processen betrokken. De selectiviteit wordt bepaald door de mate waarin de vorm en de interacties complementair zijn. Een voorbeeld van zo'n natuurlijk systeem is een enzym waarin (soms zeer selectief) een substraat gebonden kan worden vlakbij een katalytisch actief centrum. Een grote uitdaging voor chemici is het gebruiken van de concepten van de natuur om synthetische systemen te ontwikkelen die dezelfde eigenschappen en functies bezitten als de biologische systemen.

Eerder onderzoek heeft geleid tot de ontwikkeling van receptor-molecuul **1**, dat twee aromatische zijwanden bevat en in staat is dihydroxy-gesubstitueerde aromatische gastmoleculen te binden. In dit proefschrift wordt een synthese beschreven die het mogelijk maakt om receptormoleculen te maken met één aromatische wand (**2**). Vanuit dit type moleculen was het mogelijk om een scala aan nieuwe receptormoleculen te synthetiseren met verschillende zijwanden, o.a. monogefunctionaliseerde zoals **3**.

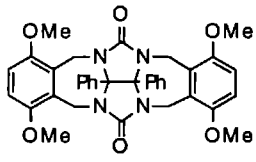

1

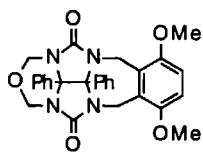

2

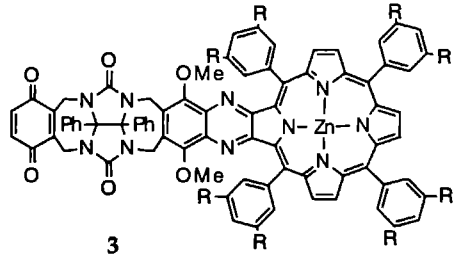

3

Door een gedetailleerde bindingsstudie aan o.a. deze nieuwe receptor-moleculen met een serie van substraatmoleculen, met behulp van ^{1}H NMR, IR en berekeningen, was het mogelijk om de bijdrage van de verschillende interacties, betrokken bij de complexvorming, te scheiden. De binding van gesubstitueerde 1,3-dihydroxybenzenen in **1** is gebaseerd op waterstofbrugvorming (bijdrage 8 kJ/mol in het geval dat 1,3-dihydroxybenzeen het substraat is), π-π interacties tussen de aromatische wanden van de receptor en het substraat (bijdrage 5 kJ/mol) en een zogenaamd 'holte effect' (bijdrage 6 kJ/mol). De bijdrage van de eerste twee genoemde interacties is afhankelijk van de substituent op het substraat. Uitbreiding van de aromatische zijwand, om de bijdrage in de π-π interactie te vergroten, resulteerde niet in stabielere complexen. In

het geval dat de wand in de hoogte werd uitgebreid (2,3-verbonden naftaleen) bleek de geometrie van het complex, opgelegd door de waterstofbrugvorming, ongunstig te zijn voor de π-π interactie. In het geval van een receptormolecuul, waarbij de naftaleenwand op de 1,8 plaats verbonden was met de difenylglycolurileenheid, resulteerde de betere π-π interactie niet in significant stabielere complexen, omdat de receptor eerst van conformatie moest veranderen om een sandwich-complex te verkrijgen. Dit laatst-genoemde receptormolecuul was ook in staat om zilverionen te complexeren.

Sommige receptormoleculen vormden een dimere structuur zowel in oplossing als in de vaste stof, waarbij de wand van de ene receptor de holte van de andere opvult. De vorming van deze dimeren is over het algemeen gebaseerd op gunstige π-π interacties tussen de zijwanden en een 'holte-effect'. In de vaste stof waren deze dimere structuren niet altijd te zien, omdat in sommige gevallen kristal-pakkingseffecten de overhand hadden. Wateroplosbare receptormoleculen, die hun wateroplosbare groep aan de difenylglycolurileenheid hebben, bleken sterke dimere associaten te vormen, omdat in dit geval een hydrofoob effect meespeelt. In het geval dat de zijwanden van deze wateroplosbare moleculen naftaleenringen waren, resulteerde deze dimerisatie in de vorming van grote 'scheermes-achtige' aggregaten met een zeer goed gedefinieerde vorm en grootte. De 'scheermes-achtige' vorm van deze aggregaten kon worden veranderd door er cafeïne of riboflavine als substraat aan toe te voegen. Door de vele evenwichten in oplossing waren de complexerende eigenschappen van de wateroplosbare receptoren moeilijk te bepalen.

Molecuul **3** is gemaakt om de lichtgeïnduceerde elektronenoverdracht van een zink-porfyrine naar een chinoneenheid te bestuderen. Een extra verval in de tijdsafhankelijke fluorescentie-meting kon aan deze elektronenoverdracht worden toegeschreven. Als een aromatisch substraat tussen de elektronendonor en acceptor werd gebonden was deze elektronenoverdracht veel sneller. Het verder bestuderen van dit systeem kan leiden tot een beter inzicht in de werking van biologische fotosynthetische reactiecentra, waarin de snelheid van elektronenoverdracht ook beïnvloed wordt door intercalerende aromatische moleculen.

Diverse monogefunctionaliseerde receptormoleculen zijn gesynthetiseerd en getest als katalysator voor verschillende reacties. Het doel om reacties uit te voeren volgens de principes van een enzym, d.w.z. een substraat binden in een holte nabij het actieve centrum, bleek niet eenvoudig. De omstandigheden zo optimaliseren, dat de bindingseigenschappen en de katalytische eigenschappen van het receptormolecuul behouden blijven, was daarbij het struikelblok. Het beste resultaat dat bereikt werd, was een verdubbeling van de reactiviteit in een koper-gekatalyseerde aziridinerings reactie.

Curriculum Vitae

De schrijver van dit proefschrift is geboren op 23 juni 1967 te 's-Hertogenbosch. In 1984 behaalde hij het HAVO-diploma en in 1986 het VWO-diploma, beide aan het Jeroen Bosch college te 's-Hertogenbosch. In 1986 is hij de studie scheikunde begonnen aan de Katholieke Universiteit van Nijmegen, waarvan het propaedeutisch diploma werd gehaald in juli 1987. Op 27 januari 1992 werd het doctoraal examen afgelegd met twee hoofdvakken, namelijk Vaste Stof Fysica bij Prof. dr. L. J. Giling en Organische Chemie bij Prof. dr. R. J. M. Nolte.

Vanaf februari 1992 was de schrijver verbonden aan de Katholieke Universiteit Nijmegen als Assistent in Opleiding (a.i.o) bij de vakgroep Organische Chemie onder begeleiding van Prof. dr. R. J. M. Nolte. In de periode 14 september tot 15 december 1992 heeft hij een stage gelopen op de Computational Medicinal Chemistry afdeling van Organon te Oss, onder begeleiding van dr. P. D. J. Grootenhuis en dr. V. J. van Geerestein.